



universität  
wien

# DISSERTATION

Titel der Dissertation

„Discovery of organellar calcium signaling components in  
*Arabidopsis thaliana*“

Verfasser

Mag. Simon Stael

angestrebter akademischer Grad

Doktor der Naturwissenschaften (Dr. rer. nat.)

Wien, 2011

Studienkennzahl lt. Studienblatt:	A 091 490
Dissertationsgebiet lt. Studienblatt:	Molekulare Biologie
Betreuerin / Betreuer:	Dr. Markus Teige

*“All truths are easy to understand once they are discovered;  
the point is to discover them.”*

Galileo Galilei

## **Thanks to...**

My supervisor Dr. Markus Teige, for the excellent guiding and opportunities he gave me within the framework of the Marie Curie Initial Training Network COSI (Chloroplast Signals).

My present and former colleagues from the lab, Bernhard, Andrea('s), Barbara, Norbert, Daniela, Przemek, Prabha, Konstantin, Karo, Helga and Sylvia for the great atmosphere, interesting discussions and help during my time in Vienna. Special thanks to Roman Bayer, for introducing me to the labwork and the fruitfull discussion and collaboration on a project that was not always riding on easy waves.

My collaboration partners, Prof. Dr. Ute Vothknecht, Prof. Dr. Andreas Weber, Prof. Dr. Halina Gabrys, Dr. Matthew Hannah, Dr. Dorothea Anrather, Dr. Edina Csazar, Philipp Schulz, Chhavi Aggarval and all people from the COSI network. Special thanks to Agostinho Rocha for the close collaboration and discussion.

Erna and Harald for the great help with logistic and administrative problems.

Finally, my parents, for all the chances they gave me untill now and to teach me that hard work pays off in the end; and my girlfriend, Lena, for being there for me.

## Abstract

My thesis is focused on the role of organelles in plant calcium signaling. Plants and other eukaryotic organisms use calcium ions as secondary messengers in order to acclimate rapidly to changes of the environment or to assist in developmental programs. The importance of calcium signaling on plant physiology is well established today, but has so far focused mainly on calcium signaling in the cytosol. To get insights into plant organellar calcium signaling, I have studied the impact of calcium on plastids, mitochondria and peroxisomes, and to a minor extent also the influence of these organelles on calcium signaling in the rest of the cell. Initially, I started with a search for calcium binding proteins in the chloroplast by targeted proteomics and data mining. However, the results of this work were in the end not only restricted to plastids as I discovered novel calcium signaling components of the mitochondria and peroxisomes.

The proteomic approaches resulted in the identification of two confirmed chloroplast calcium binding proteins. LENA (Little E-enriched protein A) is predicted to be a protein component of the long-hypothesized calcium storage of the plastid. SAMTL (*S*-adenosyl methionine transporter-like) is a member of the mitochondrial carrier family and predicted to transport SAM into chloroplasts in a calcium-dependent manner. The three calcium-dependent mitochondrial carrier family (MCF) proteins, APC1, 2 and 3 (ATP/phosphate carriers 1, 2 and 3) localize to mitochondria. Phylogenetic analysis and complementation of yeast mutants suggested APC1, 2 and 3 to be mitochondrial ATP importers, which could be needed during periods of anoxia. Furthermore an organellar EF-hand protein of 18 kDa (OEF18) was discovered in the course of a study on the impact of protein *N*-acylation for organellar targeting. This protein was identified by data mining as well as in the proteomic approach. Subsequent work showed that OEF18 is dually targeted to the plastid outer envelope and peroxisomal membrane and might be involved in the process of organellar division.

In addition to my approaches to identify novel organellar Ca<sup>2+</sup> binding proteins, I have studied a potential crosstalk between calcium signaling and protein phosphorylation in chloroplasts. Three chloroplast proteins, PsaN (subunit N of Photosystem I), the FstH protease VAR1 (Variegated 1) and CAS (Calcium sensing protein) were conclusively found to be phosphorylated in a calcium dependent manner. The implications of this novel regulation are speculative, but the presented findings provide a stable base to further investigate the impact of calcium dependent protein phosphorylation on chloroplast function.

## Zusammenfassung

In dieser Dissertation wird die Rolle von Organellen in der Kalzium-abhängigen Signaltransduktion in Pflanzen untersucht. Pflanzen und andere eukaryotische Organismen nutzen Kalzium als sekundären Botenstoff („secondary messenger“), um sich schnell an veränderte Umweltbedingungen anzupassen, oder um ihre Entwicklungsprozesse zu steuern. Die Bedeutung von Kalzium-abhängiger Signaltransduktion („calcium signaling“) in der Pflanzenphysiologie ist heute gut etabliert, ist aber bisher hauptsächlich auf zytosolische Prozesse fokussiert. Um weitere Einblicke in „calcium signaling“ in pflanzlichen Organellen zu bekommen, habe ich den Einfluss von Kalzium auf Plastiden, Mitochondrien und Peroxisomen untersucht, und zum Teil auch den Einfluss dieser Organellen auf das „calcium signaling“ im Rest der Zelle. Ich habe meine Arbeit mit einer Suche nach Kalzium-bindenden Proteinen in Chloroplasten in einem gerichteten proteomischen Ansatz und intensiven Recherchen in Datenbanken begonnen. Am Ende waren die Resultate dieser Arbeit nicht nur auf Plastiden beschränkt, da ich auch neuartige Komponenten des „calcium signaling“ in Mitochondrien und Peroxisomen entdeckt habe.

Die Proteomischen Ansätze führten zur Identifizierung von zwei bestätigten Kalzium-bindenden Proteinen im Chloroplasten: LENA (Little E-enriched protein A), welches vermutlich eine Komponente des lange gesuchten Kalziumspeichers im Plastiden darstellt, und SAMTL (Sadenosyl methionine transporter-like), einem Mitglied der Mitochondrial Carrier Familie (MCF), welches vermutlich in einer Kalzium-abhängigen Weise SAM in Chloroplasten transportiert. Zusätzlich wurden drei weitere Kalzium-abhängige MCF Proteine identifiziert, die ATP/Phosphat Carrier APC1, 2 und 3. Phylogenetische Analysen und funktionelle Komplementation von Hefemutanten legen nahe, dass APC1-3 in Mitochondrien lokalisiert sind und eine Rolle unter Sauerstoffmangelbedingungen spielen könnten. Außerdem wurde ein organellenlokalisierendes EF-Hand Protein mit einer Masse von 18 kDa (OEF18) identifiziert, welches dual im äußeren Chloroplasten Envelope und in Peroxisomen lokalisiert ist und in den Prozess der Organellenteilung involviert sein könnte.

Zusätzlich zu meinen Ansätzen, neuartige organellenlokalisierte Kalzium-bindende Proteine zu identifizieren, habe ich auch einen möglichen „cross-talk“ zwischen „calcium signaling“ und Proteinphosphorylierung im Chloroplasten untersucht. Dabei konnte eindeutig eine Kalzium-abhängige Phosphorylierung der drei Chloroplastenproteine, PsaN (Photosystem I Untereinheit N), der FtsH Protease VAR1 (Variegated 1) und CAS (Calcium Sensor Protein) gezeigt werden. Über die funktionelle Bedeutung dieser neuen Regulation kann soweit nur spekuliert werden, aber diese Ergebnisse bilden jetzt eine stabile Basis für weitere Untersuchungen über die Rolle der Kalzium-abhängigen Protein Phosphorylierung in Chloroplasten.

## Table of Contents

1. Introduction.....	10
1.1. Plant calcium signaling – the generation of calcium signals .....	10
1.2. Calcium binding proteins –storage and signaling proteins .....	15
Review - The magical life of calcium as a secondary messenger: A journey to the organelles .....	25
1.3. Main plant calcium stores .....	27
1.4. Organellar calcium signaling .....	30
1.5. Bacterial calcium signaling.....	41
1.6. Conclusions and further perspectives .....	46
2. Results and discussion .....	48
2.1. Paper 1- Mining the soluble chloroplast proteome by affinity chromatography .....	49
2.2. Paper 2 - Protein N-acylation overrides differing targeting signals .....	62
2.3. Paper 3 - Arabidopsis calcium-binding mitochondrial carrier proteins as potential facilitators of mitochondrial ATP-import and plastid SAM-import .....	68
2.4. Paper 4 - Crosstalk between calcium signaling and protein phosphorylation at the thylakoid.....	82
2.5. Organellar EF-hand protein of 18 kDa (OEF18) is a novel calcium signaling protein .....	99
2.6. Proteomics appendix - Are LENA and LENB chloroplast calcium storage proteins?.....	116
3. Conclusions and future perspectives.....	117
4. Material and methods.....	121
4.1. Used vectors.....	121
4.2. Bacteria and yeast strains .....	122
4.3. Plant material .....	123
4.4. Antibodies .....	124
4.5. Media .....	124
4.6. Buffers and solutions .....	125
4.7. RNA methods.....	126
4.8. DNA methods .....	127
4.9. Protein methods .....	131
4.10. Bacteria methods.....	139

4.11. Yeast methods.....	141
4.12. Plant methods.....	141
5. References.....	145
6. Supplementary material .....	161
7. Curriculum vitae .....	180
8. List of publications .....	181







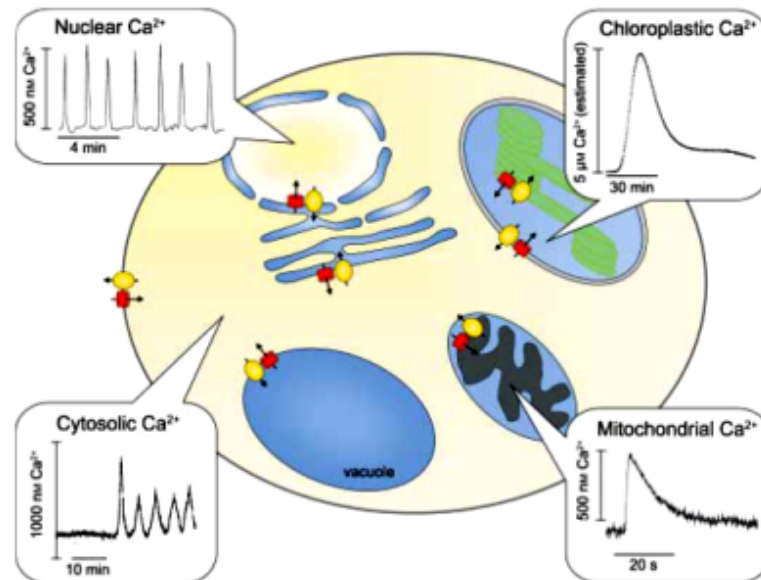
## 1. Introduction

Plants are able to react to changing environmental or stress conditions through immediate signal transduction pathways. Calcium signaling - the usage of free calcium ions as secondary messengers - is a widely accepted mechanism for immediate stress signaling in plants and other eukaryotes and is also involved in plant development. Recent advances in the field have started to uncover the potential roles that organelles play in calcium signaling and they will be discussed more in detail after a general overview of the generation and decoding of calcium signals.

### 1.1. Plant calcium signaling – the generation of calcium signals

Plant calcium signaling, on a cellular level, entails the generation of spikes, transients or oscillations of free calcium ions that can be decoded by calcium binding proteins. These calcium signals contain specific information and serve to adjust the physiological state of the cell and consequently of the whole plant in response to an external stimulus (McAinsh and Pittman, 2009; DeFalco et al., 2010; Dodd et al., 2010; Kudla et al., 2010). Due to their observed differences in duration, amplitude, frequency and spatial distribution, the fluxes of free calcium ions have come to be referred to as ‘calcium signatures’. In a non-stimulated cell, the ‘resting’ concentration of free calcium ions ( $\text{Ca}^{2+}$ ) in the cytoplasm is kept on purpose very low (appr. 100-200 nM) to prevent precipitation of  $\text{Ca}^{2+}$  with free phosphate ( $\text{P}_i$ ) groups and to prevent the competition with other metal ions for enzyme function. Therefore, all  $\text{Ca}^{2+}$  in the cell is stored in subcellular compartments or is bound to negatively charged carboxylic groups of the cell wall. The large differences in  $\text{Ca}^{2+}$  concentration between the cytoplasm and the stores provide a high potential for rapid changes in the free  $\text{Ca}^{2+}$  concentration, resulting in a great signaling effect (DeFalco et al., 2010). The calcium signatures are produced by expelling  $\text{Ca}^{2+}$  from these subcellular stores into the cytoplasm via  $\text{Ca}^{2+}$  channels. After the influx, the resting concentration is restored to its normal level by the active removal of calcium ions from the cytoplasm through  $\text{Ca}^{2+}$  efflux transporters. It is the concerted action of influx and export of  $\text{Ca}^{2+}$  from the cytoplasm that produces the typical shapes of calcium signatures (Fig. 1A).

A



B

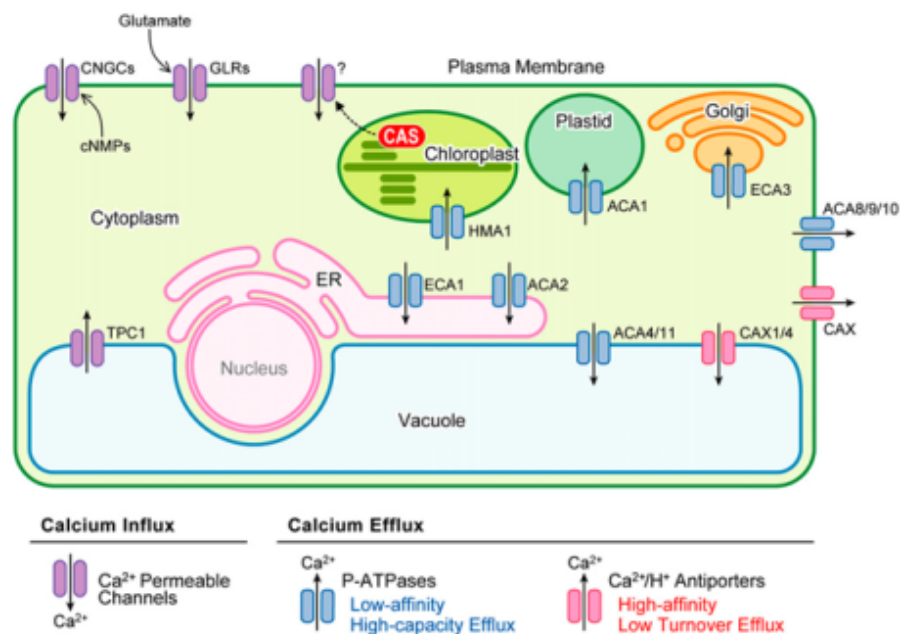


**Figure 1 Calcium signatures and calcium transporters.** (A) Different shapes of calcium fluxes are produced in various subcellular localizations (Buchanan et al., 2000). (B) Subcellular localization of calcium influx channels and calcium efflux transporters; CNGCs (cyclic nucleotide gated channels), GLRs (glutamate receptor-like channels), CAS (Calcium sensing protein), HMA1 (Heavy metal ATPase 1), ACA (Auto Inhibited  $\text{Ca}^{2+}$ -ATPase), ECA (ER-type  $\text{Ca}^{2+}$ -ATPase), CAX (Cation exchanger), TPC1 (Two-pore channel 1) (Kudla et al., 2010).

## Ca<sup>2+</sup> influx channels

Ca<sup>2+</sup> influx into the cytoplasm is a passive process in which Ca<sup>2+</sup> flows down the electrochemical gradient (so, a gradient both in concentration and in charge) through Ca<sup>2+</sup> permeable ion channels. These need to be activated for Ca<sup>2+</sup> release to happen and there are three types of influx channels that can be distinguished in the way that they are activated: voltage-dependent, ligand-dependent and stretch-activated channels. Figure 1B gives a quite complete overview of the main families of Ca<sup>2+</sup> transporters and their subcellular localization to calcium stores, known to date. It should be noted that most of these influx channels are not specific to Ca<sup>2+</sup> only, but mostly will channel a variety of other divalent and monovalent ions. Voltage-dependent channels have been characterized mainly during the 1990's through electrophysiological studies and were found to have different voltage dependencies (Sanders et al., 2002). Their presence was measured in a variety of subcellular membranes, but mainly in the plasma membrane and tonoplast. Some are activated by depolarization of the membrane, similar to neuron depolarization in the mammal system, while others are activated by hyperpolarization. Although they are quite well characterized for almost twenty years now, no molecular identity has been found for these channels so far, except for the TWO-PORE CHANNEL1 (TPC1). TPC1 localizes to the vacuolar membrane, has no other homologues in Arabidopsis, and was confirmed to be the slow vacuolar (SV) channel (Peiter et al., 2005). The protein contains two EF-hands and provides a nice example for how Ca<sup>2+</sup> might induce Ca<sup>2+</sup> release into the cytoplasm (Pottosin et al., 2009). In the case of ligand-dependent channels, similar electrophysiological experiments have uncovered Ca<sup>2+</sup> influx channels that are activated by

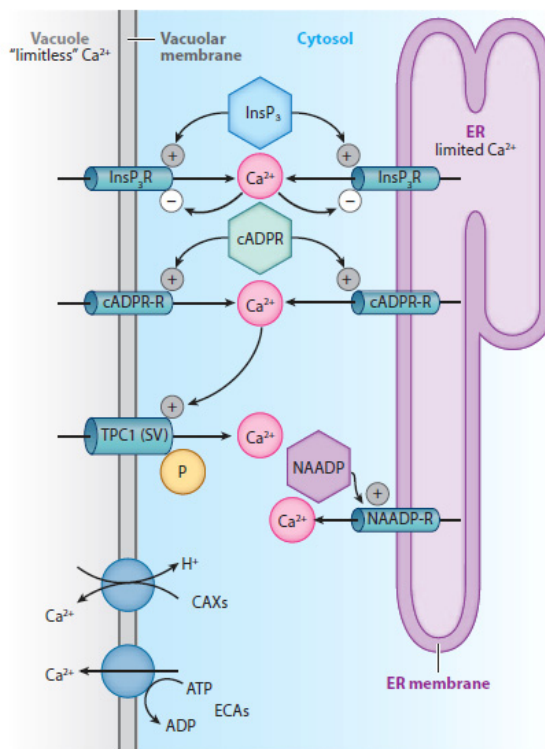


**Figure 2 Ligand-dependent channels of the vacuole and ER.** Note that NAADP only induces Ca<sup>2+</sup> release from the ER. Primary Ca<sup>2+</sup> released from the ER, might induce Ca<sup>2+</sup> release from the vacuole through TPC1 (TWO-PORE CHANNEL1) (Dodd et al., 2010).

ligands such as inositol 1,4,5-triphosphate (InsP<sub>3</sub>), cyclic ADP-ribose (cADPR) and nicotinic acid adenine dinucleotide phosphate (NAADP). These have been measured only from tonoplast and ER membrane preparations and interestingly NAADP stimulates calcium release only from the ER (Allen et al., 1995; Navazio et al., 2000) (Fig. 2). However, debate surrounds the nature of these channels while no direct homologues from the well-characterized mammal InsP<sub>3</sub>-receptor and ryanodine receptor (for cADPR) are present in higher plant genomes (Munnik and Testerink, 2009). Other ligand-gated ion channels that can mediate fluxes of Ca<sup>2+</sup> include the cyclic nucleotide-gated channels (CNGCs) and glutamate receptor-like channels (GLRs). Both gene families in *Arabidopsis* contain twenty members and they carry many ions, but some members have been implicated in mediating cytosolic increases of Ca<sup>2+</sup> (Hua et al., 2003; Ali et al., 2006; Qi et al., 2006; Ali et al., 2007; Kaplan et al., 2007). CNGCs are activated by binding of the secondary messengers cAMP and cGMP, and can be inactivated by the binding of calmodulin at a site that overlaps the binding site of the cyclic nucleotides. Members of the GLR family are differentially activated by glutamate and other amino acids (Stephens et al., 2008). All CNGCs and GLRs studied so far are targeted to the plasmamembrane. Although some of the channels have experimentally been found to transport Ca<sup>2+</sup> (Leng et al., 1999; Urquhart et al., 2007) it should be noted that non-selective ion channels might contribute to calcium influx by depolarizing the plasmamembrane, thereby activating voltage dependent Ca<sup>2+</sup> channels, instead of channeling Ca<sup>2+</sup> directly (Dodd et al., 2010). The role that they play in calcium signaling is only recently being uncovered and the sheer numbers of members in these families make them interesting candidates for the variety of calcium signatures that have been observed.

Stretch-activated channels have been implicated in the Ca<sup>2+</sup> signatures that are observed in the growing tip of pollen tubes and of root hairs, where waves of calcium alternate with periods of tip expansion (Dutta and Robinson, 2004; Hepler and Winship, 2010). The channels sense mechanical deformation of the rapidly expanding membrane via changes in their own protein conformation (Sachs, 2010; Michard et al., 2011). Proof for stretch-activated channels in the plasma membrane of pollen tubes came from electrophysiological evidences, but no molecular identity of the involved channels has been found so far. Recently, a member of the GLR family, *Atglr1.2*, was identified to be involved in pollen tube growth (Michard et al., 2011) and it would be interesting to see if this channel displays mechanosensitivity.

## Ca<sup>2+</sup> export channels

Calcium export out of the cytoplasm is an active process in which Ca<sup>2+</sup> is moved against its own electrochemical gradient through the dissipation of stored energy. Responsible for the Ca<sup>2+</sup> export are Ca<sup>2+</sup>/proton antiporters and P-type Ca<sup>2+</sup>-ATPases that are localized on various subcellular membranes (Fig. 1B). Ca<sup>2+</sup>/proton antiporters are low affinity high capacity transporters, while P-type Ca<sup>2+</sup>-ATPases are high affinity low capacity transporters (Geisler et al., 2000). For this reason, Ca<sup>2+</sup>/proton antiporters are believed to be in charge of removing the bulk of Ca<sup>2+</sup> from the cytoplasm after the induction of a Ca<sup>2+</sup> peak, whereas P-type Ca<sup>2+</sup>-ATPases make sure to keep the resting concentration of Ca<sup>2+</sup> in the cytoplasm as low as possible (McAinsh and Pittman, 2009; Kudla et al., 2010). In Arabidopsis, the Ca<sup>2+</sup>/proton antiporter family contains 6 members, known as CATION EXCHANGER 1 to -6 (CAX1-6) (Shigaki et al., 2006). CAX1 to 4 localise to the tonoplast and CAX activity has also been found in the plasma membrane (Kasai and Muto, 1990). These antiporters have an N-terminal autoinhibitory domain that can be regulated by posttranslational modification and protein interactions (Cheng et al., 2004; Mei et al., 2007). The severity of *cax1* and *cax3* single or double mutants (Cheng et al., 2005; Conn et al., 2011), together with their posttranslational regulation, suggest an important role for CAXs in Ca<sup>2+</sup> homeostasis (Dodd et al., 2010). In Arabidopsis, P-type Ca<sup>2+</sup>-ATPases are subdivided in two classes: ER-type Ca<sup>2+</sup>-ATPases (ECAs, 4 family members in Arabidopsis) and Auto Inhibited Ca<sup>2+</sup>-ATPases (ACAs, 10 family members). Despite their name, ER-type Ca<sup>2+</sup>-ATPases have not only been found in the ER (ECA1)(Liang et al., 1997), but also at the Golgi membrane and endosomes (ECA3)(Li et al., 2008; Mills et al., 2008). ECA1 and ECA3 exhibit both Ca<sup>2+</sup> and Mn<sup>2+</sup> related phenotypes and were hypothesized to have a metabolic function rather than a calcium homeostasis or signaling function (Dodd et al., 2010). ACAs, on the other hand, are recently becoming more appreciated as key players of calcium signaling. They contain an N-terminal cytosolic auto-inhibitory domain that can be relieved by the binding of calmodulin, resulting in their activation (Harper et al., 1998; Baekgaard et al., 2005). Members of the ACA family localize to the ER (ACA2), the tonoplast (ACA4 and 11)(Bonza et al., 2000; Geisler et al., 2000; Lee et al., 2007), the plasma membrane (ACA8,9 and 10)(Bonza et al., 2000; Schiott et al., 2004; George et al., 2008) and the plastid envelope (ACA1)(Huang et al., 1993). Their expression changes dramatically upon different stresses and varies between tissues and cell types of the plant (Boursiac

and Harper, 2007). ACA9 is important for pollen tube growth and knock-out mutants of ACA10 display deregulated growth of the inflorescence. Probably the best evidence for the direct involvement of a P-type ATPase in calcium signaling comes from the studies on PCAI in *Physcomitrella patens*. Disruption of PCAI leads to a sustained elevated cytosolic  $\text{Ca}^{2+}$  concentration after applying NaCl stress, which results in the upregulation of salt-stress induced genes and weaker tolerance to salt stress (Qudeimat et al., 2008).

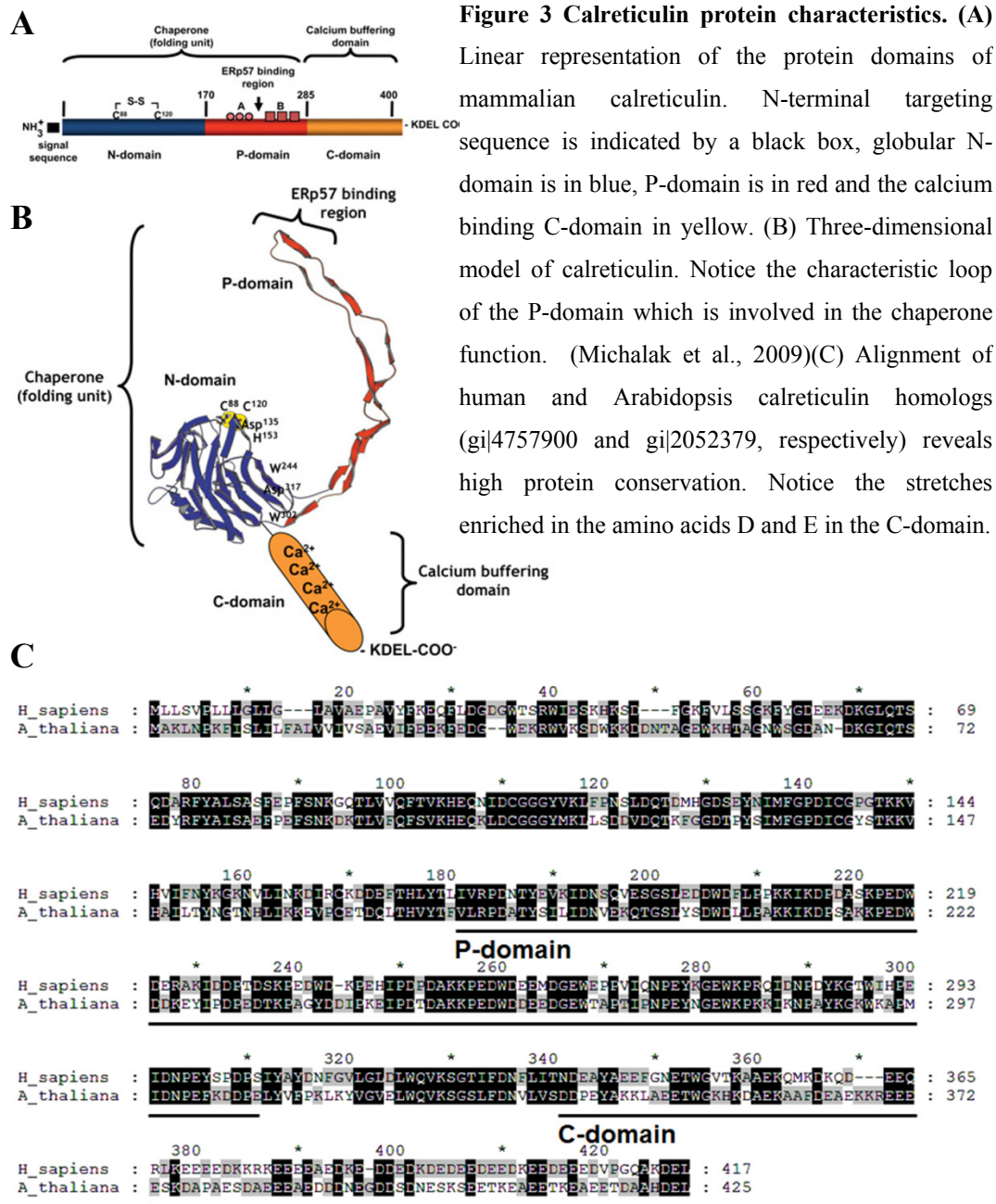
## **1.2. Calcium binding proteins –storage and signaling proteins**

Calcium binding proteins can roughly be divided in two classes based on their  $\text{Ca}^{2+}$  binding kinetics: storage proteins and signaling proteins. While storage proteins have a low-affinity/high capacity for binding calcium, signaling proteins have a high-affinity/low capacity. Both are on opposite sides of a calcium flux, meaning that, the signaling proteins perceive stimuli by binding to  $\text{Ca}^{2+}$  that is released (partly) from storage proteins. Nagata and colleagues made a quite comprehensive overview of calcium binding proteins of animals and found many, although not all, conserved proteins in Arabidopsis and Rice (Nagata et al., 2004). On the other hand, the calcium-dependent protein kinase (CDPK) family is only found in plants and some protists.

### **$\text{Ca}^{2+}$ storage proteins**

Few  $\text{Ca}^{2+}$  storage proteins are known in animals and plants. The prototypic  $\text{Ca}^{2+}$  storage protein is the ER luminal  $\text{Ca}^{2+}$ -binding protein calreticulin. It has been very well described in animals and is highly homologous to plant calreticulin (Michalak et al., 2009)(Fig. 3). It contains an N-terminal cleavable signal sequence, directing it to the ER, and an ER KDEL (Lys-Asp-Glu-Leu) retention/retrieval signal. Its three functional domains are: the globular N-domain that is important for its chaperone function, the P-domain, rich in proline, that can bind calcium with high affinity ( $\sim 1\mu\text{M}$ ) and the acidic C-domain with high capacity (25 mol of  $\text{Ca}^{2+}$  per mol of protein) and low affinity ( $K_d = 2\text{ mM}$ ) for  $\text{Ca}^{2+}$ . Highly similar to calreticulin is calnexin, with the difference that the protein contains a transmembrane helix. The  $\text{Ca}^{2+}$ -binding function of the calnexin C-domain is questionable though, because it is extruded into the cytoplasm. The Radish Vacuolar Calcium Binding protein (RVCaB) contains 4 repeats of the amino acid stretch [EET(A)PAV(A)VEEESKT(A)EE(D)VVEPKK]. The protein binds 21.6 mol of  $\text{Ca}^{2+}$  per mol of protein with an affinity of  $360\ \mu\text{M}$   $K_d$  upon which it undergoes a slight conformational change (Ishijima et al., 2007). It is clear that all calcium storage proteins

bind  $\text{Ca}^{2+}$  via an acidic domain that is significantly enriched in the negatively charged amino acids aspartate (D) and glutamate (E).





## Ca<sup>2+</sup> signaling proteins

Most Ca<sup>2+</sup> signaling proteins contain a single, or more EF-hands. It is the best known and described calcium binding protein motive and was named some 28 years ago after the protein motive of parvalbumin that contains  $\alpha$ -helices E and F, connected by a calcium-coordinating loop (Kretsinger and Nockolds, 1973). The structure resembles a hand with stretched index finger (helice E) and thumb (helice F), connected by the bent middle

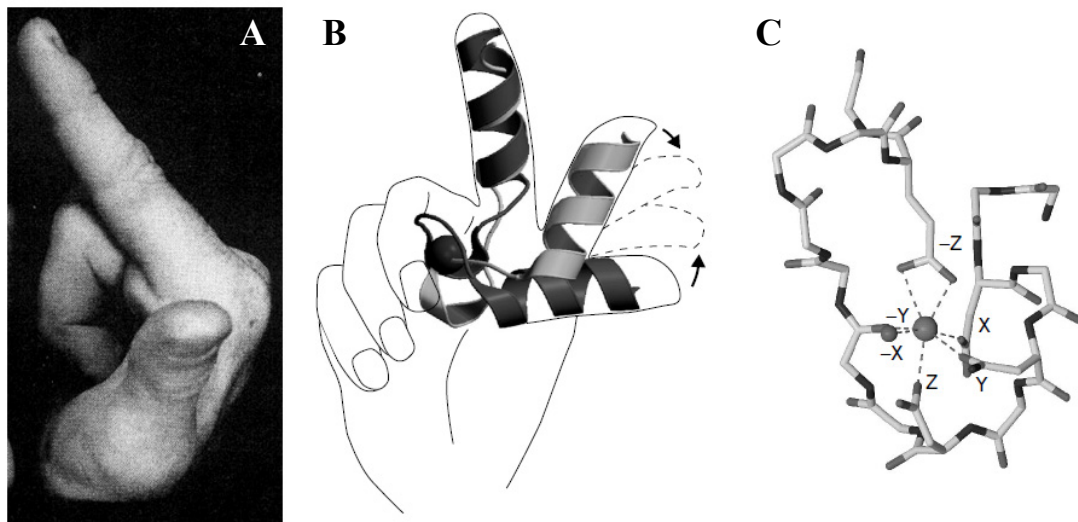


**Figure 4 EF-hand structure.** (A) Original image of Kretsinger and Nockolds describing the EF-hand fold where the index finger symbolizes the E-helice, the bent middle finger is the calcium binding loop and the thumb is the F-helice (Kretsinger and Nockolds, 1973). (B) Conformational change of the EF-hand upon binding of calcium displaces the F-helice from the light grey position to the dark grey position. (C) Representation of the axes of the pentagonal bipyramid configuration that coordinates the bound Ca<sup>2+</sup> (Lewit-Bentley and Rety, 2000).

finger (loop) that can hold the calcium ion (Fig. 4A). Since then, many more EF-hand proteins were found and its mechanistic properties and function have been well described (Lewit-Bentley and Rety, 2000; Gifford et al., 2007). In short, the calcium ion is coordinated by seven ligands of the Ca<sup>2+</sup>-binding loop, along the axes of a pentagonal bipyramid (Fig. 4C). Six of the ligands are mostly the negatively charged amino acids aspartate (D) or glutamate (E) and are ordered in a stretch of 12 amino acids that starts with the first amino acid of the loop. The amino acid stretch is commonly displayed as (1)X•(3)Y•(5)Z•(7)–Y•(9)–X••(12)–Z, where dots mark intermittent amino acids and X, Y and Z refer to the axes of the pentagonal bipyramid. The position at (12)–Z usually contributes 2 ligands for coordination and the bond of (9)–X is frequently completed by a water molecule. The protein motive prediction program ‘Prosite’ (<http://prosite.expasy.org/PDOC00018>) (de Castro et al., 2006) lists the amino acid pattern as: D-(W)-[DNS]-(ILVFYW)-[DENSTG]-[DNQGHRK]-(GP)-[LIVMC]-

[DENQSTAGC]-x(2)-[DE]-[LIVMFYW] (the amino acids in between () brackets are excluded at that position). From this pattern, one can infer that position 1 (D) and 12 (D or E) are highly conserved. Usually, position 6 is occupied by a glycine (G) residue, which allows for the middle of the loop to make a sharp turn, whereas the amino acid at position 12 is important for the selectivity of the EF-hand towards calcium (E is preferred) or its major competitor, magnesium (D is preferred). On the other hand it displays the degree of variability that EF-hands can have at the other positions, which partly explains for the different affinities that EF-hands show towards  $\text{Ca}^{2+}$ . The amino acid in position 12 falls just outside of the loop-region in the leaving  $\alpha$ -helix (F) and upon binding of  $\text{Ca}^{2+}$ , this amino acid is pulled closer into the binding site. As a consequence, the whole F  $\alpha$ -helix is shifted (Fig. 4B), leading to a conformational change of the EF-hand. It is this conformational change which leads the EF-hand motive to modulate the function of the rest of the protein or to bind to its target proteins. EF-hands are very sensitive as they usually have  $\text{Ca}^{2+}$ -binding affinities in the low micromolar range (0.1-100  $\mu\text{M}$ ).

The Arabidopsis genome contains a maximum of 250 predicted EF-hand proteins, including a variety of proteins such as enzymes, proteins involved in transcription and translation, kinases and phosphatases and ion channels and solute carriers (Day et al., 2002) (Fig. 5 displays the variety of proteins containing EF-hands). Probably best known though, are the three protein families of calmodulin and calmodulin-like proteins (CaM's and CML's), calcineurin B-like proteins (CBL's) and calcium-dependent protein kinases (CDPK's or CPK's). Calmodulins are the prototypical calcium signaling proteins. Having nothing else but 4 EF-hands and being highly conserved through all eukaryotic species, they are implicated in many processes, such as ion transport, transcription, metabolism, protein folding, cytoskeleton-associated functions, protein phosphorylation and dephosphorylation and phospholipid metabolism (Bouche et al., 2005; Reddy et al., 2011). They are small proteins (149 amino acids in Arabidopsis, ~17 kDa) that contain pairs of EF-hands connected by a flexible  $\alpha$ -helical hinge region, which upon binding of  $\text{Ca}^{2+}$ , exposes hydrophobic patches necessary for the interaction with target proteins. Containing seven functional members, the Arabidopsis genome holds a surprisingly large family of CaM genes and they are all highly identical (plants in general contain more, compared to three in humans). AtCaM1 and AtCaM4 are even completely identical and so are AtCaM2, AtCaM3 and AtCaM5 to each other. So, together with the near identical, but distinct proteins of AtCaM6 and AtCaM7, there exist only four different protein

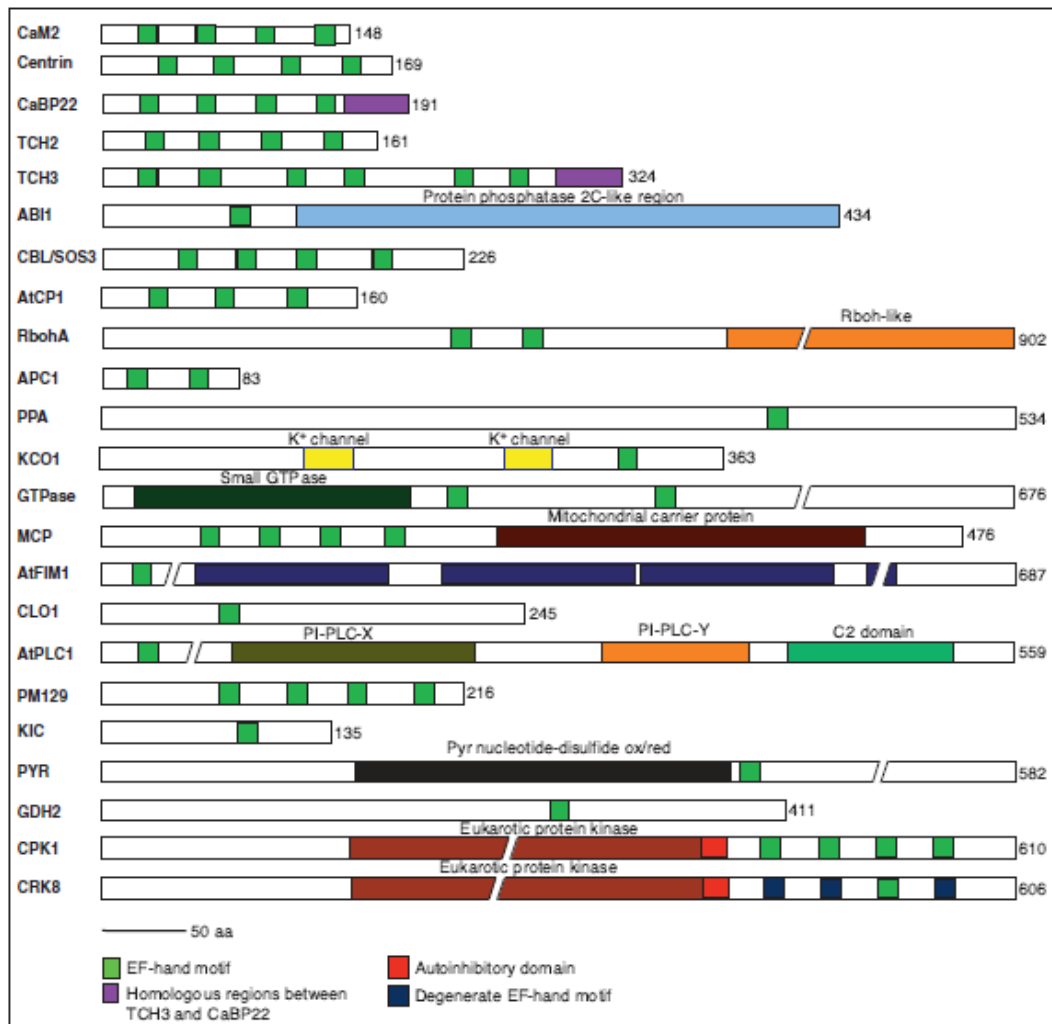


**Figure 5 Variety of EF-hand containing proteins.** Schematic diagrams of representative EF-hand proteins. EF-hands are represented by green boxes. Other domain names are written above the domain. ABH1, ABA-insensitive 1; APC1, Arabidopsis pollen  $\text{Ca}^{2+}$ -binding protein; AtCP1, Arabidopsis thaliana  $\text{Ca}^{2+}$ -binding protein; AtFIM1, Arabidopsis thaliana fimbrin 1; AtPLC1, Arabidopsis thaliana phosphatidylinositol-specific phospholipase C; CAM2, calmodulin 2; CaBP22, 22 kd  $\text{Ca}^{2+}$ -binding protein; CBL/SOS3, calcineurinB-like, salt-overlynsensitive protein; CH, calponin homology; CLO1, caleosin1; CPK,  $\text{Ca}^{2+}$ -dependent protein kinase; CRK, CPK-related kinase; GDH2, NAD(H)-dependent glutamate dehydrogenase; GTPase, small GTPase-like protein (At3g63150); KCO1, potassium channel outwardly rectifying protein 1; KIC, KCBPinteracting CCD-1-like protein; MCP, mitochondrial carrier protein (At5g61810); PM129, protein isolated from plasma-membrane enriched library; PPA, protein phosphatase 2A-like protein (At1g03960); PYR, pyridine nucleotide-disulfide oxidoreductase (At2g20800); RbohA, respiratory burst oxidase homology; TCH2 and TCH3, touch-induced proteins. // indicates a break in the protein (Day et al., 2002).

isoforms in Arabidopsis. This poses a riddle to why these highly similar proteins were not differentiating more through evolution, but strengthens the idea that their high conservation is important for function (McCormack et al., 2005). A partial explanation to the riddle is provided by the differential expression of CaM isoforms during the plant life cycle and in different plant organs. Furthermore, very small differences in the isoforms can lead to target specificity. For example, they have been shown to activate and bind to

NAD kinase and a kinesin-like motor protein with different affinities (Liao et al., 1996; Reddy et al., 1999). CaM-binding proteins have been identified by various experimental means, for example by screening of expression libraries or protein chips with labeled CaM. Based on these experimentally identified CaM-binding proteins, in a recent publication, 700 high-confidence CaM-binding proteins were predicted to exist in the Arabidopsis genome (Reddy et al., 2011). Of course, these interactions should be experimentally proven, but the study exemplifies the multitude of processes that calmodulins are involved in. CaM's are believed to reside in the cytoplasm and nucleus (DeFalco et al., 2010). However, they have been implicated in different processes in peroxisomes, chloroplasts and mitochondria. Similar to CaM's, there exists a much larger group of calmodulin-like proteins (CML's). The family contains of 50 members and has been grouped, based on the criteria that they contain only EF-hands and no other protein domains, they are small (ranging from 83-330 amino acids) and have at least 16% sequence identity with AtCaM2 (McCormack, 2003). CML's contain from 1 up to 6 EF-hands, have variable N-termini and some have predicted myristoylation motives. Their variable N-termini makes them interesting candidates for subcellular localizations other than the cytoplasm and some are highly predicted to be chloroplast-targeted by a minimum of 3 different targeting prediction programs (own unpublished data). Furthermore, the covalent attachment of myristic acid (a fatty acid) would increase the tendency of these proteins to be membrane localized. Few studies have been made on CML's, leaving great potential for these proteins in the calcium signaling research field.

The second important group of  $\text{Ca}^{2+}$ -binding proteins is the calcineurin B-like protein family (CBL's) and they are unequivocally discussed together with their target proteins, the CBL interacting protein kinases (CIPK's, reviewed in (Batistic and Kudla, 2009; Kudla et al., 2010)). They were relatively recently discovered and subsequent bioinformatic searches identified 10 CBL's and 26 CIPK's in total in the Arabidopsis genome (Liu and Zhu, 1998; Shi et al., 1999). CBL's have a high similarity to the regulatory B-subunit of calcineurin (a human phosphatase). They all share a conserved core region consisting of four EF-hands, of which the first EF-hand is atypically containing 14 residues in its  $\text{Ca}^{2+}$ -binding loop. Although they are reminiscent of CaM's, they are not homologues and are slightly larger (23 to 26 kDa). CIPK's are composed of a N-terminal kinase domain and a C-terminal regulatory domain that contains a stretch of amino acids rich in asparagine, alanine and phenylalanine (NAF domain) which is required and sufficient for mediating CBL interaction (Albrecht et al., 2001).

Autoinhibition of CIPK's is relieved by the binding of CBL's to the NAF domain (Gong et al., 2002). CBL's undergo dual lipid modifications on their N-termini, by myristoylation and palmitoylation, which help to target them to the plasma membrane and the tonoplast. Accordingly, the interaction of a CBL with a CIPK determines the subcellular localization of the active pair. Moreover, the overlapping interactions between CBL's and CIPK's provide the plant cell with the ability to react to membrane-localized  $\text{Ca}^{2+}$  fluxes with increased versatility (Batistic et al., 2010). A prominent CBL/CIPK pair exemplifies the impact that  $\text{Ca}^{2+}$  signaling proteins can have on plant physiology. Originally discovered in a reverse genetics screen for *salt overly sensitive* (SOS) mutants, AtCBL4 (SOS3) and AtCIPK24 (SOS2) mediate salt stress acclimation by regulating the  $\text{Na}^+/\text{H}^+$  antiporter SOS1 (Wu et al., 1996; Qiu et al., 2002). Furthermore, AtCIPK24 was also found to localize to the tonoplast through the specific interaction with CBL10 and is hypothesized to mediate salt stress acclimation in a similar way as the SOS pathway, by extruding  $\text{Na}^+$  from the cytoplasm to the vacuole (Weinl and Kudla, 2009). This is only a hypothesis because the vacuolar channel is unknown, but it demonstrates that CIPK's can

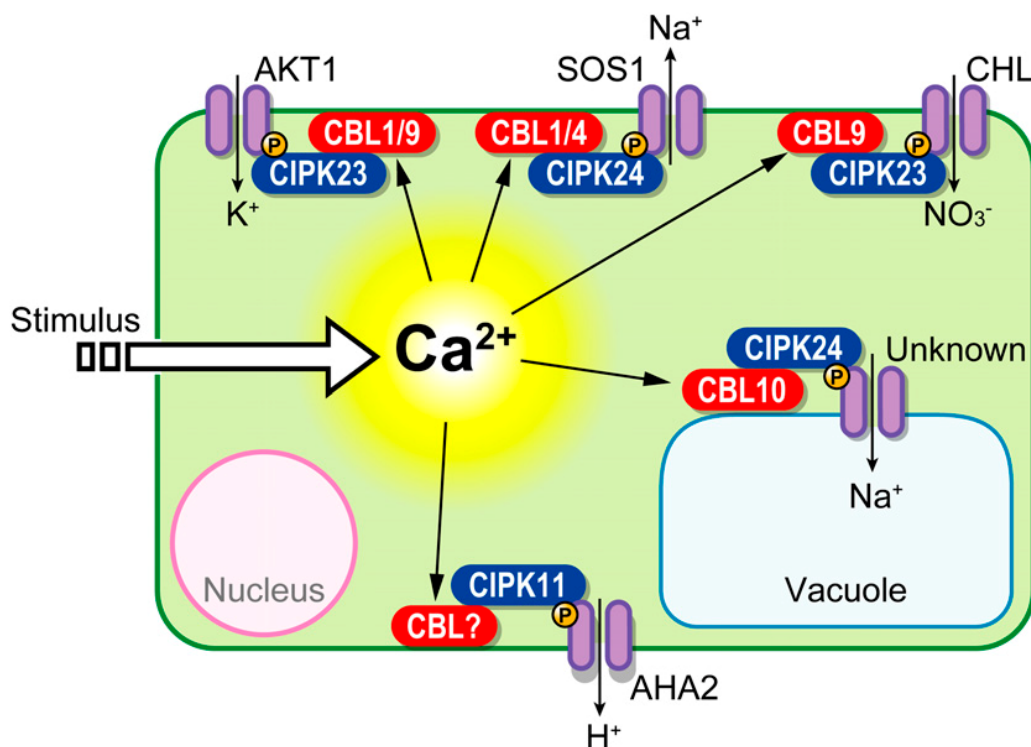


**Figure 6 CBL/CIPK pairs regulate membrane ion channels.** CBL1/4 pair targets CIPK24 to the plasma membrane for the regulation of the  $\text{Na}^+/\text{H}^+$  antiporter SOS1. The same kinase CIPK24 is targeted to the vacuole by CBL10 and there possibly regulates  $\text{Na}^+$  extrusion from the cytoplasm to the the vacuole. CBL1/9-CIPK23 pair regulates AKT1 (Arabidopsis K<sup>+</sup> transporter) and the nitrate transporter CHL1. CIPK11 phosphorylates AHA2 (Arabidopsis H<sup>+</sup> ATPase 2), but the CBL partner is unknown. More on these examples that are not discussed here can be found in (Kudla et al., 2010).

have different localizations, depending on the localization of their partner CBL. Figure 6 summarizes the most recent findings of CBL/CIPK. From this image it becomes apparent that most research so far was pointed towards regulation of membrane channels during abiotic stress, but various other calcium-dependent regulations are expected to be mediated by CBL/CIPK pairs (Kudla et al., 2010).

Calcium-dependent protein kinases (CDPK's, also called CPK's in Arabidopsis) make out the third major group of  $\text{Ca}^{2+}$ -signaling proteins. They are similar to animal  $\text{Ca}^{2+}$ /calmodulin-dependent protein kinase II (CaMKII), however they contain both the kinase- and calmodulin domain fused in one protein; a feat only known from plants and certain protists (Harper et al., 2004; Harper and Harmon, 2005). Binding of  $\text{Ca}^{2+}$  to the calmodulin-like domain (containing 4 functional EF-hands) causes the autoinhibitory domain to retract from the kinase active site (see Fig. 5 for protein domains of CDPK's). Together with autophosphorylation of the kinase, this results in the  $\text{Ca}^{2+}$ -dependent activation of CDPK's. The Arabidopsis genome contains 34 CDPK's and eight CDPK-related kinases (Hrabak et al., 2003). They occur in various subcellular localizations, such as the cytoplasm, the nucleus, the plasmamembrane and the tonoplast, as well they have been found associated with peroxisomes, mitochondria, the ER and actin filaments (Dammann et al., 2003; Mehlmer et al., 2010). The N-termini of CDPK's are highly variable of which many have predicted myristoylation and palmitoylation motives (27 out of 34 (Wurzinger et al., 2011)). Accordingly, CDPK's are mostly found associated with membranes and reversible fatty acid modification could be a means for influencing the localization and function of these kinases (Stael et al., 2011). The first physiological relevant function of a CDPK was demonstrated for CDPK2 of *Nicotiana benthamiana*. Gene silencing of NtCDPK2 resulted in a delayed hypersensitive response (wilting) of the mutant plants to the peptide elicitor Avr9 from the fungal tomato pathogen *Cladosporium fulvum* (Romeis et al., 2001). The guard cell has been extensively studied because of its crucial role for plant respiration and drought resistance through stomatal movement and is a case study for the importance of calcium signaling in plant cells (Kim et al., 2010). Abscicic acid (ABA), hydrogen peroxide, cold, delivery of external  $\text{Ca}^{2+}$  and elevated  $\text{CO}_2$  levels induce cytosolic  $\text{Ca}^{2+}$  oscillations in guard cells. AtCPK3 and AtCPK6 function in a cooperative manner in the regulation of stomatal closure in response to ABA and external  $\text{Ca}^{2+}$  fluxes through the modulation of the slow-type anion channel and calcium influx channels (Mori et al., 2006). Also AtCPK4 and AtCPK11 influence stomatal closure, but show a general defect in ABA-responsiveness that might be

explained by the observed in-vitro phosphorylation of the abscisic acid responsive element-binding factor1 (ABF1) and ABF4 proteins (Zhu et al., 2007). In *Solanum tuberosum*, two CDPK's (StCDPK4 and StCDPK5) are possibly involved in pathogen response by phosphorylating the plasma membrane localized NADPH oxidases RBOH (for Respiratory Burst Oxidase Homolog) to activate the production of reactive oxygen species (ROS) (Kobayashi et al., 2007). Recently, their Arabidopsis homologs, AtCPK4 and AtCPK5, have been implicated in pathogen response (Boudsocq et al., 2010). Through a functional genomics screen of all CPK's, combined with genome-wide gene expression profiling, the authors found these homologs and other CPK's (AtCPK6 and AtCPK11) to be deficient in the correct response to flagellin22 (flg22, a common bacterial elicitor). While single knock-out mutants did not produce pathogen related phenotypes, double, triple and quadruple mutants showed increasing defects in resistance to pathogens, as witnessed by the reduced oxidative burst in response to flg22 and increased growth of the bacterium *Pseudomonas syringae pv. tomato (Pst)* DC3000 after inoculation of leaves. AtCPK3 was recently found to be important for salt stress acclimation in a process that is independent from MAP kinase cascades (Mehlmer et al., 2010). The MAP kinase (MAPK) family is another large group of kinases that have established functions in both biotic and abiotic stress and interestingly, CDPK's and MAPK's seem to have common and separated signaling pathways (Wurzinger et al., 2011). To conclude, a wealth of literature is available on CDPK's and their regulation of the physiology of plants in development or in response to stresses. Many more CDPK targets have been identified by various authors, but they await clear confirmation in order to elucidate the mechanistic basics of how CDPK's can modulate a wide variety of physiological responses.





**Review - The magical life of calcium as a secondary messenger: A journey  
to the organelles**

Simon Stael<sup>1</sup>, Bernhard Wurzinger<sup>1</sup>, Norbert Mehlmer<sup>2</sup>, Ute C. Vothknecht<sup>2,3</sup>, and  
Markus Teige<sup>1\*</sup>

<sup>1</sup>Department of Biochemistry and Cell Biology, MFPL, University of Vienna,  
Dr. Bohrgasse 9, A-1030 Vienna. Austria.

<sup>2</sup>Department of Biology I, Botany, LMU Munich, Großhaderner Str. 2,  
D-82152 Planegg-Martinsried. Germany.

<sup>3</sup>Center for Integrated Protein Science (Munich) at the Department of Biology of the  
LMU Munich, D-81377 Munich, Germany.

Email addresses: [simon.stael@univie.ac.at](mailto:simon.stael@univie.ac.at), [bernhard.wurzinger@univie.ac.at](mailto:bernhard.wurzinger@univie.ac.at),  
[mehlmer@bio.lmu.de](mailto:mehlmer@bio.lmu.de), [vothknecht@bio.lmu.de](mailto:vothknecht@bio.lmu.de)

\* To whom correspondence should be addressed: E-mail: [markus.teige@univie.ac.at](mailto:markus.teige@univie.ac.at)  
phone: +43-1-4277-529811, fax: +43-1-4277-9528

Submission date: 25.08.2011

1 table and 1 figure

Running title: Plant organellar calcium signaling

**Abstract**

This review provides a comprehensive overview of the established and emerging roles that organelles play in calcium signaling. The function of calcium as a secondary messenger in signal transduction networks is well documented in all eukaryotic organisms, but most reviews until now have focused on calcium signaling in the cytoplasm. A short overview will be provided of the main calcium stores in plants – the vacuole, the endoplasmic reticulum and the apoplast – followed by a detailed survey of the calcium handling properties of chloroplasts, mitochondria, peroxisomes and nuclei. Recently, it became clear that these organelles not only undergo calcium regulations themselves, but are able to influence the Ca<sup>2+</sup> signaling pathways of the cytoplasm and the entire cell. When appropriate, parallels with the animal field are drawn and a short overview on bacterial calcium signaling is added to provide some ideas to the question where this typically eukaryotic signaling mechanism could have originated from during evolution.

**Key-words:** bacteria, CAS, calcium flux, chloroplast, ER, mitochondria, peroxisome, calcium signaling, EF-hand protein

**Abbreviations:** ABA, abscisic acid; CAS, calcium sensing; CDPK, calcium-dependent protein kinase; PM, plasma membrane

## Introduction

Plants react to changing environmental conditions through immediate signal transduction pathways. One integral part of many signal transduction pathways, both in plant- and animal cells, is the usage of free calcium ions ( $\text{Ca}^{2+}$ ) as secondary messengers. As  $\text{Ca}^{2+}$  forms insoluble precipitates with phosphate, which would interfere with the phosphate based metabolism, cells actively translocated  $\text{Ca}^{2+}$  from their cytoplasm to organelles and extracellular compartments throughout evolution. The resulting  $\sim 10,000$  fold difference between cytoplasmic ( $\sim 100$  nM) and non-cytoplasmic (mM)  $\text{Ca}^{2+}$  concentrations enables the generation of calcium signals by fast changes of cytoplasmic  $\text{Ca}^{2+}$  levels via membrane localized  $\text{Ca}^{2+}$  permeable channels. A wide variety of signals, including abiotic, biotic and developmental stimuli, were observed to evoke specific spatiotemporal calcium transients which are further transduced by  $\text{Ca}^{2+}$  sensor proteins into a transcriptional and metabolic response. So far in plants, most of the research on  $\text{Ca}^{2+}$  signaling has been focused on the transport mechanisms for  $\text{Ca}^{2+}$  into- and out of the cytoplasm as well as the components involved in decoding of cytoplasmic  $\text{Ca}^{2+}$  signals and this has extensively been reviewed (Clapham, 2007; McAinsh and Pittman, 2009; DeFalco et al., 2010; Dodd et al., 2010; Kudla et al., 2010). However, recent advances demonstrate how different organelles are involved in the process of  $\text{Ca}^{2+}$  signaling. This review will therefore provide a summary on the role of  $\text{Ca}^{2+}$  storage compartments, the vacuole, the endoplasmic reticulum (ER) and the apoplast, for  $\text{Ca}^{2+}$  signaling in the first section. Furthermore evidence for  $\text{Ca}^{2+}$  signaling processes in plastids, mitochondria and peroxisomes has accumulated recently and will be summarized in the second section. The third section of this review provides an overview of bacterial  $\text{Ca}^{2+}$  signaling and its implications for plant cell and especially endosymbiont  $\text{Ca}^{2+}$  signaling processes.

### 1.3. Main plant calcium stores

#### The vacuole

The main storage compartment of calcium in plants is the central vacuole. This is also the case in other species which contain large vacuoles, such as fungi. Consequently, these species become hypersensitive to  $\text{Ca}^{2+}$ , if its uptake into the vacuole is hampered (Cunningham and Fink, 1994; Cheng et al., 2005). The concentration of calcium in the vacuole varies among different plant organs and cell types. For example, in dicotyledonous plants (including *Arabidopsis thaliana*), calcium is preferentially stored in

the leaf mesophyll, rather than in the epidermal vacuole (Storey and Leigh, 2004; Conn et al., 2011). Estimates of the free vacuolar  $\text{Ca}^{2+}$  concentration range from 0,2 mM to 1-5 mM and can reach a maximum of 80 mM of total  $\text{Ca}^{2+}$  (free and bound  $\text{Ca}^{2+}$  combined, (Conn and Gilliam, 2010)). Most of the  $\text{Ca}^{2+}$  is tightly bound to chelating agents, such as malate, citrate and isocitrate and therefore, is not readily available for calcium signaling. Calcium ions might also be transiently bound to proteins, in a comparable fashion as to the classical  $\text{Ca}^{2+}$  binding storage proteins of the ER (e.g. calreticulin). An early study on the  $\text{Ca}^{2+}$ -binding properties of a vacuolar enriched protein fraction led to the conclusion that vacuoles contain a high affinity  $\text{Ca}^{2+}$  binding fraction and that the major protein  $\text{Ca}^{2+}$  binding capacity of plant extracts seemed to reside in the vacuole and ER (Randall, 1992). This indicated the presence of calcium storage proteins in these organelles and accordingly, a Radish vacuolar  $\text{Ca}^{2+}$ -binding protein (RVCaB) was found to improve calcium storage capacity of the vacuole (Yuasa and Maeshima, 2001). However, similar proteins in Arabidopsis were only found associated with the plasma membrane and probably do not play a role in calcium storage (Kato et al., 2010) and so far no other examples have been reported in any other plant species. Interestingly, a calmodulin-like protein of Arabidopsis (AtCaM15) was found to localize to the vacuolar lumen and modulate the activity of AtNHX1- the major vacuolar  $\text{Na}^+/\text{H}^+$  antiporter (Yamaguchi et al., 2005). Further evidences are emerging that calcium is not only stored in the vacuole, but plays there an important signaling role as well, mainly by influencing the activity of tonoplast (vacuolar membrane) localized ion transporters (Peiter, 2011). Various  $\text{Ca}^{2+}$  channels and transporters were reported to localize to the tonoplast. Voltage-dependent  $\text{Ca}^{2+}$  channels and ligand-gated  $\text{Ca}^{2+}$  channels release  $\text{Ca}^{2+}$  into the cytoplasm and have been characterized mainly during the 1990's through electrophysiological studies (Sanders et al., 2002). Although they are well characterized for almost twenty years now, no molecular identity was found for these channels so far, except for TPC1. AtTPC1, which has no other homologues in Arabidopsis, was confirmed to be the slow vacuolar (SV, named after its voltage-gated characteristics) channel of the tonoplast (Peiter et al., 2005). The protein contains two EF-hands and provides an example for how calcium induces  $\text{Ca}^{2+}$  release (CICR) into the cytoplasm (Pottosin et al, 2009). In the case of ligand-gated channels,  $\text{Ca}^{2+}$  fluxes were measured upon the addition of ligands such as inositol 1,4,5-triphosphate (InsP3), cyclic ADP-ribose (cADPR) and nicotinic acid adenine dinucleotide phosphate (NAADP). These have been measured only from

tonoplast and ER membrane preparations and interestingly NAADP stimulates calcium release only from the ER (Allen et al., 1995; Navazio et al., 2000).

### **The endoplasmic reticulum**

The calcium storage role of the endoplasmic reticulum (ER) is probably best known from human and animals, where the molecular mechanisms of calcium release and uptake of the sarcoplasmic endoreticulum (SR, ER of the muscle cell) during muscle contractions are described in detail (Rossi and Dirksen, 2006). In animals, the total  $\text{Ca}^{2+}$  concentration in the ER is estimated at 2 mM, while the free  $\text{Ca}^{2+}$  concentration varies between 50 to 500  $\mu\text{M}$  (Coe and Michalak, 2009). On the contrary, in plants few data is available that describes the calcium storage properties of the ER. Research is hampered mainly due to the absence of direct homologues in higher plant genomes of the well-characterized mammal  $\text{InsP}_3$ -receptor and ryanodine receptor that are responsible for ER  $\text{Ca}^{2+}$  efflux. Interestingly, the genomes of several algae species, including *Volvox* and *Chlamydomonas*, do contain these receptor proteins, suggesting they were present in ancestral eukaryotes and were lost by land plants after their divergence from the chlorophyte algae (Wheeler and Brownlee, 2008). Nonetheless, several findings of the animal and human field have been translated into plants.  $\text{InsP}_3$ , cADPR and NAADP elicited calcium fluxes have been measured from plant ER-preparations, hinting that the signaling mechanisms for  $\text{Ca}^{2+}$  release stayed conserved (although the receptors did not). Furthermore, three types of  $\text{Ca}^{2+}$  binding proteins are conserved through plant evolution: calreticulin, calnexin and Binding Protein (BiP). Calreticulin is a luminal protein of the ER and was found to be important for  $\text{Ca}^{2+}$  homeostasis, but also as a chaperone for protein folding (Christensen et al., 2010). Over-expression of maize calreticulin in tobacco cells leads to increased  $\text{Ca}^{2+}$  retention in the ER. In *Arabidopsis*, the down-regulation of calreticulin expression leads to enhanced sensitivity of the plants to low  $\text{Ca}^{2+}$ , and vice versa (Persson et al., 2001). calnexin and BiP, in plants, are better described for their chaperone function than for calcium binding (Gupta and Tuteja, 2011). In animals and humans, an unrelated protein, calsequestrin is the major  $\text{Ca}^{2+}$  storage protein of the ER. The lack of calsequestrin in higher plants together with the findings mentioned before, suggest that calreticulin is the major  $\text{Ca}^{2+}$  storage protein in plant ER. In conclusion, little is known about plant ER  $\text{Ca}^{2+}$  storage and release compared to the animal field, which is reflected by the fact that the molecular identity of the plant ER  $\text{Ca}^{2+}$  release channel(s) is still unknown to date.

## The apoplast

The apoplast is another major plant  $\text{Ca}^{2+}$  store. Though at the same time it acts as the ‘highway’ through which  $\text{Ca}^{2+}$  is trafficking to the cells by means of the water transpiration stream and it should not be regarded as a terminal store, like the vacuole. Furthermore the  $\text{Ca}^{2+}$  concentration in the apoplast needs to be tightly regulated because a high apoplastic  $\text{Ca}^{2+}$  concentration impairs stomatal movement (Kim et al., 2010) and plant cell wall rigidity depends on  $\text{Ca}^{2+}$  for pectate cross linking (Hepler, 2005). That these two reasons can drastically influence plant growth, was recently demonstrated by the analysis of a mutant plant that is deficient in the main vacuolar  $\text{Ca}^{2+}$  transporters AtCAX1 and AtCAX3 (Conn et al., 2011). The authors reasoned that deficient  $\text{Ca}^{2+}$  sequestration in the vacuole led to an increase of free  $\text{Ca}^{2+}$  in the apoplast, with the above-mentioned defects as a consequence. Most of the  $\text{Ca}^{2+}$  in the apoplast is bound to negatively charged carboxyl groups of pectin and oxalates and reports on the concentration of  $\text{Ca}^{2+}$  vary from 10  $\mu\text{M}$  to 10 mM (Hepler, 2005). Conn and colleagues (2011) estimated the free  $\text{Ca}^{2+}$  concentration in Arabidopsis leaf apoplast to be approximately 0,33 mM, while the bound  $\text{Ca}^{2+}$  concentration was 0,5 mM. In addition to the voltage gated  $\text{Ca}^{2+}$  channels, other ligand-gated ion channels, that can mediate fluxes of  $\text{Ca}^{2+}$  into the cytoplasm, include the cyclic nucleotide-gated channels (CNGCs) and glutamate receptor-like channels (GLRs). Both gene families in Arabidopsis contain twenty members and they can carry a diversity of ions, but some members have been implicated in mediating cytosolic increases of  $\text{Ca}^{2+}$  (Hua et al., 2003; Ali et al., 2006; Qi et al., 2006; Ali et al., 2007; Kaplan et al., 2007). All CNGCs and GLRs studied so far are targeted to the plasma membrane.

### 1.4. Organellar calcium signaling

The focus of this chapter lies on the emerging calcium signaling processes of the chloroplast, mitochondria, peroxisomes and briefly the nucleus. In the context of cytoplasmic  $\text{Ca}^{2+}$  signaling these organelles seem to partly act as  $\text{Ca}^{2+}$  stores. However, the discovery of  $\text{Ca}^{2+}$  dependent regulatory processes and specific  $\text{Ca}^{2+}$  transients within these organelles, add up to a more complete picture of  $\text{Ca}^{2+}$  signaling within the plant cell, which is summarized in figure 7.

### **Chloroplast calcium signaling**

Early investigations showed that  $\text{Ca}^{2+}$  modulates the metabolic reactions of the chloroplast. Elevated  $\text{Ca}^{2+}$  concentration effectively inhibits the Calvin cycle enzymes fructose-1,6-bisphosphatase and sedoheptulose bisphosphatase, leading to a halt of photosynthetic  $\text{CO}_2$  fixation (Racker and Schroeder, 1958; Portis and Heldt, 1976; Charles and Halliwell, 1980). The total concentration of  $\text{Ca}^{2+}$  in the chloroplast has been estimated at 15 mM or higher (Nobel, 1969; Portis and Heldt, 1976) and increases upon illumination, by the uptake of  $\text{Ca}^{2+}$  from the external medium during the daylight (Kreimer, 1985; Roh et al., 1998). Because a high amount of free chloroplastic  $\text{Ca}^{2+}$  would inhibit photosynthesis and precipitate with abundant chloroplastic phosphate, most of the  $\text{Ca}^{2+}$  is bound to thylakoid membranes or to stromal proteins (Gross and Hess, 1974; Davis and Gross, 1975; Kreimer, 1987). Accordingly, the resting free  $\text{Ca}^{2+}$  concentration in the stroma during the day was estimated to be ~150 nM (Johnson et al., 1995). Calcium also affects the photosynthetic reactions from the luminal side of the thylakoid. It is an essential cofactor of the oxygen evolving complex and binds the 8 kDa subunit of the ATP synthase, thereby regulating the photosynthetic proton-flow and ATP production (Zakharov et al., 1993; Ifuku et al., 2010). So, the chloroplast has an essential requirement for  $\text{Ca}^{2+}$ , but needs tight control over its distribution.

Calcium fluxes occur in the chloroplast and follow a daily rhythm (Johnson et al., 1995; Sai and Johnson, 2002). Each day, five minutes after the transition from light to dark, a  $\text{Ca}^{2+}$  flux is generated in the stroma that reaches a maximum after approximately 25 minutes. This  $\text{Ca}^{2+}$  flux is proposed to be responsible for inhibiting photosynthetic  $\text{CO}_2$  fixation during the night and could help to entrain the circadian clock. Based on the characteristics of the  $\text{Ca}^{2+}$  flux, the authors proposed that in the light, the chloroplast takes up  $\text{Ca}^{2+}$  from the cytosol and stores it in the thylakoid membrane or a so far unknown store. Upon transition from light to dark the  $\text{Ca}^{2+}$  is subsequently released from the store back into the cytosol. Light, via the thylakoid proton gradient, seems to drive  $\text{Ca}^{2+}$  uptake into the thylakoid lumen as well, through the activity of a  $\text{Ca}^{2+}/\text{H}^+$  exchanger (Ettinger et al., 1999). However, the inhibition of the photosynthetic electron transport chain, and correspondingly the proton gradient, resulted in a slight increase of stromal  $\text{Ca}^{2+}$  during the light period, but did not inhibit the charging of the  $\text{Ca}^{2+}$  store that was discharged by lights off (Sai and Johnson, 2002). Hence, the authors proposed the existence of an unknown alternative stromal  $\text{Ca}^{2+}$  store.

Active  $\text{Ca}^{2+}$  transport has also been measured across the chloroplast inner envelope and could account for the observed  $\text{Ca}^{2+}$  uptake of the chloroplast during the light period. A negative inside membrane potential driven  $\text{Ca}^{2+}$  transport was measured from inner envelope membrane vesicles of *Pisum sativum*, confirming previous experiments from intact chloroplasts (Kreimer, 1985; Roh et al., 1998). However, the molecular identity of this channel has not been described. On the other hand, two potential  $\text{Ca}^{2+}$  ATPases were identified in the chloroplast envelope. The first is AtACA1 from the Auto-inhibited  $\text{Ca}^{2+}$ -ATPases family and is most likely found only in root plastids (Huang et al., 1993). Strangely though, both the labs of Huang and Roh could not find  $\text{Ca}^{2+}$ -ATPase activity at the envelope. Furthermore, since its description in 1993, ACA1 has been found in cauliflower tonoplast and Arabidopsis ER, prompting further study on this  $\text{Ca}^{2+}$ -ATPase (Malmstrom et al., 1997; Dunkley et al., 2006). The second  $\text{Ca}^{2+}$ -ATPase might be AtHMA1: a member of the heavy metal P-type ATPases that was shown to have high-affinity  $\text{Ca}^{2+}$  transport activity and is specifically inhibited by the sarco/endoplasmic reticulum  $\text{Ca}^{2+}$ -ATPase (SERCA) inhibitor, thapsigargin (Moreno et al., 2008). There is dispute about its exact role, because originally it was described to transport  $\text{Cu}^+$  into the chloroplast (Seigneurin-Berny et al., 2006) but later on it was shown to function in the tolerance to excess Zn, by extruding it from the chloroplast (Kim et al., 2009). ALBINO3 (ALB3), the integral membrane protein and translocase that is involved in chloroplast biogenesis (Sundberg et al., 1997; Lewis et al., 2010), might function as a  $\text{Ca}^{2+}$  transporter at the thylakoid. The Pea homolog of ALB3, Pisum-post-floral-specific gene 1 (PPF1), produces significant inward calcium ion currents in Novikoff human hepatoma cells and the  $\text{Ca}^{2+}$  homeostasis of plants with altered expression of PPF1/ALB3 is disrupted in Arabidopsis guard cells leading to severe growth phenotypes (Wang et al., 2003; Li et al., 2004). In conclusion, although several transporters are hypothesized to aid chloroplast  $\text{Ca}^{2+}$  influx, a more comprehensive analysis is needed to directly link these proteins to chloroplast  $\text{Ca}^{2+}$  homeostasis. Furthermore, how  $\text{Ca}^{2+}$  is exported from the thylakoid lumen to the stroma and subsequently to the cytosol remains largely open. To this end, Roh and colleagues could show that  $\text{Ca}^{2+}$  can traverse the inner envelope through a reversal of the membrane potential driven  $\text{Ca}^{2+}$  transporter (Roh et al., 1998). From more recent work, it became apparent that calmodulin (CaM) has regulatory roles in chloroplasts. The best example is the import of nuclear encoded chloroplast proteins via the TOC (translocon at the outer envelope of chloroplasts) and TIC (translocon at the inner envelope of chloroplasts) complexes. Calcium/CaM was found to promote



chloroplast import and this is most likely due to the direct interaction of calmodulin to the stromal side of Tic32 (TIC protein of 32kDa)(Chigri et al., 2005; Chigri et al., 2006). Furthermore, in a different study, it was found by electrophysiological measurements, that the gating properties of the main pore forming subunit of the TIC complex, Tic110, were affected in a specific manner by  $\text{Ca}^{2+}$  (Balsera et al., 2009). Taken together,  $\text{Ca}^{2+}$  seems to influence chloroplast protein import at these closely linked sites. Another function of the chloroplast that was found to be modulated by  $\text{Ca}^{2+}$  is the chloroplast inner vesicle transport system (Morre et al., 1991). This system is proposed to have a role in thylakoid membrane biogenesis and was found to be disrupted by CaM inhibitors as well as calcium depletion (Westphal et al., 2001, 2003). Chloroplast division might also be regulated in a  $\text{Ca}^{2+}$  dependent manner by AtMinD1 (Arabidopsis Minicell D1), which is part of the chloroplast division machinery, because its ATPase activity depends on  $\text{Ca}^{2+}$  rather than  $\text{Mg}^{2+}$  as it is the case in bacteria (Aldridge and Moller, 2005). Furthermore, two chloroplastic mechanosensitive ion channels MSL2 and 3 (homologs of the bacterial mechanosensitive (MS) channel MscS: MscS-Like 2 and 3) were found to influence chloroplast division and act in concert with the Min proteins (Haswell and Meyerowitz, 2006; Wilson et al., 2011). It would be interesting to see if MSL2-3 can directly influence the  $\text{Ca}^{2+}$  dependent activity of AtMinD1, either by mediating  $\text{Ca}^{2+}$  fluxes or through a depolarization of the chloroplast envelope. Chloroplast movement in response to fluctuating light conditions is another  $\text{Ca}^{2+}$  dependent process shown to occur in different species, such as *Lemna trisulca* and Tobacco (Tlalka and Fricker, 1999; Anielska-Mazur et al., 2009). Chloroplasts move along the actin cytoskeleton in plant cells (Kong and Wada, 2011) and accordingly the use of  $\text{Ca}^{2+}$  chelators and calmodulin inhibitors revealed the stabilizing effect of  $\text{Ca}^{2+}$  on actin polymerization and its importance for chloroplast movement. However, chloroplast movement was influenced even in the presence of an intact actin network, thereby evoking a signaling function of  $\text{Ca}^{2+}$  in light-induced chloroplast movements. NAD kinase (NADK) is an intriguing case for chloroplastic calcium dependent regulations. Through the use of CaM inhibitors, NADK was the first plant enzyme found to be activated by CaM and the majority of its activity was found to localize to the chloroplast (Jarrett et al., 1982). Jarrett and colleagues purified a CaM-containing fraction from Pea chloroplasts to near homogeneity, but did not identify the protein responsible for NADK activation. The initial increase of  $\text{Ca}^{2+}$  in the chloroplast upon illumination was proposed to activate NAD kinase via the interaction with CaM. NADK catalyzes the light-dependent conversion of NAD to NADP, which is the final

electron acceptor of the photosynthetic electron transport chain. Thereby it provides important reduction potential for the plant, which becomes obvious in the reduced growth and hypersensitivity to oxidative stress of chloroplastic NADK knock-out plants (Chai et al., 2005; Takahashi et al., 2006). From more recent work, it became apparent that one of the three *Arabidopsis* NADK isoforms, AtNADK2, is responsible for the calmodulin-dependent NAD kinase activity in chloroplasts (Turner et al., 2004; Waller et al., 2010). A region of 45 amino acids within the long N-terminal extension of AtNADK2 was found to be sufficient and necessary to bind to CaM. Other examples of chloroplast proteins that were found to interact with calmodulin are AtPsaN (a sub-unit of photosystem I), the chaperonin AtCpn10, and AtAFG1L1, an AAA<sup>+</sup>-ATPase (Yang and Poovaiah, 2000; Reddy et al., 2002; Bussemer et al., 2009). However, the functional relevance of these interactions need further study. To conclude, it became apparent that various stromal proteins are able to bind to CaM, leading to a change of their activity. Nonetheless, the chloroplastic CaM or CaM-like protein is still unknown and its identification is expected to greatly advance the understanding of the physiological relevance of these calcium/CaM dependent regulations.

So far there are two reports of EF-hand containing proteins in the chloroplast. The best documented is the Ca<sup>2+</sup>-activated RelA/SpoT homolog protein (CRSH), that is novel both for being a chloroplastic EF-hand protein and for its alleged function. CRSH contains two EF-hands and a RelA/SpoT enzymatic domain, which is responsible for the calcium-dependent production of a small signaling nucleotide, guanosine 5'-diphosphate 3'-diphosphate (ppGpp) (Masuda et al., 2008). ppGpp signaling was discovered in bacteria as a response to stress conditions, such as nutrient deprivation, in a process called 'the bacterial stringent response', and homologous proteins have since been found in various plant species (Tozawa et al., 2007; Masuda et al., 2008). The bacterial RelA and SpoT proteins do not contain EF-hands, which seems to be an exclusive trait of CRSH in higher plants. ppGpp was found mainly in the chloroplast and the levels changed after different stress- and hormonal treatments and upon the transition from light to dark (Takahashi et al., 2004). Similar to its function in transcription and translation in bacteria, ppGpp was found to modulate exclusively the function of the bacterial type plastid-encoded plastid RNA polymerase (PEP), but not the nuclear-encoded plastid RNA polymerase (NEP) (Sato et al., 2009). It seems that the bacterial stringent response has been conserved in chloroplasts from its cyanobacterial origin, but more experimental work is needed to elucidate its physiological function and the interplay with Ca<sup>2+</sup> signaling, in plants. The

second chloroplastic EF-hand protein is a substrate carrier (AtSUC) that contains a single EF-hand and belongs to the mitochondrial carrier protein family. It was recently found in a targeted proteomics screen and was confirmed to reside in the chloroplast envelope by YFP-fusion analysis, however, its function is unknown to date (Bayer et al., 2011).

Reports from a chloroplast localized protein involved in ‘calcium sensing’ (AtCAS) evoke the idea that chloroplasts may modulate cytoplasmic  $\text{Ca}^{2+}$  signaling. AtCAS was first reported as a plasma membrane localized  $\text{Ca}^{2+}$ -sensing receptor, important for inducing stomatal closure provoked by elevation of the extracellular  $\text{Ca}^{2+}$  concentration ( $[\text{Ca}^{2+}]_{\text{ext}}$ ; a hallmark of stomatal movement) (Han et al., 2003). The protein was found to bind  $\text{Ca}^{2+}$  with a low affinity and high capacity and down-regulation of its expression impaired the production of  $[\text{Ca}^{2+}]_{\text{ext}}$  induced cytoplasmic  $\text{Ca}^{2+}$  oscillations. However, subsequent reports identified AtCAS to be targeted to the thylakoid membrane (Friso et al., 2004; Nomura et al., 2008; Vainonen et al., 2008; Weinl et al., 2008). Nevertheless, knock-out of AtCAS was still confirmed, by different labs, to impair  $[\text{Ca}^{2+}]_{\text{ext}}$  induced stomatal closure, whereas over-expression of CAS promoted stomatal closure in the absence of externally applied  $\text{Ca}^{2+}$  (Nomura et al., 2008; Weinl et al., 2008). Disruption of AtCAS in Arabidopsis retarded plant growth and AtCAS was found to be increasingly phosphorylated by the state transition kinase AtSTN8 under increasing light intensities (Vainonen et al., 2008). Stomata of *cas* Arabidopsis plants displayed normal closure after the application of externally imposed cytoplasmic  $\text{Ca}^{2+}$  oscillations, indicating that the guard cells are still responsive to  $\text{Ca}^{2+}$  signals but most likely have a defect in the generation of  $\text{Ca}^{2+}$  fluxes (Weinl et al., 2008). This suggests that the chloroplast can sense and influence cytoplasmic  $\text{Ca}^{2+}$  levels, but, the molecular mechanism behind these processes still await discovery.

### **Mitochondrial calcium signaling**

In contrast with the animal and human field, where mitochondrial calcium uptake and release is well studied and known to play important cellular roles, relatively few data is available on calcium signaling in plant mitochondria. It is now well established that mitochondria in animals function as transient calcium stores that can produce  $\text{Ca}^{2+}$  microdomains through a close interaction with the ER, thereby modulating  $\text{Ca}^{2+}$  signatures (Clapham, 2007; Laude and Simpson, 2009). On a different account, the elevation of  $\text{Ca}^{2+}$  inside of the mitochondria positively affects ATP production by up-regulating the major limiting enzymes of the citric acid cycle (similar to the up-regulation

of the Calvin cycle in chloroplasts) (McCormack et al., 1990). The over-accumulation of  $\text{Ca}^{2+}$  in the mitochondria is linked to the induction of apoptosis by opening of the mitochondrial permeability transition pore (mPTP) and the subsequent release of mitochondrial apoptosis markers, such as cytochrome c (Giacomello et al., 2007; Szabadkai and Duchen, 2008). This process apparently occurs in plants as well (Arpagaus et al., 2002; Tiwari et al., 2002; Virolainen et al., 2002).

In plants, the resting free  $\text{Ca}^{2+}$  concentration in the mitochondria was estimated to be ~200 nM (Logan and Knight, 2003), with most of the mitochondrial  $\text{Ca}^{2+}$  probably being bound in the form of a ready-releasable amorphous phosphate precipitate (Chalmers and Nicholls, 2003; Starkov, 2010).  $\text{Ca}^{2+}$  fluxes in *Arabidopsis* mitochondria have been observed upon various stimulations (Logan and Knight, 2003). Whereas most mitochondrial  $\text{Ca}^{2+}$  fluxes were similar,  $\text{H}_2\text{O}_2$  and touch stimulation produced a signal that was different to the concurrently occurring cytosolic  $\text{Ca}^{2+}$  fluxes. This indicates that mitochondria are not just passive calcium sinks, but are able to regulate their own  $\text{Ca}^{2+}$  fluxes.

Surprisingly little information about  $\text{Ca}^{2+}$  transporters of plant mitochondria exists, compared to the intensive research on this topic in the animal and human field (Collins and Meyer, 2010; Starkov, 2010). There, high concentrations or low concentrations of  $\text{Ca}^{2+}$  are taken up differently by the mitochondria and various  $\text{Ca}^{2+}$  channels have recently been described (Hajnoczky and Csordas, 2010; Hoppe, 2010). Highly elevated cytosolic  $\text{Ca}^{2+}$  levels, such as in microdomains, are transported into the mitochondria via a directional  $\text{Ca}^{2+}$  influx transporter, called the mitochondrial calcium uniporter (MCU). It has been extensively studied and its properties well delineated: (1) electrogenic transport that is driven by a negative inside membrane potential, (2) sensitivity to ruthenium red, (3) low affinity for  $\text{Ca}^{2+}$ , and (4) regulation by  $\text{Ca}^{2+}$ . After almost 50 years, the molecular nature of the uniporter has been discovered in a series of recent studies (Perocchi et al., 2010; Baughman et al., 2011; De Stefani et al., 2011). In an integrative genomics and proteomics search, Perocchi and colleagues found an EF-hand containing protein, which is targeted to the mitochondrial inner membrane, to induce a  $\text{Ca}^{2+}$ -dependent calcium influx into the mitochondria. They called it MICU1, for mitochondrial  $\text{Ca}^{2+}$  uptake 1, and reasoned that it most likely is not the uniporter itself, but the sensor for  $\text{Ca}^{2+}$  that regulates the MCU. In two independent follow-up experiments, based on the phylogenetic profile, protein distribution and characteristics of MICU1, a 40 kDa protein was identified as the actual  $\text{Ca}^{2+}$  pore and therefore it was called MCU. The MCU protein contains two

transmembrane helices, connected by a conserved loop containing the amino acids DIME, and most likely oligomerizes in the mitochondrial inner membrane. Earlier research pointed out a role for uncoupling protein 2 and 3 (UCP2 and 3) as the potential MCU, however these findings are under debate (Trenker et al., 2007; Brookes et al., 2008). Nonetheless UCP2 and 3 show robust  $\text{Ca}^{2+}$  transporter activities, so still, they might be involved in mitochondrial  $\text{Ca}^{2+}$  homeostasis. On the other hand, mitochondria take up  $\text{Ca}^{2+}$  at low concentration levels via the high-affinity  $\text{Ca}^{2+}/\text{H}^+$  antiporter, LETM1 (Jiang et al., 2009). Calcium efflux from mitochondria can occur through a reversal of LETM1 or through the  $\text{Na}^+/\text{Ca}^{2+}$  exchanger NCLX, that was recently found to be targeted to the mitochondria (Palty et al., 2010). To conclude, the presence of homologs in the Arabidopsis genome of all the before-mentioned proteins raises the interesting possibility of translating these findings directly into plants.

Calcium/CaM was reported to promote mitochondrial protein import in a similar manner as it occurs in chloroplasts (Kuhn et al., 2009). Furthermore, it was found to be a plant-specific trait, because yeast mitochondria were not susceptible to the CaM inhibitors and calcium ionophores used in the study. Pyruvate dehydrogenase activity was also found to decline with the use of CaM inhibitors (Miernyk et al., 1987). The pyruvate dehydrogenase complex (PDC) assists in the conversion of pyruvate into acetyl-CoA and therefore, an important connection between glycolysis and the citric acid cycle might be regulated by  $\text{Ca}^{2+}$  in plants. The finding of a CaM-binding  $\text{AAA}^+$ -ATPase, AtAFG1L1, with dual localization to chloroplasts and mitochondria further suggest the presence of CaM in the plant mitochondria (Bussemer et al., 2009). So far, the only report on CaM in the mitochondria came from Biro and colleagues, who found an Oat calmodulin in the intermembrane space that was lost upon removal of the outer mitochondrial membrane (Biro et al., 1984).

The glutamate dehydrogenase  $\beta$  sub-unit (GD- $\beta$ ) localizes to the mitochondrial matrix, contains a single EF-hand, and its activity was reported to be stimulated by the addition of  $\text{Ca}^{2+}$  (Turano et al., 1997). Two isoforms of the type II NAD(P) H:quinone oxidoreductases of *A. thaliana*, AtNDB1 and AtNDB2 were found to be externally attached to the inner membrane of mitochondria and contain functional EF-hands (Geisler et al., 2007). Interestingly, the closest Arabidopsis homolog of LETM1, the mitochondrial high-affinity  $\text{Ca}^{2+}/\text{H}^+$  antiporter, contains two EF-hands and was recently found to localize to the mitochondria by GFP-fusion analysis (Van Aken et al., 2009). In this study the authors attempted to delineate the mitochondrial stress response by searching for

mitochondrial proteins that show the greatest expression variation upon 16 selected stress treatments. The fact that the AtLETM1-like protein was included in this set further prompts the study of this protein for its  $\text{Ca}^{2+}/\text{H}^{+}$  activity and the involvement of mitochondrial calcium signaling upon stress conditions in Arabidopsis.

Ample evidence for the influence of mitochondrial  $\text{Ca}^{2+}$  on cytoplasmic  $\text{Ca}^{2+}$  fluxes exist in animals (Laude and Simpson, 2009) and these observations probably hold true for plants, given that plant mitochondria exhibit a similar handling of  $\text{Ca}^{2+}$  (Silva et al., 1992). Maize mitochondria have been shown to release  $\text{Ca}^{2+}$  upon hypoxia and their internal  $\text{Ca}^{2+}$  concentration changes rapidly and in a reversible manner when returning back to normoxia (Subbaiah et al., 1994, 1998). Other evidence for mitochondrial  $\text{Ca}^{2+}$  efflux comes from the measurement of  $\text{Ca}^{2+}$  changes in the root hair in response to the disruption of actin polymerization by latrunculin B (Lat-B) and jasplakinolide (Jas) (Wang et al., 2010). Root hair cells produce a tip-focused  $\text{Ca}^{2+}$  gradient with  $\text{Ca}^{2+}$  oscillation lagging behind growth oscillation, in a similar fashion to growing pollen tubes (Cardenas et al., 2008; Monshausen et al., 2008). Modulation of actin polymerization caused a release of  $\text{Ca}^{2+}$  from the mitochondria, probably via the mPTP, and a concurrent increase in cytosolic  $\text{Ca}^{2+}$  concentrations. Furthermore, Wang and colleagues showed that the concentration of free  $\text{Ca}^{2+}$  in mitochondria displays a gradient from high concentration at the growing tip (~500 nM) to low at the base (~200 nM). Together with the observation that mitochondria shuttle up and down the actin filaments through the root hair (Zheng et al., 2009), mitochondria may play a role in the removal or buffering of the  $\text{Ca}^{2+}$  fluxes in the root hair apex, as was previously hypothesized (Hetherington and Brownlee, 2004).

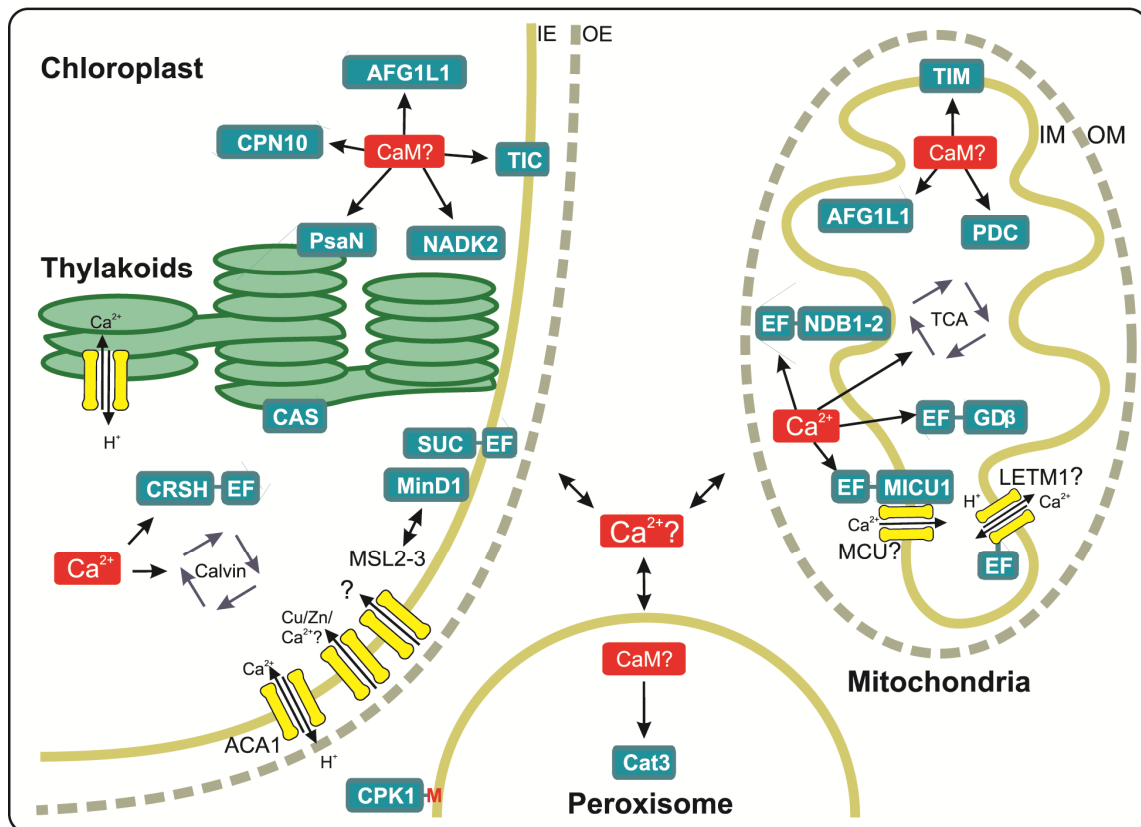


**Figure 7 Overview of proteins that are involved in calcium signaling in chloroplasts, mitochondria and peroxisomes.** Abbreviations of the proteins are indicated in the text. Calcium transporters are depicted in yellow and calmodulin/calcium binding proteins in green. EF-hand containing proteins are indicated by the addition of an 'EF-box' to the respective proteins. Proteins of uncertain nature (lack of protein identity or uncertain function) are indicated with a (?). The central  $\text{Ca}^{2+}$  (?) symbol indicates the possibility of  $\text{Ca}^{2+}$  exchange between organelles and the contribution of organelles to cytoplasmic calcium signaling. Other abbreviations are Calvin (Calvin-Benson cycle), TCA (tricarboxylic acid cycle), IE (inner envelope), OE (outer envelope), IM (inner membrane), OM (outer membrane).

### Peroxisomal calcium signaling

Information on calcium signaling in the peroxisome is scarce. It was only until recently that the occurrence of calcium fluxes in the peroxisome was recognized in animals (Raychaudhury et al., 2006; Drago et al., 2008; Lasorsa et al., 2008). A similar study, based on the expression of a peroxisomal targeted chameleon probe (a  $\text{Ca}^{2+}$  reporter protein construct), showed that plant peroxisomes undergo  $\text{Ca}^{2+}$  fluxes as well (Costa et al., 2010). Furthermore, the peroxisomal  $\text{Ca}^{2+}$  increase was found *in vivo* to enhance the detoxification of the reactive oxygen species (ROS)  $\text{H}_2\text{O}_2$  through the activity of the catalase isoform 3 (AtCAT3), as was proposed earlier. In 2002, Yang and Poovaiah demonstrated the *in vitro* stimulation of AtCAT3 activity by the calcium dependent binding of CaM and provided evidence for the presence of CaM in peroxisomes, however

they did not find its molecular identity (Yang and Poovaiah, 2002). A member of the Arabidopsis calcium-dependent protein kinase family, AtCPK1, was found to bind to the external surface of peroxisomes (Dammann *et al.*, 2003) and lipid bodies, which is most likely due to an N-terminal myristoylation signal, which determines the localization of many CDPKs and other kinases (Lu and Hrabak, 2002; Benetka *et al.*, 2008; Stael *et al.*, 2011). AtCPK1 was shown to mediate pathogen resistance (Dammann *et al.*, 2003; Coca and San Segundo, 2010). Given the few reports, the already presented interplay between calcium and ROS prompts the further study of the molecular nature of calcium handling and signaling in and around peroxisomes.

### **Nuclear calcium signaling**

In order to be complete, a short overview of calcium signaling in the nucleus is presented here. For a more comprehensive overview, the reader may consider the excellent reviews by Mazar and colleagues (Mazars *et al.*, 2009; Mazars *et al.*, 2011). Calcium signals in the nucleus enable the cell to react to environmental changes by alteration of gene expression in animals and plants (Ikura *et al.*, 2002; Kim *et al.*, 2009; Galon *et al.*, 2010; Reddy *et al.*, 2011). This may sound straightforward, however, only recently target genes of Ca<sup>2+</sup>-dependent gene expression in Arabidopsis were reported (Kaplan *et al.*, 2006), mainly because it is difficult to distinguish them from non- Ca<sup>2+</sup>-dependent gene expression changes by other nuclear signaling routes upon stress treatment (Finkler *et al.*, 2007; Wurzinger *et al.*, 2011). From this study it became apparent that many of the Ca<sup>2+</sup>-regulated genes contained abscisic acid-responsive element (ABRE) -related *cis*-elements and were already implicated in abiotic stress response before. Ca<sup>2+</sup> can influence transcription through Ca<sup>2+</sup>-binding transcription factors, CaM-binding transcription activators (AtCAMTAs, six members in Arabidopsis (Bouche *et al.*, 2002)), or phosphorylation of transcription factors by calcium dependent protein kinases (CDPKs), of which quite a number are present in the nucleus (Dammann *et al.*, 2003; Choi *et al.*, 2005; Zhu *et al.*, 2007; Boudsocq *et al.*, 2010; Mehlmer *et al.*, 2010).

Various stimuli elicit nuclear Ca<sup>2+</sup> fluxes: wind or cold shock of tobacco seedlings (van Der Luit *et al.*, 1999), the application of nodulation (nod) factors to *Medicago truncatula* root hairs (Sieberer *et al.*, 2009), the application of mastoporan, biotic elicitors and jasmonates to tobacco cells (Pauly *et al.*, 2000; Lecourieux *et al.*, 2005; Walter *et al.*, 2007) or the osmotic shock of tobacco cells (Mithofer and Mazars, 2002). A lot of the research on nuclear Ca<sup>2+</sup> signaling has been focused on the question if nuclei can generate



$\text{Ca}^{2+}$  fluxes autonomously from the cytosol. Given that the nucleoplasm and cytosol are connected by relatively large pores in the nuclear envelope, one can imagine that nuclear  $\text{Ca}^{2+}$  fluxes are the result of passive influx from the cytosol. However, the delays that have been measured between cytosolic and nuclear  $\text{Ca}^{2+}$  fluxes in the previously quoted studies, implicate the opposite. Furthermore, when tobacco cells were treated with a biologically active derivative of jasmonate (jasmonate-isoleucine), nuclei were able to generate  $\text{Ca}^{2+}$  fluxes without any measurable cytosolic  $\text{Ca}^{2+}$  responses (Walter et al., 2007). Experiments with isolated nuclei further emphasized the autonomous nature of plant nuclei from the extranuclear environment with regards to  $\text{Ca}^{2+}$  signaling (Xiong et al., 2004; Xiong et al., 2008).

If the nucleus is able to produce its own  $\text{Ca}^{2+}$  fluxes, then the nuclear envelope is most likely to serve as the responsible  $\text{Ca}^{2+}$  store. The nuclear envelope contains an inner and outer membrane, punctured by the nuclear pores, and the lumen is continuous with the ER. Analysis of its protein components has been hampered by the difficult extraction of intact nuclei and the contamination by ER membranes (Matzke et al., 2010). Nonetheless, several  $\text{Ca}^{2+}$  channels and transporters have been found at the inner and outer membrane of the nuclear envelope and it is hypothesized that the nuclear pores can act as  $\text{Ca}^{2+}$  selective channels. Two interesting examples of nuclear ion channels are Castor and Polux. Originally they were reported to localize to chloroplasts (Imaizumi-Anraku et al., 2005), but further work has unequivocally proven their presence in the nuclear envelope (Charpentier et al., 2008). Mutation of Castor and Polux abolishes perinuclear  $\text{Ca}^{2+}$  spiking and, concurrently, root symbioses with arbuscular mycorrhizal fungi and rhizobial bacteria in legume species, such as *Lotus japonicas* or non-legume species, such as rice (Chen et al., 2009). Root symbiosis in legumes is probably the best example to demonstrate the importance of nuclear calcium signaling and has been extensively reviewed elsewhere (Oldroyd and Downie, 2006; Murray, 2011).

### **1.5. Bacterial calcium signaling**

Compared to bacteria, the function of  $\text{Ca}^{2+}$  as a second messenger in signal transduction networks is well documented in eukaryotic cells. However,  $\text{Ca}^{2+}$  mediated signaling seems not to be exclusive to eukaryotes. As already mentioned, the active exclusion of  $\text{Ca}^{2+}$  from the cytosol has been a driving force during evolution to prevent the precipitation of insoluble phosphate. Hence, archaea and bacteria, which also rely on a

phosphate based metabolism, should exhibit an unequal distribution of  $\text{Ca}^{2+}$  between cytoplasm similar to eukaryotic cells as well.

Indeed it has been shown in several studies that the intracellular free  $\text{Ca}^{2+}$  concentration in bacteria is actively maintained in the range of 100 - 300 nM (Knight et al., 1991; Herbaud et al., 1998; Jones et al., 1999; Torrecilla et al., 2000). Like in eukaryotes distinct transient changes in the cytoplasmic  $\text{Ca}^{2+}$  concentration for different stimuli like heat, cold (Torrecilla et al., 2000), salt, osmotic (Torrecilla et al., 2001), oxidative (Herbaud et al., 1998) stress and different compounds ranging from heavy metals to organic acids (Barran-Berdon et al., 2011) were observed in bacteria too (Dominguez, 2004). Furthermore data of several studies suggest that chemotaxis in *E.coli* is at least partially mediated by  $\text{Ca}^{2+}$  signaling as the movement of the bacteria could be directly correlated to the  $\text{Ca}^{2+}$  transients observed during exposure of *E.coli* to an attractant or repellent (summarized in (Dominguez, 2004)). Interestingly, in the non-diazotrophic cyanobacterium *Synechococcus elongatus* PCC 7942 as well as in the diazotrophic cyanobacterium *Nostoc (Anabaena) sp.* PCC 7120 an increase in the intracellular free  $\text{Ca}^{2+}$  concentration is among the first signals observed after deprivation of combined nitrogen from the growth medium (Torrecilla et al., 2004; Zhao et al., 2005; Shi et al., 2006; Leganes et al., 2009). Furthermore in both species the  $\text{Ca}^{2+}$  transients were found to be down stream of NtcA activity, a transcriptional regulator of many genes involved in nitrogen metabolism. Indirect evidence exists that the observed  $\text{Ca}^{2+}$  transient is a part in the signaling cascade leading to phycobiliprotein degradation, a response to nutrient deprivation in *Synechococcus elongatus* PCC 7942 (Leganes et al., 2009). In case of *Nostoc (Anabaena) sp.* PCC7120 alterations of the nitrogen depletion induced  $\text{Ca}^{2+}$  transient led to an arrest of heterocyst (specialized cells capable of fixing  $\text{N}_2$ ) differentiation (Torrecilla et al., 2004). In addition, the authors of this study report that the  $\text{Ca}^{2+}$  transient is of intracellular origin.

To maintain and regulate the  $\text{Ca}^{2+}$  gradient at the plasma membrane bacterial cells must contain  $\text{Ca}^{2+}$  transport proteins. This is probably best illustrated in a study where it was shown that the active exclusion of  $\text{Ca}^{2+}$  from the cytoplasm via CaxP, a P-type  $\text{Ca}^{2+}$ -ATPase, is crucial for survival of *Streptococcus pneumoniae* in its host (Rosch et al., 2008). However, already an early bioinformatic investigation revealed the presence of  $\text{Na}^+$ ,  $\text{K}^+$  and  $\text{Ca}^{2+}$  selective voltage gated ion channels,  $\text{Ca}^{2+}$  cation antiporters and P-type  $\text{Ca}^{2+}$ -ATPases in 18 bacterial genomes based on sequence homology to eukaryotic counterparts (Paulsen et al., 2000). LMCA1 from *Listeria monocytogenes* has been

demonstrated to be a functional  $\text{Ca}^{2+}$ -ATPase *in vitro* (Faxen et al., 2011). In *Bacillus subtilis*, the YolB gene product was identified as a P-type  $\text{Ca}^{2+}$ -ATPase that is only expressed during late stage of sporulation but not in vegetative cells (Raeymaekers et al., 2002). Knock out mutants of YolB exhibited less resistant spores to heat stress than did wild type spores. More recently it was shown that the ChaA gene product from *Bacillus subtilis* encodes for a  $\text{Ca}^{2+}$  specific  $\text{Ca}^{2+}/\text{H}^+$  antiporter (Fujisawa et al., 2009). Furthermore it was found that ChaA is under control of the sigma factors B and G which, according to the authors, is an indication for its transcription during stress adaptation and sporulation. In *Synechococcus elongatus* PCC 7942, the PacL gene product was demonstrated to be a P-type  $\text{Ca}^{2+}$ -ATPase (Berkelman et al., 1994). Deletion of the pacL gene led to the absence of  $\text{Ca}^{2+}$ -ATPase activity from plasma membranes of this strain, indicating that PacL might be the only  $\text{Ca}^{2+}$ -ATPase in *Synechococcus elongatus* PCC 7942. The  $\Delta\text{pacL}$  mutant exhibited no phenotype under standard growth conditions but showed an osmosensitive phenotype (Kanamaru et al., 1993; Berkelman et al., 1994). In *Synechocystis sp.* PCC 6803 the mechanosensitive ion channel MscL was reported to be responsible for major  $\text{Ca}^{2+}$  effluxes observed after membrane depolarization and high temperature (Nazarenko et al., 2003).  $\text{Ca}^{2+}/\text{H}^+$  antiporters, homologous to the CAX gene family in *Arabidopsis* have been identified in cyanobacterial genomes too (Waditee et al., 2004). The Cax protein from *Synechocystis sp.* PCC 6803 was shown to be biochemically functional, localized at the plasma membrane and required for salt tolerance, as well as for adaptation to an alkaline milieu in this strain.

Molecular identities of  $\text{Ca}^{2+}$  specific influx systems in bacteria are largely missing so far. Studies in *E.coli* suggest at least two independent  $\text{Ca}^{2+}$  influx systems, one which can be inhibited by  $\text{La}^{3+}$  and one which is insensitive towards  $\text{La}^{3+}$  exist (Jones et al., 1999). Butane 2,3 diol was found to induce  $\text{Ca}^{2+}$  influx via  $\text{La}^{3+}$  sensitive  $\text{Ca}^{2+}$  channels in *E.coli* (Campbell et al., 2007). Interestingly poly-3-hydroxy-butyrate/phosphate complexes, which are also present in eukaryotes (Reusch, 1989), were shown to be voltage activated  $\text{Ca}^{2+}$  channels in *E.coli* plasma membranes (Reusch et al., 1995).  $\text{Ca}^{2+}$  currents via these non-protein channels are inhibited by  $\text{La}^{3+}$ . However, data presented so far cannot exclude the existence of a  $\text{La}^{3+}$  sensitive protein  $\text{Ca}^{2+}$  channels in *E.coli*. In addition to these data, ionotropic glutamate receptor channels were identified in several bacterial genomes which could be involved in  $\text{Ca}^{2+}$  influx too (Ger et al., 2010).

If intracellular  $\text{Ca}^{2+}$  mediated signaling should take place in bacteria like in eukaryotic cells, then calcium sensors in form of  $\text{Ca}^{2+}$  binding proteins must exist in bacteria as well.

The best understood  $\text{Ca}^{2+}$  binding protein motive so far is the EF-hand motive (Grabarek, 2006; Zhou et al., 2006; Gifford et al., 2007). During the last decade various successful attempts have been made to identify EF-hand containing proteins in bacterial genomes (Michiels et al., 2002; Zhou et al., 2006; Rigden et al., 2011). Summarizing, it can be said that EF-hand containing proteins are found in most bacterial genomes and that they are evenly distributed throughout families and genera. Furthermore, sequence homology searches revealed that EF-hand containing proteins are present in diverse functional categories including transporters, genes for DNA/RNA- as well as energy-metabolism and cell structure. The majority of EF-hand containing proteins (~90 %) just contain a single EF-hand motive and ~10 % were found to contain more than one EF-hand motives (Zhou et al., 2006). In addition to EF-hands new calcium binding motives of proteins are predicted and found in bacterial genomes, further rising the number of potential  $\text{Ca}^{2+}$  binding proteins in bacteria (Morgan et al., 2006; Hu et al., 2011; Rigden et al., 2011). Therefore, the following short summery will only contain genetically and biochemically characterized  $\text{Ca}^{2+}$  binding proteins involved in bacterial signaling processes. In *Streptomyces coelicolor* a cell differentiation phenotype, was observed when the  $\text{Ca}^{2+}$  buffering EF-hand containing protein CabC was knocked out and the mutant was grown under  $\text{Ca}^{2+}$  limiting conditions, whereas over-expression of cabC led to a delay in development (Wang et al., 2008). The extracellular EF hand containing CiaX protein of *Streptococcus mutans*, the primary pathogen of dental caries in humans, was found to bind  $\text{Ca}^{2+}$  and to influence the expression of the CiaHR two component system, which is involved in the signaling process that leads to biofilm formation of *S. mutans*, in a  $\text{Ca}^{2+}$  dependent manner (He et al., 2008). Furthermore it was shown that  $\text{Ca}^{2+}$  regulated biofilm formation is at least partially mediated by CiaX and sequence analysis of the CiaHR operon revealed that CiaX is an integral part of it making it in fact a three component system. CasA from the symbiotic bacterium *Rhizobium etli* has been demonstrated to be a secreted calmodulin-related  $\text{Ca}^{2+}$  binding protein which is only expressed during infection and colonization of its plant host (Xi et al., 2000). Interruption of the casA gene or over expression of its transcriptional repressor led to a lower number of bacteroids in the nodules and hence a reduced nitrogen fixation rate. CcbP, a non-EF hand containing protein, from *Nostoc (Anabaena) sp. PCC7120* has been demonstrated to be an intracellular  $\text{Ca}^{2+}$  binding protein which is involved in heterocyst differentiation upon limitation of combined nitrogen (Zhao et al., 2005; Hu et al., 2011). At the initial stage of differentiation, CcbP gets degraded by hetR, a serine protease specifically expressed at

that stage of development, resulting in a rise of intracellular free  $[Ca^{2+}]$  and subsequently heterocyst formation (Shi et al., 2006).

In table one, 19 conserved proteins between *A.thaliana* and *Nostoc (Anabaena) sp. PCC7120*, containing the  $Ca^{2+}$  binding motive Dx[DN]xDG in the homologous sequences of both organisms, are summarized. It is interesting that most of these proteins localize, or are predicted to localize to different compartments than to the plastid. Nevertheless, together with 2 more proteins, CML41 is predicted to localize to the plastid, which may

**Table 1.** Conserved Dx[DN]xDG motive containing proteins in *A.thaliana*.

AGI code	description	plastid	mito	sec pathw	MS/MS
At3g12290	Amino acid dehydrogenase family protein	1.2	0	0	PM, plastid
At3g09090	DEX1 defective in exine formation	0	3.3	28.2	PM
At2g34020	Calcium-binding EF-hand family protein	5	6.2	16	
At3g50770	CML41 calmodulin-like 41	11.4	2.3	0	
At4g10060	$\beta$ -glucosidase GBA2 type family protein	0	0	0	
At1g33700	$\beta$ -glucosidase GBA2 type family protein	0	0	0	PM
At5g49900	$\beta$ -glucosidase GBA2 type family protein	0	0	0.8	vacuole
At1g74960	KAS2 Fatty acid biosynthesis 1	27.2	0	7.5	plastid
At2g04540	mtKAS1 $\beta$ -ketoacyl synthase	2.2	19	0.5	
At1g62810	Copper amine oxidase family protein	0.4	0	30.6	
At1g31690	Copper amine oxidase family protein	3.3	0	27.7	peroxisomes
At3g43670	Copper amine oxidase family protein	0.1	0	35.2	
At1g31670	Copper amine oxidase family protein	0	0	29.1	
At4g12290	Copper amine oxidase family protein	2.2	0	24.3	PM
At4g14940	AO1 amine oxidase 1	0	0	28.9	extracellular
At3g48560	CSR1 Chlorsulfuron/imidazolinone resistant	30.6	0.6	0	plastid
At5g04130	GYRB2 DNA gyrase B2	3.6	18.9	2.6	mitochondrion
At3g10270	GYRB1 DNA gyrase B1	0	0	0	mitochondrion
At3g23890	TOPII topoisomerase II	4	3.2	0	

Aramemnon score refers to the likelihood of localisation for a protein predicted with Aramemnon (Schwacke *et al.*, 2003). MS/MS indicates evidence for the localisation of the protein in a cellular compartment based on proteomics studies summarised in the SUBA database (Haezelwood *et al.*, 2007); PM = plasma membrane.

suggest that the so far "missing" plastidal CaM might be a calmodulin like protein. This is further supported by the observation of a calmodulin like activity from *Anabaena sp.* which stimulates bovine brain cyclic AMP phosphodiesterase and the *Anabaena*

adenylate cyclase in a similar way as does calmodulin (Bianchini et al., 1990). However, since the eukaryotic cell is more complex in terms of compartmentalization than a bacterial cell, it needs a signaling system which allows for adjustment of all processes taking part in different sub cellular compartments, to a single stimulus affecting the whole cell. The  $\text{Ca}^{2+}$  signaling system seems to be such a global signaling system in plant cells. This is also reflected by the fact that highly conserved proteins such as MinD and the RelA/SpoT homolog CRSH are  $\text{Ca}^{2+}$  regulated in *A.thaliana* but not in *E.coli* (Givens et al., 2004; Aldridge and Moller, 2005).

### **1.6. Conclusions and further perspectives**

A central question in  $\text{Ca}^{2+}$  signaling is how such a simple ion can mount an appropriate and specific physiological response, when almost every stress or developmental process elicits calcium fluxes in the cell? While the answer to the specificity question is manifold (Sanders et al., 2002), it can partly be explained by the compartmentalized nature of calcium signaling. In other words, the possibility to mobilize  $\text{Ca}^{2+}$  from various subcellular stores, including chloroplasts and mitochondria, combined with its rapid release and uptake, implies that the effect of a  $\text{Ca}^{2+}$  flux can be highly localized to microdomains in the cytosol (Laude and Simpson, 2009). Furthermore, through the physical separation of organelles from the cytosol,  $\text{Ca}^{2+}$ -dependent regulations inside of organelles, such as chloroplasts, mitochondria, peroxisomes and nuclei can be exerted in a highly localized and specific manner.

It should be noted that being a large calcium store does not automatically equal the vacuole to be the most important organelle for calcium signaling in plants. The vacuole, ER and apoplast each contain an equally high potential for unloading  $\text{Ca}^{2+}$  into the cytoplasm. Furthermore, the sequestering of such high amounts of  $\text{Ca}^{2+}$  does not play a role in signaling only, but also in the general ion homeostasis of the plant. Also the types and amounts of channels that are present at the respective subcellular membranes to generate specific  $\text{Ca}^{2+}$  fluxes should be considered. To this end, various calcium influx channels from these different subcellular calcium stores were found to influence specific  $\text{Ca}^{2+}$  fluxes (reviewed in (McAinsh and Pittman, 2009)).

The question arises than: what is the contribution of the other organelles to cellular  $\text{Ca}^{2+}$  signaling? At least in chloroplasts, the impact of impaired organellar  $\text{Ca}^{2+}$  handling on plant physiology has already been demonstrated by CAS and PPF1. The mutation of,

respectively, a putative chloroplastic  $\text{Ca}^{2+}$  sensor and a transporter led to impaired stomatal movement and impaired plant growth. To provide further insight into the physiological relevance of organellar  $\text{Ca}^{2+}$  signaling, it will be crucial to identify the proteins that are responsible for calcium transport (channels and transporters), storage and decoding of the  $\text{Ca}^{2+}$  signals that have been observed. Likewise, more should be known on the stimuli that provoke  $\text{Ca}^{2+}$  signals in mitochondria and peroxisomes and especially in chloroplasts, where until now only light and dark were found to induce  $\text{Ca}^{2+}$  fluxes. The combination of the molecular players and the elicitors of calcium signaling in organelles should provide fruitful grounds for further discovery.

Interplay between organelles can greatly affect  $\text{Ca}^{2+}$  signaling. In human and animal cells the intimacy of ER and mitochondria was found to be beneficial for movement of  $\text{Ca}^{2+}$  between the two stores and this was further strengthened by the identification of the molecular bridge between them (Kornmann et al., 2009; de Brito and Scorrano, 2010). Similarly in plants,  $\text{Ca}^{2+}$  might be exchanged between chloroplasts, mitochondria and peroxisomes, while they are required to be closely connected for photorespiration and the exchange of metabolites (Gowik et al., 2011). Moreover,  $\text{Ca}^{2+}$  exchange between chloroplasts and ER cannot be excluded, while they were also found to be closely associated in plants (Schattat et al., 2011; Schattat et al., 2011).

The data on bacterial calcium-signaling clearly indicates that the prerequisites for eukaryotic  $\text{Ca}^{2+}$  signaling, an actively maintained  $\text{Ca}^{2+}$  gradient across membranes and  $\text{Ca}^{2+}$  sensor proteins, are already present in bacteria. The even distribution and frequent occurrence of  $\text{Ca}^{2+}$  transporters and EF-hand containing proteins throughout genomes of bacterial families (Paulsen et al., 2000; Zhou et al., 2006) further indicate a prokaryotic origin of these core elements in eukaryotic  $\text{Ca}^{2+}$  signaling. For this, it is reasonable to search for conserved  $\text{Ca}^{2+}$  signaling processes between bacteria, eukaryotes and their endosymbionts, mitochondria and plastids, too.

### **Acknowledgements**

This work has been funded by the Austrian GEN-AU program in the ERA-PG project *CROPP* (Project No. 818514), the Austrian Science Foundation (P19825-B12), and by the EU in the Marie-Curie ITN *COSI* (ITN 2008 GA 215-174).

## 2. Results and discussion

The results part includes work that has been published (paper 1 and 2) or has been submitted for review (paper 3 and 4). Thereafter, unpublished results on OEF18 and LENA were added. Since each paper already includes the discussion, results and discussion were joined together in this chapter also for OEF18 and LENA. This is an overview of my contributions to each paper:

- 1) Bayer RG, **Stael S**, Csaszar E, Teige M. Mining the soluble chloroplast proteome by affinity chromatography. **Proteomics**. 2011 Apr. PMID: 21365755.

*Stael S contributed the part of the proteomics with Eu<sup>3+</sup>-IDA and helped with the confirmation of localization for the selected proteins by YFP-fusion. Stael S helped with the correction and discussion of the manuscript.*

- 2) **Stael S**, Bayer RG, Mehlmer N, Teige M. Protein N-acylation overrides differing targeting signals. **FEBS Lett**. 2011 Feb 4. PMID: 21219905.

*Stael S did the YFP-fusion analysis and western blots on FNR, RCA and CPK16. Stael S helped with the correction and discussion of the manuscript.*

- 3) **Stael S**, Rocha AG, Robinson AJ, Kmiecik P, Vothknecht UC, Teige M. Arabidopsis calcium-binding mitochondrial carrier proteins as potential facilitators of mitochondrial ATP-import and plastid SAM-import. **FEBS Lett** (first revision submitted, 07/10/2011)

*Stael S performed most experimental work; except for the <sup>45</sup>Ca overlay assay and the bio-informatic analysis of SAMTL. The manuscript was written by Stael S.*

- 4) **Stael S**, Rocha AG, Wimberger T, Anrather D, Vothknecht UC, Teige M. Crosstalk between calcium signaling and protein phosphorylation at the thylakoid. **Journal of Experimental Botany** (first submission, 07/10/2011).

*Stael S did the 2D experiments and prepared the samples for MS/MS. Stael S expressed most proteins for the confirmatory kinase assays. The manuscript was written by Stael S.*

**Stael S**, Wurzinger B, Mehlmer N, Vothknecht UC, Teige M. The magical life of calcium as a secondary messenger: A journey to the organelles. **Journal of Experimental Botany** (first revision, 26/09/2011).

*Stael S wrote the parts on major calcium stores, organellar calcium signaling and discussion.*



## RESEARCH ARTICLE

**2.1. Paper 1- Mining the soluble chloroplast proteome by affinity chromatography***Roman G. Bayer, Simon Stael, Edina Csaszar and Markus Teige*

Department of Biochemistry and Cell Biology, Max F. Perutz Laboratories, University of Vienna, Austria

Chloroplasts are fundamental organelles enabling plant photoautotrophy. Besides their outstanding physiological role in fixation of atmospheric CO<sub>2</sub>, they harbor many important metabolic processes such as biosynthesis of amino acids, vitamins or hormones. Technical advances in MS allowed the recent identification of most chloroplast proteins. However, for a deeper understanding of chloroplast function it is important to obtain a complete list of constituents, which is so far limited by the detection of low-abundant proteins. Therefore, we developed a two-step strategy for the enrichment of low-abundant soluble chloroplast proteins from *Pisum sativum* and their subsequent identification by MS. First, chloroplast protein extracts were depleted from the most abundant protein ribulose-1,5-bisphosphate carboxylase/oxygenase by SEC or heating. Further purification was carried out by affinity chromatography, using ligands specific for ATP- or metal-binding proteins. By these means, we were able to identify a total of 448 proteins including 43 putative novel chloroplast proteins. Additionally, the chloroplast localization of 13 selected proteins was confirmed using yellow fluorescent protein fusion analyses. The selected proteins included a phosphoglycerate mutase, a cysteine protease, a putative protein kinase and an EF-hand containing substrate carrier protein, which are expected to exhibit important metabolic or regulatory functions.

Received: August 10, 2010

Revised: December 15, 2010

Accepted: December 29, 2010

**Keywords:**

Affinity chromatography / ATP-binding / Chloroplast / Metal-binding / Plant proteomics / YFP-fusion protein

**1 Introduction**

Chloroplasts are semi-autonomous organelles of endosymbiotic origin found in all plant and algal cells. They have essential roles in processes such as photosynthesis, biosynthesis of amino acids and vitamins, lipid synthesis, or storage of starch. Analysis of the chloroplast proteome helps to elucidate the multitude of chloroplast functions by providing information about the protein composition and

compartmentalization of metabolic pathways [1-4].

Beginning with the completion of the genome sequence of *Arabidopsis thaliana* in the year 2000 various efforts have been made to estimate the size of the chloroplast proteome using sequenced-based prediction programs. The Arabidopsis Genome Initiative calculated an overall number of ~3600 chloroplast proteins using TargetP [5], whereas usage of ChloroP resulted in the prediction of ~1900-2500 chloroplast proteins [6]. This difference can be explained by the fact that chloroplast transit peptides (cTPs) do not share distinct consensus motifs in their primary structure and by their remarkable diversity [7]. Therefore, an improved prediction strategy was applied accepting cTPs only when they were identified by at least three out of four different programs [8]. This resulted in the prediction of ~2100 proteins, which probably fits best to the actual size of the chloroplast proteome. However, as reliable information on the subcellular localization of proteins cannot be deduced

**Correspondence:** Dr. Markus Teige, Department of Biochemistry and Cell Biology, Max F. Perutz Laboratories, University of Vienna, Dr. Bohrgasse 9/5, A-1030 Vienna, Austria

**E-mail:** markus.teige@univie.ac.at

**Fax:** 143-14277-9528

**Abbreviations:** **AGI**, *Arabidopsis* gene identifier; **cTP**, chloroplast transit peptide; **PGL**, phosphoglycerate mutase; **PPDB**, Plant Proteome Database; **PPK**, putative protein kinase; **PurB**, purva- lanol B; **Rubisco**, ribulose-1,5-bisphosphate carboxylase/oxygenase; **YFP**, yellow fluorescent protein

[www.proteomics-journal.com](http://www.proteomics-journal.com)

from genome sequences alone [1, 4], it is indispensable to analyze the chloroplast proteome experimentally.

Since the first plant genomes were published, large-scale MS-coupled proteomic approaches have routinely been employed to directly detect proteins in organellar preparations [9], and the obtained data have been integrated into several protein databases. For example, the Plant Proteome Database (PPDB) contains ~1200 manually curated chloroplast proteins including data of a recently published chloroplast study, which claims to be the most comprehensive chloroplast proteome analysis to date [10, 11]. Thus, PPDB provides by far the most extensive, curated resource for experimentally verified chloroplast-localized proteins. In combination with protein data from a recently published chloroplast proteomic study integrated into the novel database AT\_CHLORO [12], both databases make up a total of ~1700 unique chloroplast-localized proteins. This number probably reflects the amount of chloroplast proteins that is accessible with the current MS technologies and traditional preparation techniques.

Up to date, neither the proteome of an organism nor an organelle has been experimentally identified completely. This is due to the inaccessibility of certain proteins to proteomic techniques as a consequence of their physico-chemical properties and the dynamic range of proteins ( $10^6$  magnitudes) leading to a repeated detection of abundant proteins. To overcome the dynamic range problem, it is necessary to modify the fractionation techniques prior to MS [1]. In accordance with Ferro et al. [12] we think that classical large-scale chloroplast proteomic approaches have reached their limit and only directed approaches have the potential to unveil low-abundant proteins. To date, there are only very

few reports about studies aiming at the targeted identification of organellar proteins present in the literature. Examples are the identification of thioredoxin-interacting proteins in the stroma of chloroplasts by using immobilized thioredoxin affinity columns and the analysis of ATP-binding proteins in chloroplast membranes or in the mitochondrial matrix by ATP-affinity chromatography [13-16].

We set out to identify novel, low-abundant soluble proteins localized in the chloroplast by applying a targeted fractionation approach prior to protein detection by MS. In order to reduce the sample complexity we decided to implement a two-step strategy (Fig. 1A). In a first step, we either performed SEC of extracted stroma proteins, or we performed a heat treatment of isolated chloroplasts. Both strategies led to an almost complete separation of the most abundant protein ribulose-1,5-bisphosphate carboxylase/oxygenase (Rubisco) from the rest of the soluble proteins. In a second step, we performed affinity chromatography using different ligands, which not only further reduced the complexity of the sample but also allowed a specific enrichment of proteins according to their biological function [17]. In the end we were able to detect a subset of ~20% of the expected 2100 chloroplast proteins including novel chloroplast-localized proteins. The chloroplast localization

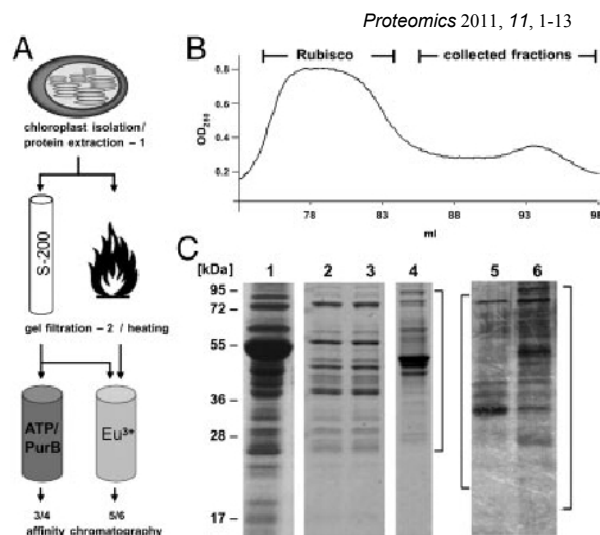


**Figure 1.** Experimental strategy and procedure. A, Flow scheme. B, Elution profile of gel filtration. X-axis shows milliliters of eluting sample. Y-axis shows absorbance at 280 nm indicating relative protein content. C, Affinity chromatography. 1-6, protein samples analyzed by SDS-PAGE: 1, crude chloroplast protein extract. 2, sample after gel filtration prior to affinity chromatography. 3, sample after heating. 4, elution of ATP-affinity column. 5, citrate elution of  $\text{Eu}^{3+}$ -affinity column. 6, EDTA strip of  $\text{Eu}^{3+}$ -affinity column. In lanes 4-6 the region, where protein bands were cut, is indicated.

of 13 selected candidate proteins was confirmed by yellow fluorescent protein (YFP) fusion analysis.

## 2 Materials and methods

### 2.1 Chloroplast isolation - *A. thaliana*

A comparison of several published chloroplast isolation protocols revealed that an adapted version of the protocol by Kunst [18] resulted in the highest yield of intact chloroplasts. Briefly, *Arabidopsis* plants were grown for approximately 8 wk under short day conditions (8 h light/16 h dark photoperiod at  $100\text{--}150\text{ mmol m}^{-2}\text{s}^{-1}$ ,  $22\pm 5^\circ\text{C}$ , humidity  $60\pm 20\%$ ). Leaves were harvested and homogenized in the HB buffer (450 mM sorbitol, 20 mM Tricine, 10 mM  $\text{Na}_2\text{EDTA}$ , 5 mM  $\text{NaHCO}_3$ , 0.1% BSA, 10 mM isoascorbic acid, 1 mM reduced glutathione, pH 8.4 with KOH) using a Waring blender (3 pulses: low-low-high; 2-3 s each). In comparison to the original chloroplast isolation protocol, addition of isoascorbic acid and glutathione to the homogenization buffer resulted in a significant increase in the yield of intact chloroplasts. After filtration and centrifugation the chloroplasts were purified over continuous Percoll gradients, which consisted of Percoll (GE Healthcare) mixed in a 1:1 ratio with  $2 \times \text{RB}$  buffer (600 mM sorbitol, 40 mM Tricine, 10 mM  $\text{MgCl}_2$ , 5 mM  $\text{Na}_2\text{EDTA}$ , pH 7.6 with KOH). The gradient was formed by centrifugation for 30 min at

3 R. G. Bayer et al.

53 000 × g and then the chloroplasts were centrifuged for 6 min at 10700 × g. Intact chloroplasts were recovered from the gradient, washed with 1 × RB buffer and stored at -80°C.

## 2.2 Chloroplast isolation - *Pisum sativum*

The chloroplast isolation procedure was adapted from [19]. Briefly, *P. sativum* plants were grown for 8-9 days under long day conditions (16/8 h photoperiod at ~70 mmol m<sup>-2</sup>s<sup>-1</sup>, 21±5°C, humidity 70-90%). Leaves were cut and homogenized using a Waring blender. The homogenate was filtered through Miracloth (Merck, Germany) and centrifuged. The resuspended pellets were loaded on top of 2-4 preformed Percoll step gradients consisting of 12 mL 40% Percoll and 7 mL 80% Percoll (in 330 mM sorbitol, 50 mM Hepes/KOH pH 7.6). After centrifugation intact chloroplasts were recovered from the 40-80% interphase and washed. Isolated chloroplasts were pooled and immediately frozen in liquid nitrogen and stored at -80°C.

## 2.3 Stromal protein extraction and gel filtration

Chloroplasts (~20 mg of chlorophyll; measured according to Arnon [20]) were incubated in the breaking buffer (10 mM Tricine pH 8, 10 mM MgCl<sub>2</sub>, 1 mM DTT, supplemented with protease inhibitor cocktail Complete Mini EDTA-free (Roche Applied Science) on ice for 5 min. After centrifugation for 6 min (12 000 × g, 4°C) the supernatant was transferred to a new tube and the extraction was repeated. Subsequently, the extracts were pooled and the buffer was exchanged to buffer A (50 mM Tris pH 7.8, 50 mM NaCl, 10 mM MgCl<sub>2</sub>) using PD-10 Desalting columns (GE Healthcare). The sample was concentrated to ~500 µL using a Centriprep Centrifugal Filter Unit (NMWL: 10 kDa; Millipore). After clarification by centrifugation for 10 min (16100 × g, 4°C) the supernatant was applied to a Superdex 200 (GE Healthcare) gel filtration column and SEC was performed on an FPLC system (GE Healthcare) at a flow rate of 0.8 ml/min (buffer A).

## 2.4 Heat treatment of isolated chloroplasts and protein extraction

Isolated pea chloroplasts were lysed by addition of 7 mL of lysis buffer (20 mM DTT, 0.1% Triton X-100, protease inhibitor cocktail Complete Mini EDTA-free) to 3 mL of chloroplasts (containing ~4 mg/mL chlorophyll) and incubation for 10 min on ice. The chloroplast suspension was divided into 1 mL aliquots, rapidly heated to 75°C for 5 min, and immediately cooled on ice. Heat-denatured proteins and thylakoid membranes were pelleted by centrifugation at 20 000 × g for 10 min. After centrifugation for 30 min at 100 000 × g (TLS55 rotor, Optima Ultracentrifuge;

*Proteomics* 2011, 11, 1-13

Beckman Coulter) and 4°C, the supernatant was rebuffed to IDA column-loading buffer (100 mM Tris-HCl pH 7.5, 3 M NaCl, 200 mM CaCl<sub>2</sub>) on a PD-10 column (GE Healthcare).

## 2.5 Affinity chromatography ATP/Purvalanol B (Pur B)

C10-linked Aminophenyl-ATP-Sepharose was purchased from JENA Bioscience (Jena, Germany). Preparation of PurB affinity sepharose was done as previously described [21]. In both cases the affinity sepharose was poured into disposable polystyrene columns (Thermo Scientific) and the columns were run by gravity flow at room temperature.

**PurB column:** The column (500 mL of slurry) was equilibrated with 10 column volumes of PurB buffer (buffer A + 350 mM NaCl, 0.5% Triton X-100). Nearly, 1.5 mg protein sample (gel-filtrated chloroplast stroma) was adjusted by the PurB buffer and then applied to the column. Subsequently, the column was washed with 20 column volumes of the PurB buffer and bound proteins were eluted with 6 column volumes of 0.5% SDS.

**ATP column:** The column (500 mL of slurry) was equilibrated with 10 column volumes of ATP buffer (buffer A + 100 mM NaCl, 0.05% NP-40). Nearly, 1.5 mg protein sample (gel-filtrated chloroplast stroma) was adjusted by the ATP buffer and then applied to the column. Subsequently, the column was washed with 20 column volumes of the ATP buffer and bound proteins were eluted with 6 column volumes 0.5% SDS.

All fractions were precipitated with TCA using a standard protocol (LabFAQS, <http://www.roche-applied-science.com/labfaqs/intro.htm>). The pellets were resuspended in the SDS loading buffer and the precipitated proteins were resolved by a 12% SDS-PAGE. Proteins were visualized by Coomassie or silver staining (using formaldehyde instead of glutaraldehyde), and bands were excised and subjected to MS.

## 2.6 Eu<sup>3+</sup>-IDA column affinity chromatography

The Eu<sup>3+</sup>-IDA column affinity chromatography was adapted from [22]. To prepare the Eu<sup>3+</sup>-IDA affinity column, a disposable polystyrene column was filled with 1 mL of IDA-sepharose (Thermo Scientific) and washed with 5 mL of 100 mM EDTA (pH 7.0), followed by 10 mL of double distilled water. A 50 mM EuCl<sub>3</sub> (Alfa Aesar, USA) solution was applied to the column, followed by washing with 25 mL double-distilled water. The column was equilibrated with 10 mL of the equilibration buffer (100 mM Tris-HCl pH 7.5, 2 M NaCl, 200 mM CaCl<sub>2</sub>). Samples were obtained either from SEC of chloroplast stroma or from heat denaturation of isolated chloroplasts. In the case of fractionated stroma salts were added to match the IDA column-loading buffer. After loading of a sample,

the column was washed with 10 mL equilibration buffer, 5 mL of sulfate buffer (600 mM Na<sub>2</sub>SO<sub>4</sub>, 100 mM Tris-HCl pH 7.5, 2 M NaCl) and 2.5 mL of malonate buffer (40 mM malonate, 600 mM Na<sub>2</sub>SO<sub>4</sub>, 100 mM Tris-HCl pH 7.5, 2 M NaCl). Protein was eluted with a citrate solution (0.2 M phosphate buffer pH 7.5, 3 M NaCl, 200 mM citrate) and afterwards the column was stripped with 100 mM EDTA. The citrate eluate and EDTA-strip were buffer-exchanged to 50 mM Tris-HCl pH 7.5 on a PD-10 column and precipitated in four volumes of cold acetone. Eluted proteins were separated by SDS-PAGE and visualized by silver staining. Bands were excised and subjected to MS.

## 2.7 MS analyses

Coomassie or silver-stained gel bands were used for the nano-electrospray LC-MS/MS analyses as described previously [23]. The gel bands were cut out, and in case of Coomassie stained bands destained with a mixture of ACN and 50 mM ammonium hydrogen carbonate. Proteins were reduced by DTT and alkylated by iodoacetamide. Trypsin was used as protease. Samples were digested overnight at 37°C and the digest was stopped by addition of 10% formic acid in water to an end concentration of approximately 1%.

Peptides were separated on an UltiMate™ HPLC system (Dionex) equipped with a PepMap C18 column (300 mm × 5 mm) and a 75 mm × 150 mm analytical column of the same material. About 0.1% TFA was used for binding of the peptides and elution was performed using a linear gradient of ACN and 0.1% formic acid in water. LC-MS/MS analyses were carried out using the UltiMate™ system interfaced to an LTQ (Thermo Scientific) linear ion trap mass spectrometer. The electrospray voltage was set to 1500 V and peptide spectra were recorded over the mass range of m/z 450-1600. MS/MS spectra were recorded in information-dependent data acquisition with a default charge state set to 3. The mass range for MS/MS measurements was calculated according to the masses of the parent ions. One full spectrum was recorded followed by four MS/MS spectra for the most intense ions, automatic gain control was applied and the collision energy was set to the arbitrary value of 35. Helium was used as the collision gas. Fragmented ions were set onto an exclusion list for 20 s. Raw spectra were interpreted by Mascot 2.2.04 (Matrix Science) using Mascot Daemon 2.2.2. The peptide tolerance

was set to 72 Da, MS/MS tolerance was set to 70.8 Da. Carbamidomethylcysteine was set as static modification, oxidation of methionine residues was set as the variable modification. Trypsin was selected as protease and two missed cleavages were allowed. MASCOT results were loaded into Scaffold (Ver. 2.01.01.1; Proteome Software) for an X! Tandem Search. Peptide identifications were accepted, if they could be established at greater than 95% probability as specified by the Peptide Prophet algorithm [24]. Protein identifications

were accepted, if they could be established at greater than 99% probability as assigned by the Protein Prophet algorithm [25]. Additionally, at least two identified peptides were required. Proteins were identified from the full genome sequence of TAIR in the case of Arabidopsis samples and from the recently created EST database in the case of pea samples [26].

## 2.8 Data validation

Identified proteins (always referring to Arabidopsis gene identifier (AGI) codes) were imported into Microsoft Excel for further analyses. Redundant protein identifications were removed using the advanced filter. Proteins were searched against PPDB [10], pIprot [27], AMPDB [28], SUBA [29] and AraPerox [30] databases. All proteins not found in any of the abovementioned databases were manually inspected regarding experimental verification of subcellular localization by searching in publications found in the TAIR AGI entry ([www.arabidopsis.org](http://www.arabidopsis.org)) or in the ENTREZ search engine ([www.ncbi.nlm.nih.gov/sites/gquery](http://www.ncbi.nlm.nih.gov/sites/gquery)). Targeting prediction was done with TargetP [31], ChloroP [32], Aramemnon consensus prediction [33] and MultiP [34]. To test for the presence of a P-LOOP motif in proteins, a regular expression of the motif, which was obtained from the PROSITE database [35], was created using Microsoft Excel and queried against all protein sequences (TAIR8 release). Furthermore, the nucleotide- and metal-binding features of identified proteins were individually analyzed using the annotated protein function and the databases PROSITE and ENZYME [35, 36].

## 2.9 Subcellular localization studies

The coding sequences of the analyzed candidate genes were obtained by RT-PCR from total leaf RNA or in the case of OTL by PCR from a RIKEN BRC Arabidopsis Full-Length clone (RAFL21-73-A21) [37-39]. C-terminal YFP-fusions of the candidate genes were cloned into the binary plant expression vector pBIN19 [40]. Tobacco transfection and subcellular localization analysis were done as previously described [41].

## 3 Results and discussion

### 3.1 Enrichment and identification of low-abundant chloroplast proteins

As most chloroplast proteomics studies focussed on the exploration of the thylakoid protein complement, mining the soluble proteome has the highest potential to discover new proteins. Furthermore, soluble proteins are easily accessible by standard chromatographic separation techniques in

contrast to hydrophobic proteins originating from thylakoid preparations.

We decided to use chloroplasts isolated from pea, because they are known to be highly pure and intact in contrast to Arabidopsis chloroplasts, which tend to break and lose their stromal content during isolation [42]. As the pea genome has not been sequenced yet, we employed a recently created pea EST database that already proved to be useful in proteomic studies of the chloroplast envelope [26].

In a first step, after extraction of stromal proteins from isolated pea chloroplasts, we performed gel filtration in order to enrich for low-abundant proteins. By this means, we separated the most abundant protein, the multimeric Rubisco protein complex with a size of ~540 kDa, from the majority of other proteins that are of much smaller size (Fig. 1B). Compared to other purification strategies, such as employing Rubisco antibody columns, SEC had the advantage that also ribosomes were removed [43]. This led to a depletion of the abundant ribosomal proteins, which would normally exacerbate the detection of low-abundant proteins.

In a second purification step, we subjected the pooled fractions eluting after the prominent Rubisco peak from the gel filtration column to affinity chromatography. This method is based on the specific and reversible interaction of a ligand with its target protein, thus presenting a major advantage over the multidimensional protein identification technology MudPIT, which is applied to peptide mixtures [44].

We combined the selection of ligands with the general interest in understanding cellular signaling including protein kinases [45], and extended our approach to ATP-binding proteins as a whole. Therefore, we used ATP and the ATP-binding site directed protein kinase inhibitor PurB as ligands in independent chromatographic runs. Additionally, we used a ligand specific for metal-binding proteins. Initially, we aimed at calcium-binding proteins, but it is known that  $\text{Ca}^{2+}$  easily gets desorbed from affinity matrices in a process called metal ion transfer. Hence, we used the ligand  $\text{Eu}^{3+}$ , which in contrast to  $\text{Ca}^{2+}$  was demonstrated to be stably attached to the affinity matrix, and which is even able to adsorb calcium-binding proteins [22]. The Rubisco-depleted fractions after gel filtration were applied to all three different affinity ligands.

As an alternative to SEC, we performed a heat treatment of isolated chloroplasts and recovered soluble proteins and soluble fragments of membrane proteins after centrifugation. Originally, this step was established to enrich for heat-stable calmodulins [46], but empiric results in our lab showed that this procedure was also very efficient for the removal of Rubisco resulting in an enrichment particularly of heat-stable proteins. However, in contrast to SEC, heating did not lead to a depletion of ribosomes. After the heat treatment the sample was applied only to the  $\text{Eu}^{3+}$ -column.

In order to achieve a maximal resolution for the subsequent protein identification by MS, eluted proteins from all three affinity columns were further separated by SDS-PAGE (Fig. 1C). A comparison of the original sample to the eluting

fractions revealed a specific enrichment of proteins. Separated gel lanes of all eluting fractions were cut into slices and after extraction and digestion proteins were identified by MS/MS using the pea EST database [26]. Each identified protein was queried against the Arabidopsis genome database and the corresponding AGI of the closest homologue was determined. All further analyses were carried out using the respective Arabidopsis genes.

### 3.2 Saturation of protein identifications

The analysis of three biological replicates and several technical replicates resulted in the identification of 448 unique proteins with high confidence (Supporting Information Table S1). Based on all obtained results we calculated saturation curves referring to identified proteins (Supporting Information Fig. S1). For each affinity strategy we analyzed three biological samples and plotted the percentage of all new identified proteins per sample. Using the ATP-affinity strategy we identified in total 319 proteins. Already, 82% of all proteins were identified in the first biological sample, and the second biological replicate led to the detection of only additional 4%. A significant improvement in the discovery of new proteins (14%) could be obtained only after changing the ligand from PurB to ATP for the third biological replicate.

Similar results were obtained using the  $\text{Eu}^{3+}$ -column. In total, we identified 273 proteins. 54% of all proteins were discovered in the first biological sample, and the second biological sample gave again no significant improvement (only 1%). In both cases heat-treated chloroplast extracts were applied to affinity chromatography, whereas gel-filtrated stroma extracts were used for the third biological replicate. This led to a significant increase in newly identified proteins (45% of all identified proteins).

### 3.3 Subcellular localization of identified proteins

In order to get an idea about the enrichment of chloroplast-localized proteins in our data set, we analyzed the number of predicted chloroplast proteins using TargetP. Out of the 448 identified proteins 84.3% are predicted to contain a cTP compared to 14.9% proteins of the whole Arabidopsis proteome (TAIR9 release). Furthermore, to assess the quality of our data set regarding the amount of already experimentally verified chloroplast proteins and non-chloroplast contaminants, we queried available organellar protein databases. We used the databases PPDB and plprot [27], which focus on chloroplasts, the mitochondrial AMPDB [28], the peroxisomal AraPerox [30] and the database SUBA [29], which integrates data of all subcellular compartments. The localization of all remaining proteins, which were not found in any database, was manually curated. Only if no experimental information on the subcellular localization of a protein could be found, it was considered to be a putative novel chloroplast protein.

Overall, this analysis revealed a good quality of our chloroplast isolations as reflected by the high rate of known chloroplast proteins being 84% (376 proteins) and the low contamination rate of 6.5% (29 proteins). It is important to note here that dual targeting [47] is not considered and therefore the real contamination rate will most likely be lower. In total, 9.6% (43 proteins) were classified as putative new to the chloroplast (Table 1). Notably, knockout mutants of eight of these proteins in *Arabidopsis* do exhibit a chloroplast-related phenotype according to the Chloroplast 2010 database ([www.plastid.msu.edu](http://www.plastid.msu.edu)).

According to TargetP 30 out of the 43 putative new chloroplast proteins are predicted to be chloroplast-localized indicating that the majority of putative new proteins are targeted via the canonical import pathway. Interestingly, one protein (AT3G55870) is predicted to enter the secretory pathway. This protein is annotated as subunit of anthranilate synthase, which is an enzyme of the plastidial-localized shikimate pathway for the synthesis of aromatic amino acids [48]. It may be targeted to the chloroplast via the ER, a non-nanonical import pathway that has already been described for the carbonic anhydrase CAH1 from *Arabidopsis*, the rice  $\alpha$ -amylase AmyI-1 and the rice nucleotide pyrophosphatase/phosphodiesterase NPP1 [49-51].

During preparation of this article the new chloroplast protein database AT\_CHLORO was launched and also publications confirming the localization of some novel chloroplast proteins were released. In response to these new findings, which nonetheless support the quality of our experimental approach, we reevaluated our putative novel chloroplast proteins (Table 1).

### 3.4 Ligand-binding affinity of identified proteins

We performed affinity chromatography using the ligands ATP, PurB and  $\text{Eu}^{3+}$ . With each affinity ligand we are able to identify a specific subset of proteins (Supporting Information Fig. S2). As expected, the overlap between ATP and PurB was larger (75 proteins) than between ATP and  $\text{Eu}^{3+}$  (14 proteins) or PurB and  $\text{Eu}^{3+}$  (39 proteins) reflecting the different nature of the ligand's binding affinities. Nevertheless, even with PurB and ATP several unique proteins could be identified indicating a slightly different mode of action on ATP-binding proteins.

We analyzed all 319 proteins that were identified with the ATP-affinity strategy for the presence of a P-LOOP signature, which is a classical and well-characterized ATP-binding motif [52]. While in the whole proteome (TAIR9 release) only 6.3% of all proteins contain a P-LOOP, this motif is enriched to 11.6% within all 319 identified proteins. But it has to be considered that a number of proteins are binding ATP via a completely different motif. As proteins interacting with nucleotides similar to ATP such as FAD, NAD or GTP could have bound to the ATP and PurB columns, we manually investigated all identified proteins for their bind-

ing affinities based on their annotated function. In total, 47.7% of the 319 proteins exhibited affinity to ATP or a similar nucleotide. Furthermore, in line with Ito et al. [15], who analyzed the ATP-binding proteome of mitochondria, we identified many classical nucleotide-binding proteins such as HSPs, isoforms of the elongation factor Tu and different dehydrogenases and reductases.

All 273 proteins identified with the  $\text{Eu}^{3+}$ -column were individually analyzed for their ability to bind metal ions based on their annotated function. In total 23% of the proteins are able to bind to Zn, Ca or other metal ions, which is a clear enrichment compared to the average amount of 12% metal-binding (e.g. Zn and Fe) proteins that are present in eukaryotic proteomes according to the analysis of 57 sequenced species using the SCOP (Structural Classification of Proteins) database [53]. However, also here it has to be considered that this analysis is only based on available annotations and that therefore the number of genuine metal binding proteins in this data set will most probably be much higher.

### 3.5 Subcellular localization of candidate proteins

As MS detection of proteins in organellar preparations alone is not a convincing proof of localization due to the risk of detecting contaminants, we selected 13 candidates for further experimental investigation by YFP fusion analysis (Table 2; for identified peptides see Supporting Information Table S2).

We chose to analyze the protease OTL, the protein HAC, which belongs to the superfamily of haloacid dehalogenases, the aminotransferase ATF and the two unknown proteins CUP1 and CUP2. Furthermore, we selected the protein PIF, which was shown to interact with the nuclear factor PRL1, the ATP sulfurylase APS2, the 2-dehydro-3-deoxyphospho-heptonate aldolase DAS, the oxidoreductase ORE and the phosphoglycerate mutase PGL. By using relaxed identification criteria we even could identify a putative protein kinase, PPK and an EF-hand containing substrate carrier protein, SUC, which had already been detected in a chloroplast envelope proteomic study [54]. Both proteins were also included in our verification experiments. Finally, we added the P-type ATPase PAP to our test set, which had also been identified in a chloroplast proteomics study before, but only with one peptide [11]. The subcellular localization of all candidate proteins was analyzed by confocal laser scanning microscopy using C-terminal YFP fusion proteins. In all cases except for SUC full-length coding sequences were used. In the case of SUC only the N-terminal part of the protein was analyzed, but it is known that the N-terminus harboring the cTP is sufficient to mediate chloroplast import [7, 34]. For the protein kinase PPK both, the N-terminal part and the full-length protein were analyzed.

All of the 13 candidate genes showed chloroplast localization indicated by an overlap of the YFP signal with the

**Table 1.** The 43 identified putative novel chloroplast proteins

AGI code	Functional annotation (TAIR9)	TargetP	ATP/PurB	Eu <sup>3</sup>	Chloroplast 2010
<b>AT1G06510</b>	<b>Unknown protein</b>	<b>C</b>	-	+	<b>WP</b>
<b>AT1G15730<sup>a,b)</sup></b>	<b>PRL1-interacting factor L, putative</b>	<b>C</b>	+	-	<b>WP, CF</b>
<b>AT1G19920<sup>a)</sup></b>	<b>ATP sulfurylase</b>	<b>C</b>	+	-	-
AT1G21500 <sup>a)</sup>	Chloroplast Unknown protein 1	C	-	+	-
<b>AT1G22410</b>	<b>2-Dehydro-3-deoxyphosphoheptonate aldolase</b>	<b>C</b>	+	+	<b>WP, SAA</b>
AT1G23800	ALDH2B7; 3-chloroallyl aldehyde dehydrogenase (NAD)	M	+	-	-
AT1G30510 <sup>a)</sup>	ATRFNR2; root FNR 2)	C	+	-	-
AT1G36280 <sup>a,b)</sup>	Adenylosuccinate lyase	C	+	-	WP
AT1G42430	Chloroplast Unknown protein 1	O	+	+	-
AT1G54310	RNA binding	M	+	-	-
AT1G60000 <sup>a,b)</sup>	29 kDa ribonucleoprotein	C	+	+	-
AT1G66530	Arginyl-tRNA synthetase, putative	O	+	-	-
AT1G71720 <sup>b)</sup>	S1 RNA-binding domain-containing protein	C	-	+	-
AT1G71920 <sup>a)</sup>	Histidinol-phosphate aminotransferase, putative	C	+	-	-
AT1G74920	ALDH10A8; 3-chloroallyl aldehyde dehydrogenase	O	+	-	-
AT1G76690	OPR2; 12-oxophytodienoate reductase	O	+	-	-
AT1G77122	Unknown protein	C	+	+	-
<b>AT1G77670<sup>a)</sup></b>	<b>Aminotransferase class I and II family protein</b>	<b>M</b>	+	-	-
AT1G77930	DNAJ heat shock N-terminal domain-containing protein	C	-	+	WP
AT1G79530 <sup>c)</sup>	GAPCP-1; glyceraldehyde-3-phosphate dehydrogenase	C	+	-	WP, LFA
AT1G79870 <sup>a)</sup>	Oxidoreductase family protein	O	+	-	-
<b>AT2G17240</b>	<b>Unknown protein</b>	<b>C</b>	-	+	-
AT2G17340	Pantothenate kinase-related	O	+	-	-
AT2G21350	RNA binding	C	-	+	-
AT2G23390	Acyl-CoA N-acyltransferase	M	+	-	-
<b>AT2G25870</b>	<b>Haloacid dehalogenase-like family protein</b>	<b>M</b>	+	-	-
AT2G31890 <sup>b)</sup>	ATRAP; putative RNA binding domain	C	+	-	-
AT2G44760	Unknown protein	C	+	-	-
AT3G02900 <sup>a)</sup>	Unknown protein	C	-	+	-
<b>AT3G04650</b>	<b>FAD-dependent oxidoreductase</b>	<b>C</b>	+	-	-
AT3G25110	AtFaTA; <i>Arabidopsis</i> FatA acyl-ACP thioesterase	C	+	-	-
AT3G29185 <sup>a)</sup>	Unknown protein	C	+	+	-
AT3G55870	Anthranilate synthase, a subunit, putative	S	+	-	-
<b>AT3G57810</b>	<b>OTU-like cysteine protease family protein</b>	<b>M</b>	-	+	-
AT3G59040	Pentatricopeptide (PPR) repeat-containing protein	C	+	-	-
AT4G27070 <sup>a)</sup>	TSB2; tryptophan synthase b subunit 2	C	+	+	WP
AT5G02590	Tetrapentapeptide (TPR) repeat-containing protein	C	-	+	-
AT5G14460	Pseudouridine synthase/transporter	C	+	-	-
AT5G15390	tRNA/rRNA methyltransferase (SpoU) family protein	C	+	-	-
<b>AT5G22620<sup>a,b)</sup></b>	<b>Phosphoglycerate mutase family protein</b>	<b>C</b>	+	-	<b>LAA</b>
AT5G52010	Zinc finger (C2H2 type) family protein	C	+	-	-
AT5G62990	Embryo defective 1692 (ubiquitin thioesterase)	C	+	+	-
AT5G64840 <sup>b)</sup>	ATGCN5; <i>A. thaliana</i> general control non-repressible 5	C	+	-	-

AGI codes of all proteins together with functional annotation from TAIR9 and TargetP prediction are shown. C, chloroplast; M, mitochondrion; S, secretory system; O, other localization. Whether or not a protein was identified with the ATP/PurB and/or Eu<sup>3+</sup> strategy is depicted by + or -, respectively. When an identified protein exhibits a certain phenotype according to the Chloroplast 2010 database, this is indicated: WP, Whole Plant Morphology; CF, Chlorophyll Fluorescence; SAA, Seed Amino Acid; LFA, Leaf Fatty Acid; LAA, Leaf Amino Acid. Proteins that have been selected for YFP localization study are written in bold. Proteins that have been reported to be localized in the chloroplast during preparation of this publication are labelled by superscript lowercase letters, which are explained at the bottom of the table.

a) Protein is present in the AT\_CHLORO database.

b) Protein is chloroplast localized according to the recent PPDB update. c) Chloroplast - localized according to [71].

autofluorescence signal of chlorophyll (Fig. 2). Interestingly, the proteins PAP, HAC, PGL, DAS, CUP1 and PPK exhibited speckled chloroplast localization, which was similar to the localization pattern of the known chloroplast proteins ferredoxin-NADP+ reductase (AT5G66190) and Rubisco

activase (AT2G39730) (Supporting Information Fig. S3). In the case of PPK, the speckled pattern could only be observed for the full-length protein but not for the N-terminal portion. This indicated that PPK carries internal information within its protein sequence that is needed to target it to

**Table 2.** The 13 candidate proteins selected for YFP localization

AGI code	Name	Functional annotation (TAIR9)	TargetP	ChloroP	MultiP	Aram.	ATP/PurB	Eu <sup>3+</sup>
AT1G06190	PAP	P-type ATPase, cation-transport	C	C	C	C	-	+
AT1G06510	CUP1	Chloroplast unknown protein 1	C	C	C	C	-	+
AT1G15730	PIF	PRL1-interacting factor L, putative	C	C	C	C	+	-
AT1G19920	APS2	ATP sulfurylase	C	C	C	C	+	-
AT1G22410	DAS	2-Dehydro-3-deoxyphosphoheptonate aldolase	C	C	C	C	+	+
AT1G77670	ATF	Aminotransferase class I and II family protein	M	C	O	O	+	-
AT2G17240	CUP2	Chloroplast unknown protein 1	C	C	C	C	-	+
AT2G25870	HAC	Haloacid dehalogenase-like family protein	M	C	O	M	+	-
AT2G35800	SUC	Substrate carrier family protein	O	O	O	O	-	+
AT3G04650	ORE	FAD-dependent oxidoreductase	C	C	C	C	+	-
AT3G57810	OTL	OTU-like cysteine protease family protein	M	C	C	C	-	+
AT5G16810	PPK	Putative protein kinase	C	O	C	O	+	+
AT5G22620	PGL	Phosphoglycerate mutase family protein	C	C	C	C	+	-

AGI codes of selected proteins, arbitrary name and functional annotation from TAIR9 are shown. YFP indicates the experimentally determined subcellular localization. Results of targeting prediction by TargetP, ChloroP, MultiP and Aramemnon (Aram.) are included as well. C, chloroplast; M, mitochondrion; O, other localization. Whether or not a protein was identified with the ATP/PurB and/or Eu<sup>3+</sup> strategy is depicted by + or -, respectively.

a specific subcompartment within the chloroplast. We suppose that this holds true also for the other proteins with a similar localization pattern.

Furthermore, in both the cases the localization was not exclusively observed in chloroplasts, ATF was detected also in the cytoplasm and CUP2 in the nucleus. This might be an experimental artifact due to overexpression of the proteins using the strong 35S promoter from Cauliflower mosaic virus. But since all other analyzed proteins do not show any background localization to other cellular compartments than the chloroplast, ATF and SUC could also be dually targeted. Furthermore, overexpression of proteins seems to lead to mislocalization rather when multiple copies of the 35S promoter are used. For example the nuclear-localized putative ion channels CASTOR and POLLUX were mistargeted to the chloroplast only when a double 35S promoter was used [55]. The most interesting novel chloroplast proteins will be discussed below.

### 3.6 OTL (OTU-like cysteine protease)

OTL belongs to the OTU-like superfamily of predicted cysteine proteases [56]. In chloroplasts an unknown cysteine protease activity was shown to be involved in the turnover of Rubisco as well as Rubisco activase and the regulation of the general chloroplast protein composition was effected by overexpression of the cysteine protease inhibitor cystatin in tobacco leaves [57]. OTL is now the first identified chloroplast-localized cysteine protease in Arabidopsis.

### 3.7 PGL (phosphoglycerate mutase)

Phosphoenolpyruvate, together with erythrose 4-phosphate, is the precursor of aromatic amino acids synthesized via the

shikimate pathway and is therefore a key metabolite in plants. In principle, phosphoenolpyruvate can be formed from 3-phosphoglycerate in two consecutive reaction steps involving a phosphoglycerate mutase, PGL, and an enolase. In Arabidopsis the enolase ENO1 was already shown to be localized within the chloroplast [58]. In this study we were able to identify the missing chloroplast-localized phosphoglycerate mutase, PGL. During preparation of this article PGL was also identified in another independent chloroplast proteomic study [59]. Interestingly, integrated data analysis of shotgun proteomics and RNA profiling indicated a significant molecular mass bias for the detection of proteins, which are expressed at very low levels [60]. This seems to be the case for the plastidial PGL, thus explaining why its detection by MS had been so difficult. In contrast other metabolic enzymes like transketolase accumulate at much higher levels as related metabolic enzymes [61] or as it would be expected based on their transcript levels [60], even enabling its protein purification from plant tissues [62].

### 3.8 PPK (plastidial protein kinase)

Protein phosphorylation by protein kinases is a key mechanism to transduce signals within a cell and to regulate processes according to environmental changes. The chloroplast with its numerous metabolic processes is integrated into the cellular signaling network, but so far only a handful chloroplast protein kinases have been identified. Examples are the state transition kinases STN7 and STN8 [63], which are involved in photosynthetic acclimation, the plastid transcription kinase CKIIa [64], and the recently described chloroplast sensor kinase CSK [65], which controls transcription of several chloroplast genes. Here, we provide evidence for a novel chloroplast-localized putative



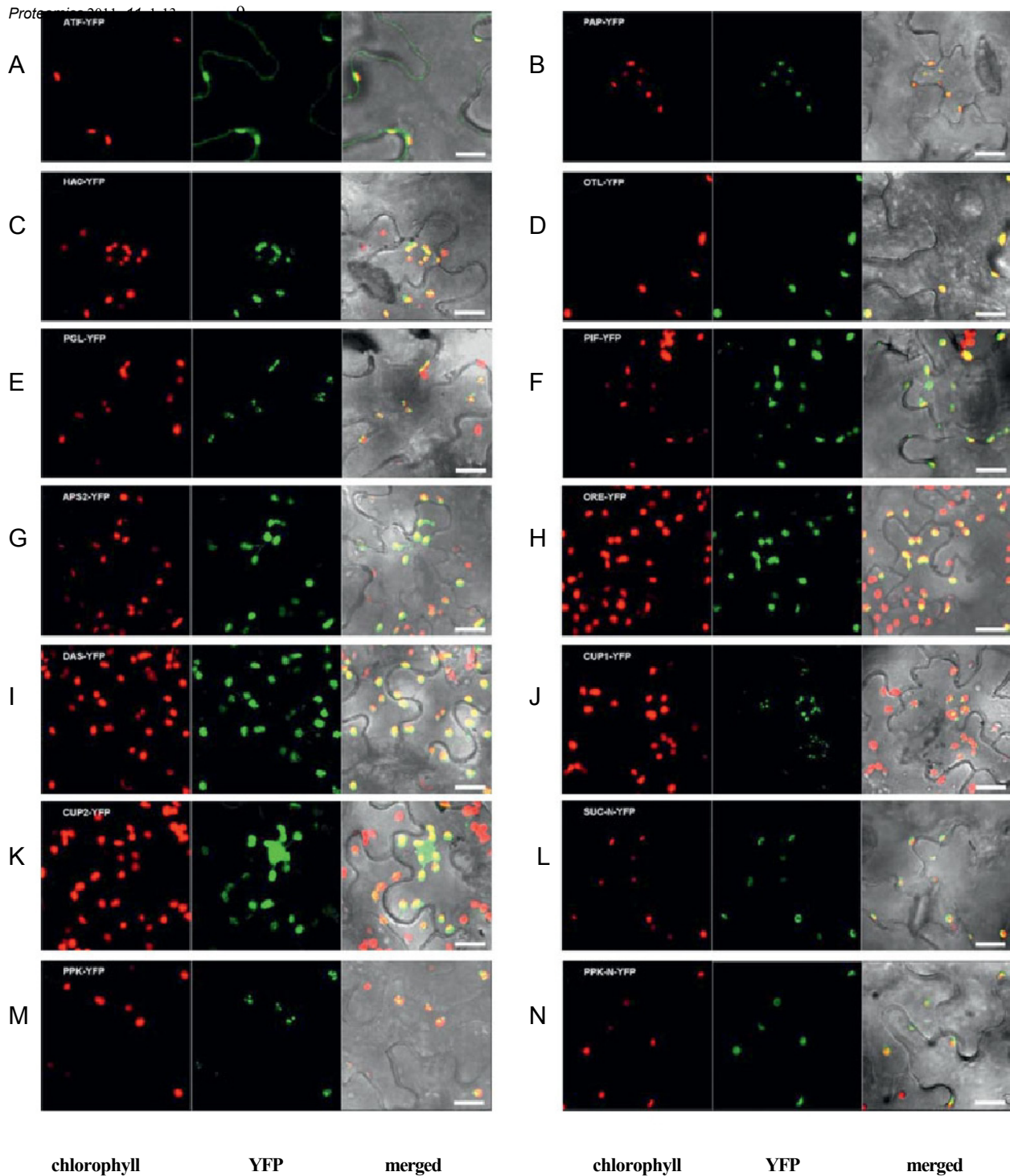


**Figure 2.** YFP localization of selected candidate proteins. Tobacco leaves infiltrated with constructs in which the gene of interest was fused in front of YFP were analyzed by confocal laser scanning microscopy two days after infiltration. Chlorophyll autofluorescence is shown in the first channel and the YFP signal in the second channel. The third channel is a merged image of the previous two plus transmitted light. N after the name of a protein indicates that only its N-terminus was fused to YFP. Bar 5 20 nm.

protein kinase. Notably, quite a number of different protein kinases are predicted to be localized in chloroplasts but systematic analysis of their localization revealed that most of them are not targeted to chloroplasts in vivo [66].

For example, the  $\text{Ca}^{2+}$ -dependent protein kinase CPK3 has a firm prediction for chloroplast targeting, but turned out to be localized to the nucleus and different cellular membranes [67].

[www.proteomics-journal.com](http://www.proteomics-journal.com)

### 3.9 SUC (substrate carrier protein)

SUC is a member of the mitochondrial carrier family (MCF), which consists of 58 putative members in Arabidopsis [68]. Some are known to carry specific substrates not only across the mitochondrial membrane (as the family name might suggest), but also across the chloroplast envelope [69]. The identification of SUC in a previous proteomics study of the chloroplast envelope [54] prompted further evaluation of its localization. An N-terminal YFP-fusion protein of SUC clearly localizes to ring-like structures around the chloroplast, hinting at envelope localization. Furthermore, SUC is one of the four predicted MCF proteins to have at least one functional EF-hand. Together, we present here new evidence for a potentially calcium-regulated substrate carrier protein at the chloroplast envelope.

### 3.10 HAC (haloacid dehalogenase)

The haloacid dehalogenase superfamily is a large family of proteins dominated by phosphotransferases. It includes phosphoesterases, ATPases, phosphonases, dehalogenases and sugar phosphomutases, which act on a remarkably diverse set of substrates and contain a specific form of the Rossmannoid fold [70]. Interestingly, eight different haloacid dehalogenase-like proteins, which are evolutionary highly conserved, were also identified in the recent proteomic study by Olinares et al. [43], thus pointing toward an ancient group of regulatory proteins in chloroplast metabolism inherited from their prokaryotic progenitors.

### 3.11 Comparison of the pea EST with the Arabidopsis genome database

In order to assess the identification potential of the pea EST database compared to the complete genome database of Arabidopsis, we repeated the affinity approach using ATP-Sepharose with chloroplasts isolated from mature Arabidopsis plants. The procedure was exactly the same as for pea.

Although the same amount of chloroplasts was used, after gel filtration only 0.82 mg protein could be recovered compared to 1.5 mg with pea, which reflects the well-known fact that during isolation Arabidopsis chloroplasts break and lose parts of their stromal content. Remarkably, although less protein was present in the sample, 365 proteins could be identified with Arabidopsis in contrast to 234 with pea (Supporting Information Table S3). This is most probably due to the lower sequence coverage of the pea EST database compared to the complete genome database of Arabidopsis. Furthermore, the overlap of identified proteins between both organisms accounts for only 160 proteins. This indicates that the usage of pea gave rise to the identification of a different subset of chloroplast proteins, which could be

based on two reasons. On the one hand, this is most likely due to species-specific differences in the chloroplast protein content. On the other hand, this probably also reflects differences in the developmental state of the analyzed chloroplasts as seedlings were used for chloroplast isolation from pea, whereas leaves of mature plants were used in the case of Arabidopsis.

With the data from the recently published AT\_CHLORO database already integrated, out of the 365 Arabidopsis proteins 94% were already known to be localized in the chloroplast compared to 86.3% with the pea approach. Strikingly, although approximately 50% more proteins were identified with Arabidopsis only nine (2.5%) putative novel chloroplast proteins were found compared to 21 (7.3%) with pea.

## 4 Concluding remarks

At a time where classical top-down organellar proteomic approaches are reaching their detection limits, we have shown that applying a targeted proteomic approach on chloroplasts from the non-model organism pea has the potential to identify novel chloroplast proteins. The use of different affinity ligands could further lead to novel protein identifications and eventually to deeper understanding of chloroplast function.

The comparison of the stromal proteomes of pea and Arabidopsis confirmed the expected species- and/or developmental state-specific differences between chloroplasts isolated from mature leaves of Arabidopsis and seedlings of pea. Most importantly, the use of the non-model organism pea gave rise to the identification of new chloroplast proteins (e.g. DAS, HAC, ORE) that were not accessible in Arabidopsis before. In this context, a further improvement of the targeted approach presented in this study would be the sequencing of the complete pea genome. We predict that usage of a whole genome database for the identification of chloroplast proteins from pea would result in the detection of more (novel) chloroplast proteins, accompanied with a decrease in the contamination rate.

Data on protein identifications associated with this article may be downloaded as Scaffold SFD files from Proteome-Commons.org Tranche using following hashes:

```
bkNL8osY7uDT6RyhN9K9hbRAKzkUZrH08vjd71
coXUGYkcPWQbQCTEWmfL/7kQvF7lsXd2L6dm1
dExwk1s29tUwTTcAAAAAAAABkw 5 5
tyvgY1UhiPBmFytFipsUzNspkE6Gn7oJcPcqP38X-
FrIMjpYWYVoo6Y8a1chlWvcRjuWdsuHGLuq
byUKXrKgHBirKWgAAAAAAAABkw 5 5
kxF5p9j0zIb1lmQWPgEzHy3HL1iH915WFO1G/j1
B4X6aKA/1FWPhH5hM71ZZ93B0u59N3dgRu/9Wc6by/
DKzvXqaTwAAAAAAAABjQ 5 5
3jYp8J6PZsOY39cTeDsGkT4xx7PP6PMbAQWH37SKb6
JK7KcmMkr8ywyq7EafETTbeywuy/R0Aa1Y2AiuCsuBpilh-
n5UwAAAAAAAABtg 5 5
```

[www.proteomics-journal.com](http://www.proteomics-journal.com)

The hashes may be used to prove exactly what files were published as part of this article's data set, and the hash may also be used to check that the data have not changed since publication.

This work has been funded by the Austrian GEN-AU program in the ERA-PG project CROPP (Project No. 818514) and by the EU in the Marie-Curie ITN COSI (GA 215-174).

The authors thank Andreas Weber and Andrea Brautigam (Institute for Plant Biochemistry, Heinrich-Heine-University Dusseldorf) for providing access to their pea EST database prior to publication and for their valuable support and discussion of the results. Furthermore, the authors thank Gustav Ammerer and all members of the mass spectrometry facilities of the MFPL for the good collaboration and they are indebted to Helga Waltenberger for technical assistance.

The authors have declared no conflict of interest.

## 5 References

- [1] Baginsky, S., Plant proteomics: concepts, applications, and novel strategies for data interpretation. *Mass Spectrom. Rev.* 2009, **28**, 93-120.
- [2] Jan van Wijk, K., Proteomics of the chloroplast: experimentation and prediction. *Trends Plant Sci.* 2000, **5**, 420-425.
- [3] Jarvis, P., Organellar proteomics: chloroplasts in the spotlight. *Curr. Biol.* 2004, **14**, R317-R319.
- [4] Lilley, K. S., Dupree, P., Plant organelle proteomics. *Current Opin. Plant Biol.* 2007, **10**, 594-599.
- [5] AGI, Analysis of the genome sequence of the flowering plant *Arabidopsis thaliana*. *Nature* 2000, **408**, 796-815.
- [6] Abdallah, F., Salamini, F., Leister, D., A prediction of the size and evolutionary origin of the proteome of chloroplasts of *Arabidopsis*. *Trends Plant Sci.* 2000, **5**, 141-142.
- [7] Jarvis, P., Targeting of nucleus-encoded proteins to chloroplasts in plants. *New Phytol.* 2008, **179**, 257-285.
- [8] Richly, E., Leister, D., An improved prediction of chloroplast proteins reveals diversities and commonalities in the chloroplast proteomes of *Arabidopsis* and rice. *Gene* 2004, **329**, 11-16.
- [9] Haynes, P. A., Roberts, T. H., Subcellular shotgun proteomics in plants: looking beyond the usual suspects. *Proteomics* 2007, **7**, 2963-2975.
- [10] Sun, Q., Zybailov, B., Majeran, W., Friso, G. et al., PPDB, the Plant Proteomics Database at Cornell. *Nucleic Acids Res.* 2009, **37**, D969-D974.
- [11] Zybailov, B., Rutschow, H., Friso, G., Rudella, A. et al., Sorting signals, N-terminal modifications and abundance of the chloroplast proteome. *PLoS One* 2008, **3**, e1994.
- [12] Ferro, M., Brugiére, S., Salvi, D., Seigneurin-Berny, D. et al., AT\_CHLORO: a comprehensive chloroplast proteome database with subplastidial localization and curated information
- [13] Balmer, Y., Koller, A., del Val, G., Manieri, W. et al., Proteomics gives insight into the regulatory function of chloroplast thioredoxins. *Proc. Natl. Acad. Sci. USA* 2003, **100**, 370-375.
- [14] Motohashi, K., Kondoh, A., Stumpp, M. T., Hisabori, T., Comprehensive survey of proteins targeted by chloroplast thioredoxin. *Proc. Natl. Acad. Sci. USA* 2001, **98**, 11224-11229.
- [15] Ito, J., Heazlewood, J. L., Millar, A. H., Analysis of the soluble ATP-binding proteome of plant mitochondria identifies new proteins and nucleotide triphosphate interactions within the matrix. *J. Proteome Res.* 2006, **5**, 3459-3469.
- [16] Kishimoto, K., Ishijima, S., Ohnishi, M., ATP-binding proteins of spinach chloroplast membranes. *J. Biol. Macromol.* 2003, **3**, 69-74.
- [17] Azarkan, M., Huet, J., Baeyens-Volant, D., Looze, Y., Vandebussche, G., Affinity chromatography: a useful tool in proteomics studies. *J. Chromatogr.* 2007, **849**, 81-90.
- [18] Kunst, L., Preparation of physiologically active chloroplasts from *Arabidopsis*. *Methods Mol. Biol.* 1998, **82**, 43-48.
- [19] Schleiff, E., Soll, J., Kuchler, M., Kuhlbrandt, W., Harrer, R., Characterization of the translocon of the outer envelope of chloroplasts. *J. Cell Biol.* 2003, **160**, 541-551.
- [20] Arnon, D. I., Copper enzymes in isolated chloroplasts. Polyphenoloxidase in *Beta vulgaris*. *Plant Physiol.* 1949, **24**, 1-15.
- [21] Wissing, J., Jansch, L., Nimtz, M., Dieterich, G. et al., Proteomics analysis of protein kinases by target class-selective prefractionation and tandem mass spectrometry. *Mol. Cell. Proteomics* 2007, **6**, 537-547.
- [22] Chaga, G. S., Ersson, B., Porath, J. O., Isolation of calcium-binding proteins on selective adsorbents. Application to purification of bovine calmodulin. *J. Chromatogr. A* 1996, **732**, 261-269.
- [23] Spirek, M., Estreicher, A., Csaszar, E., Wells, J. et al., SUMOylation is required for normal development of linear elements and wild-type meiotic recombination in *Schizosaccharomyces pombe*. *Chromosoma* 2010, **119**, 59-72.
- [24] Keller, A., Nesvizhskii, A. I., Kolker, E., Aebersold, R., Empirical statistical model to estimate the accuracy of peptide identifications made by MS/MS and database search. *Anal. Chem.* 2002, **74**, 5383-5392.
- [25] Nesvizhskii, A. I., Keller, A., Kolker, E., Aebersold, R., A statistical model for identifying proteins by tandem mass spectrometry. *Anal. Chem.* 2003, **75**, 4646-4658.
- [26] Brautigam, A., Shrestha, R. P., Whitten, D., Wilkerson, C. G. et al., Low-coverage massively parallel pyrosequencing of cDNAs enables proteomics in non-model species: comparison of a species-specific database generated by pyrosequencing with databases from related species for proteome analysis of pea chloroplast envelopes. *J. Biotechnol.* 2008, **136**, 44-53.
- [27] Kleffmann, T., Hirsch-Hoffmann, M., Gruissem, W., Baginsky, S., plprot: a comprehensive proteome database

www.proteomics-journal.com

- for different plastid types. *Plant Cell Physiol.* 2006, **47**,
- [28] Heazlewood, J. L., Tonti-Filippini, J. S., Gout, A. M., Day, D. A. et al., Experimental analysis of the *Arabidopsis* mitochondrial proteome highlights signaling and regulatory components, provides assessment of targeting prediction programs, and indicates plant-specific mitochondrial proteins. *Plant Cell* 2004, **16**, 241-256.
- [29] Heazlewood, J. L., Tonti-Filippini, J., Verboom, R. E., Millar, A. H., Combining experimental and predicted datasets for determination of the subcellular location of proteins in *Arabidopsis*. *Plant Physiol.* 2005, **139**, 598-609.
- [30] Reumann, S., Ma, C., Lemke, S., Babujee, L., AraPerox. A database of putative *Arabidopsis* proteins from plant peroxisomes. *Plant Physiol.* 2004, **136**, 2587-2608.
- [31] Emanuelsson, O., Nielsen, H., Brunak, S., von Heijne, G., Predicting subcellular localization of proteins based on their N-terminal amino acid sequence. *J. Mol. Biol.* 2000, **300**, 1005-1016.
- [32] Emanuelsson, O., Nielsen, H., von Heijne, G., ChloroP, a neural network-based method for predicting chloroplast transit peptides and their cleavage sites. *Protein Sci.* 1999, **8**, 978-984.
- [33] Schwacke, R., Fischer, K., Ketelsen, B., Krupinska, K., Krause, K., Comparative survey of plastid and mitochondrial targeting properties of transcription factors in *Arabidopsis* and rice. *Mol. Genet. Genomics* 2007, **277**, 631-646.
- [34] Lee, D. W., Kim, J. K., Lee, S., Choi, S. et al., *Arabidopsis* nuclear-encoded plastid transit peptides contain multiple sequence subgroups with distinctive chloroplast-targeting sequence motifs. *Plant Cell* 2008, **20**, 1603-1622.
- [35] Hulo, N., Bairoch, A., Bulliard, V., Cerutti, L. et al., The 20 years of PROSITE. *Nucleic Acids Res.* 2008, **36**, D245-D249.
- [36] Bairoch, A., The ENZYME database in 2000. *Nucleic Acids Res* 2000, **28**, 304-305.
- [37] Sakurai, T., Satou, M., Akiyama, K., Iida, K. et al., RARGE: a large-scale database of RIKEN *Arabidopsis* resources ranging from transcriptome to phenome. *Nucleic Acids Res.* 2005, **33**, D647-D650.
- [38] Seki, M., Carninci, P., Nishiyama, Y., Hayashizaki, Y., Shinozaki, K., High-efficiency cloning of *Arabidopsis* full-length cDNA by biotinylated CAP trapper. *Plant J.* 1998, **15**, 707-720.
- [39] Seki, M., Narusaka, M., Kamiya, A., Ishida, J. et al., Functional annotation of a full-length *Arabidopsis* cDNA collection. *Science* 2002, **296**, 141-145.
- [40] Bevan, M., Binary *Agrobacterium* vectors for plant transformation. *Nucleic Acids Res.* 1984, **12**, 8711-8721.
- [41] Benetka, W., Mehler, N., Maurer-Stroh, S., Sammer, M. et al., Experimental testing of predicted myristoylation targets involved in asymmetric cell division and calcium-dependent signalling. *Cell Cycle* 2008, **7**, 3709-3719.
- [42] Halliwell, B., The chloroplast at work. A review of modern developments in our understanding of chloroplast metabolism. *Prog. Biophys. Mol. Biol.* 1978, **33**, 1-54.
- [43] Olinares, P. D., Ponnala, L., van Wijk, K. J., Megadalon 432-436. complexes in the chloroplast stroma of *Arabidopsis thaliana* characterized by size exclusion chromatography, mass spectrometry, and hierarchical clustering. *Mol. Cell. Proteomics* 2010, **9**, 1594-1615.
- [44] Wolters, D. A., Washburn, M. P., Yates, J. R., 3rd, An automated multidimensional protein identification technology for shotgun proteomics. *Anal. Chem.* 2001, **73**, 5683-5690.
- [45] Baginsky, S., Grussem, W., The chloroplast kinase network: new insights from large-scale phosphoproteome profiling. *Mol. Plant* 2009, **2**, 1141-1153.
- [46] Huo, L., Lee, E. K., Leung, P. C., Wong, A. O., Goldfish calmodulin: molecular cloning, tissue distribution, and regulation of transcript expression in goldfish pituitary cells. *Endocrinology* 2004, **145**, 5056-5067.
- [47] Karnieli, S., Pines, O., Single translation - dual destination: mechanisms of dual protein targeting in eukaryotes. *EMBO Rep.* 2005, **6**, 420-425.
- [48] Tzin, V., Galili, G., The Biosynthetic Pathways for Shikimate and Aromatic Amino Acids in *Arabidopsis thaliana*. *The Arabidopsis Book* 2010, **8**, eo132 doi: 10-1199/ Aali0.132.
- [49] Villarejo, A., Buren, S., Larsson, S., Dejardin, A. et al., Evidence for a protein transported through the secretory pathway en route to the higher plant chloroplast. *Nature Cell Biol.* 2005, **7**, 1224-1231.
- [50] Kitajima, A., Asatsuma, S., Okada, H., Hamada, Y. et al., The rice alpha-amylase glycoprotein is targeted from the Golgi apparatus through the secretory pathway to the plastids. *The Plant Cell* 2009, **21**, 2844-2858.
- [51] Nanjo, Y., Oka, H., Ikarashi, N., Kaneko, K. et al., Rice plastidial N-glycosylated nucleotide pyrophosphatase/ phosphodiesterase is transported from the ER-golgi to the chloroplast through the secretory pathway. *The Plant Cell* 2006, **18**, 2582-2592.
- [52] Saraste, M., Sibbald, P. R., Wittinghofer, A., The P-loop - a common motif in ATP- and GTP-binding proteins. *Trends Biochem. Sci.* 1990, **15**, 430-434.
- [53] Dupont, C. L., Yang, S., Palenik, B., Bourne, P. E., Modern proteomes contain putative imprints of ancient shifts in trace metal geochemistry. *Proc. Natl. Acad. Sci. USA* 2006, **103**, 17822-17827.
- [54] Ferro, M., Salvi, D., Brugiare, S., Miras, S. et al., Proteomics of the chloroplast envelope membranes from *Arabidopsis thaliana*. *Mol. Cell. Proteomics* 2003, **2**, 325-345.
- [55] Charpentier, M., Bredemeier, R., Wanner, G., Takeda, N. et al., *Lotus japonicus* CASTOR and POLLUX are ion channels essential for perinuclear calcium spiking in legume root endosymbiosis. *Plant Cell* 2008, **20**, 3467-3479.
- [56] Makarova, K. S., Aravind, L., Koonin, E. V., A novel superfamily of predicted cysteine proteases from eukaryotes, viruses and *Chlamydia pneumoniae*. *Trends Biochem. Sci.* 2000, **25**, 50-52.
- [57] Prins, A., van Heerden, P. D., Olmos, E., Kunert, K. J., Foyer, C. H., Cysteine proteinases regulate chloroplast protein content and composition in tobacco leaves: a model for dynamic interactions with ribulose-1,5-bisphosphate

*Proteomics* 2011, **11**, 1-13

carboxylase/oxygenase (Rubisco) vesicular bodies. *J. Exp. Botany* 2008, **59**, 1935-1950.

[58] Prabhakar, V., Lottgert, T., Gigolashvili, T., Bell, K. et al., Molecular and functional characterization of the plastid-localized Phosphoenolpyruvate enolase (ENO1) from *Arabidopsis thaliana*. *FEBS Lett.* 2009, **583**, 983-991.

[59] Joyard, J., Ferro, M., Masselon, C., Seigneurin-Berny, D. et al., Chloroplast proteomics highlights the subcellular compartmentation of lipid metabolism. *Prog. Lipid Res.* 2009, **49**, 128-158.

[60] Baginsky, S., Kleffmann, T., von Zychlinski, A., Gruissem, W., Analysis of shotgun proteomics and RNA profiling data from *Arabidopsis thaliana* chloroplasts. *J. Proteome Res.* 2005, **4**, 637-640.

[61] Teige, M., Kopriva, S., Bauwe, H., Suss, K. H., Chloroplast pentose-5-phosphate 3-epimerase from potato: cloning, cDNA sequence, and tissue-specific enzyme accumulation. *FEBS Lett.* 1995, **377**, 349-352.

[62] Teige, M., Melzer, M., Suss, K. H., Purification, properties and in situ localization of the amphibolic enzymes D-ribulose 5-phosphate 3-epimerase and transketolase from spinach chloroplasts. *Eur. J. Biochem.* 1998, **252**, 237-244.

[63] Bonardi, V., Pesaresi, P., Becker, T., Schleiff, E. et al., Photosystem II core phosphorylation and photosynthetic acclimation require two different protein kinases. *Nature* 2005, **437**, 1179-1182.

[64] Ogrzewalla, K., Piotrowski, M., Reinbothe, S., Link, G., The plastid transcription kinase from mustard (*Sinapis alba* L.). A nuclear-encoded CK2-type chloroplast enzyme with redox-sensitive function. *Eur. J. Biochem.* 2002, **269**, 3329-3337.

13

[65] Puthiyaveetil, S., Kavanagh, T. A., Cain, P., Sullivan, J. A. et al., The ancestral symbiont sensor kinase CSK links photosynthesis with gene expression in chloroplasts. *Proc. Natl. Acad. Sci. USA* 2008, **105**, 10061-10066.

[66] Schliebner, I., Pribil, M., Zuhlke, J., Dietzmann, A., Leister, D., A survey of chloroplast protein kinases and phosphatases in *Arabidopsis thaliana*. *Curr. Genomics* 2008, **9**, 184-190.

[67] Mehlmer, N., Wurzing, B., Stael, S., Hofmann-Rodriguez, D. et al., The Ca<sup>2+</sup>-dependent protein kinase CPK3 is required for MAPK-independent salt-stress acclimation in *Arabidopsis*. *Plant J.* 2010, **63**, 484-498.

[68] Picault, N., Hodges, M., Palmieri, L., Palmieri, F., The growing family of mitochondrial carriers in *Arabidopsis*. *Trends Plant Sci.* 2004, **9**, 138-146.

[69] Palmieri, F., Rieder, B., Ventrella, A., Blanco, E. et al., Molecular identification and functional characterization of *Arabidopsis thaliana* mitochondrial and chloroplastic NAD1 carrier proteins. *J. Biol. Chem.* 2009, **284**, 31249-31259.

[70] Burroughs, A. M., Allen, K. N., Dunaway-Mariano, D., Aravind, L., Evolutionary genomics of the HAD superfamily: understanding the structural adaptations and catalytic diversity in a superfamily of phosphoesterases and allied enzymes. *J. Mol. Biol.* 2006, **361**, 1003-1034.

[71] Munoz-Bertomeu, J., Cascales-Minana, B., Mulet, J. M., Baroja-Fernandez, E. et al., Plastidial glyceraldehyde-3-phosphate dehydrogenase deficiency leads to altered root development and affects the sugar and amino acid balance in *Arabidopsis*. *Plant Physiol.* 2009, **151**, 541-55



## 2.2. Paper 2 - Protein N-acylation overrides differing targeting signals

Simon Stael<sup>1</sup>, Roman G. Bayer<sup>1</sup>, Norbert Mehlmer<sup>2</sup>, Markus Teige<sup>1</sup> 

Department of Biochemistry and Cell Biology, MFPL, University of Vienna, Dr. Bohrgasse 9, A-1030 Vienna, Austria

article info abstract

### Article history:

Received 30 November 2010

Revised 30 December 2010

Accepted 4 January 2011

Available online 8 January 2011

Edited by Ulf-Ingo Flügge

### Keywords:

Protein kinase

Chloroplast targeting

Myristoylation

Palmitoylation

Calcium-dependent protein kinase

**In a bioinformatics based screen for chloroplast-localized protein kinases we noticed that available protein targeting predictors falsely predicted chloroplast localization. This seems to be due to interference with N-terminal protein acylation, which is of particular importance for protein kinases. Their N-myristoylation was found to be highly overrepresented in the proteome, whereas myristoylation motifs are almost absent in known chloroplast proteins. However, only abolishing their myristoylation was not sufficient to target those kinases to chloroplasts and resulted in nuclear accumulation instead. In contrast, inhibition of N-myristoylation of a calcium-dependent protein kinase was sufficient to alter its localization from the plasma membrane to chloroplasts and chloroplast localization of ferredoxin-NADP<sup>+</sup> reductase and Rubisco activase could be efficiently suppressed by artificial introduction of myristoylation and palmitoylation sites.**

© 2011 Federation of European Biochemical Societies. Published by Elsevier B.V. All rights reserved.

### 1. Introduction

The subcellular localization of proteins is crucial for their physiological function [1,2]. Accordingly, the correct assignment of protein localization is a prerequisite to understand its biological function. The rapidly increasing amount of sequenced genomes generated an increasing need to predict the subcellular localization of proteins from available sequence data. Protein sorting mechanisms are dependent on the presence of certain targeting sequences, mostly in the N-terminal parts of the protein, as well as on the general properties of the protein, for example its hydrophobicity [3,4]. Based on the physico-chemical properties of its targeting peptides, several algorithms have been developed to predict the subcellular localization of proteins [5].

It is estimated that ~30% of all cellular proteins are targeted to membranes [6], which can be achieved via hydrophobic transmembrane domains, electrostatic interaction with membrane components or lipid modifications [7]. The two major mechanisms of lipid modification are acylation and prenylation. While prenylation modifies C-terminal ends of proteins by covalent attachment of a farnesyl or geranylgeranyl moiety to a cysteine residue [8],

protein acylation occurs mainly in the N-terminal part [9] and does therefore potentially interfere with protein sorting. Numerous proteins involved in signal transduction, are myristoylated and palmitoylated [9–11]. N-Myristoylation is the irreversible, co-translational attachment of myristic acid (C14:0) to an N-terminal glycine that is required at position 2 of a protein. Accordingly the mutation of this glycine (i.e. G2A) abolishes N-myristoylation of this protein. During translation, following the removal of the N-terminal methionine residue by a methionylaminopeptidase, myristic acid is linked to the N-terminal glycine via an amide bond by a N-myristoyltransferase (NMT) [12]. NMT recognizes a certain consensus motif - in many cases MGXXX(S/T) - which can be predicted by various programs [13–16]. In contrast, palmitoylation is the post-translational attachment of palmitic acid (C16:0) to N-terminal or internal cysteine residues of proteins via a reversible thioester bond catalyzed by a protein palmitoyltransferase (PPT). PPTs are much likely located at membranes, for example the ER or the Golgi apparatus [11], but the mechanism of their action is still unclear [17,18]. Internal palmitoylation of proteins is myristoylation-independent, whereas N-myristoylation is a prerequisite for N-terminal palmitoylation in most cases. Furthermore, palmitoylation is not restricted to the presence of a specific consensus motif [13].

Myristoylation facilitates only reversible membrane binding of proteins because the energy provided by myristate-lipid interaction alone is too low for a stable membrane attachment [19]. Palmitoylation in contrast is suggested to mediate a stable membrane anchoring, which corresponds to the fact that palmitoylated proteins are found almost exclusively in membrane preparations

Abbreviations: CDPK, calcium-dependent protein kinase; FNR, ferredoxin-NADP<sup>+</sup> reductase; PPDB, plant protein database; RCA, Rubisco activase

† Corresponding author. Fax: +43 1 4277 9528.

E-mail address: [Markus.Teige@Univie.ac.at](mailto:Markus.Teige@Univie.ac.at) (M. Teige).

<sup>1</sup> These authors contributed equally.

<sup>2</sup> Present address: Biozentrum der LMU Munchen, Department Biologie I - Botanik, Biozentrum GroBhaderner Str. 2-4, D-82152 Planegg-Martinsried, Germany.

whereas myristoylated proteins are also present in soluble protein extracts [9,10]. Stable membrane attachment of myristoylated proteins can only be achieved by additional factors that support membrane binding such as palmitoylation, interaction of a polybasic amino acid stretch with acidic phospholipids or interaction with a membrane protein [18,20]. Acylation of proteins can influence their membrane targeting, their structure and activity or their interaction with other proteins [21].

The physiological relevance of protein N-acylation has already been demonstrated for a number of different examples, particularly for proteins involved in signal transduction and stress response [7,22,23]. For example, the plasma membrane  $\text{Na}^+/\text{H}^+$  exchanger SOS1 is regulated in a calcium-dependent manner via the joint action of SOS3, a calcineurin B-like protein (CBL) and SOS2, a protein kinase in response to salt stress in Arabidopsis [24]. The salt-hypersensitive *sos3-1* mutant exhibits impaired SOS1 activity, which could only be complemented by wild-type SOS3, but not by the non-myristoylatable SOS3 G2A mutant [23,24]. Similarly, *cb11* mutants are hypersensitive to salt, and again only wild-type CBL1 but not CBL1 G2A was able to partially complement the mutant. Furthermore, CBL1 C3S in which the cysteine on position 3 has been exchanged for serine to prevent its palmitoylation, was also not able to complement the salt-sensitive phenotype of the *cb11* mutant. This indicates that palmitoylation as well as N-myristoylation has strong effects on the physiological function of signaling components [7]. However, the interference of protein N-acylation and other targeting mechanisms has so far almost been overlooked, particularly in the plant field. In 2005, Colombo et al. [25] reported that N-myristoylation determines dual targeting of mammalian NADH-cytochrome b5 reductase to the ER and to mitochondrial outer membranes by a mechanism of kinetic partitioning, and here we show that protein N-acylation is able to override other targeting signals like chloroplast targeting peptides, which has strong implications particularly for protein kinases.

## 2. Materials and methods

### 2.1. Cloning of genes and production of mutants

The coding sequences of all investigated genes were amplified by PCR from Arabidopsis cDNA. All analyzed mutants were created by PCR mutagenesis using 5' oligonucleotides carrying the indicated base changes. Subsequently, all constructs were sequenced and cloned into the vector pBAT [26], for the analysis of N-myristoylation, and into the vector pBIN-Basta, a derivative of pBIN 19 [27] carrying a C-terminal YFP fusion for localization studies.

### 2.2. In vitro myristoylation assays

Analysis of protein N-myristoylation was carried out exactly as previously described [28], using a cell free system (TNT Coupled Wheat Germ Extract System, Promega). In vitro translation was carried out either in the presence of 10  $\mu\text{Ci}$  of L-[ $^{35}\text{S}$ ] methionine (1175 Ci/mmol, Perkin-Elmer) for total protein labelling, or 50  $\mu\text{Ci}$  of [9,10- $^3\text{H}$ ]-labelled myristic acid (60 Ci/mmol, American Radiolabeled Chemicals). Reaction products were separated on 12% (w/v) SDS-polyacrylamide gels and incubated with autoradiography intensifier (Amersham) before detection on X-ray film.

### 2.3. YFP localization studies

The localization of proteins fused to YFP was investigated by confocal laser scanning microscopy after agrobacterium-mediated transfection of *Nicotiana tabacum* epidermal leaf cells two days after transfection as described previously [28].

### 2.4. Western blotting

After microscopy, transfected leaves of *N. tabacum* expressing the YFP-fusion proteins were ground in liquid nitrogen. Proteins were extracted in denaturing extraction buffer (0.175 M Tris-HCl pH 8.8, 5% SDS, 15% glycerol, 0.2 M DTT), precipitated with four volumes of cold acetone and resuspended in standard SDS-PAGE loading buffer. Western blot was carried out as described previously [29], and detection was carried out with anti-GFP primary antibody (1:1000 dilution, Roche) and anti-mouse secondary antibody (1:10 000 dilution, GE healthcare). Western blots were developed with SuperSignal West Pico Chemiluminescent Substrate (Pierce). Protein amounts were equalized in order to have similar signal strengths.

## 3. Results

### 3.1. N-Myristoylation affects particularly the subcellular localization of protein kinases

Initially we set out to identify chloroplast localized protein kinases in a bioinformatics based approach using multiple prediction methods. To experimentally test the in vivo localization of our selected candidate genes, we generated C-terminal YFP-fusion proteins and studied their localization by laser scanning microscopy after transient expression in tobacco leaves. Disappointingly, none out of the 10 protein kinases we tested appeared in chloroplasts, instead most of them (8/10) showed a predominant extra-plastidic membrane localization. Typical results are exemplified in Fig. 1B for four serine/threonine-specific protein kinases: Kin1 (At1g14370), Kin2 (At2g02800), Kin3 (At2g17220), and Kin4 (At4g35600), which were all highly predicted to be targeted to chloroplasts by at least three different prediction methods. The N-terminal sequences of these kinases are shown in Fig. 1C including their TargetP score for chloroplast targeting. Considering that the known true positive rate of chloroplast prediction by TargetP in Arabidopsis is ~86%, whereas the false positive rate of prediction is ~35% [30] this was a very unexpected result. A similar observation has also been published by Schliebner et al. [31], who analyzed the localization of nine different protein kinases, which were also chloroplast predicted by several algorithms, and found only two of them localized in the chloroplast. As the overlap between the two studies is only one kinase (Kin3, At2g 17220), there is now a total number of 18 protein kinases with high prediction for chloroplast localization by different methods of which only two (11%) appeared in chloroplasts. This prompted us to have a closer look at the N-terminal sequences where we noticed that most (9/10) of the kinases we studied contained motifs for N-myristoylation and many (8/10) also cysteines for additional palmitoylation (Fig. 1C).

Therefore, we extended our analysis to the entire Arabidopsis proteome and asked whether N-myristoylation of protein kinases might be a more general phenomenon to regulate their subcellular localization. Strikingly, 7% of all 965 Arabidopsis protein kinases [32] but only 1.2% (320 proteins) of all other 26270 proteins (TAIR8 release) were predicted to be myristoylated using the myristoylation prediction program Myrist Predictor (<http://plantsp.genomics.purdue.edu/html/myrist.html>) [16]. On the other hand, only 0.2% (2 proteins) out of the ~1100 experimentally confirmed chloroplast proteins listed in the plant proteome database (PPDB) [33] are predicted to be myristoylated by the Myrist Predictor (Fig. 1D). When we looked more specifically at predicted chloroplast-localized protein kinases we found that 36.8% of those were predicted to be myristoylated whereas only 22.8% of all predicted chloroplast proteins were also predicted to be myristoylated. Looking at the

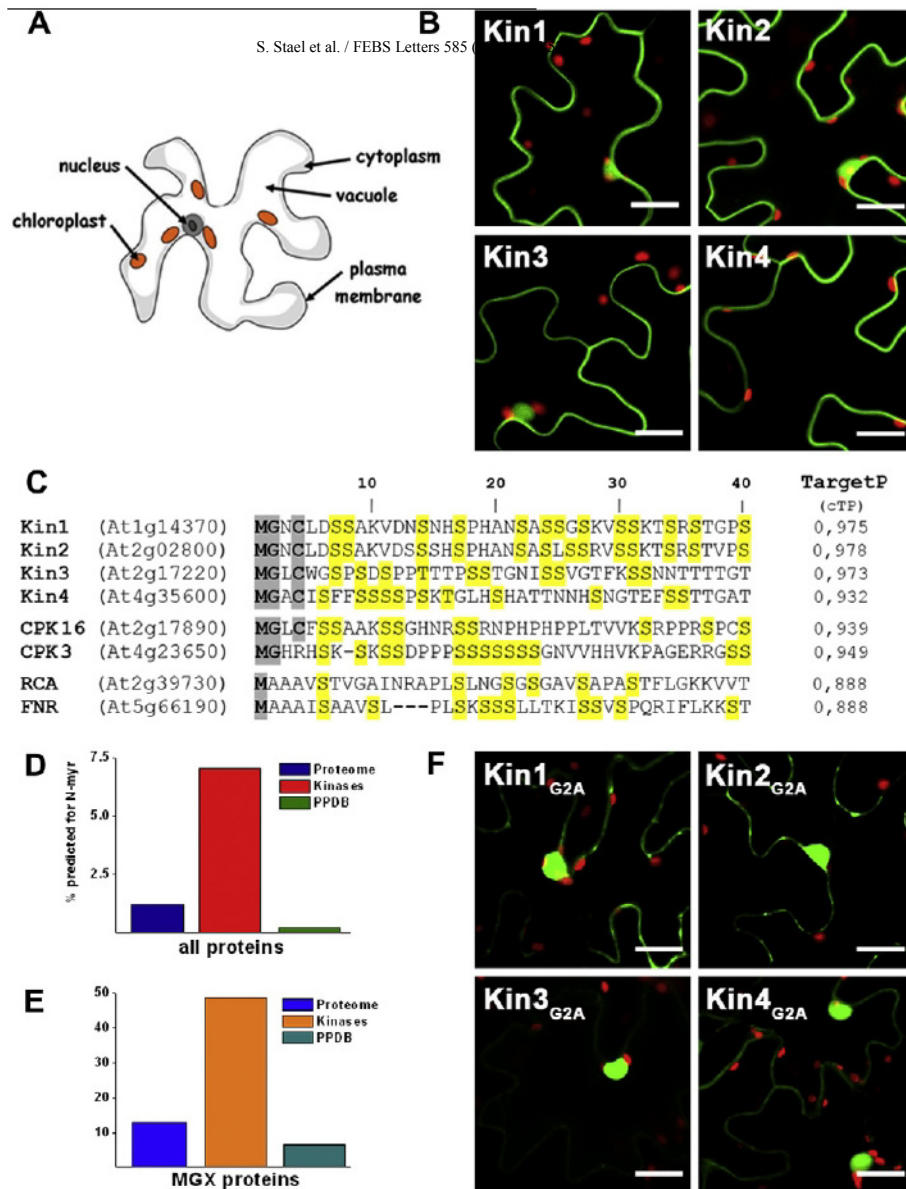


Fig. 1. (A) Scheme of a leaf epidermal cell in which the vacuole fills most of the intracellular space. (B) Confocal microscopy images of tobacco epidermal leaf cells expressing YFP-fusions of Kin1-4 (kinases, green; chloroplasts, red; scale bar = 20  $\mu$ m). (C) Alignment of the N-terminal 40 amino acids of Kin 1-4, CPK3 and 16, RCA and FNR. TargetP score indicates chloroplast prediction. Residues important for myristoylation and palmitoylation are shaded in grey and serines in yellow to illustrate their enrichment. (D) Comparison of myristoylation prediction for protein kinases compared to the entire Arabidopsis proteome and the chloroplast proteome (PPDB). (E) The same analysis as in (D) but considering only proteins starting with MGX. (F) Confocal microscopy images of tobacco epidermal leaf cells expressing YFP-fusions of the G2A versions of Kin1-4.

experimentally identified proteins this difference becomes even more obvious: In total, 31 chloroplast annotated proteins in the PPDB database [30] have a glycine at position 2, and only two of them (i.e. At4g03415 and At2g25840) are predicted to be myristoylated. An alignment of the N-termini of 898 annotated chloroplast proteins revealed that clearly the penultimate position of these known chloroplast proteins is typically an Ala (56% of cases), Ser (10%) or Pro (7%) and not a Gly [30]. In comparison, 12.9% of all Arabidopsis proteins starting with a MGX sequence are predicted to be myristoylated compared to 48.6% of all protein kinases (Fig. 1E). The two experimentally identified chloroplast proteins that are predicted to be myristoylated are a protein phosphatase (At4g03415) and a tRNA synthetase (At2g25840) that has been shown to be dually targeted to chloroplasts and mitochondria [34]. However, it is still unclear whether these two proteins are really myristoylated in vivo. We could confirm that Kin1 and Kin3 are indeed N-myristoylated in vitro (Supplementary Fig. 1)

and therefore continued to test the effect of N-myristoylation on the chloroplast predicted protein kinases Kin1, Kin2, Kin3, and Kin4 in vivo. We generated non-myristoylatable G2A mutants of those kinases and studied their localization in tobacco epidermal leaf cells. As expected, the localization of all four candidate protein kinases was altered, when myristoylation was abolished (Fig. 1F). The membrane localization was drastically reduced and the proteins accumulated strongly in the nucleus compared to the wild-type proteins but not in the chloroplast as we would have expected.

### 3.2. N-Acylation overrides chloroplast localization of a calcium-dependent protein kinase (CDPK)

A much more striking effect of N-myristoylation on the subcellular localization of a protein kinase became obvious when analyzing the calcium-dependent protein kinase CPK16 (AT2G17890).



520

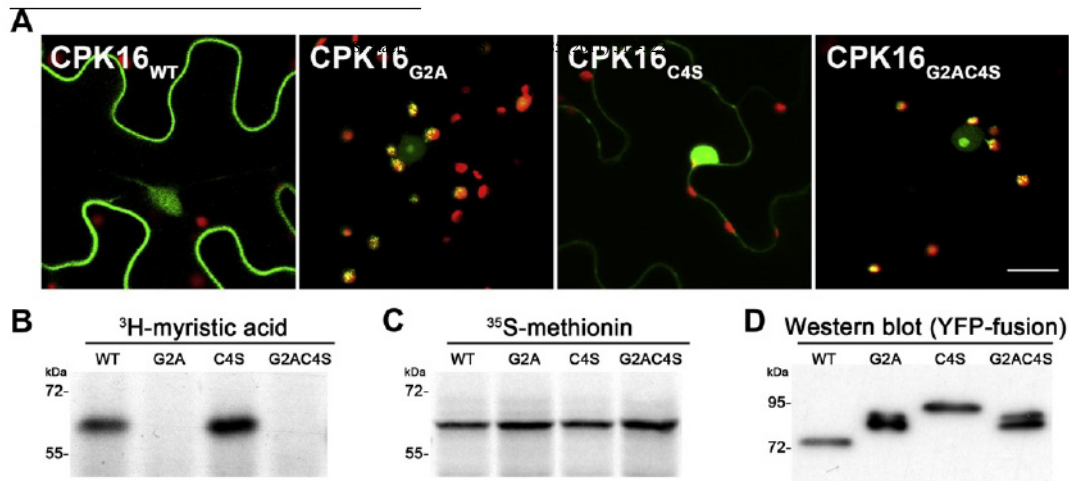


Fig. 2. (A) Confocal microscopy images of CPK16 YFP-fusion proteins and mutant versions as indicated in image. The size of the scale bar is 20  $\mu$ m. (B) Autoradiograph of myristoylation assays of CPK16 and mutants. (C) Autoradiograph of the translation controls. (D) Western blot of CPK16 YFP-fusion proteins and mutant versions from infiltrated tobacco leaves.

CPK16 is also highly predicted to be localized in the chloroplast and harbors N-myristoylation and palmitoylation sites (Fig. 1C). Consistent with its predicted N-acylation, CPK16 appeared predominantly at the plasma membrane in the wild-type form (Fig. 2A). CPK16 is efficiently myristoylated in vitro (Fig. 2B and C), and intriguingly, CPK16 was relocated to chloroplasts when the glycine on position 2 was exchanged for an alanine (Fig. 2A). This implies that myristoylation interferes with chloroplast localization. As CPK16 harbors both an N-terminal myristoylation and palmitoylation site, we set out to study the interference of these two modifications with chloroplast localization in more detail. Therefore, the CPK16 mutants C4S and G2AC4S were created in addition to the G2A mutant. They have the cysteine on position 4 exchanged for serine and thus cannot be palmitoylated anymore. Analysis of YFP-fusion proteins in infiltrated tobacco leaves revealed that the C4S mutant, which can still be myristoylated but not palmitoylated, was not targeted to chloroplasts but showed a much stronger nuclear accumulation instead (Fig. 2A). In contrast, the G2AC4S mutant was localized again in chloroplasts, thus suggesting that myristoylation alone inhibits chloroplast localization of CPK16 (Fig. 2A). As expected, only wild-type CPK16 and the C4S mutant could be myristoylated in vitro as shown by the incorporation of <sup>3</sup>H-labeled myristic acid (Fig. 2B), while all proteins were translated with similar efficiencies (Fig. 2C). Notably the G2A and the G2AC4S mutant showed also a stronger accumulation in the nucleolus as compared to the wild-type. To rule out that the exchange of amino acids led to chloroplast import inhibition due to perturbation of the chloroplast transit peptide, additional control mutations were generated. A G2V version was created, as alanine is known to be the most frequently occurring amino acid on position 2 of chloroplast proteins, which might be a possible chloroplast targeting determinant [30,35]. Nevertheless, CPK16 G2V still localized to chloroplasts and showed also nuclear accumulation (Supplementary Fig. 2). Furthermore, we wanted to back-up our microscopical studies with a biochemical assay. Therefore we extracted total protein extracts of the tobacco leaves expressing the YFP-fusion proteins and analyzed them by Western blotting using an antibody directed against GFP. The wild-type version of CPK16 appeared at a molecular mass of about 75 kDa (Fig. 2D), which was unexpected, but seemed not to be caused by chloroplast import-related processing. Comparison with in vitro translated CPK16-YFP (Supplementary Fig. 1C) revealed that the "full-length" (non-processed) protein appeared at a molecular mass of 93 kDa

like the C4S mutant. Most importantly, the G2A and G2AC4S mutants of CPK16-YFP appeared at 85 kDa. TargetP or ChloroP ([www.cbs.dtu.dk/services/](http://www.cbs.dtu.dk/services/)) predicted a targeting peptide of 75 amino acids for CPK16, which would correspond to 8,3 kDa. Thus, the observed size difference of about 8 kDa would be in perfect agreement with the removal of the chloroplast transit peptide in these mutants after import into the chloroplast, demonstrating that CPK16 harbors a canonical targeting signal that is masked by N-myristoylation.

### 3.3. Artificial N-acylation of chloroplast localized proteins inhibits their import

Based on these results we asked, whether it is possible to prevent import of canonical chloroplast proteins by the artificial introduction of N-myristoylation and palmitoylation. Therefore we selected the chloroplast proteins ferredoxin-NADP<sup>+</sup> reductase (FNR) (At5g66190) and Rubisco activase (RCA) (At2g39730), which are both lacking a glycine on position 2 and therefore cannot be myristoylated per se. FNR and RCA show exclusive chloroplast localization as YFP-fusion proteins (Fig. 3A and E). However, according to the Myrist Predictor, the exchange of alanine on position 2 for a glycine results in the introduction of a strong myristoylation consensus motif in both proteins. Consequently, both FNR A2G and RCA A2G could be efficiently myristoylated in vitro (Fig. 3B, C and F, G). Interestingly, YFP-fusion proteins of FNR A2G and RCA A2G were still localized predominantly in chloroplasts and only a minor fraction appeared outside of chloroplasts (Fig. 3A and E). Therefore we introduced additional palmitoylation sites by generating A2GA4C mutants of FNR and RCA to test the effect of both N-terminal modifications on chloroplast import. Both mutants were still myristoylated in vitro, indicating that introduction of the cysteine did not eliminate the myristoylation consensus motif (Fig. 3B, C and F, G). But now the analysis of YFP-fusion proteins of FNR A2GA4C and RCA A2GA4C in tobacco leaves revealed that a great part of those mutants was not localized in the chloroplast but showed a strong membrane attachment instead (Fig. 3A and E). This indicates that introduction of myristoylation and palmitoylation impedes chloroplast localization in these cases. To exclude again that the observed changes in localization are caused by mutating the critical alanine at position 2 or by introducing a cysteine at position 4, we generated an A2V and A2VA4S mutant for RCA. Nevertheless, both mutants still showed chloroplast

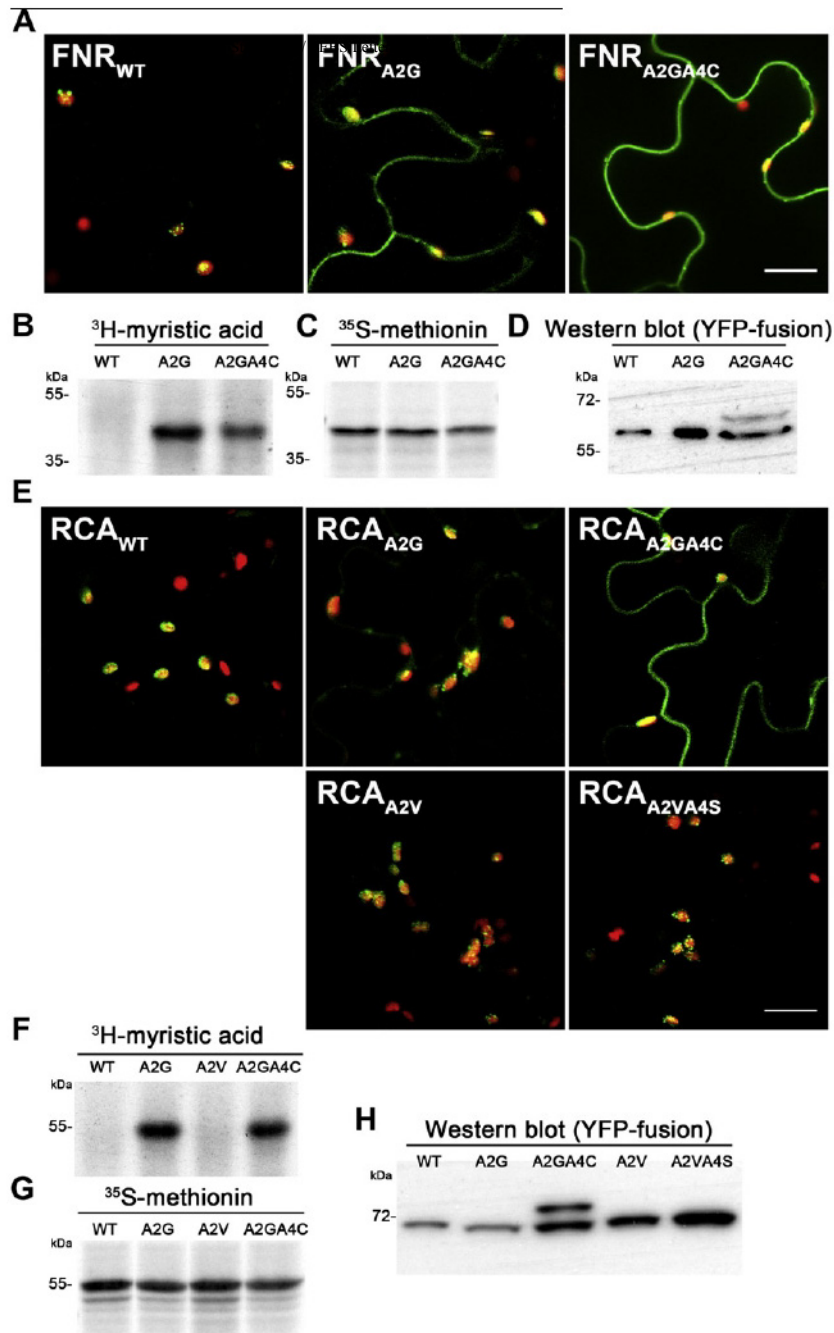


Fig. 3. (A, E) Confocal microscopy images of FNR and RCA YFP-fusion proteins and mutant versions, respectively (as indicated in image). The scale bar indicates 20  $\mu\text{m}$ . (B, F) Autoradiograph of myristoylation assays of FNR and RCA with their corresponding mutants. (C-G) Autoradiograph of translation controls of FNR and RCA with their corresponding mutants, respectively. (D, H) Western blot of FNR and RCA YFP-fusion proteins and the corresponding mutant versions from infiltrated tobacco leaves.

localization as shown in Fig. 3E. These results clearly indicated that chloroplast localization of FNR, and RCA could efficiently be inhibited by N-terminal acylation.

As already done for CPK16 we analyzed also protein extracts from infiltrated leaves by Western-blotting using the GFP antibody. These results confirmed the observations from fluorescence microscopy. We found that both A2G mutants were still perfectly processed and no unprocessed precursor was detectable in Western blots (Fig. 3D and H), which is in agreement with the observed predominant chloroplast localization. However, the introduction of an additional palmitoylation site, lead to the accumulation of unprocessed precursor in both A2GA4C mutants (Fig. 3D and H). This indicated that for FNR and RCA

the N-terminal palmitoylation prevents their chloroplast localization.

#### 4. Discussion

We noticed that currently all methods for prediction of subcellular protein localization do not consider N-terminal acylation. While this weakness seems to be of minor importance in the analysis of diverse protein sets, it becomes particularly important for protein kinases. At the proteome wide scale, they seem to be much more affected as other proteins, notably 48.6% of all protein kinases starting with MGX are predicted to be N-myristoylated. On the other hand, only two proteins with predicted N-myristoylation

have been experimentally identified in chloroplasts. Our analysis of predicted chloroplast-localized protein kinases and their G2A mutants clearly showed that N-myristoylation strongly affects their localization, leading to a predominant extra-plastidic membrane attachment of the (wild-type) proteins. Moreover, YFP localization studies on CPK16, FNR, RCA and their acylation mutants revealed that myristoylation as well as palmitoylation is able to interfere with chloroplast localization. However, it seems that this is not a general mechanism but has to be analyzed for each protein separately. In the case of CPK16 abolishing myristoylation in the G2A mutant led to its accumulation in chloroplasts, but removal of only the palmitoylation site in the C4S mutant had no effect on the chloroplast localization and rather affected nuclear accumulation. Thus, we concluded that myristoylation alone did not inhibit chloroplast import of CPK16 *in vivo*. In contrast, abolishing N-myristoylation of CPK3 (At4g23650), another myristoylated CDPK which is also highly predicted to be targeted to chloroplasts (Fig. 1C), did not lead to chloroplast localization as we have shown previously [29].

The artificial introduction of N-myristoylation sites in FNR and RCA in the A2G mutants did only slightly influence chloroplast targeting. Only the additional introduction of palmitoylation sites in the A2GA4C mutants led to a strong accumulation of the proteins outside the chloroplast and appearance of the unprocessed precursor in Western blots from leaf extracts. It seems that in these cases inhibition of chloroplast localization must primarily be attributed to palmitoylation. An explanation therefore would be that acylation does not inhibit the passage of proteins through the chloroplastic TOC-TIC apparatus *per se*. Acylation may rather direct proteins to different compartments before they can be recognized by chloroplast import components *in vivo*. For example it is possible that myristoylated CPK16 is recognized by SRP, co-translationally targeted to the ER where it is palmitoylated and subsequently transported to the plasma membrane. In contrast, non-myristoylated CPK16 G2A would not be recognized by SRP and therefore, after completed translation, CPK16 G2A would be available for components of the chloroplast import machinery. Altogether, our studies show that N-terminal protein acylation offers an additional layer to regulate protein targeting, which is of particular importance for protein kinases and needs clearly to be considered in the context of potential organellar targeting.

#### Acknowledgements

We thank Helga Waltenberger for excellent technical support. This work has been funded by the Austrian GEN-AU program in the ERA-PG project CROPP (Project No. 818514), and by the EU in the Marie-Curie ITN COSI (GA 215-174).

#### Appendix A. Supplementary data

Supplementary data associated with this article can be found, in the online version, at doi:10.1016/j.febslet.2011.01.001.

#### References

- [1] Scott, M.S., Calafell, S.J., Thomas, D.Y. and Hallett, M.T. (2005) Refining protein subcellular localization. *PLoS Comput. Biol.* 1, e66.
- [2] Lunn, J.E. (2007) Compartmentation in plant metabolism. *J. Exp. Bot.* 58, 35-47.
- [3] Blobel, G. (1980) Intracellular protein topogenesis. *Proc. Natl. Acad. Sci. USA* 77, 1496-1500.
- [4] von Heijne, G. (1981) On the hydrophobic nature of signal sequences. *Eur. J. Biochem.* 116, 419-422.
- [5] Emanuelsson, O. and von Heijne, G. (2001) Prediction of organellar targeting signals. *Biochim. Biophys. Acta* 1541, 114-119.
- [6] Kleinschmidt, J.H. (2003) Membrane proteins - introduction. *Cell. Mol. Life Sci.* 60, 1527-1528.
- [7] Baticic, O., Sorek, N., Schultke, S., Yalovsky, S. and Kudla, J. (2008) Dual fatty acyl modification determines the localization and plasma membrane targeting of CBL/CIPK Ca<sup>2+</sup> signaling complexes in *Arabidopsis*. *Plant Cell* 20, 1346-1362.
- [8] Zhang, F.L. and Casey, P.J. (1996) Protein prenylation: molecular mechanisms and functional consequences. *Annu. Rev. Biochem.* 65, 241-269.
- [9] Towler, D.A., Gordon, J.I., Adams, S.P. and Glaser, L. (1988) The biology and enzymology of eukaryotic protein acylation. *Annu. Rev. Biochem.* 57, 69-99.
- [10] Taniguchi, H. (1999) Protein myristoylation in protein-lipid and protein-protein interactions. *Biophys. Chem.* 82, 129-137.
- [11] Iwanaga, T., Tsutsumi, R., Noritake, J., Fukata, Y. and Fukata, M. (2009) Dynamic protein palmitoylation in cellular signaling. *Prog. Lipid Res.* 48, 117-127.
- [12] Farazi, T.A., Waksman, G. and Gordon, J.I. (2001) The biology and enzymology of protein N-myristoylation. *J. Biol. Chem.* 276, 39501-39504.
- [13] Sorek, N., Bloch, D. and Yalovsky, S. (2009) Protein lipid modifications in signaling and subcellular targeting. *Curr. Opin. Plant Biol.* 12, 714-720.
- [14] Maurer-Stroh, S., Eisenhaber, B. and Eisenhaber, F. (2002) N-Terminal N-myristoylation of proteins: prediction of substrate proteins from amino acid sequence. *J. Mol. Biol.* 317, 541-557.
- [15] Bologna, G., Yvon, C., Duvaud, S. and Veuthey, A.L. (2004) N-Terminal myristoylation predictions by ensembles of neural networks. *Proteomics* 4, 1626-1632.
- [16] Podell, S. and Gribskov, M. (2004) Predicting N-terminal myristoylation sites in plant proteins. *BMC Genomics* 5, 37.
- [17] Yalovsky, S., Rodr Guez-Concepcion, M. and Gruissem, W. (1999) Lipid modifications of proteins - slipping in and out of membranes. *Trends Plant Sci.* 4, 439-445.
- [18] Weber, C.N. (2006) Molekulare determinanten für die palmitoylierung integraler membranproteine. Ph.D. thesis. In Institut für Immunologie und Molekularbiologie (Eds). Freie Universität Berlin, Berlin.
- [19] Peitzsch, R.M. and McLaughlin, S. (1993) Binding of acylated peptides and fatty acids to phospholipid vesicles: pertinence to myristoylated proteins. *Biochemistry* 32, 10436-10443.
- [20] Murray, D., Ben-Tal, N., Honig, B. and McLaughlin, S. (1997) Electrostatic interaction of myristoylated proteins with membranes: simple physics, complicated biology. *Structure* 5, 985-989.
- [21] Beven, L., Adenier, H., Kichenama, R., Homand, J., Redeker, V., Le Caer, J.P., Ladant, D. and Chopineau, J. (2001) Ca<sup>2+</sup>-myristoyl switch and membrane binding of chemically acylated neurocalcins. *Biochemistry* 40, 8152-8160.
- [22] Pierre, M., Traverso, J.A., Boisson, B., Domenichini, S., Bouchez, D., Giglione, C. and Meinel, T. (2007) N-Myristoylation regulates the SnRK1 pathway in *Arabidopsis*. *Plant Cell* 19, 2804-2821.
- [23] Ishitani, M., Liu, J., Halfter, U., Kim, C.S., Shi, W. and Zhu, J.K. (2000) SOS3 function in plant salt tolerance requires N-myristoylation and calcium binding. *Plant Cell* 12, 1667-1678.
- [24] Qiu, Q.S., Guo, Y., Dietrich, M.A., Schumaker, K.S. and Zhu, J.K. (2002) Regulation of SOS1, a plasma membrane Na<sup>+</sup>/H<sup>+</sup> exchanger in *Arabidopsis thaliana*, by SOS2 and SOS3. *Proc. Natl. Acad. Sci. USA* 99, 8436-8441.
- [25] Colombo, S., Longhi, R., Alcaro, S., Ortuso, F., Sprocati, T., Flora, A. and Borgese, N. (2005) N-Myristoylation determines dual targeting of mammalian NADH-cytochrome b5 reductase to ER and mitochondrial outer membranes by a mechanism of kinetic partitioning. *J. Cell Biol.* 168, 735-745.
- [26] Annweiler, A., Hipskind, R.A. and Wirth, T. (1991) A strategy for efficient *in vitro* translation of cDNAs using the rabbit beta-globin leader sequence. *Nucleic Acids Res.* 19, 3750.
- [27] Bevan, M. (1984) Binary *Agrobacterium* vectors for plant transformation. *Nucleic Acids Res.* 12, 8711-8721.
- [28] Benetka, W. et al. (2008) Experimental testing of predicted myristoylation targets involved in asymmetric cell division and calcium-dependent signalling. *Cell Cycle* 7, 3709-3719.
- [29] Mehlmer, N., Wurzinger, B., Stael, S., Hofmann-Rodrigues, D., Csaszar, E., Pfister, B., Bayer, R. and Teige, M. (2010) The Ca<sup>2+</sup>-dependent protein kinase CPK3 is required for MAPK-independent salt-stress acclimation in *Arabidopsis*. *Plant J.* 63, 484-498.
- [30] Zybailov, B., Rutschow, H., Friso, G., Rudella, A., Emanuelsson, O., Sun, Q. and van Wijk, K.J. (2008) Sorting signals, N-terminal modifications and abundance of the chloroplast proteome. *PLoS One* 3, e1994.
- [31] Schliebner, I., Pribil, M., Zuhlke, J., Dietzmann, A. and Leister, D. (2008) A survey of chloroplast protein kinases and phosphatases in *Arabidopsis thaliana*. *Curr. Genomics* 9, 184-190.
- [32] Gribskov, M., Fana, F., Harper, J., Hope, D.A., Harmon, A.C., Smith, D.W., Tax, F.E. and Zhang, G. (2001) PlantsP: a functional genomics database for plant phosphorylation. *Nucleic Acids Res.* 29, 111-113.
- [33] Sun, Q., Zybailov, B., Majeran, W., Friso, G., Olinares, P.D. and van Wijk, K.J. (2009) PPDB, the plant proteomics database at cornell. *Nucleic Acids Res.* 37, D969-D974.
- [34] Duchene, A.M. et al. (2005) Dual targeting is the rule for organellar aminoacyl-tRNA synthetases in *Arabidopsis thaliana*. *Proc. Natl. Acad. Sci. USA* 102, 16484-16489.
- [35] Pujol, C., Marechal-Drouard, L. and Duchene, A.M. (2007) How can organellar protein N-terminal sequences be dual targeting signals? *In silico* analysis and mutagenesis approach. *J. Mol. Biol.* 369, 356-367.

### **2.3. Paper 3 - Arabidopsis calcium-binding mitochondrial carrier proteins as potential facilitators of mitochondrial ATP-import and plastid SAM-import**

Simon Stael<sup>1</sup>, Agostinho G. Rocha<sup>2</sup>, Alan J. Robinson<sup>3</sup>, Przemyslaw Kmiecik<sup>1</sup>, Ute C. Vothknecht<sup>2,4</sup>, and Markus Teige<sup>1\*</sup>

<sup>1</sup>Department of Biochemistry and Cell Biology, MFPL, University of Vienna,  
Dr. Bohrgasse 9, A-1030 Vienna. Austria.

<sup>2</sup>Department of Biology I, Botany, LMU Munich, Großhaderner Str. 2,  
D-82152 Planegg-Martinsried. Germany.

<sup>3</sup>The Medical Research Council, Mitochondrial Biology Unit, Hills Road, Cambridge  
CB2 0XY, United Kingdom.

<sup>4</sup>Center for Integrated Protein Science (Munich) at the Department of Biology of the  
LMU Munich, D-81377 Munich, Germany.

\* To whom correspondence should be addressed: E-mail: markus.teige@univie.ac.at  
phone: +43-1-4277-529811, fax: +43-1-4277-9528

Key words: chloroplast, mitochondria, mitochondrial carrier protein, calcium-binding, ATP-phosphate carrier, SAM transporter

Abbreviations: APC, ATP/phosphate carrier; BKA, bongkrelic acid; MCF, mitochondrial carrier family; SAM, S-adenosyl methionine; SAMTL, SAM transporter-like; TM, transmembrane domain; YFP, yellow fluorescent protein

**Abstract**

Chloroplasts and mitochondria are central to crucial cellular processes in plants and contribute to a whole range of metabolic pathways. The use of calcium ions as a secondary messenger in and around organelles is increasingly appreciated as an important mediator of plant cell signaling, enabling plants to develop or to acclimatize to changing environmental conditions. Here, we have studied the four calcium-dependent mitochondrial carriers that are encoded in the *Arabidopsis* genome. An unknown substrate carrier, which was previously found to localize to chloroplasts, is proposed to present a calcium-dependent *S*-adenosyl methionine carrier. For three predicted ATP/phosphate carriers, we present experimental evidence that they can function as mitochondrial ATP-importers.

## Introduction

Plants can react rapidly to a changing environment or stress conditions by employing immediate signaling pathways, such as calcium signaling. This involves the generation of specific information in transient or oscillating spikes of free calcium ions that are decoded by calcium binding proteins ultimately leading to a physiological change of the plant (recently reviewed in (DeFalco et al., 2010; Dodd et al., 2010; Kudla et al., 2010)). Canonical calcium binding proteins contain EF-hands with a high affinity for calcium ions ( $\text{Ca}^{2+}$ ) (Kretsinger and Nockolds, 1973; Gifford et al., 2007). Fluxes of free  $\text{Ca}^{2+}$  have been reported to occur upon a myriad of stresses and developmental cues and take place mainly in the cytoplasm (McAinsh and Pittman, 2009). However,  $\text{Ca}^{2+}$  fluxes and  $\text{Ca}^{2+}$ -dependent signaling pathways in and around plant organelles, such as mitochondria and chloroplasts have also been reported (Bussemer et al., 2009). In chloroplasts,  $\text{Ca}^{2+}$  fluxes have been measured upon the transition from light to dark (Sai and Johnson, 2002) and in mitochondria, they were elicited by a range of stimuli, including application of  $\text{H}_2\text{O}_2$ , touch stimulation and anoxia (Subbaiah et al., 1998; Logan and Knight, 2003). An evolutionary conserved enzyme of the bacterial stringent response, which contains two EF-hands (CRSH) and a non-canonical calcium binding protein that influences the cytosolic calcium fluxes observed during stomatal closure (CaS) localize to chloroplasts (Han et al., 2003; Masuda et al., 2008; Nomura et al., 2008; Vainonen et al., 2008; Weinl et al., 2008). In addition, the mitochondrial type II NAD(P)H:quinone oxidoreductases contain EF-hands and are  $\text{Ca}^{2+}$ -regulated (Geisler et al., 2007). Despite these initial reports, only a few more  $\text{Ca}^{2+}$ -binding proteins have been found in these organelles and even less data exist on the roles that  $\text{Ca}^{2+}$  signaling in mitochondria or chloroplasts play in adjusting the physiology of the plant to its changing environment.

The mitochondrial carrier family (MCF) contains transmembrane transporter proteins that transport a diverse set of substrates such as ATP/ADP (Fiore et al., 1998), citrate (Kaplan et al., 1995) and glutamate (Fiermonte et al., 2002) (for a complete overview see (Palmieri et al., 2011)). Originally they were found to localize exclusively to mitochondria (Palmieri, 1994), however, in plants certain prominent members are also located in other organelles. For example, the *S*-adenosylmethionine (SAM) transporter SAMT1 localizes to chloroplasts (Bouvier et al., 2006) and the peroxisomal ATP/ADP translocases PNC1 and PNC2 localize to peroxisomes (Linka et al., 2008). MCF proteins have three tandemly repeated homologous domains (Wohlrab, 2010), each containing two

transmembrane helices that form a pore lined with specific amino acids that determine the substrate specificity (Robinson and Kunji, 2006). This protein family is conserved in eukaryotes and contains 35 putative members in *Saccharomyces cerevisiae*, about 50 in *Homo sapiens* and 58 in *Arabidopsis thaliana*. The rare examples found in pathogenic prokaryote genomes appear to be pseudogenes resulting from horizontal gene transfer. The high conservation of functional residues between species allows the predictive assignment of substrate specificity based on protein homology (Palmieri et al., 2011). Interestingly, the aspartate/glutamate and ATP-Mg/P<sub>i</sub> carrier subfamilies, which have been described in yeast and human have EF-hands containing N-terminal protein extensions and their transport activities are Ca<sup>2+</sup>-dependent (Chen, 2004; Contreras et al., 2007; Traba et al., 2008; Marmol et al., 2009). Out of our interest for calcium signaling in organelles we set out to describe and characterize the four EF-hand containing MCF proteins that are present in the Arabidopsis genome.

## Material and methods

### Plant material and yeast strains

Tobacco plants (*Nicotiana tabacum* cv. Petite Havana SR1) were grown in soil for approximately 6-7 weeks under short day conditions (8h light) in a climate chamber with a light strength of 150  $\mu\text{M}$  photons/m<sup>2</sup> sec. Yeast strains were W303 (MAT $\alpha$  leu2-3,112 trp1-1 can1-100 ura3-1 ade2-1 his3-11,15) and  $\Delta$ sal1 (as W303, but, AAC1-3,  $\Delta$ sal1::kanMX4). *Agrobacterium tumefaciens* strain was AGL1 (recA::bla pTiBo542 $\Delta$ T Mop<sup>+</sup> CbR; Lazo et al, 1991).

### Computational procedures

Sequences of plant orthologs from SAMTL (At2g35800) and APC1 (At5g61810.1), APC2 (At5g51050), and APC3 (At5g07320) were retrieved from the Phytozome database (<http://www.phytozome.net/>). Algae sequences and the sequences from *Saccharomyces cerevisiae* and *Homo sapiens* were obtained from a BLAST search of the NCBI nr protein sequence database (<http://blast.ncbi.nlm.nih.gov/Blast.cgi>) (Duy et al., 2007). Sequences were screened with ScanProsite (<http://www.expasy.org/tools/scanprosite/>) (de Castro et al., 2006) and only those containing EF-hands were considered for further evaluation. Transmembrane domains were predicted by Aramemnon (<http://aramemnon.botanik.uni-koeln.de/>) (Schwacke et al., 2003). Sequences (NCBI protein accession numbers listed in suppl. Table1) were aligned with the ClustalW2 program

(<http://www.ebi.ac.uk/Tools/msa/clustalw2/>) (Pohlmeier et al., 1998) and visualized as phylogenetic tree. For substrate prediction of SAMTL, all plant and algae orthologs were aligned and the relative positions of the functional residues were compared to the sequence of the bovine ATP/ADP carrier. Residues that line the carrier cavity were identified in particular the contact points of the predicted substrate binding site and the salt bridge networks. These were compared to known transporters to predict the nature of the substrate and the translocation mechanism (Robinson and Kunji, 2006; Kunji and Robinson, 2010).

### **Subcellular localization analysis of YFP-fusion proteins**

Full-length coding sequences of APC1, 2 and 3 were cloned in the plant binary expression vector pBIN19 containing a C-terminal YFP-tag, transformed into AGL1 and infiltrated in tobacco leaves as described previously (Benetka et al., 2008). Tobacco protoplasts were prepared from infiltrated leaves two days after transfection according to (Yoo et al., 2007) and stained with MitoTracker Red CMXRos (Molecular Probes; final concentration of 100 nM). Images were taken on a confocal laser scanning microscope Zeiss 510 model, with a Plan-Neofluar 40x/1.3 oil DIC objective.

### **Radiolabeled calcium overlay assays**

Assays were performed as described earlier (Maruyama et al., 1984) with minor modifications using recombinant proteins expressed in *Escherichia coli*. The N-terminal parts of SAMTL (amino acids 1-424), APC1 (1-187), APC2 (1-200) and APC3 (1-188) were expressed and purified with the IMPACT<sup>TM</sup> System (New England Biolabs) that allows the purification of untagged proteins. After purification 2.5 and 0.5 µg of protein were spotted on PVDF membranes. As controls, the recombinant EF-hand protein aequorin and commercially available bovine serum albumin (BSA, New England Biolabs) were used. Membranes were incubated three times for 20 min at room temperature with buffer containing 60 mM KCl, 5 mM MgCl<sub>2</sub>, 60 mM imidazole-HCl (pH 6.8), before incubation in the same buffer containing 0.1 µM <sup>45</sup>CaCl<sub>2</sub> (13.90 mCi/mg; Perkin Elmer) and 0.1 mM 'cold' CaCl<sub>2</sub> for 10 min at room temperature. Membranes were subsequently washed for 5 minutes with 50% ethanol. Autoradiographs were visualized on a FUJI FLA-3000 (FUJIFILM). Membranes were subsequently stained with amido black.



**Yeast functional complementation assay**

Full-length coding sequences of APC1, 2 and 3 were cloned in the yeast expression vector YEp351 behind the constitutive methionine-repressible promoter (pMet25) and were transformed into W303 and  $\Delta$ sal1 yeast strains. An empty vector served as a negative control. Cultures were grown aerobically to an OD600 of 1.0 and were subsequently diluted to an OD600 of 0.1, 0.01, and 0.001. 5  $\mu$ l of each dilution were plated on SD-Leu plates (pH4.0) containing 0.0, 0.5 or 1  $\mu$ M bongkreikic acid (BKA, Enzo Life Sciences) and the plates were incubated for 2 days at 30°C according to (Laco et al., 2010).

**Results****The calcium-binding MCF proteins form two phylogenetically distinct groups in plants**

In a proteomic approach aiming at the identification of novel  $\text{Ca}^{2+}$ -binding proteins in the chloroplast, we identified recently a member of the MCF with unknown function containing one EF-hand, to be targeted to the chloroplast envelope and called it SUC (substrate carrier) (Bayer et al., 2011). To avoid confusion with the sucrose- $\text{H}^+$  symporters, named SUC1-9 (Williams et al., 2000), we will refer to this protein from now on as SAMTL, for SAM transporter-like. From the 58 other members of this family in Arabidopsis, three more MCF proteins contain EF-hands: APC1, 2 and 3 (ATP/Phosphate Carrier 1, 2 and 3) as referred to by Palmieri and colleagues (Palmieri et al., 2011), due to their high homology to the mitochondrial ATP-Mg/ $\text{P}_i$  carriers in yeast and human. These carriers have not been described experimentally before in Arabidopsis.

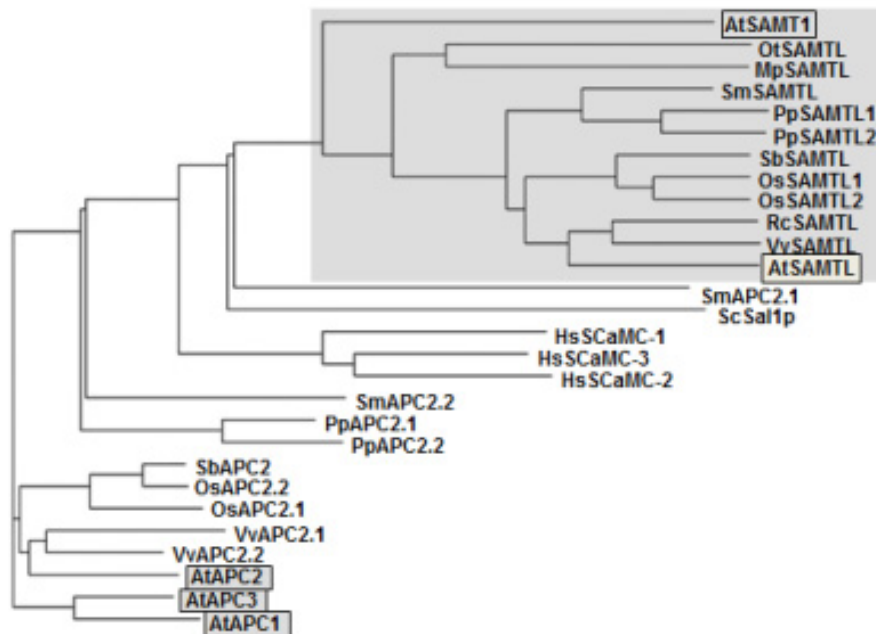
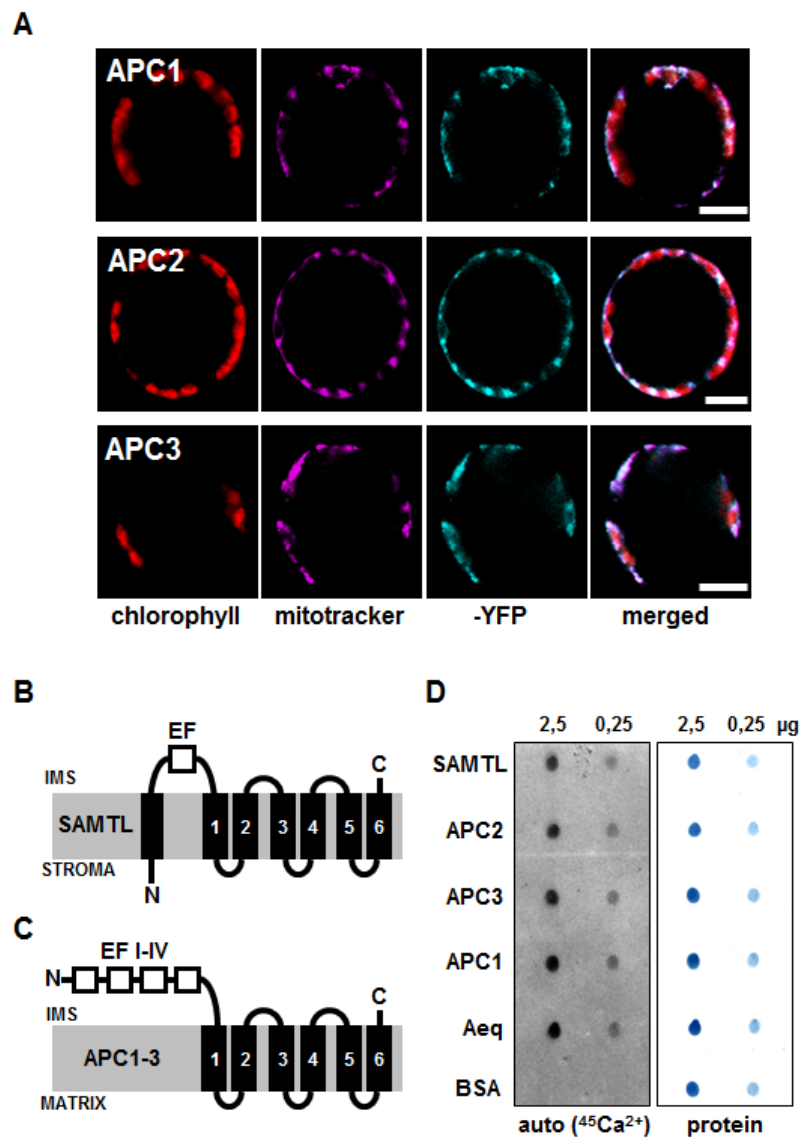


Figure 1 **Phylogenetic tree** generated using ClustalW2 of the calcium-binding MCF proteins of the SAMTL subfamily (grey box), and APC1, 2 and 3 with their orthologs in dicots, monocots, mosses, green algae, yeast, and humans including the Arabidopsis chloroplast SAM transporter (AtSAMT1). NCBI protein accessions are listed in suppl. Table 1. Species: At, *Arabidopsis thaliana*; Hs, *Homo sapiens*; Mp, *Micromonas pusilla*; Os, *Oryza sativa*; Ot, *Ostreococcus tauri*; Pp, *Physcomitrella patens*; Rc, *Ricinus communis*; Sb, *Sorghum bicolor*; Sc, *Saccharomyces cerevisiae*; Sm, *Selaginella moellendorffii*; Vv, *Vitis vinifera*.

A phylogenetic analysis of the aforementioned Arabidopsis proteins with their orthologs in dicots, monocots, mosses, green algae, fungi and humans is shown in Fig. 1. Based on phylogenetic distance as well as on differences in their primary protein structure and functional residues in the predicted binding site, SAMTL and APC1, 2 and 3 are most likely not functionally related. SAMTL seems to be specific for higher plants, mosses and algae. No homologues proteins containing EF-hands could be found in the genomes of yeast and humans. The closest homolog found, using profile hidden Markov models of conserved portions of SAMTL, is the SAM transporter of plants (Arabidopsis SAMT1), animals and fungi. However, the SAM transporters do not contain EF-hands. *S. cerevisiae* has a single ortholog of the APC1, 2 and 3 proteins, named Suppressor of Aac2 Lethality 1 (SAL1; (Chen, 2004)), and humans have three orthologs, called Short Calcium-binding Mitochondrial Carriers 1-3 (SCaMC1-3 (del Arco and Satrustegui, 2004)). Interestingly, only APC2 clusters together with its orthologs in monocots and dicots, whereas APC1 and 3 most likely duplicated later in evolution and therefore are paralogs of APC2.

**The MCF proteins APC1, 2 and 3 localize to mitochondria and all EF-hand containing MCF proteins bind  $\text{Ca}^{2+}$  *in vitro***

YFP-fusion analysis of the full-length APC1, 2 and 3 proteins transiently expressed in tobacco protoplasts clearly shows that they are localized to mitochondria, judged by the



**Figure 2. Localisation, calcium-binding and domain structure of the MCF proteins APC1, 2 and 3.** (A) Localization analysis of APC1, 2 and 3 in tobacco protoplasts. Chlorophyll autofluorescence is shown in red, the mitochondrial marker MitoTracker in magenta, and the APC1-, 2- and 3-YFP-fusion proteins in cyan. Scale bar = 10  $\mu\text{m}$ . (B) and (C) Scheme of the protein domains and predicted membrane topology of SAMTL and APC1-3, respectively displaying the EF-hands as white and the TM domains as black boxes. IMS, intermembrane space. (D) Radiolabeled calcium ( $^{45}\text{Ca}$ ) overlay assay showing the binding of  $^{45}\text{Ca}^{2+}$  to the purified N-terminal EF-hand containing parts of SAMTL and APC1-3, spotted on a PVDF membrane. Aeq, aequorin; BSA, bovine serum albumin. The left panel shows the binding of  $^{45}\text{Ca}^{2+}$  on the autoradiogram and right panel shows the presence of the protein (2.5  $\mu\text{g}$  and 0.25  $\mu\text{g}$ , respectively).

overlap of the YFP-signal with MitoTracker (magenta fluorescence Fig. 2A). This is the first experimental subcellular localization evidence for the full-length APC1, 2 and 3 proteins, whilst these carriers have not been found in any proteomic study to date. SAMTL was previously found to localize to the chloroplast by three independent proteomic studies and could be confirmed to reside in the chloroplast envelope by YFP-fusion analysis (Ferro et al., 2003; Ferro et al., 2010; Bayer et al., 2011).

To test the  $\text{Ca}^{2+}$ -binding capacity of the EF-hands of SAMTL and APC1, 2 and 3, which are depicted in the scheme of their protein domains (Fig. 2B and C), we performed radiolabeled calcium ( $^{45}\text{Ca}$ ) overlay assays on the N-terminal extensions of the carriers, containing the EF-hands, but excluding the carrier domains. Aequorin served as a positive control and BSA as a negative control (Fig. 2D). Further controls showing the purity of the recombinant proteins and more negative controls are shown in suppl. Fig. 2. All four EF-hand containing MCF proteins were clearly able to bind  $\text{Ca}^{2+}$  *in vitro*. Unexpectedly, the intensity of the autoradiogram of SAMTL appeared to be similar to that of aequorin even though the latter should be stronger, given that aequorin contains three EF-hands and SAMTL contains only one EF-hand. However, this calcium ( $^{45}\text{Ca}$ ) overlay assay is only qualitative and obtaining quantitative measures of  $\text{Ca}^{2+}$ -binding capacities were beyond the scope of this study.

### **Prediction of substrate specificity suggests SAMTL to be a plastidial SAM importer**

Because there are no clear orthologs of SAMTL experimentally described yet, we made a prediction for the type of substrate it could carry based on a multiple sequence alignment of all SAMTL orthologs in plants and algae. We focused on the 6 transmembrane (TM) domains forming the central carrier pore as depicted in Fig. 2B (suppl. Fig. 1). According to Robinson and Kunji (Robinson and Kunji, 2006), MCF proteins can be classified in three major subfamilies based on their functional residues that protrude into the central carrier pore: keto acid carriers, amino acid carriers and carriers of adenine-containing substrates. In the case of SAMTL, the presence of positively and negatively charged amino acids (RE) at position 692-693 in TM4 indicates that the protein transports a charged amino acid or a zwitterionic compound (Fig. 3). The substrate most likely has a negatively charged side chain that could be coordinated by the positively charged stretch (SxxHR) at position 605 in TM2. The transport activity is not proton-coupled, because the non-charged residues at position 555-556 (ST) in TM1 cannot carry protons to

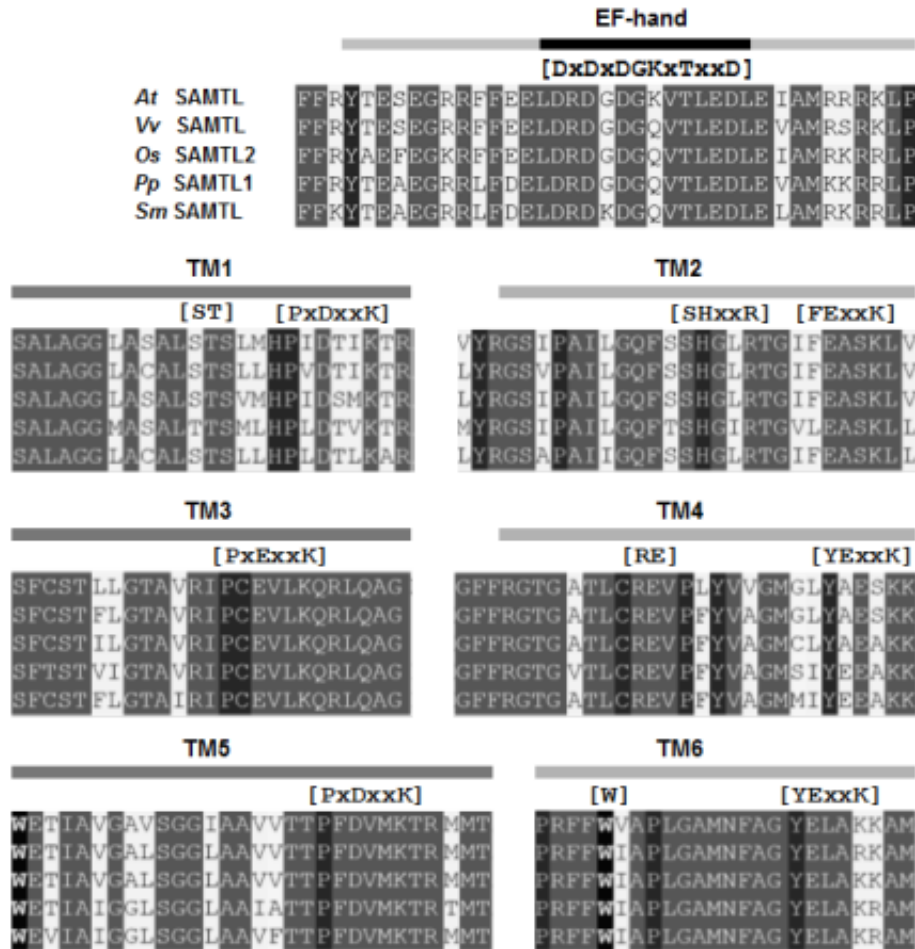


**Figure 3** Multiple sequence alignment of the EF-hand domain and the six TM domains of the active pore (as depicted in Fig. 2B) of the green plant SAMTL sub-family of MCF proteins of Arabidopsis (At), wine (Vv), rice (Os), Physcomitrella (Pp), and Selaginella (Sm). The EF-hand is indicated with gray lines for the  $\alpha$ -helical parts and a black line for the central  $\text{Ca}^{2+}$ -binding loop. Indicated in brackets are the amino acids 1, 3, 5, 7, 9 and 12, which are involved in the pentagonal bipyramidal orientated binding of  $\text{Ca}^{2+}$  and position 1,3 and 12 are the most conserved. The central glycine at position 6 allows for the  $\text{Ca}^{2+}$ -binding loop to make a sharp turn. The essential amino acids for interaction with substrates in the TM domains are indicated in brackets.

mediate a carboxyl-carboxylate interaction between substrate and carrier, as seen in other proton-coupled carriers (Kunji and Robinson, 2010). Furthermore, the presence of a complete salt-bridge network on both the cytoplasmic side and the matrix (stromal) side indicates that the carrier is a substrate exchanger. In this network, the charged residues of the [(F/Y)(D/E)xxK] motifs at the C-termini of all three even-numbered TM helices interact by hydrogen bonding and electrostatic interactions to close the pore to the cytoplasm and the [Px(D/E)xxK] motif at the C-termini of odd-numbered TM helices closes the pore to the stromal side of the carrier. Instead of the conserved tryptophan W786 in Arabidopsis SAMTL (TM6), almost always basic residues are present at this position in most other mitochondrial carriers. Interestingly, a similarly conserved

tryptophan is also found in *S*-adenosyl methionine (SAM) carriers. In combination with the overall homology to the SAM carrier and the fitting substrate description, SAMTL is therefore highly likely to exchange SAM for *S*-adenosyl homocysteine (SAHC), as it was experimentally found for the SAM transporter of Arabidopsis (SAMT1; (Bouvier et al., 2006; Palmieri et al., 2006)).

### APC1, 2 and 3 are able to complement an ATP-importer deficient yeast strain

To prove the predicted activity of APC1, 2 and 3 as ATP-Mg/P<sub>i</sub> transporters to import ATP into mitochondria in exchange for phosphate, we have exploited the high homology between APC1-3 and their yeast ortholog SAL1. In a recent study, Laco and colleagues have shown that SAL1 becomes essential for the viability of yeast growing in the presence of bongkreikic acid (BKA), a potent inhibitor of the major ATP/ADP carrier AAC2 (Laco et al., 2010). The lack of AAC2 can be compensated by SAL1 under growth conditions where ATP export from mitochondria is expendable, e.g. on glucose media. We expressed the Arabidopsis APC1, 2 and 3 genes under a constitutive promoter in a

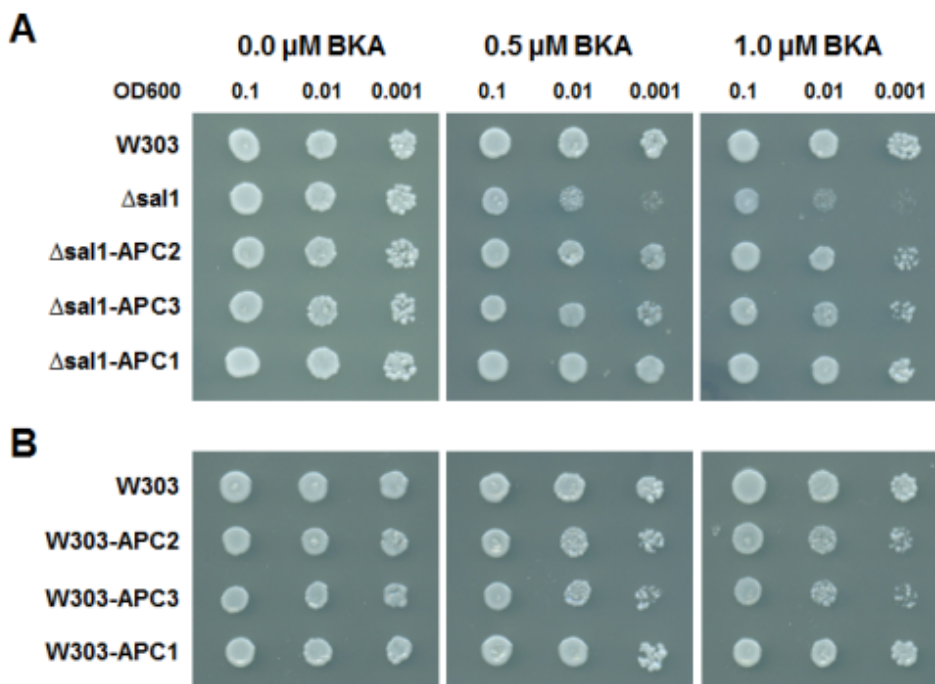


**Figure 4** Yeast functional complementation of SAL1 deficient yeast with APC1-3. **(A)** Dilution series (OD600 of 0.1, 0.01, and 0.001) of wild type (W303), SAL1 deficient ( $\Delta sal1$ ) and  $\Delta sal1$  expressing APC1-3 ( $\Delta sal1$ -APC1-3) yeast strains, growing on glucose-containing plates (pH4.0), containing 0, 0.5, and 1.0  $\mu$ M of bongkreikic acid (BKA). **(B)** Dilution series of control yeast strains (W303) expressing APC1-3 (W303-APC1-3) on glucose-containing plates (pH4.0) containing 0, 0.5 and 1.0  $\mu$ M of BKA.

SAL1 knock-out ( $\Delta sal1$ ) yeast strain and compared their growth in the presence of increasing amounts of BKA (0.5 and 1  $\mu$ M) (Fig. 4). Without BKA all strains grew like

the wild type, but with increasing amounts of BKA, the  $\Delta sal1$  strain showed severe growth retardation, as reported before (Laco et al., 2010). Clearly, the expression of APC1, 2 and 3 in the  $\Delta sal1$  strain ( $\Delta sal1$ -APC1-3) fully restored yeast growth back to the wild-type level (W3030-APC1-3) on both amounts of BKA. This indicates that APC1, 2 and 3 can functionally substitute for SAL1 and because of their orthology and localization they are likely mitochondrial ATP-Mg/P<sub>i</sub> transporters in Arabidopsis.

## Discussion

We present evidence for a plant Ca<sup>2+</sup>-binding subfamily of mitochondrial carriers containing two types of functionally unrelated proteins. On the one hand there is SAMTL, which has an unusually long N-terminal extension that targets it to chloroplasts, as previously reported (Bayer et al., 2011). In addition, the observation that SAMTL is only present in the green lineage (plants and green algae) correlates with its chloroplast localization. Hence, SAMTL is another exception to the exclusive mitochondrial localization of members of this carrier family. Also its single EF-hand is rather unusual, as EF-hands mostly occur in pairs in order to bind Ca<sup>2+</sup> in a cooperative manner (Lewitt-Bentley and Rety, 2000). Nonetheless, SAMTL was still able to bind specifically to Ca<sup>2+</sup> *in vitro* (Fig. 2D) and this has been reported for other single EF-hand proteins as well (Gutierrez-Ford et al., 2003; Reddy et al., 2004). While protein homo-dimerization is disputed to influence the activity of MCF proteins (Schroers et al., 1998; Postis et al., 2005; Kunji and Robinson, 2010), it might be a means for the EF-hand of SAMTL to be fully responsive to the Ca<sup>2+</sup> fluxes of the cell. In addition highly conserved cysteine residues might play a role in dimerization, as it was reported for other MCF proteins (Dyall et al., 2003; Wohlrab, 2010). The localization of SAMTL to the inner envelope (Fig. 2B) was tentatively assigned based on two facts. First, small molecules are able to freely pass the outer plastid envelope through specific solute channels (OEP's, outer envelope proteins (Pohlmeyer et al., 1998; Duy et al., 2007)) and second, at least in mitochondria, most MCF proteins localize to the inner membrane with both N- and C-terminus facing the inner membrane space (Picault et al., 2004). Accordingly, the EF-hand of SAMTL would be located in the inner membrane space. Based on predictions, the most likely substrate of SAMTL is *S*-adenosyl methionine (SAM). Chloroplasts have a high requirement for SAM as a methyl donor in a variety of methylation processes, most notably in the biosynthesis of prenyllipids and chlorophyll (Weber and Fischer, 2007). However, SAM is only produced in the cytoplasm and hence needs to be imported into

chloroplasts. SAMT1 was found to localize to chloroplasts and was experimentally proven to carry SAM (Bouvier et al., 2006; Palmieri et al., 2006). Interestingly, deletion of SAMT1 in Arabidopsis does not completely abolish SAM levels in chloroplasts, thus suggesting the presence of another SAM transporter, a role that could be fulfilled by SAMTL. Data from the publically available gene expression data mining interface GENEVESTIGATOR (Zimmermann et al., 2004), indicates that the SAMTL gene is expressed throughout the whole plant with globally higher expression in green tissues than in roots. Intriguingly, the biggest variation in gene expression is brought about by mutants affecting chlorophyll biosynthesis, where SAM is involved through the enzymatic action of Magnesium protoporphyrin IX *O*-methyltransferase (Vothknecht U.C., 1995). The *gun1/gun5* mutant lacks certain enzymes for the biosynthesis of chlorophyll (Mochizuki et al., 2001). The *flu* mutant over-accumulates protochlorophyll because it is defective in a negative feedback loop of chlorophyll biosynthesis (Meskauskiene et al., 2001). Taken together, SAMTL gene expression is down-regulated upon accumulation of protochlorophyll and vice versa. We speculate that the amount of SAM in the chloroplast is fine-tuned by SAMTL in response to the varied consumption of SAM in chlorophyll biosynthesis. Notably, the gene expression of SAMT1 is not altered in the aforementioned mutants.

On the other hand, there are the mitochondria localized carriers APC1, 2 and 3. Based on prediction and the results of this work we can confidentially suggest that APC1-3 are  $\text{Ca}^{2+}$ -regulated ATP-Mg/ $\text{P}_i$  transporters in Arabidopsis, a group of proteins best studied in human and yeast. The yeast ortholog, SAL1, was hypothesized to be a target of glucose-induced  $\text{Ca}^{2+}$  signals (Eilam et al., 1990; Nakajima-Shimada et al., 1991; Groppi et al., 2011) that would activate its ATP-Mg/ $\text{P}_i$  exchange activity resulting in the rapid increase of mitochondrial ATP levels (Cavero et al., 2005). As such, mitochondria are ATP consumers during aerobic growth on glucose-containing medium (Traba et al., 2008). Furthermore, the activity of SAL1 was found to be strictly dependent on calcium binding to its EF-hands (Chen, 2004). During anaerobic growth the import of cytosolic ATP into mitochondria becomes essential for mitochondrial viability because it helps to maintain the mitochondrial membrane potential by a reversal of the  $\text{F}_0\text{F}_1$   $\text{H}^+$ -ATP synthase and proton pumping of the respiratory complexes (Traba et al., 2009). These findings could be translated directly to plants. Under increased glucose/sucrose concentrations, an ATP excess from glycolysis could be shuttled into the mitochondria. This would promote the



proliferation of mitochondria and plant growth, while only the ATP-Mg/P<sub>i</sub> transporter adds nucleotides to the net content of the mitochondrial ATP/ADP pool (in contrast to AAC, the ADP/ATP exchanger; (Traba et al., 2009)). During hypoxia, for example during waterlogging of plant roots, the loss of mitochondrial oxidative phosphorylation could be counter balanced by APC1-3, to provide the mitochondria with ATP. Cytosolic Ca<sup>2+</sup> fluxes have been observed upon the addition of glucose to plant cell cultures and seedlings on plate (Furuichi et al., 2001; Furuichi and Muto, 2005) and in seedlings subjected to anoxia (Sedbrook et al., 1996). In this case the Ca<sup>2+</sup> flux might originate from the mitochondria themselves (Subbaiah et al., 1994, 1998) and accordingly, APC1, 2 and 3 might be a direct target of these Ca<sup>2+</sup>-fluxes.

To conclude, SAMTL and APC1, 2 and 3 can be added to a growing list of plant organellar calcium signaling proteins. We present here basic evidence for a hypothetical function, topology and Ca<sup>2+</sup> regulation of SAMTL, which provides good ground for further work on this MCF protein. We propose that SAMTL might help to import SAM into chloroplasts in addition to SAMT1, perhaps under conditions of increased need. Also for APC1, 2 and 3, the Arabidopsis ATP-Mg/P<sub>i</sub> transporters, we have drawn several scenarios, based on the yeast and human orthologs. The future challenge will be to prove or disprove these scenarios for SAMTL and APC1-3 *in planta* and connect them to Ca<sup>2+</sup> signaling in organelles.

### **Acknowledgements**

This work has been funded by the Austrian GEN-AU program in the ERA-PG project *CROPP* (Project No. 818514), and by the EU in the Marie-Curie ITN *COSI* (ITN 2008 GA 215-174). AJR is funded by the UK Medical Research Council. We thank Dr. J. Laco (Comenius University Bratislava) for kindly providing the W303 and  $\Delta$ sal1 yeast strains, Dr. N. Mehlmer (LMU Munich) for kindly providing the aequorin protein and Andreas PM Weber (University of Düsseldorf) for discussions about transporter phylogeny.

## **2.4. Paper 4 - Crosstalk between calcium signaling and protein phosphorylation at the thylakoid**

Simon Stael<sup>1</sup>, Agostinho G. Rocha<sup>2</sup>, Terje Wimberger<sup>1</sup>, Dorothea Anrather<sup>3</sup>, Ute C. Vothknecht<sup>2,4</sup> and Markus Teige<sup>1\*</sup>

<sup>1</sup>Department of Biochemistry and Cell Biology, MFPL, University of Vienna, Dr. Bohrgasse 9, A-1030, Vienna. Austria.

<sup>2</sup>Department of Biology I, Botany, LMU Munich, Großhaderner Str. 2, D-82152 Planegg-Martinsried. Germany.

<sup>3</sup>Christian Doppler Laboratory for Proteomics, MFPL, University of Vienna, Dr. Bohrgasse 9, A-1030, Vienna, Austria.

<sup>4</sup>Center for Integrated Protein Science (Munich) at the Department of Biology of the LMU Munich, D-81377 Munich, Germany.

Email addresses: [simon.stael@univie.ac.at](mailto:simon.stael@univie.ac.at), [rocha@bio.lmu.de](mailto:rocha@bio.lmu.de), [terje.wimberger@gmail.com](mailto:terje.wimberger@gmail.com), [dorothea.anrather@univie.ac.at](mailto:dorothea.anrather@univie.ac.at), [vothknecht@bio.lmu.de](mailto:vothknecht@bio.lmu.de), [markus.teige@univie.ac.at](mailto:markus.teige@univie.ac.at)

\* To whom correspondence should be addressed: E-mail: [markus.teige@univie.ac.at](mailto:markus.teige@univie.ac.at), phone: +43-1-4277-529811, fax: +43-1-4277-9528

Submission date: 05.10.2011

1 table and 3 figures + 2 suppl. tables and 7 suppl. figures

Running title: CALCIUM DEPENDENT THYLAKOID PROTEIN PHOSPHORYLATION

**Abstract**

The role of protein phosphorylation for adjusting chloroplast functions to changing environmental needs is well established, whereas calcium signaling in the chloroplast is only recently becoming appreciated. The presented work explores the potential crosstalk between calcium signaling and protein phosphorylation in chloroplasts and provides first evidence for targets of calcium dependent protein phosphorylation at the thylakoid membrane. We screened thylakoid proteins for calcium dependent phosphorylation by 2D gel electrophoresis combined with phospho-specific labeling and repeatedly identified PsaN, CAS and VAR1, among other proteins by mass spectrometry. Subsequently their calcium dependent phosphorylation was confirmed in kinase assays using the purified proteins and chloroplast extracts. This is the first report on protein targets of calcium dependent phosphorylation of thylakoid proteins and provides ground for further studies in this direction.

## Introduction

The chloroplast harbours many cellular processes that require tight regulation allowing plants to grow efficiently under fluctuating environmental conditions. Protein phosphorylation is important for the post-translational control of these processes and seems to be dominated in the chloroplast by three protein kinases: chloroplast casein kinase 2 (cpCK2) and the state transition kinases STN7 and STN8 (Bayer *et al.*, JXB, submitted). cpCK2 localizes to the stroma and plays a role in chloroplast transcription and translation, as it was found to associate with the RNA polymerase complex and to phosphorylate parts of the transcription machinery and RNA-binding proteins (Baginsky *et al.*, 1999; Ogrzewalla *et al.*, 2002). The functional impact of cpCK2 phosphorylation of the chloroplast transcription machinery on plant growth was recently demonstrated by the use of phosphorylation site mutants of the *Arabidopsis thaliana* sigma factor 6 (AtSIG6) (Schweer *et al.*, 2010). However, the action of cpCK2 is most likely not restricted to the control of chloroplastic gene regulation alone, as its preferred phosphorylation motive is strongly overrepresented in a diverse set of 174 identified chloroplast phosphoproteins (Reiland *et al.*, 2009). This notion is further supported by the observation that cpCK2 seems to be responsible for the main protein kinase activity in the stroma. This conclusion was based on the observation that stromal protein extracts are equally well phosphorylated in the presence of GTP, a known and specific co-substrate of CK2 (Niefind *et al.*, 1999), as by ATP (Bayer *et al.*, JXB, submitted). STN7 and STN8 are integral membrane protein kinases of the thylakoid and their function is to optimize light harvesting for photosynthesis to fluctuating light conditions and repair of high-light photo-damaged photosynthetic complexes, respectively (Rochaix, 2007; Tikkanen and Aro, 2011). Accordingly, stunted growth of the *stn7* and *stn7/stn8* double mutants becomes especially visible under fluctuating light conditions (Tikkanen *et al.*, 2010). STN7 mainly phosphorylates the light harvesting complex (LHC) proteins, while STN8 specifically phosphorylates the subunits D1, D2 and CP43 of photosystem II (PSII). These proteins represent the majority of phosphorylated proteins in thylakoids, and recently a hypothesis has been put forward that phosphorylation of PSII regulates the cation-dependent stacking of thylakoids because thylakoid stacking was found to be less dependent on  $Mg^{2+}$  in *stn8* mutants (Fristedt *et al.*, 2009; Fristedt *et al.*, 2010). The authors reason that increased phosphorylation of the main thylakoid proteins in the thylakoid stack (grana) would provide repulsion of negative phosphoryl groups between

adjacent grana membranes and therefore provide space for the cycling of photo-damaged PSII proteins to the lamellae, where they are degraded and replaced (Tikkanen et al., 2008). STN7 and STN8 are responsible also for minor phosphorylations of other thylakoid proteins, respectively TSP9, a soluble protein involved in the regulation of light harvesting (Hansson et al., 2007; Fristedt et al., 2009) and the calcium sensing protein (CaS), an integral membrane protein involved in the process of stomatal closure (Nomura et al., 2008; Vainonen et al., 2008; Weinl et al., 2008). Notably, in the *stn7/stn8* double mutant, remainders of unknown phosphorylated thylakoid proteins could be detected, albeit to a much lower extent than the main phosphorylated proteins (Fristedt et al., 2009). Responsible for this phosphorylation could be TAK (thylakoid associated kinase) (Snyders and Kohorn, 1999), or an as yet unidentified protein kinase. Moreover, cross-phosphorylation of stromal protein kinases can also not be excluded. In addition, the recently discovered chloroplast protein kinases, such as the ABC1 kinases (Ytterberg et al., 2006) Bayer *et al.*, JXB, submitted) and plastid protein kinase (PPK) (Bayer et al., 2011) together with the variety of identified chloroplast phosphoproteins (Reiland et al., 2009) opens many new possibilities for future discoveries and broadens the potential impact of chloroplast phosphorylation on plant physiology.

Calcium signaling in organelles is a relatively new topic (Stael *et al.*, JXB, submitted). Compared to protein phosphorylation (Bennett, 1977), it was only recently appreciated that fluxes of free calcium ions ( $\text{Ca}^{2+}$ ) occur in the chloroplast and the topic has not been extensively studied yet (Johnson et al., 1995; Sai and Johnson, 2002).  $\text{Ca}^{2+}$  fluxes occur in the chloroplast stroma upon the transition from light to dark, as measured with a stromal targeted aequorin protein construct (a  $\text{Ca}^{2+}$  sensor protein) (Johnson et al., 1995; Sai and Johnson, 2002). The resting level of free  $\text{Ca}^{2+}$  was estimated at ~150 nM and increased five minutes after dark to a peak concentration of 5 to 10  $\mu\text{M}$  in a time frame of 20-25 minutes. Interestingly, when the plants were exposed for several days to continuous light, the amount of  $\text{Ca}^{2+}$  release was found to be proportional to the light period. From earlier work it is known that chloroplasts take up  $\text{Ca}^{2+}$  from the surrounding media (cytosol) upon illumination (Kreimer, 1985; Roh et al., 1998). Given the characteristics of the  $\text{Ca}^{2+}$  flux, the chloroplast most likely takes up  $\text{Ca}^{2+}$  from the cytosol and stores it in the thylakoid membrane or a so far unknown store, which is then released on the transition from dark to light. The thylakoid lumen needs to take up  $\text{Ca}^{2+}$  in order to provide the oxygen evolving complex (OEC) with one of its necessary cofactors (Cinco et al., 2004).

Accordingly,  $\text{Ca}^{2+}$  uptake into the lumen was found to be driven by the proton gradient through the activity of an unknown  $\text{Ca}^{2+}/\text{H}^+$  exchanger (Ettinger et al., 1999). The increase of the  $\text{Ca}^{2+}$  concentration in the stroma was hypothesized to have a direct effect (inhibition) on the enzyme functions of the Calvin-Benson cycle, as it was observed *in vitro* (Racker and Schroeder, 1958; Portis and Heldt, 1976; Charles and Halliwell, 1980). More recently, the discovery of calmodulin dependent processes, such as protein import (Chigri et al., 2005; Chigri et al., 2006) and NAD kinase activity (Jarrett et al., 1982; Turner et al., 2004) suggest a role for  $\text{Ca}^{2+}$  as a secondary messenger in the chloroplast. Furthermore, two EF-hand ( $\text{Ca}^{2+}$ -binding motive) containing proteins localize to the chloroplast. The  $\text{Ca}^{2+}$ -activated RelA/SpoT homolog protein (CRSH) that resides in the chloroplast and is most likely involved in an evolutionary conserved signaling process called the ‘bacterial stringent response’ (Takahashi et al., 2004; Tozawa et al., 2007; Masuda et al., 2008) and an unknown substrate carrier (SUC) that localizes to the chloroplast envelope (Bayer et al., 2011). The impact of chloroplast calcium handling on plant physiology is probably best illustrated by a rather unusual  $\text{Ca}^{2+}$  binding protein. CAS, for ‘calcium sensing’, binds  $\text{Ca}^{2+}$  with a low affinity and high capacity and down-regulation of its expression impairs the induction of  $[\text{Ca}^{2+}]_{\text{ext}}$  cytoplasmic  $\text{Ca}^{2+}$  oscillations in guard cells, thereby affecting stomatal movement (Han et al., 2003; Nomura et al., 2008; Weinl et al., 2008). First reported as a plasmamembrane localized  $\text{Ca}^{2+}$ -sensing receptor (Han et al., 2003), it was later unequivocally established as an integral thylakoid membrane protein (Friso et al., 2004; Nomura et al., 2008; Vainonen et al., 2008; Weinl et al., 2008). As mentioned earlier, CAS is increasingly phosphorylated under increasing light intensities in an STN8-dependent manner (Vainonen et al., 2008). It is still unclear how exactly CAS is able to ‘sense’ extracellular  $\text{Ca}^{2+}$  ( $[\text{Ca}^{2+}]_{\text{ext}}$ ) variations and influence stomatal closure. To conclude, the chloroplast has all prerequisites for calcium signaling, namely a low resting free  $\text{Ca}^{2+}$  concentration, the ability to produce  $\text{Ca}^{2+}$  fluxes as well as proteins to decode the calcium signal.

## Material and methods

### Calcium dependent phosphorylation assays of thylakoid membranes

*Pisum sativum* (Pea) or *Arabidopsis* chloroplasts were isolated as previously described (Bayer et al., 2011). For two reactions, Percoll-purified chloroplasts containing 140  $\mu\text{g}$  of chlorophyll (*chl*) were lysed by adding 5 equal volumes of lysis buffer (25 mM Tris-HCl pH 7.8, 75 mM NaCl, 10 mM  $\text{MgCl}_2$ , 1 mM NaF, 0.5 mM  $\text{NaVO}_3$ , 15 mM  $\beta$ -

Glycerophosphate, 1 mM DTT and complete, EDTA-free Protease Inhibitor Cocktail (Roche), and incubating for five min on ice. Thylakoids were spun down for 2 min at 20.000g on 4°C and were washed with 5 volumes of lysis buffer. After centrifugation, the thylakoid pellet was re-suspended in 80 µl of lysis buffer and divided to two Eppendorf tubes (so, two reactions with 70 µg *chl*). To one tube, 1 µl of CaCl<sub>2</sub> (of varying concentrations; 40, 10 or 1 mM) was added and to the other tube, 1 µl of the calcium-specific chelator EGTA (of varying concentrations; 40, 10 or 1 mM) was added. The tubes were gently mixed and incubated for 5 min on room temperature in the dark. The kinase reactions were started by adding 1 µl of an 8 mM ATP solution (final concentration of 0.2 mM ATP) and were incubated for 20 min on room temperature in the dark. The kinase reactions were stopped by the addition of 400 µl methanol, and thylakoid proteins were precipitated according to the chloroform/methanol technique (Wessel and Flugge, 1984).

## **2D protein separation by isoelectric focusing and SDS-PAGE gel electrophoresis**

After chloroform/methanol precipitation, the protein pellets were solubilized in 125 µl of rehydration buffer (7 M urea, 2 M thiourea, 2% CHAPS, 2% IPG buffer (pH3-11 NL, GE Healthcare), 0.002% bromphenol blue and 50 mM DTT). The protein solutions were applied to immobilized pH gradient strips (IPG strips Immobiline™ DryStrip gels pH 3-11 NL, 7 cm, GE Healthcare). After covering of the strips with mineral oil (Immobiline™ DryStrip Cover Fluid, GE Healthcare), they were left to rehydrate overnight. The day after, the strips were placed in a Multiphor II focusing unit (GE Healthcare) that was connected to an EPS 3501 XL power supply (GE Healthcare) and the strips were run according to manufacturer's protocol. Afterwards, the strips were equilibrated in SDS equilibration buffer (75 mM Tris-HCl pH 8.8, 6 M urea, 29.3% glycerol, 2% SDS, 0.002% bromphenol blue) containing DTT (100 mg/ 10 ml buffer) for 20 min and subsequently in SDS equilibration buffer containing iodacetamid (250 mg/ 10 ml buffer) for 20 min. Both strips, containing the phosphorylated proteins in the presence of Ca<sup>2+</sup> and EGTA, were loaded on top of the same SDS-PAGE gel. The gel was run in a PROTEAN II system (Bio-Rad) at a current of 10 mA/gel until the proteins from the strip had entered the SDS-PAGE. Subsequently, the current was increased to 30 mA/gel.

**Visualization of phosphorylated thylakoid proteins**

To visualize phosphorylated thylakoid proteins, the 2D gels were stained by Pro-Q Diamond phosphoprotein gel stain according to manufacturer's protocol (Invitrogen). Alternatively, proteins of the 2D gels were transferred to polyvinylidene fluoride membranes (PVDF, Immobilon-P, Millipore) by western blotting according to manufacturer's protocol (Trans-Blot SD semi-dry electrophoretic transfer cell, Bio-Rad). The PVDF membranes were incubated with a phospho-threonine specific primary antibody (Cell Signaling #9381) and an ECL Rabbit IgG, HRP-linked secondary antibody (from donkey, GE healthcare). Immuno-labeled spots were detected with the ECL Plus Western Blotting Detection System (GE Healthcare) and films (Fujifilm) were developed in a CURIX60 table-top processor (AGFA). After completion of the phospho-specific stains, the gels and PVDF membranes were stained by silver stain or Coomassie Brilliant Blue (CBB) stain.

**Excision of proteins spots and identification by mass spectrometry**

Protein spots that showed differences in intensity between the  $\text{Ca}^{2+}$  and EGTA phosphorylation assays on the phospho-specific stained gel were manually mapped to the protein spots of the corresponding silver stained or CBB stained gel. The protein spots were excised and prepared for mass spectrometry analysis (MS) as previously described (Bayer et al., 2011). For the Pea samples, MS/MS analysis was carried out as previously described (Bayer et al., 2011) and proteins were identified from a recently created Pea EST database (Brautigam et al., 2008). For the Arabidopsis samples, peptides were separated on an UltiMate 3000 HPLC system (Dionex), by loading the sample digests on a trapping column (PepMap C18, 5 $\mu\text{m}$  particle size, 300  $\mu\text{m}$  i.d. x 5mm) equilibrated with 0.1% TFA (trifluoric acetic acid) and separating on an analytical column (PepMap C18, 3  $\mu\text{m}$ , 75  $\mu\text{m}$  i.d. x 150mm), applying a 90 minutes linear gradient from 2.5% up to 40% ACN with 0.1% formic acid. The HPLC was directly coupled to a LTQ-Orbitrap Velos mass spectrometer (Thermo Fisher Scientific) equipped with a nanoelectrospray ionization source (Proxeon), for which the electrospray voltage was set to 1500 V. The mass spectrometer was operated in the data-dependent mode: 1 full scan ( $m/z$ : 300-1800, resolution 60000) with lock mass enabled was followed by maximal 20 MS/MS scans. The lock mass was set at the signal of polydimethylcyclsiloxane at  $m/z$  445.120025. Screening of the charge state was on, singly charged signals and ions with no charge state



assigned were excluded from fragmentation. The collision energy was set at 35%, Q-value at 0.25 and the activation time at 10 msec. Fragmented ions were set onto an exclusion list for 90 s. Raw spectra were interpreted by Mascot 2.2.04 (Matrix Science) using Mascot Daemon 2.2.2. The peptide tolerance was set to 2 ppm, MS/MS tolerance was set to 0.8 Da. Proteins were identified from the full genome sequence of TAIR9 ([ftp://ftp.arabidopsis.org/home/tair/Genes/TAIR9\\_genome\\_release/](ftp://ftp.arabidopsis.org/home/tair/Genes/TAIR9_genome_release/), on [www.arabidopsis.org](http://www.arabidopsis.org)). Carbamidomethylcysteine was set as a static modification and oxidation of methionine as a variable modification. Trypsin was selected as protease and two missed cleavages were allowed. MASCOT results were loaded into Scaffold (Ver. 3.00.02; Proteome Software) for an X! Tandem Search. Peptide identifications were accepted at a probability greater than 95% and protein identifications at a probability greater than 99%, as assigned by the Protein Prophet algorithm (Keller et al., 2002; Nesvizhskii et al., 2003). Mostly, multiple proteins were identified per spot. Therefore, peptide count was used as a relative measure of protein abundance and this was combined with information on predicted pI and mass to single out the most likely protein per spot. All identified proteins per spot are summarized in Supplementary table 2.

### **Preparation of chloroplast soluble and extrinsic membrane proteins for recombinant phosphorylation assay**

Arabidopsis chloroplasts were hypotonically disrupted in lysis buffer (20 mM Tricine pH 7.6, 10% glycerol, 0.5% DTT), supplemented with protease inhibitors (complete EDTA-free Protease Inhibitor Cocktail, Roche), phosphatase inhibitors (Phospho-Stop, Roche) and 5 mM EGTA. After incubation on ice for 15 min, membranes and soluble components were separated by centrifugation at 60.000g for 10 min. To solubilize extrinsic membrane proteins, the membrane fraction was washed with lysis buffer containing 0.8 M NaCl. The 60.000g supernatants of the first and second centrifugation were combined, desalted and concentrated using Vivaspin 500 spin columns (3 kDa cutoff, GE Healthcare). All operations were carried out either on ice or at 4°C.

### **Calcium dependent phosphorylation assays of selected recombinant proteins**

PsaN, lacking the N-terminal 81 amino acids (forward primer: 5'-TTATTATCCA TGGCTGCTTCTGCTAATGCTGGCGTCAT-3' and reverse primer: 5'-AATATAGCGG CCGCATATAAGAATAGATGAAAAC-3'), the C-terminus of CAS

(amino acids 216-387; forward primer: 5'-GATCGGGCCCATGGGTTACAAAGGTGATCTTACGCC-3' and reverse primer: 5'-ACTAGCGGCCGCAGTCGGAGCTAGGAAGGAAC-3'), the C-terminus of VAR1 (amino acids 221-704, forward primer: 5'-GATCGGGCCCATGGGTGGTCCTG GAGGTTTAGG-3' and reverse primer: 5'-ACTAGCGGCCGCAAGAAACATA TAACTCGGCT-3') and the C-terminus of VAR2 (amino acids 198-695; forward primer: 5'-GATCGGGCCCATGGGTGGACCTGGTGGTCC-3' and reverse primer: 5'-ACTAGCGGCC GCAGACAGCAGCTGGTGTGGT-3') were obtained by PCR from Arabidopsis cDNA using primers containing the restriction sites for NcoI (or ApaI) and NotI. The PCR products of PsaN and CAS were cloned in frame with an N-terminal intein tag into pTWIN (New England Biolabs) and the PCR products of VAR1 and VAR2 were cloned in frame with a glutathione-S-transferase (GST) tag into pGEX4T-3 (GE Healthcare). Proteins were expressed according to manufacturer's protocol, which resulted in the removal of the intein tag from PsaN and CAS. Protein phosphorylation assays were carried out in kinase buffer (20 mM Tricine pH 7.6, 10 mM MgCl<sub>2</sub>, 5 μM cold ATP and 2–5 μCi [ $\gamma$ -<sup>32</sup>P] ATP (3000 Ci/mmol, Perkin Elmer), 10% glycerol, 0.5% DTT) supplemented with either 2 mM EGTA or 5 mM CaCl<sub>2</sub>. In a total reaction mix of 50 μl was added 5 μl of chloroplast soluble and extrinsic membrane proteins. Reactions were stopped after 25 min at room temperature by the addition of 12 μl of 4x SDS-sample buffer and were separated by SDS-PAGE gel electrophoresis and stained with CBB. Radio-labeled proteins were detected by exposure for 3 days on a x-ray film (FUJI) at -80°C.

## Results

### Several thylakoid proteins are phosphorylated in a calcium-dependent manner in pea and Arabidopsis

In order to identify targets of Ca<sup>2+</sup> dependent phosphorylation in thylakoids, we subjected Percoll-purified chloroplasts of Pea to *in vitro* phosphorylation assays in the presence of Ca<sup>2+</sup>. Control experiments were performed in the presence of EGTA to chelate any contaminating Ca<sup>2+</sup>. The higher specificity of EGTA towards Ca<sup>2+</sup> combined with the saturating amount of Mg<sup>2+</sup> in the kinase buffer assured that all differences in phosphorylation were Ca<sup>2+</sup> specific. Initial experiments were performed with pea in the presence of 1 mM Ca<sup>2+</sup>, and the concentration of Ca<sup>2+</sup> was lowered to 25 μM in the subsequent experiments using Arabidopsis thylakoids. After loading the two kinase

reactions (+/-  $\text{Ca}^{2+}$ ) on a denaturing SDS-PAGE gel, phosphorylated bands were visualized with Pro-Q Diamond phosphoprotein gel stain. Protein bands at approximately 65, 35 and 10 kDa, respectively, showed a clear dependence on  $\text{Ca}^{2+}$  for phosphorylation as displayed for pea thylakoids in Fig. 1A.

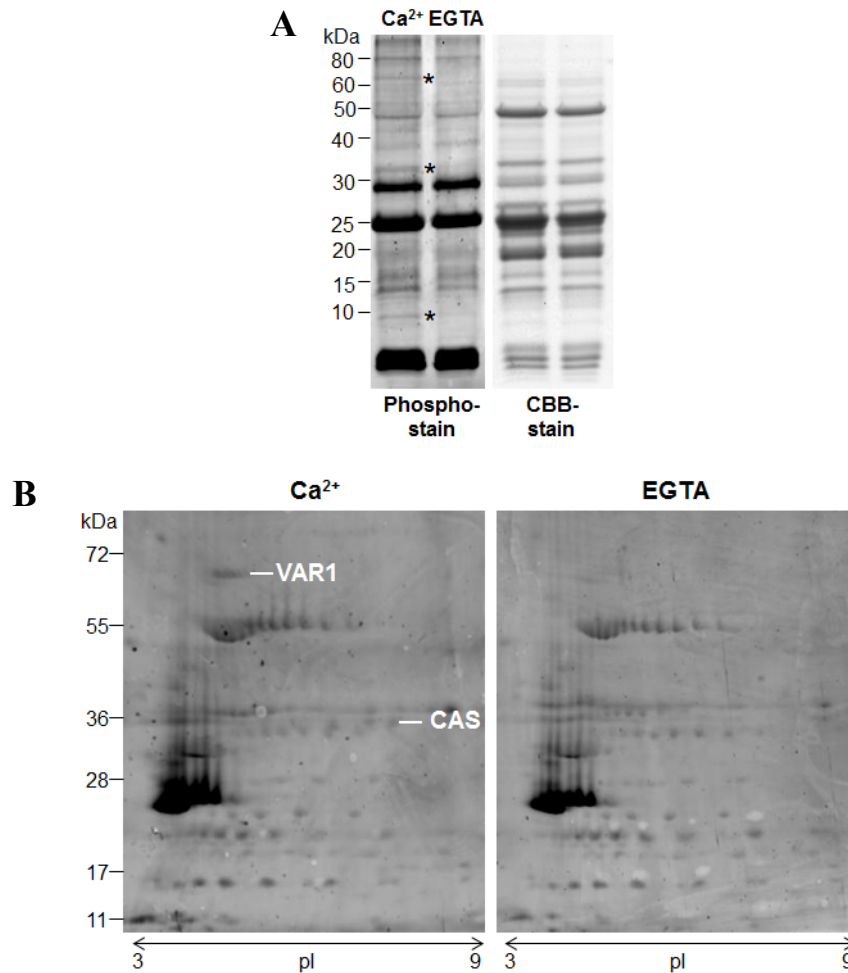


**Figure 1 Calcium dependent phosphorylation of pea thylakoid proteins.** (A) The left panel displays a Pro-Q Diamond phosphoprotein gel stain that reveals three differentially phosphorylated protein bands (indicated with an asterisk) upon the addition of 1 mM  $\text{Ca}^{2+}$ , compared to 1 mM EGTA. The right panel is the protein loading control (CBB = Coomassie Brilliant Blue). (B) 2D protein separation according to isoelectric point (pI) and size (kDa) of the same  $\text{Ca}^{2+}$  dependent phosphorylation assay followed by a Pro-Q Diamond phosphoprotein gel stain (experiment 1). Two protein spots were identified as the FtsH protease, Variegated 1 (VAR1) and ‘Calcium sensing’ protein (CAS).

### 2D gel analysis identifies VAR1 and CAS as targets of $\text{Ca}^{2+}$ dependent phosphorylation

To identify the  $\text{Ca}^{2+}$  dependent phosphorylated proteins, the proteins from the two phosphorylation assays of pea thylakoids (1 mM  $\text{Ca}^{2+}$  and 1mM EGTA) were separated in a 2D approach. In the first dimension the proteins were separated according to their pI

on a non-linear pH gradient from pH 3-11, and in the second dimension on a 12 % SDS-PAGE gel. Phosphorylated proteins were again visualized with Pro-Q Diamond phosphoprotein stain and the gel was subsequently stained with Coomassie Brilliant Blue (CBB). Protein spots, corresponding to a molecular mass of 65 kDa and 35 kDa, respectively showed differences in phosphorylation (Fig. 1B) confirming the first observation from the initial experiment (Fig. 1A). The protein spots from the phosphostain were manually mapped to the CBB stained gel, cut out and analyzed by tandem mass spectrometry. After parsing of all identified proteins (see material and methods), the protein spots at 65 kDa and 35 kDa corresponded, respectively, to Variegated 1 (VAR1) and CAS.

### **Repeated 2D gel analysis of Arabidopsis thylakoids confirms results obtained in pea and uncovers additional targets of Ca<sup>2+</sup> dependent phosphorylation**

In subsequent experiments, the Ca<sup>2+</sup> dependent phosphorylation assays were repeated with thylakoids from Percoll-purified chloroplasts of Arabidopsis. In order to get closer to physiological relevant Ca<sup>2+</sup> concentrations, the experiment was repeated three times with 250 μM Ca<sup>2+</sup>/EGTA and three times with 25 μM Ca<sup>2+</sup>/EGTA. Furthermore, two complementary approaches were used to detect phosphorylated proteins. In four of the six experiments, a western blot with a phosphothreonine-specific antibody was used, and for the remaining two experiments the Pro-Q Diamond phosphoprotein stain was used. When phosphorylated proteins were detected by western blot, a reference gel was run under identical conditions and the protein spots were mapped to this reference gel with the help of the CBB stain of the western blot. The results of these seven independent experiments are summarized in Supplementary Table 1. Those proteins, which were identified multiple times in independent experiments, are presented in Table 1. From these proteins, PsaN (subunit N of photosystem 1) was identified most frequently and it probably represents the phosphorylated band appearing at a molecular mass of 10 kDa in the initial Pea experiment (Fig. 1A). Following in number of identifications were CAS, PsbP (subunit P of photosystem 2) and PsaH-2 (subunit H-2 of photosystem 1). VAR1 and VAR2 were both included in this table, because protein identification ambiguity existed between these closely homologous proteins.

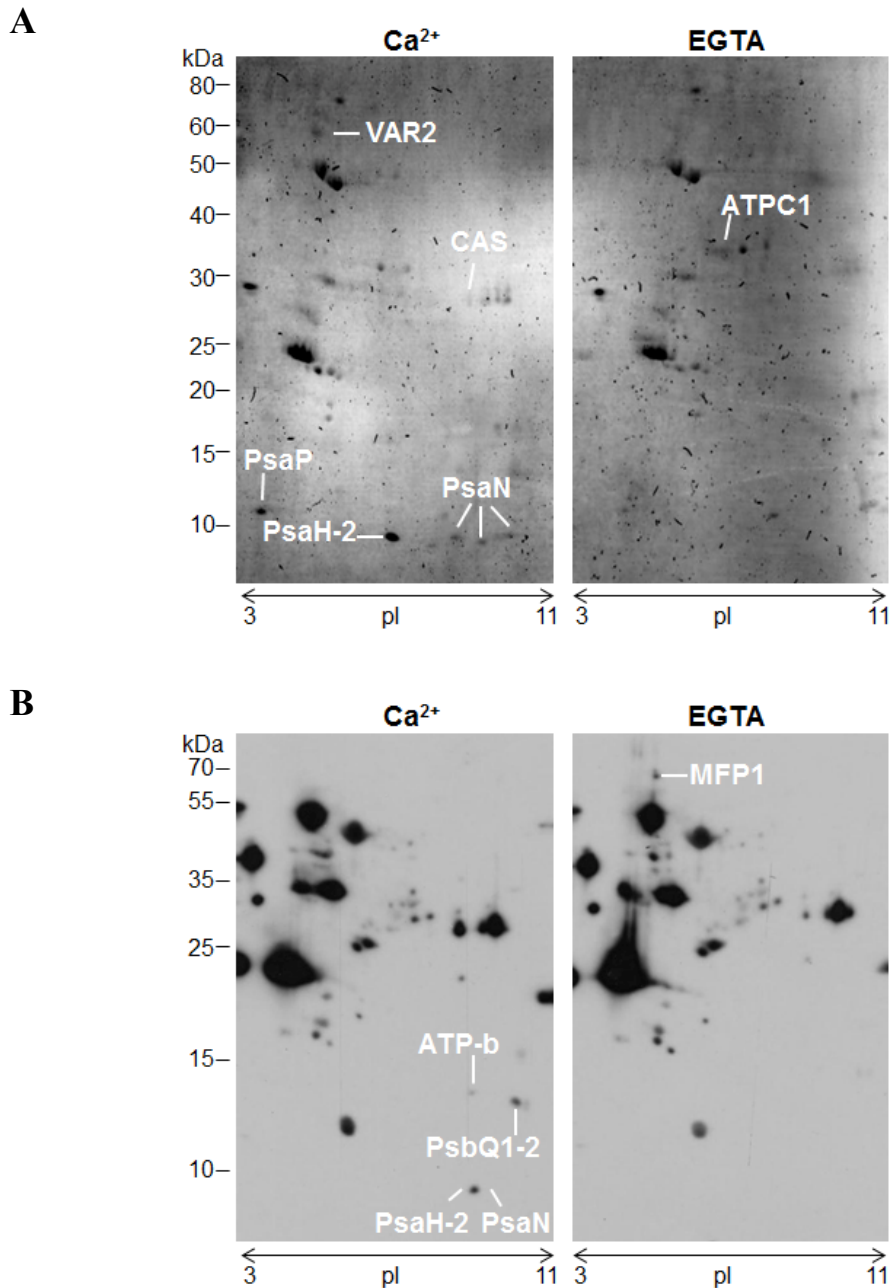


**Figure 2 Calcium dependent phosphorylation of Arabidopsis thylakoid proteins visualized by Pro-Q Diamond phosphoprotein gel stain (A) and phospho-threonine specific antibody (B) after 2D-gel separation according to isoelectric point (pI) and size (kDa).** (A) Protein spots identified in experiment 4 (250  $\mu$ M  $\text{Ca}^{2+}$ /EGTA) are the FtsH protease, Variegated 2 (VAR2), ‘Calcium sensing’ protein (CAS), Photosystem I subunit P (PsaP), Photosystem I subunit H-2 (PsaH-2) and Photosystem I subunit N (PsaN; three times identified). (B) Protein spots identified in experiment 3 (250  $\mu$ M  $\text{Ca}^{2+}$ /EGTA) are the ATPase subunit F (ATPF), the Photosystem II subunits Q1 and Q2 (PsbQ1-2), PsaH-2 and PsaN. Stronger phosphorylation of spots were also observed in the EGTA samples, as it is the case in (A) for the ATPase C1 subunit (ATPC1) and in (B) for the MAR binding filament-like protein 1 (MFP1).

**Table 1.** Overview of most frequently identified calcium dependent phosphorylated proteins.

ID	AGI code	Description	Species	pro-Q	p-Thr	PhosPhat	Experiment
PsaN	At5g64040	Photosystem I subunit N	At	4	4	y	(3)(4)(5) (6)(7)
CAS	At5g23060	'Calcium sensing' protein	Ps/At	2	1	y	(1)(2)(4)
VAR1/ VAR2	At5g42270/ At2g30950	Variegated 1 and 2, FtsH proteases	Ps/At	2	0	y/n	(1)(4)
PsbP-1	At1g06680	Photosystem II subunit P-1	At	1	1	y	(2)(7)
PsaH-2	At1g52230	Photosystem I subunit H-2	At	1	1	n	(3)(4)

Indicated is in which species the proteins were identified (At = *Arabidopsis thaliana*; Ps = *Pisum sativum*), which stain was used to reveal the phosphorylated proteins (Pro-Q = Pro-Q Diamond phosphoprotein gel stain; pThr = phospho-Threonine specific antibody), if the protein is included in the phospho-peptide database PhosPhat 3.0 (Heazlewood et al., 2008; Durek et al., 2010), and in which experiment the protein was identified. Images to the seven experiments are included in the supplementary figures.

### Kinase assays on purified proteins confirm the calcium dependent phosphorylation of VAR1, CAS and PsaN

The four proteins PsaN, CAS, VAR1 and VAR2, which were identified with highest confidence as targets of Ca<sup>2+</sup> dependent phosphorylation at thylakoid membranes (Table 1) were recombinantly expressed and purified from *E. coli* to test the Ca<sup>2+</sup> dependency of their phosphorylation in an independent approach. In the case of CAS, VAR1 and VAR2, only the C-termini of the proteins without the transmembrane domains were expressed, in order to avoid protein solubility problems. The C-termini were chosen as they contain the known phosphorylation sites of these proteins (Vainonen et al., 2008; Reiland et al., 2009). PsaN and CAS were purified without a protein tag, whereas the addition of a glutathione-S-transferase (GST) protein tag to VAR1 and VAR2 seemed to increase their protein stability (data not shown). For the kinase assays, soluble and extrinsic proteins of Percoll-purified Arabidopsis chloroplasts were used to phosphorylate the purified proteins in the presence of Ca<sup>2+</sup> or EGTA (two middle lanes of Fig. 3). No phosphorylation was detected when only the recombinant proteins were incubated with ATP (two left lanes of Fig.3). Phosphorylation assays without purified proteins were included for comparison to the background phosphorylation of the chloroplast extract (two right lanes of Fig. 3). As a control, kinase assays were performed on GST. A clear

calcium dependent phosphorylation was visible for PsaN, CAS and VAR1. VAR2, on the other hand, was notably less phosphorylated than VAR1, if compared to the background phosphorylation. All together, these data do also confirm the previously reported phosphorylation of those proteins from an unbiased phosphoproteomics study (Reiland et al., 2009).

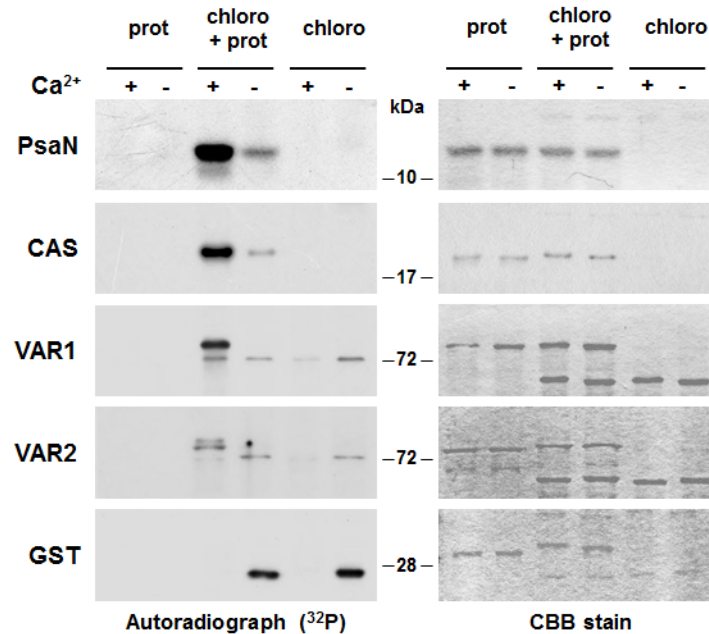


**Figure 3 Calcium dependent phosphorylation assays on recombinant PsaN, CAS, VAR1, VAR2 and GST protein.** The two middle lanes of the left panel display the autoradiograph of  $^{32}\text{P}$ -labeled proteins of a  $\text{Ca}^{2+}$  dependent phosphorylation assay of recombinant protein (prot) by an Arabidopsis chloroplast protein extract (chloro). The two left lanes are a control of protein only, whereas the two right lanes are a control for the background phosphorylation in the chloroplast protein extract. Note that GST is not being phosphorylated, instead a strong phosphorylation is visible in the EGTA sample of the chloroplast protein extract. The right panel is the protein loading control (CBB = Coomassie Brilliant Blue).

## Discussion

The exploration of potential crosstalk between calcium signaling and protein phosphorylation at chloroplast thylakoid membranes has delivered first evidence for the calcium dependent phosphorylation of PsaN, CAS and VAR1, among other proteins. This leads to the question what might be the function of this calcium dependent phosphorylation? While this is difficult to answer for PsaN, one can speculate about the impact of calcium dependent phosphorylation on VAR1 and CAS. VAR1, which is also called FTSH5, is a conserved thylakoid localized protease that together with its close homolog VAR2 (or FTSH2) is responsible for the protein turnover of photo-damaged D1 subunits of photosystem II (Lindahl et al., 2000; Aro et al., 2005; Kato et al., 2009).

Subunit D1 seems to be the main ‘victim’ of the reactive photochemical reactions of the photosystem II and constantly needs to be recycled, even under low light, to prevent photo-inhibition of the photosystems (Aro et al., 1993). The important function of VAR1 and VAR2 for the plant becomes obvious in their loss-of-function mutants, which exhibit variegated leaf phenotypes (green and white sectoring of the leaf) (Sakamoto et al., 2003). Phosphorylation of VAR1 might be a means to altering its proteolytic activity, as it is known for another important group of proteases, the caspases (Kurokawa and Kornbluth, 2009). Accordingly, we hypothesize that an increase of free stromal  $\text{Ca}^{2+}$  on the transition from light to dark (Sai and Johnson, 2002) could mediate the phosphorylation of VAR1, a protease that degrades photo-damaged D1 protein in the light, to switch of its activity when it is no longer needed in the dark. From our experiments it seems that mainly VAR1 is subjected to posttranslational modification, since VAR2 was not phosphorylated significantly above background levels (Fig. 3). As both VAR1 and VAR2 are operating in heterocomplexes (Sakamoto et al., 2003; Zhang et al., 2010), the posttranslational modification of VAR1 could have an influence on the activity of VAR2. In this respect, phosphorylation of VAR1 could affect complex formation, as it is known for the photosynthetic complexes (Tikkanen and Aro, 2011). For CAS it is tempting to speculate that the observed increase of phosphorylation under increased light intensities (Vainonen et al., 2008) is mediated by an increase of  $\text{Ca}^{2+}$  uptake into the chloroplast under light (Kreimer, 1985; Roh et al., 1998). How this behaviour than relates to the observed function in ‘calcium sensing’ of CAS for stomatal movement remains an open question. CAS was shown to bind  $\text{Ca}^{2+}$  with low affinity/high capacity to a part of the protein N-terminal of the transmembrane region (Han et al., 2003). Interestingly, for the phosphorylation assay of Fig. 3 we have used the C-terminal part of CAS, because it was proven to be phosphorylated (Vainonen et al., 2008; Reiland et al., 2011). How the binding of  $\text{Ca}^{2+}$  to the N-terminus of CAS relates to the  $\text{Ca}^{2+}$  dependent phosphorylation of the C-terminus adds to question on the function of CAS. It should be noted that CAS was found in this study through a naïve search for calcium dependently phosphorylated proteins. Nevertheless its prior connection to chloroplast calcium signalling fits nicely with the finding of calcium dependent protein phosphorylations in the thylakoid. Further detailed studies are necessary to elucidate the functional impact of calcium dependent phosphorylation on VAR1 and CAS.



What is the nature of the kinase responsible for the calcium dependent protein phosphorylation? Most likely several protein kinases are involved, since protein substrates from both sides of the thylakoid membrane have been identified. For example, the C-terminal part of VAR1 faces the stromal side of the thylakoid (Sakamoto et al., 2003), whereas, PsaN and the oxygen evolving complex subunit PsbP are attached to the luminal side of the thylakoid membrane. Another clue comes from the confirmation experiments (Fig. 3) in which the recombinantly purified proteins PsaN, VAR1 and CAS were phosphorylated by a salt-washed soluble chloroplast extract. This would rather exclude the membrane-intrinsic thylakoid protein kinases STN7 and STN8 as responsible kinases for this phosphorylation. A possible candidate kinase for calcium dependent phosphorylation could be CIPK13, which is supposed to be soluble and was reported to reside in the chloroplast (Schliebner et al., 2008). CIPK's are CBL interacting protein kinases that are known to be regulated in a calcium dependent manner through the interaction with the EF-hand containing calcineurin B-like proteins (CBL) (Weinl and Kudla, 2009). However, CIPK13 has not been characterized in detail so far and the absence of CBL proteins in the chloroplast casts doubt on the function of CIPK13 in the chloroplast. Also several other calcium dependent protein kinases are predicted to be localized to plastids. However, it turned out that they are membrane-localized due to *N*-acylation, which prevents their chloroplast import (Mehlmer et al., 2010; Stael et al., 2011) Bayer *et al.*, JXB, submitted).

It should be noted that through the use of phosphatase inhibitors (NaF, NaVO<sub>3</sub> and β-Glycerophosphate) the influence of phosphatases can be excluded in this experimental set-up. Of course, it cannot be excluded that *in vivo* protein phosphatases could play a role in calcium dependent protein phosphorylations of the thylakoid. On the other hand, instead of Ca<sup>2+</sup> influencing the kinase, Ca<sup>2+</sup> might also bind first the substrate protein leading to a conformational change or enhancing the interaction with a protein kinase, which in turn could phosphorylate the substrate. This could be the case for CAS and PsbP, which are known to bind calcium. Similarly, conformational changes, which are induced by depletion of Ca<sup>2+</sup> (upon addition of EGTA), could be the reason for observed increases in phosphorylation, which is visible for ATPC1 and MFP1 in Fig 2A and B, respectively. We observed this effect also in other experiments (see suppl. Figures).

In the future, the functional impact of calcium dependent phosphorylation on plant physiology can be estimated through targeted mutations of the phosphorylation sites of

VAR1 and CAS. Quantitative phosphoproteomics were proven to work for chloroplasts (Reiland et al., 2011) and could be used to obtain an even more comprehensive overview of calcium dependent phosphorylated proteins of the thylakoid, including the mapping of exact phosphorylation sites.

### **Supplementary data**

Supplementary Table S1. Overview of all identified calcium or EGTA dependent phosphorylated proteins.

Supplementary Table S2. Excel table of all identified protein spots from different 2D gels. (Not supplied with this thesis)

Supplementary Fig. S1 – S7. Pictures of all 2D experiments done with Arabidopsis using different Ca<sup>2+</sup> concentrations and different detection methods (Pro-Q Diamond staining and phospho-Threonine specific antibodies).

### **Acknowledgements**

This work has been funded by the Austrian GEN-AU program in the ERA-PG project *CROPP* (Project No. 818514), the Austrian Science Foundation (P19825-B12), and by the EU in the Marie-Curie ITN *COSI* (ITN 2008 GA 215-174).

## **2.5. Organellar EF-hand protein of 18 kDa (OEF18) is a novel calcium signaling protein**

The discovery of OEF18 was connected to the work on acylation and chloroplast targeting of protein kinases (Stael et al., 2011) and was rather a case of serendipity. What we noticed in this study was a severe underrepresentation of predicted myristoylated proteins in the chloroplast, compared to the full Arabidopsis genome. To test this, a former colleague (Dr. Roman Bayer) screened the available chloroplast proteomic databases for proteins with a predicted myristoylation signal. Next to two Arabidopsis proteins which were previously shown to reside inside the chloroplast (Duchene et al., 2005; Schliebner et al., 2008), the localization of one protein from rice was tested by YFP-fusion analysis. The YFP-fusion chimera of the Arabidopsis homolog (At1g64850) did not localize inside the chloroplast, but rather at the envelope of chloroplasts and some undefined spots outside of the chloroplasts, thereby confirming the underrepresentation of acylated proteins inside of the chloroplast (Stael et al., 2011). Interestingly, we realized that this protein contained an EF-hand and therefore I decided to work further on it within the frame of my thesis. The protein was described as an unknown protein, thus we named it Organellar EF-hand protein of 18 kDa (OEF18).

### **OEF18 localizes to the peroxisomal membrane and chloroplast outer envelope with the EF-hand facing to the cytosol**

Data from three independent localization approaches were considered, to establish the localization of OEF18 to certain organelles. YFP-fusion studies and OEF18 was first identified by proteomics in the plastid envelope of etiolated rice seedlings (von Zychlinski et al., 2005). Since then it was found to be localized to the plastid envelope in two further proteomic approaches (Brautigam and Weber, 2009; Ferro et al., 2010) and to the peroxisome (Reumann et al., 2009). It was also identified in our earlier described chloroplast proteomics approach (Bayer et al., 2011), however, it was below the acceptance threshold. To assess the localization of OEF18 in an independent approach, it was fused to yellow fluorescent protein (YFP), transiently expressed in tobacco leaf epidermal cells and viewed after two days of incubation with a confocal microscope. OEF18 displayed a dual localization to the chloroplast envelope and to peroxisomes, judged by the overlap of the YFP-signal with co-expressed subcellular protein markers (Fig. 8A). OEF18-YFP signal did not overlap with other subcellular protein markers, such

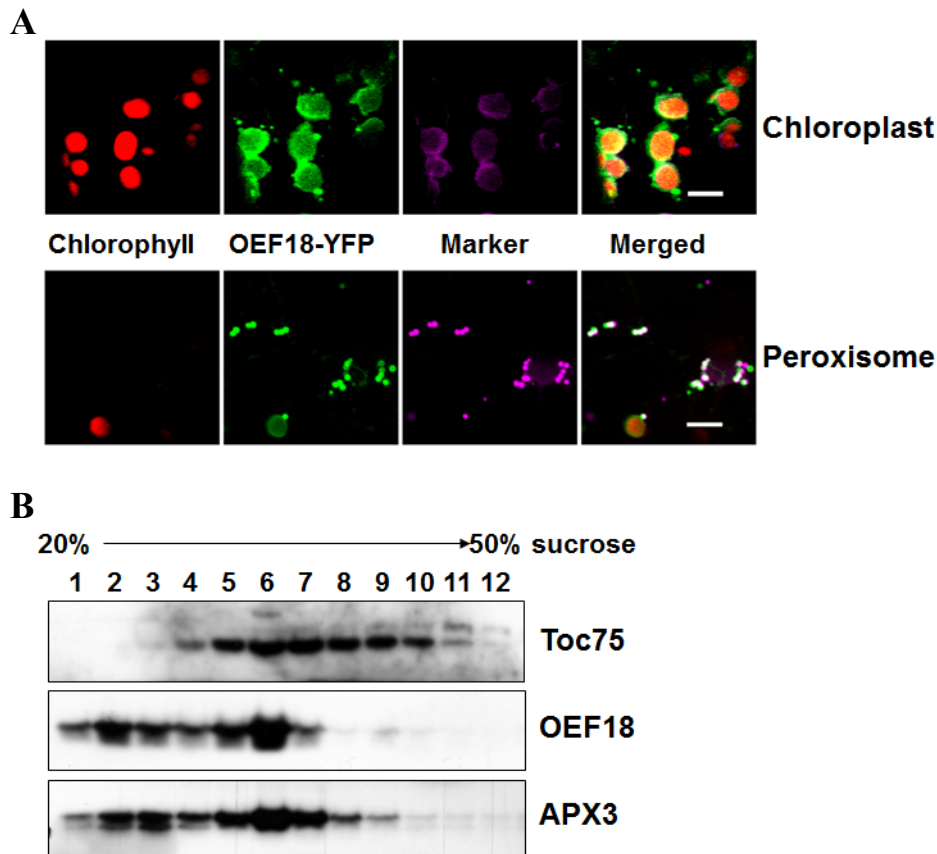


**Figure 8 OEF18 is dually localized to the plastid envelope and peroxisomes.** (A) YFP-fusion localization study of OEF18 in tobacco epidermal leaf cells. OEF18-YFP signal overlaps with the signal from a plastid outer envelope marker (OEP7-mCherry marker, top row) and with a peroxisomal membrane marker (mCherry-SKL marker, bottom row). Autofluorescence of chloroplasts is in red, OEF18-YFP is green, mCherry marker is magenta and a merged image is presented on the right. Size of the scalebar is 10  $\mu$ m. (B) Western blot of 12 fractions from a total leaf membrane extract separated on a sucrose density gradient (~20-50%). Endogenous OEF18 protein is detected with a specific antibody in the middle panel. The top panel displays the presence of the outer envelope marker protein Toc75 in the different fractions, whereas the bottom panel shows the distribution of the peroxisomal membrane marker APX3.

as an ER-, a Golgi complex-, and an oilbody-protein marker (data not shown). In an

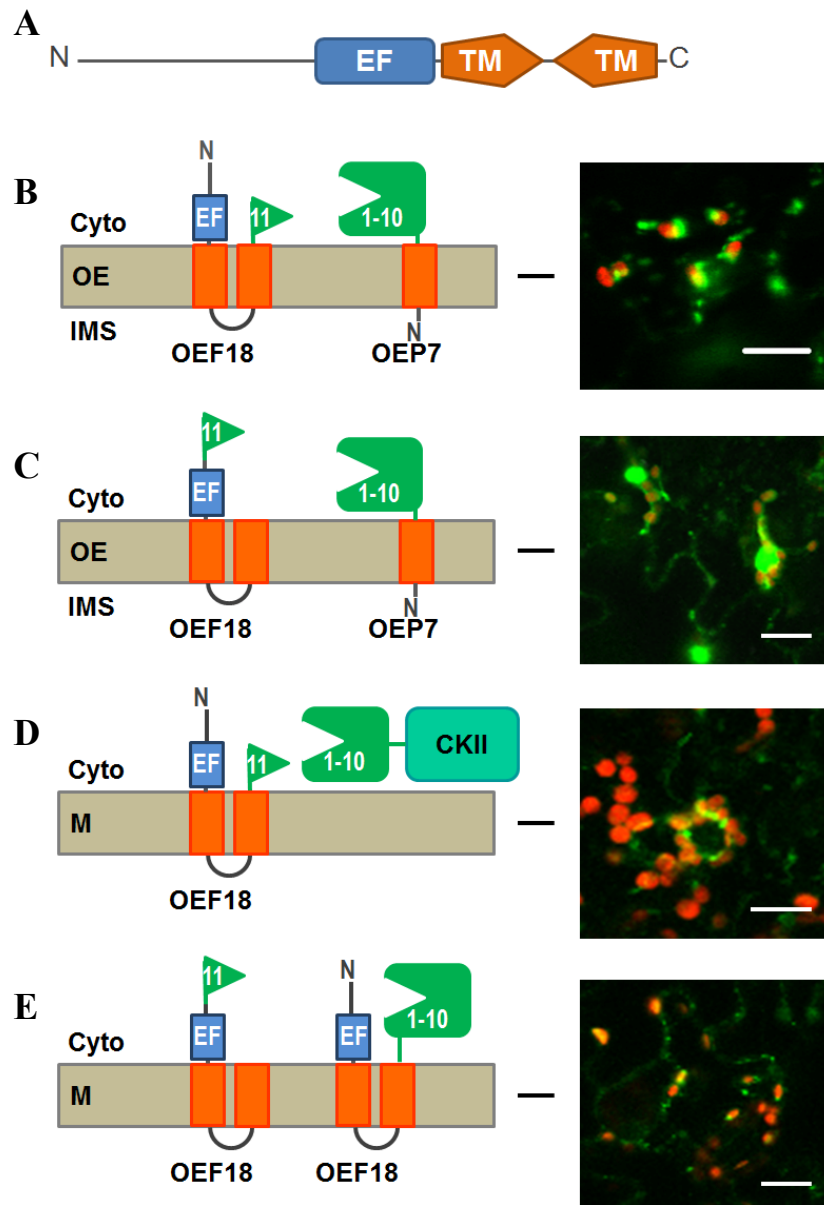


**Figure 9 Determining the topology of OEF18 with self-assembly GFP.** (A) Representation of predicted protein domains of OEF18 shows the EF-hand (EF in blue box) and two C-terminal transmembrane domains (TM in orange boxes). (B) The 11th  $\beta$ -strand of GFP (indicated with number 11 in the green flag) attached to the C-terminus of OEF18 is able to interact with  $\beta$ -strands 1-10 of GFP attached to the C-terminus of the outer envelope marker OEP7, as symbolized in the left scheme. On the right, the merged confocal microscopy image reveals the presence of reconstituted GFP-signal (in green) and chloroplast autofluorescence (in red). Size of the scalebar is 20  $\mu$ m. (C) The 11th  $\beta$ -strand of GFP attached to the N-terminus of OEF18. (D) The 11th  $\beta$ -strand of GFP attached to the C-terminus of OEF18 can interact with  $\beta$ -strands 1-10 of GFP attached to the C-terminus of the cytoplasmic marker protein casein kinase II (CKII). (E) The 11th  $\beta$ -strand of GFP attached to the N-terminus of OEF18 can interact with  $\beta$ -strands 1-10 of GFP attached to the C-terminus of OEF18, demonstrating that both termini face the same side of the membrane.

alternative experimental approach, an Arabidopsis leaf membrane extract was separated by centrifugation on a sucrose gradient and the 12 obtained fractions were subsequently western blotted and probed with an OEF18-specific antibody. The same western blot was

probed with an antibody for APX3 (ascorbate peroxidase 3), which localizes to the peroxisomal membrane (Shen et al., 2010), and Toc75 (Translocon outer membrane complex 75), which localizes to the plastid outer envelope. In this approach, the signal of OEF18 showed the best overlap with that of APX3 (fraction 1 to 6), favouring a peroxisomal localization of OEF18. However, some overlap with Toc75 was also detected in fractions 4 to 7, which argues for a dual localization of OEF18.

From the localization data and protein prediction it became evident that OEF18 was an integral membrane protein that potentially contained two transmembrane  $\alpha$ -helices positioned in the C-terminal domain of the protein (Fig. 9A). The question then arised: to which compartment of the cell does the EF-hand of OEF18 localize? To answer this question, the topology of OEF18 was determined using a relatively new technique based on split-GFP technology, called self-assembly GFP (saGFP). This technique was successfully employed to pinpoint the localization of Omp85 (Outer membrane protein 85) in the complex plastid of the diatom *Phaeodactylum tricornutum* (Bullmann et al., 2010) and to determine the disputed topology of the Arabidopsis homologs, AtToc75-III and AtToc75-V (Sommer et al., 2011). It works similar to the better known bi-molecular fluorescence complementation (BiFC) assay, but the difference with saGFP is that unequal parts of GFP are splitted, namely  $\beta$ -strands 1-10 and 11, which have a much higher affinity for each other than is the case with BiFC. This will lead to an efficient reconstitution of the GFP signal when the two parts of saGFP are expressed in pair in the same compartment of the cell, regardless of a potential interaction between the proteins they are fused to. When this is combined with the knowledge of topology for one of the proteins in the pair, the unknown topology of the other protein can be deduced. The system proofs to be very flexible as complex localizations or topologies can be assessed for wich other techniques are coming short and various combinations of the saGFP tags (N- or C-terminal) can be used to obtain a confident idea of a protein's topology. These combinations are summarized in Fig. 9B-E and lead to the conclusion that both N- and C-termini of OEF18 face the same membrane side, that OEF18 localizes to the peroxisome membrane and the plastid outer envelope and that the EF-hand is facing the cytosol.

### **OEF18 binds calcium and is myristoylated *in vitro***

OEF18 has a single predicted EF-hand (depicted in Fig. 10A), which is rather unusual for EF-hand containing  $\text{Ca}^{2+}$  binding proteins. Therefore overlay assays with radiolabeled calcium ( $^{45}\text{Ca}$ ) were performed using the N-terminal part of OEF18, excluding the

transmembrane (TM) domains. The protein was expressed in *Escherichia coli* and purified with the IMPACT<sup>TM</sup> system (New England Biolabs) in which the purification tag is cleaved off, resulting in an untagged OEF18 protein of high purity. This protein was then dot-blotted on a PVDF membrane and incubated with <sup>45</sup>Ca in a standard overlay assay (Fig. 10B). Mutating the first and highly conserved aspartate of the EF-hand Ca<sup>2+</sup>-binding loop to an alanine (D2A), resulted in the inability of the protein to bind Ca<sup>2+</sup> and served as a control to the <sup>45</sup>Ca overlay assay. Accordingly, OEF18 is able to bind Ca<sup>2+</sup> *in vitro* with its EF-hand. Building further on the work of protein acylation and chloroplast targeting (Stael et al., 2011), the predicted myristoylation site of OEF18 (indicated with a G for glycine in Fig. 10A) was experimentally tested in a radiolabeled myristoylation (<sup>3</sup>H) assay. To this end, full-length OEF18 was expressed in wheat germ lysate in the presence of <sup>3</sup>H labelled myristate or <sup>35</sup>S labelled methionine, as an expression control, and incorporated radioactivity was visualized on an SDS-PAGE gel (Fig. 10C). OEF18 is myristoylated *in vitro*, similar to the positive control, calcium-dependent protein kinase 2 (CPK2). Nevertheless, the role of myristoylation for OEF18 is still unclear, since the protein is already membrane bound by two transmembrane domains. However, it might play a role in the function of OEF18 or in targeting to the peroxisomal membrane and chloroplast envelope, as highlighted in the next paragraph.

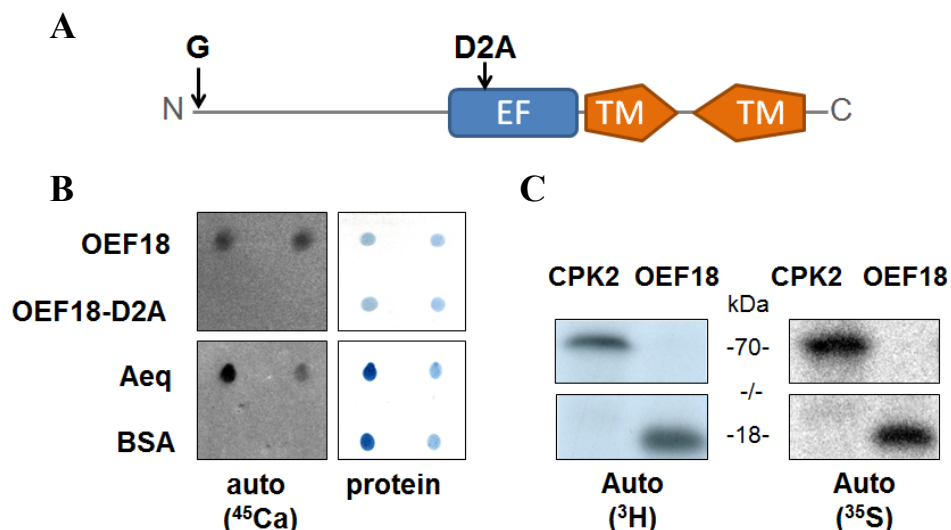


**Figure 10 Calcium binding and myristoylation assays of OEF18.** (A) Approximate position of the N-terminal glycine (G) and aspartate to alanine mutation (D2A) on the OEF18 protein scheme. (B) Radiolabeled calcium (<sup>45</sup>Ca) overlay assay displays the binding of <sup>45</sup>Ca to the N-terminal part of OEF18 including the EF-hand, but excluding the TM domains. The OEF18-D2A protein is unable to bind <sup>45</sup>Ca, although a similar amount of protein was loaded (right panels are the protein loading control). Positive control is aequorin (Aeq, contains 3 EF-hands) and negative control is bovine serum albumin (BSA). (C) Radiolabeled myristoylation assay shows the labeling of the published positive control protein, calcium-dependent protein kinase 2 (CPK2) (Lu and Hrabak, 2002), and OEF18 with <sup>3</sup>H myristate (left panels). Right panels display the translation control of <sup>35</sup>S methionine labeled protein from the cell-free wheat germ lysate.

### The localization of OEF18 is determined by the transmembrane domains, myristoylation and a positively charged double lysine motive

Various factors influence the remarkable dual localization and targeting of OEF18 to the peroxisomal membrane and plastid outer envelope. The C-terminal transmembrane domain of OEF18 was fused C-terminally to the fluorescence tag mCherry and expressed transiently in tobacco leaf epidermal cells (Fig. 11A). This seemed to be sufficient to target the fluorophore to the same localization as observed for the whole protein (Fig. 11B). On the contrary, the localization of the N-terminal part only of OEF18 did not

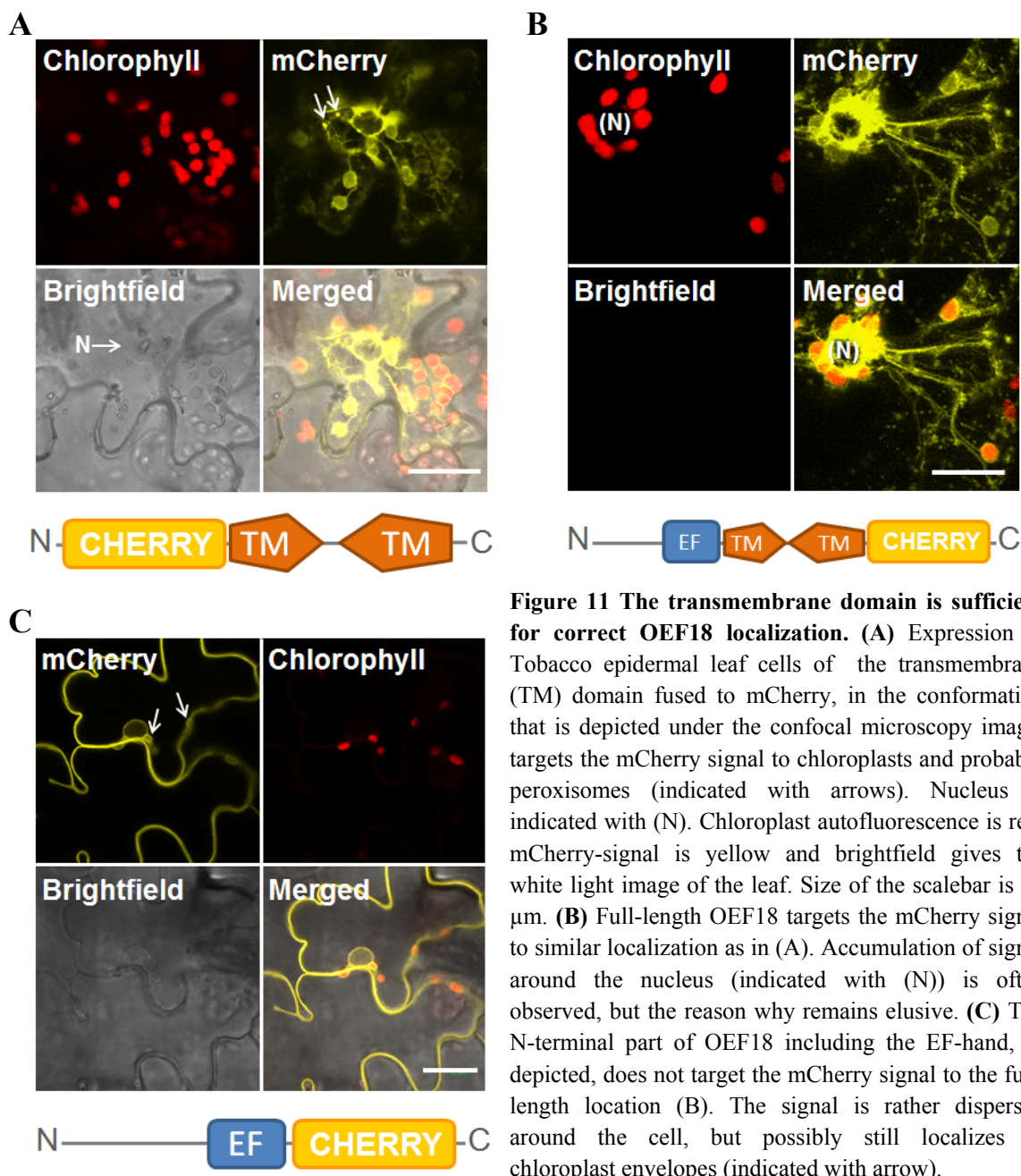


**Figure 11 The transmembrane domain is sufficient for correct OEF18 localization. (A)** Expression in Tobacco epidermal leaf cells of the transmembrane (TM) domain fused to mCherry, in the conformation that is depicted under the confocal microscopy image, targets the mCherry signal to chloroplasts and probably peroxisomes (indicated with arrows). Nucleus is indicated with (N). Chloroplast autofluorescence is red, mCherry-signal is yellow and brightfield gives the white light image of the leaf. Size of the scalebar is 20  $\mu$ m. **(B)** Full-length OEF18 targets the mCherry signal to similar localization as in (A). Accumulation of signal around the nucleus (indicated with (N)) is often observed, but the reason why remains elusive. **(C)** The N-terminal part of OEF18 including the EF-hand, as depicted, does not target the mCherry signal to the full-length location (B). The signal is rather dispersed around the cell, but possibly still localizes to chloroplast envelopes (indicated with arrow).



resemble the localization of the full-length protein, but was completely dispersed throughout the cell (Fig. 11C). Possibly, the N-terminal part still localized to the chloroplast envelope (indicated with arrows in Fig. 11C), however this would need further experimentation to be unequivocally proven. The role of myristoylation in the localization of OEF18 was investigated by mutating the N-terminal glycine to an alanine residue (G2A, represented in Fig. 12A), as this was demonstrated to have a severe effect on the localization and function of other proteins (Ishitani et al., 2000; Batistic et al., 2008; Stael et al., 2011).

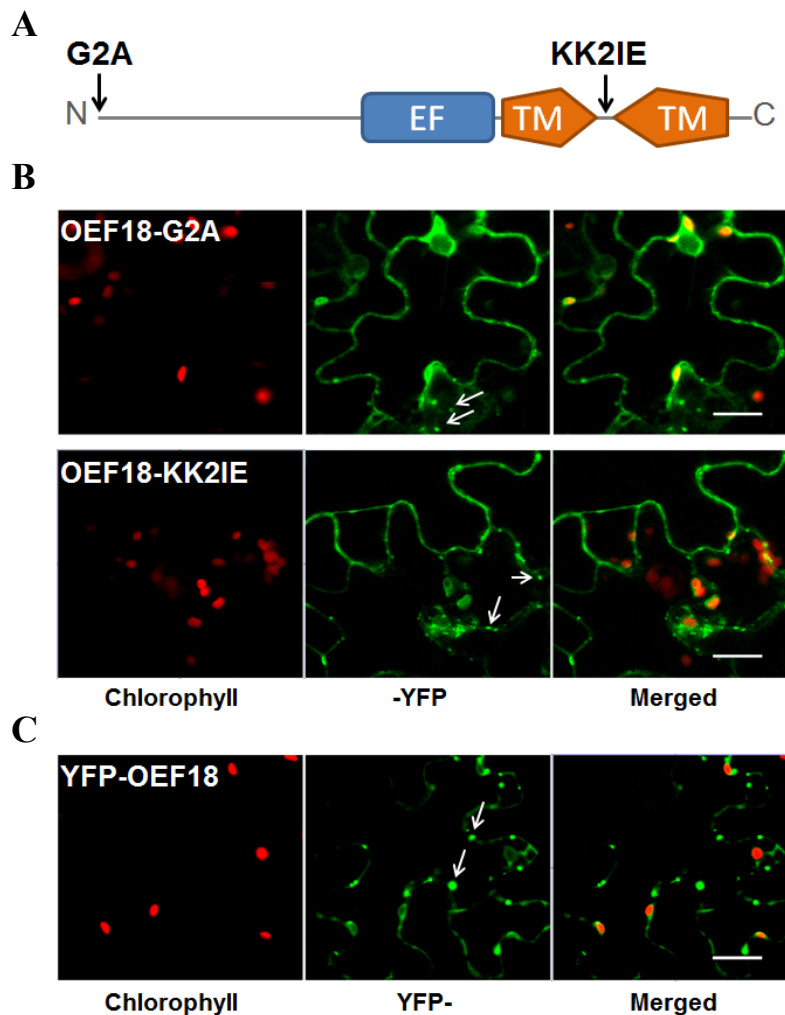


**Figure 12 Factors that influence localization of OEF18.** (A) Approximate position of the point mutations that affect localization on the OEF18 protein scheme. (B) Mutation of the first glycine to alanine (G2A) disturbs the localization of the OEF18\_G2A-YFP fusion product when expressed in Tobacco epidermal leaf cells. The YFP-signal (green) still localizes to chloroplasts (in red) and peroxisomes (indicated with arrows), but is more dispersed through the rest of the cell. Similarly, mutation of the double lysine motive to an isoleucine and glutamate residue (KK2IE) disperses the YFP-signal of OEF18\_KK2IE through the cell. (C) Orientation of the fluorophore does not greatly affect the localization of OEF18, as OEF18 with a fusion of YFP to its N-terminus (YFP-OEF18) still localizes to chloroplasts and peroxisomes (indicated with arrow). Nonetheless, the YFP-signal is a bit dispersed. Size of the scalebar is 20  $\mu$ m.

Again, the YFP-signal of the OEF18 G2A mutant did not fully resemble the localization of the wild-type protein but was somewhat more dispersed throughout the cell (Fig. 12B). A similar distribution was observed for an OEF18 mutant protein in which the conserved positively charged double lysine motive in between the two TM domains was mutated to a negatively charged glutamate and isoleucine residue (KK2IE; Fig. 12B). This is in line with reports for other outer envelope membrane proteins that lysine residues flanking the TM domain can influence their localization and positive charges in general influence TM helices insertion into the membrane (Lee et al., 2001; Lee et al., 2004; Lerch-Bader et al., 2008; Lee et al., 2011). Apparently, the main targeting factor for OEF18 seems to be the transmembrane domain and correct targeting is influenced by myristoylation and a conserved positively charged double lysine motive.

### **OEF18 has orthologs in plants and algae and a single homolog in Arabidopsis**

Arabidopsis OEF18 has orthologs in higher plant species, embryophytes (*Selaginella moellendorffii* and *Physcomitrella patens*) and chlorophytes (*Chlamydomonas reinhardtii* and *Volvox carteri*), but not in cyanobacteria or other bacteria. From an alignment of selected higher plant species orthologs it became obvious that OEF18 is fairly conserved along the entire length of the protein, with the N-terminus being least conserved and two regions being highly conserved (marked HCR1 and 2 in Fig. 13A). HCR2 encompasses the protein region around the double lysine motive (KK) in between the two transmembrane domains (TM1 and 2) and is probably conserved for protein targeting reasons. The reason for the high conservation of HCR1 remains elusive. Going further down the evolutionary tree, a clear ortholog for *Chlamydomonas* was hard to find from a straightforward BLAST search and involved the parsing of low-homology candidates for specific OEF18 protein features. An unknown *Chlamydomonas* protein (gi 159483337) fitted best as it was of similar size to OEF18 and contained two EF-hands, followed directly by a single lysine in between of two predicted TM domains (aligned with OEF18 in Fig. 13B). Interestingly, when ‘going up’ the evolutionary tree, there seemed to be a degeneration of EF-hands: the *Chlamydomonas* ortholog contains two predicted fully functional EF-hands (predicted by Prosite; <http://prosite.expasy.org/>), the *Selaginella* ortholog contains one fully functional EF-hand and one ‘incomplete EF-hand’ and all higher plant species contain one ‘incomplete EF-hand’ (Fig. 13C). Perhaps, the HCR1 is what remains of the second EF-hand. One unknown Arabidopsis protein, At4g37445, is homologous to OEF18 and contains all its protein features except for the EF-hand

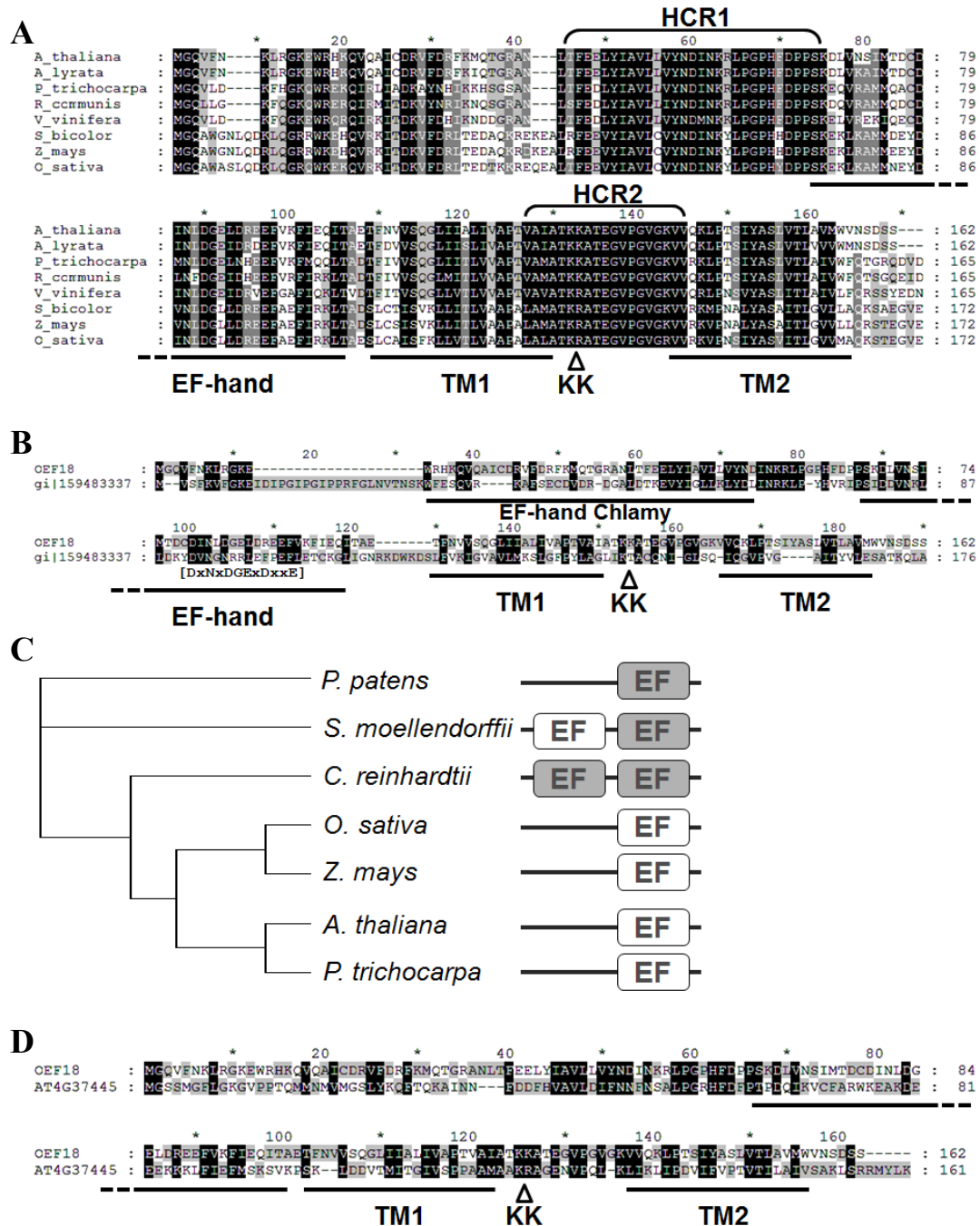


**Figure 13 OEF18 phylogeny.** (A) Alignment of higher plant orthologs of OEF18 displays the high conservation of OEF18. Two highly conserved regions (HCR1 and HCR2) are indicated with brackets. The position of the single EF-hand and the two transmembrane domains (TM1 and TM2) are underlined. KK marks the double lysine motive in between TM1 and TM2. (B) Alignment of OEF18 with a probable *Chlamydomonas reinhardtii* ortholog (gene identifier 159483337). The *Chlamydomonas* ortholog has an extra EF-hand (indicated with EF-hand Chlamy). The calcium binding motive of the OEF18 EF-hand is indicated at its approximate position ([DxNxDGExDxxE]). (C) Phylogenetic tree of selected OEF18 orthologs displaying the number of EF-hands per protein. EF-hands in the dark grey boxes are predicted to be fully functional, whereas EF-hands in the white boxes are incomplete. In the case of OEF18, the leucine in position 4 of the calcium binding motive [DxNLDGExDxxE] should not be there, according to the Prosite prediction motive: D-(W)-[DNS]-(ILVFIYW)-[DENSTG]-[DNQGHRK]-(GP)-[LIVMC]-[DENQSTAGC]-x(2)-[DE]-[LIVMFYW] (the amino acids in between () brackets are excluded at that position). (D) Alignment of OEF18 with its only Arabidopsis homolog (At4g37445). The position of the EF-hand is underlined, but is absent in At4g37445. On the other hand, TM1, the KK-motive and TM2 are present and underlined.

(aligned with OEF18 in Fig. 13D). The relationship of this protein to OEF18 remains to be solved.

### OEF18 is expressed throughout the plant and expression increases with the age of leafs and osmotic stress

The expression pattern of the OEF18 protein in Arabidopsis was investigated with the use of an OEF18 specific antibody on western blots of various Arabidopsis protein extracts. The antibody was raised in a rabbit that was immunized with the native N-terminal part of the OEF18 protein (excluding the transmembrane domain). OEF18 was present in all major plant tissues, except in the seeds (Fig. 14A). Its presence in the root was double-checked by comparison with a root protein extract from an OEF18 knock-out allele, *oef18-1* (Fig. 14C). These findings are in good agreement with publically available RNA expression data. Next, the protein amount of OEF18 in leaves of different ages was tested (Fig. 14B). Interestingly, significantly more OEF18 protein was detectable in old leaf (still green) and senescent leaf (old leaves that started to yellow) than in young total leaf (still green) and senescent leaf (old leaves that started to yellow) than in young total

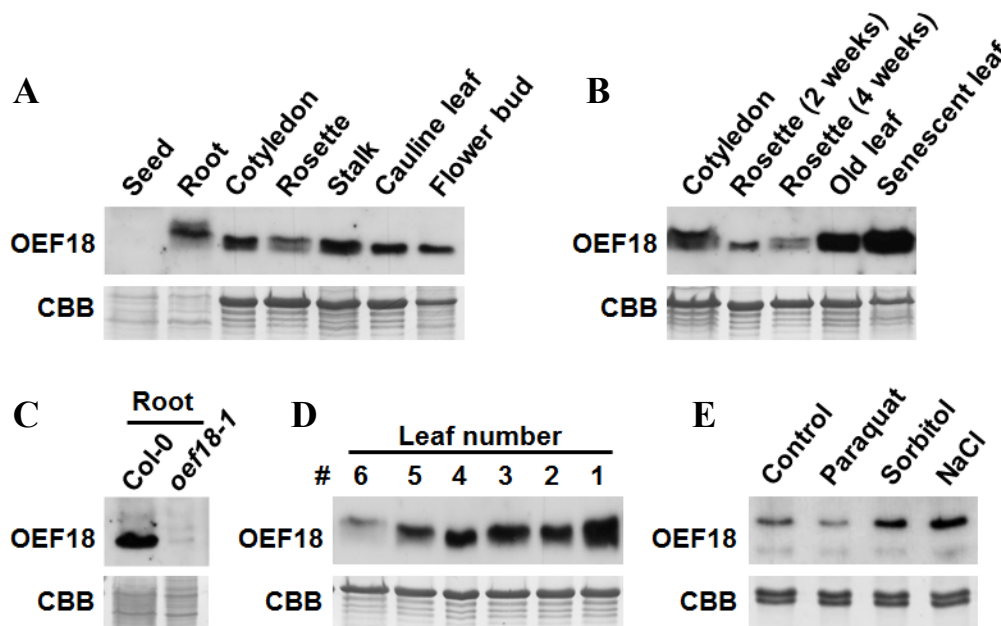


Figure 14 Expression analysis of OEF18 by western blot. **(A)** Anti-OEF18 antibody reveals the presence of OEF18 in all major plant tissues, except seeds (top panel). Bottom panel shows an inset of the Coomassie brilliant blue (CBB) stained blot as an approximate control of equal protein load per lane (strongest band is Rubisco). **(B)** Expression of OEF18 in leaf tissue of various ages. Cotyledons were 10 days old at harvest. Complete rosette was 2 and 4 weeks old. Single full-grown leaves at approximately 2 months of age were harvested still green (old) and clearly yellowing (senescent). **(C)** Root protein extract of wild-type (Col-0) and OEF18 knock-out (*oef18-1*) Arabidopsis plants. **(D)** Expression of OEF18 in single leaves of increasing age of a single rosette. Leaves were numbered according ascending order in the rosette, excluding the cotyledons. Accordingly, leaf number 1 is the oldest and 6 the youngest. **(E)** Expression of OEF18 in complete seedlings (2 weeks) on agarose plates (1/2 MS, 1% sugar) under different stresses: reactive oxygen species (1  $\mu$ l/L paraquat), osmotic (100 mM sorbitol) and salt (75 mM NaCl).

rosette leaflets (2 weeks and 4 weeks). In line with this finding, the OEF18 protein level of single leaves going up the rosette spiral (numbered 1 (oldest) to 6 (youngest) in Fig. 14D) was tested. Similarly to the old and senescent leaves, the protein levels increased with increasing leaf age, although to a lesser extent. A slight increase in protein level of OEF18 was also observed upon abiotic stress treatment, when seedlings (2 weeks) were grown on agarose plates (1% sugar) under osmotic stress (100 mM sorbitol) and salt stress (75 mM NaCl) (Fig. 14E). Given the similar OEF18 expression levels under salt and osmotic stress, the difference to standard conditions under salt stress was probably due to the osmotic component of salt stress. Upon the addition of paraquat, a ROS-inducing agent, the OEF18 protein level slightly dropped below standard level. It seems that OEF18 is ubiquitously expressed throughout the plant and thereby forms a general part of the plant cell protein complement. Since its expression is varied only minimal upon the experimentally tested abiotic stresses and other untested stresses (inferred from publically available RNA expression data), OEF18 might rather be involved in signaling for general housekeeping functions or in developmental functions.

### **Two knock-out and overexpressing alleles pave the way for a genetic analysis of OEF18**

After the discovery of OEF18 and the initial experiments on its localization and calcium binding properties, several T-DNA insertion lines (see supplementary table 1) were screened to identify *Arabidopsis* knock-out alleles of OEF18 (Fig. 15B and C). Eventually, two lines with T-DNA insertions inside of the OEF18 gene were identified and named *oef18-1* (WiscDsLox461-464A5) and *oef18-2* (SK40148). The *Arabidopsis oef18-1* line was obtained from the Wisconsin DsLox T-DNA mutant collection (Woody et al., 2007) and is in the Col-0 genetic background with the T-DNA inserting most likely in the third and last intron (Fig. 15A). The *Arabidopsis oef18-2* line was obtained from the relatively new Saskatoon T-DNA mutant collection (Robinson et al., 2009) and is in the Col-4 genetic background with the T-DNA inserting most likely in the third exon or third intron (Fig. 15A). Both lines were found to be homozygous for the T-DNA insertion. Although *oef18-1* exhibited a slight residual expression of full-length OEF18 (indicated with a star in Fig. 15B), no OEF18 protein could be detected in both lines (Fig. 15D). At the same time, *Arabidopsis* lines overexpressing a Strep-tagged OEF18 construct under the control of a 35S promoter were prepared and screened for homozygosity. Two of these lines, called OEF18-1 and OEF18-2 (Fig. 15D) revealed to be weak/medium

overexpressors of OEF18, whereas others expressed OEF18 to much higher levels (not shown). These alleles enabled a genetic analysis of OEF18 function for which initial steps have been taken, as detailed in the next paragraphs.

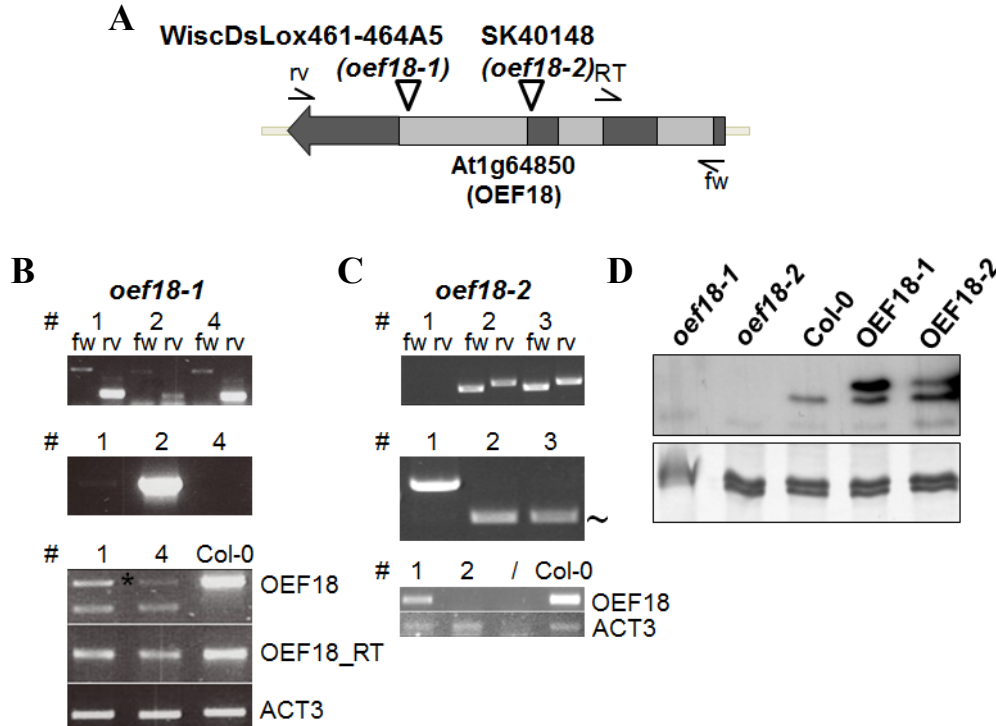


**Figure 15 T-DNA insertion alleles of OEF18.** (A) Scheme of the *OEF18* gene indicating the approximate position of two different T-DNA insertions. Exons are dark grey and introns light grey. The Arabidopsis T-DNA insertion line WiscDsLox461-464A5 is referred to as *oef18-1* and SK40148 as *oef18-2*. Primers used for the genotyping of the lines are indicated with fw (forward), rv (reverse) and RT (primers spans intron 2 for use with RT-PCR). (B) Genotyping of *oef18-1* by PCR. Top panel displays the search for positive T-DNA insertion lines by PCR on genomic DNA with fw and rv primers in combination with the left border primer of the T-DNA. Various plants were tested, but only 3 representative plants are shown (plant #1,2 and 4). Middle panel shows the search for homozygous T-DNA insertion lines. To this end, PCR on genomic DNA with fw and rv primers was performed. The increased size of the PCR product, due to the insertion of the T-DNA, leads to the absence of PCR product as observed for plant #1 and 4, under conditions were a non-inserted or heterozygous plant shows product (plant #2). Bottom panel shows the product of RT-PCR for full-length *OEF18* (fw and rv primer) in plant #1 and 4 compared to wild-type (Col-0; residual *OEF18* expression in #4 indicated with a star). *OEF18\_RT* is the product of RT-PCR for an N-terminal part of *OEF18* (fw and RT primer). *Actin3* (*act3*) is a loading control. (C) Genotyping of *oef18-2*, similarly to (B). Here, plant # 2 and 3 are homozygous (unspecific product indicated with a (~)) and the RT-PCR product of *OEF18* is absent in plant # 2. (In the bottom panel, the lane indicated with (/) is a water control without cDNA.) (D) Western blot for the expression of endogenous *OEF18* protein shows the absence of protein in the *oef18-1* (plant #4) and *oef18-2* lines (plant #2), whereas 35S-driven overexpressor lines *OEF18-1* and *OEF18-2* contain a bit more of *OEF18*-STREP protein. The increased size of the protein in *OEF18-1* and *OEF18-2* is likely due to the STREP-tag.

### **OEF18 function influences plant growth and sugar levels**

Altering the expression levels of OEF18 revealed an influence on plant growth already under normal growth conditions. When grown under standard long day conditions, *oef18-1* and *oef18-2* knock-out mutants were growing slightly smaller than the wildtype allele, whereas OEF18-1 and OEF18-2 plants grew slightly bigger (Fig. 16A). For this analysis, the seeds of all 5 plant lines were harvested from plants growing under identical conditions for two consecutive generations, to reduce seed-derived effects on plant growth. Fig. 16D shows the expression level of OEF18 in these alleles. In a confirmation experiment in cooperation with Bayer Bioscience, a large set of seedlings (minimally 75 per genotype) was grown on agarose plates (1 % sugar; Fig. 16B shows an example plate) under standard growth conditions and the average leaf area of each plant line was determined by quantitative image analysis. The graph in Fig. 16C summarizes the average difference in leaf area to the wildtype allele (Col-0) over a timeline of day 8 until day 17. Similarly to the soil-experiments, *oef18-1* and *oef18-2* alleles were gradually lacking behind in growth to approximately 20% in leaf area of the wildtype allele at day 17, whereas OEF18-1 and OEF18-2 had a remarkable headstart in growth until day 11, after which their leaf areas dropped back to a similar size as the wildtype allele. The reason for this sudden drop remains elusive. These initial phenotypic observations suggested that OEF18 is involved in plant growth and perhaps plant development. In an attempt to learn more about the function of OEF18 and to shed light on the growth-phenotype, a metabolic screen was performed on the OEF18 alleles in collaboration with the lab of Prof. Andreas Weber (University of Düsseldorf). A total of 40 general plant metabolites were measured in two biological replicates. For the first replicate, samples were taken only at midday, but for the second replicate the samples were taken also at midnight. The mutant alleles OEF18-1 and OEF18-2 consistently had lower levels of sucrose (Fig. 16D-F) and glucose (Fig. 16G-I) than the wildtype, whereas the *oef18-1* and *oef18-2* alleles displayed an unreliable variation in the accumulation of these metabolites. Other changes in metabolite levels were not consistent between the two biological repeats and therefore are not presented. This drop in sugar levels for the plants overexpressing OEF18 seems interesting, but needs confirmation via another experiment to substantiate this claim. It has been reported though that increased plant growth negatively correlates with abundance of the main plant metabolites, such as the sugars, because the plant supposedly has a higher turnover of metabolites (Meyer et al., 2007; Sulpice et al., 2010).

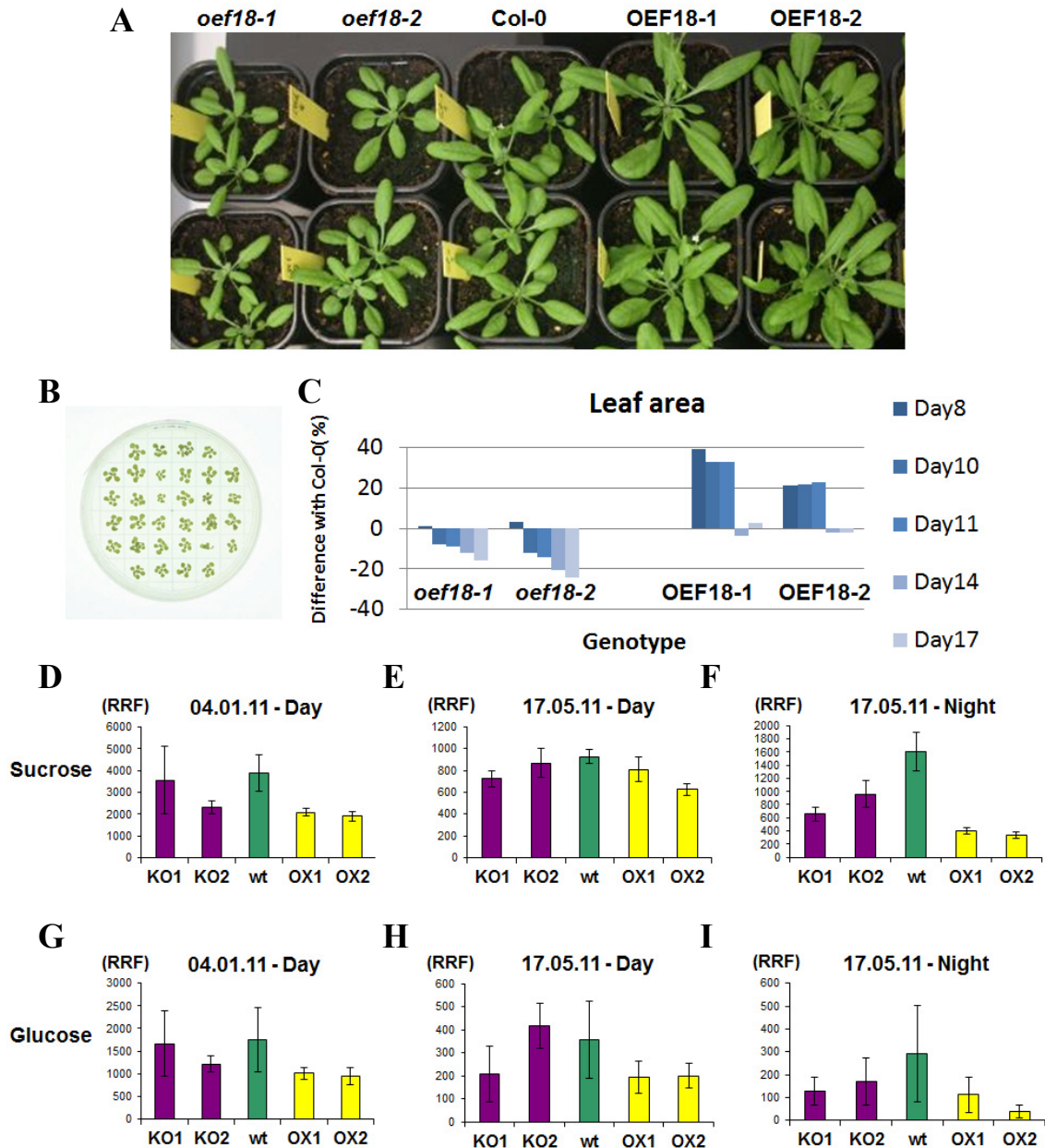


**Figure 16 Growth and metabolite analysis of OEF18 knock-out and overexpressing plants. (A)** Top view of Arabidopsis plants grown for 4 weeks under long day conditions in soil at a light intensity of  $\pm 100 \text{ mmol m}^{-2}\text{s}^{-1}$ ,  $\pm 22^\circ\text{C}$  and humidity of  $\pm 60\%$ . *oef18-1* and *oef18-2* are knock-out alleles and OEF18-1 and OEF18-2 are overexpressing alleles of OEF18. **(B)** Example plate of the leaf-area experiment. Seedlings were spaced well apart to reduce neighboring effects on agarose plates containing  $\frac{1}{2}$  MS medium and 1% sugar. Images were taken of all plates at day 8, 10, 11, 14 and 17. Leaf area was calculated with a custom program in ImageJ and statistics were performed in R. **(C)** The column graph summarizes the difference in leaf area of the indicated OEF18 alleles to wild-type plants (Col-0), over a period of 10 days from day 8 to day 17. P-values of main differences were for the most significant differences smaller than 0.001. **(D)(E)(F)** Quantification of sucrose in the full rosette of 4 week old Arabidopsis plants for the different alleles of OEF18 (KO1=*oef18-1*, KO2=*oef18-2*, WT=Col-0, OE1=OEF18-1, OE2=OEF18-2) by GC-MS analysis according to (Brautigam et al., 2011). Experiment was repeated three times: at midday on 04.01.2011 (D), at midday on 17.05.2011 (E) and at midnight on 17.05.2011 (F). Metabolites were quantified relative to ribitol, an added internal standard, and therefore the y-axis is named ribitol response factor (RRF). In (E) and (F), less metabolite extract was loaded, leading to lower RRF values. **(G)(H)(I)** Quantification of glucose, similar to (D)(E)(F). Values are the mean of 4 replicas and standard errors are depicted.



**Overexpression of OEF18-YFP in Arabidopsis leads to clustering of the chloroplast**

In order to double-check the localization of OEF18 in Arabidopsis plants, transgenic lines were produced that overexpress an OEF18-YFP fusion protein under the control of a 35S promoter. Upon examining the plants by confocal laser scanning microscopy it became immediately evident that OEF18-YFP localized to the envelope and that the chloroplasts had an aberrant morphology that is best described by the word: clusters (Fig. 17A-E). Furthermore, these chloroplast clusters were most evident in the petiole (observation not quantified), but the meaning of this observation again remains elusive. On a related note, the transient overexpression of the OEF18\_EFD2A mutant, which is mutated in the EF-hand and unable to bind  $\text{Ca}^{2+}$ , as a YFP-fusion protein in tobacco epidermal cells, produced big buds on the chloroplast that were not observed with the wild-type protein (Fig. 17F-K). Taken together these findings suggest a possible role of OEF18 in plastid division.

**Discussion of OEF18 targeting and potential function**

The novelty of OEF18 lies in its localization and single EF-hand. Most of my research until now was focused on localization and targeting of OEF18, as the observed dual localization to the plastid outer envelope and peroxisomal membrane is rather unusual. In fact, only one other transmembrane protein, called SMP2 was reported to localize to the chloroplast, peroxisome and mitochondria and apart from its localization nothing else is known about this protein (Abu-Abied et al., 2009). On the other hand, the dual targeting of soluble organellar proteins is much more common, especially between plastids and mitochondria (Carrie et al., 2009). How might OEF18 than be targeted to both the plastid outer envelope and peroxisomal membrane? Apparently, the C-terminal transmembrane part of OEF18 is sufficient for its targeting and it contains a positively charged region behind the first transmembrane domain. These characteristics are reminiscent of tail-anchored (TA) membrane proteins with the difference that TA membrane proteins only have a single transmembrane domain at their very C-terminus (Abell and Mullen, 2011), and OEF18 has two. An increasing number of TA proteins have recently been found to localize to the plastid envelope (Kriechbaumer et al., 2009) and peroxisome (Narendra et al., 2006; Aung et al., 2010) and one factor seems to be crucial for the targeting of these proteins: the outer envelope protein chaperone/receptor, Ankyrin-repeat containing

protein 2A (AKR2A) (Bae et al., 2008; Dhanoa et al., 2010; Shen et al., 2010; Zhang et al., 2010). AKR2A is believed to specifically bind the TM domain and to guide proteins for the posttranslational insertion into the plastid envelope and peroxisomal membrane. It would be very interesting to see if AKR2A is involved in the dual targeting of OEF18. Another possibility for the peroxisomal targeting of OEF18 would be to first traverse the ER en route to the peroxisome as other peroxisomal membrane proteins are known to do (Karnik and Trelease, 2007; van der Zand et al., 2010). However, this would not explain the plastid localization, as a similar ER-plastid route for membrane proteins is unknown to date. Furthermore, a recent study showed that transmembrane domains followed by positively charged residues, so called signal anchors, with a low hydrophobicity (<0.4 on the Wimley and White scale) preferably insert into the membranes of endosymbiotic organelles and with a high hydrophobicity preferably insert into the ER membrane (Lee et al., 2011). The transmembrane domains of OEF18 have a low average hydrophobicity (0.2 and 0.13 on the Wimley and White scale) that would favour their insertion into the plastid envelope. Of course, this is only prediction and the possibility of an OEF18 ER-targeting route should be investigated. Anyhow, the high conservation of the C-terminal transmembrane domain (Fig. 13A) emphasizes the importance of correct OEF18 targeting. The single EF-hand of OEF18 is one of the few experimentally documented single EF-hand proteins in Arabidopsis, despite the fact that almost 40% of the 250 predicted EF-hand proteins in Arabidopsis contain a single EF-hand (Day et al., 2002). The best documented Arabidopsis single EF-hand protein is KIC (KCBP-interacting  $\text{Ca}^{2+}$  binding protein), which is involved in the  $\text{Ca}^{2+}$ -dependent binding of Kinesin-like calmodulin binding protein (KCBP) and trichome morphogenesis (Reddy et al., 2004). KIC is required for the microtubule-stimulated ATPase activity of KCBP and was shown to bind  $\text{Ca}^{2+}$  at physiological levels in the process. Similarly, OEF18 is able to bind  $\text{Ca}^{2+}$  by its single EF-hand in a  $^{45}\text{Ca}$  overlay assay, however the kinetics and specificity of  $\text{Ca}^{2+}$  binding should be investigated in order to assess if OEF18 would be able to sense physiological changes in the concentration of  $\text{Ca}^{2+}$ . To conclude, the unique localization of OEF18 and its EF-hand at the interface with the cytosol bestow the possibility upon plastids and peroxisomes to perceive first-hand the information of cytoplasmic  $\text{Ca}^{2+}$  signaling. On the other hand, possible  $\text{Ca}^{2+}$  signals emanating from internal plastid or peroxisome  $\text{Ca}^{2+}$  stores might influence functions at the periphery of the respective organelles.

Apart from the novelty, the main question about OEF18 is of course: what is its function? As for all reverse genetics approaches, this has been a hard question to answer. Probably the best hint came from Arabidopsis plants overexpressing an YFP-tagged version of OEF18. These plants displayed abnormal chloroplast behaviour, forming clusters of tightly packed chloroplasts that seemed to be incompletely divided of one another and especially seemed to affect the petiole (Fig. 17A-E). So far, there are no other reports in the literature of clustering plastids, but if it is true that the chloroplasts are incompletely divided and not merely 'sticking together', then OEF18 might be involved in the act of plastid division. A defect in the development of plastids could result in the defective growth of the OEF18 knock-out mutant plants *oef18-1* and *oef18-2*, whereas slight overexpression in OEF18-1 and OEF18-2 might boost chloroplast division and plant growth. Important for this effect is the expression level of OEF18, because an expression as high as it is visible in the OEF18-YFP plants would lead to a clustering of plastids, which most likely is not beneficial anymore to the plant. Furthermore, expression of OEF18 across the entire plant further suggests that its function is central to the development of plastids and plants and the localization of OEF18 surely fits this hypothesis. On the other hand, the increased expression of OEF18 in aging leaves (Fig. 14B and D) contradicts a function of OEF18 in development of plastids, but rather speaks for a role in degradation of plastids. Of course, both processes could involve the function of OEF18 for division or fragmentation of the plastid. Components of the division machinery of plastids peroxisomes and mitochondria are known to be shared (Aung et al., 2010) and one protein, DRP5B, localizes both to plastids and peroxisomes. DRP5B (Dynamamin-related protein 5B), also called ARC5 (for accumulation and replication of chloroplasts), is a cytosolic protein that originally was identified as a component of plastid division, because cells that lack the protein contain enlarged dumbbell-shaped chloroplasts (Gao et al., 2003). Later on it was found to localize to peroxisomes and to be involved in their division as well (Zhang and Hu, 2010). Since DRP5B does not contain any transmembrane domains, but specifically localizes to the chloroplast and peroxisome membrane, it would be interesting to test if OEF18 is able to interact with DRP5B. To conclude, OEF18 might bring a signaling dimension to the act of plastid and peroxisome division, which would be a new invention of plants to possibly coordinate plastid and peroxisome division with processes of the rest of the cell involving calcium signals.

## 2.6. Proteomics appendix - Are LENA and LENB chloroplast calcium storage proteins?

In a confirmation experiment of the chloroplast proteomics approach, the newly identified chloroplast protein, described as CUP2 in the Bayer 2011 proteomics paper (CHLOROPLAST UNKNOWN 2, At2g17240; Fig. 18A) was tested for its ability to bind  $\text{Ca}^{2+}$  in a radiolabeled calcium ( $^{45}\text{Ca}$ ) overlay assay. CUP2 was chosen because it has a remarkable acidic stretch of amino acids enriched in glutamic acid (E), which is known to be involved in low affinity/high capacity  $\text{Ca}^{2+}$  binding in  $\text{Ca}^{2+}$  storage proteins (see introduction). It is a very small protein, of which the acidic stretch takes up almost 40 % of the predicted 9.7 kDa mature protein (without transit peptide). Therefore, the protein was renamed more aptly to LITTLE E-ENRICHED protein A (LENA) and Fig. 18B shows that LENA, similarly to the positive control Aequorin, was able to bind  $\text{Ca}^{2+}$  *in vitro*. The Arabidopsis genome contains one highly homologous gene to LENA, which codes for an unknown protein and tentatively was named LENB (At3g24506). LENB has a good chloroplast prediction and a high similarity of the predicted mature protein to

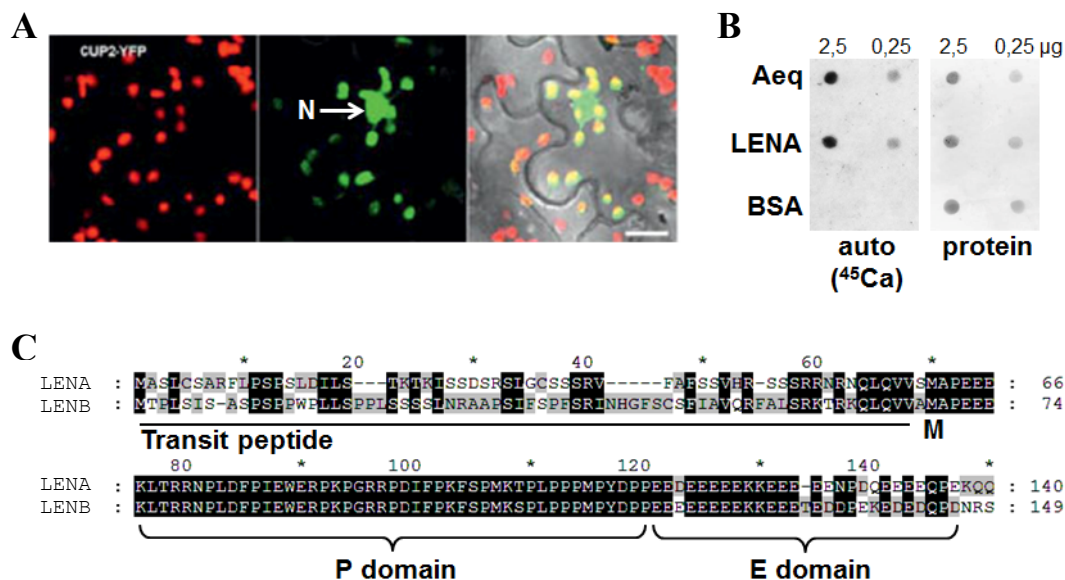


**Figure 17 LENA overview.** (A) LENA-YFP localizes to the chloroplast in Tobacco leaf epidermal cells (image taken from Bayer et al, 2010). The accumulation of LENA in the nucleus (indicated with N) is probably due to overexpression from an alternative start-codon, which is probably the second methionine (indicated in (C) with M). (B) Full-length LENA is able to bind  $\text{Ca}^{2+}$  in a  $^{45}\text{Ca}$ -overlay assay, as is visible from the autoradiograph (left panel). Positive control is aequorin (Aeq) and negative control is bovine serum albumin (BSA). Right panel is the protein loading control. 2.5 and 0.25  $\mu\text{g}$  of recombinant protein were spotted on the PVDF membrane. (C) Alignment of LENA and its closest Arabidopsis homolog LENB. The predicted chloroplast transit peptide is underlined. The P-domain is enriched in proline residues and the E-domain is enriched in glutamate residues. Notice the high conservation of the mature proteins (without transit peptide).

LENA (Fig. 18C). Although it was not studied experimentally, LENB is expected to have the same localization and  $\text{Ca}^{2+}$ -binding capacities as LENA. Both proteins are differentially expressed, according to publically available RNA expression data, with LENA being higher expressed than LENB (data not shown). Interestingly, these two proteins not only have an acidic domain (E domain in Fig. 18C), but they also contain a domain that is highly conserved and enriched in proline (P domain in Fig. 18C), similar to calreticulin - the main calcium storage protein of the ER (compare to Fig. 3 of the introduction). Further experimentation is required, but nonetheless, the resemblance of LENA and LENB as a ‘miniaturized version’ of calreticulin adds to the argument that these proteins might be involved in  $\text{Ca}^{2+}$  storage of the chloroplast.

### 3. Conclusions and future perspectives

I have presented evidence for a range of new  $\text{Ca}^{2+}$  binding proteins of Arabidopsis located at plastids, peroxisomes and mitochondria. Understanding of the influence of  $\text{Ca}^{2+}$  signaling in these organelles and the impact on the rest of the cell is still in its infancy. The insights from the presented research have therefore helped to enrich the knowledge about - and to cement the position of - calcium signaling in the organelles.

An initial search for  $\text{Ca}^{2+}$  binding proteins in the chloroplast by means of proteomics led to the discovery of various new chloroplast proteins, of which two proteins, SAMTL and LENA were confirmed to bind  $\text{Ca}^{2+}$  *in vitro*. The chloroplast is hypothesized to be a  $\text{Ca}^{2+}$  storage organelle in which most of the mobilizable  $\text{Ca}^{2+}$  is transiently bound to a yet unknown stromal  $\text{Ca}^{2+}$  store (Kreimer, 1987; Sai and Johnson, 2002). Based on its protein characteristics and resemblance to the main ER  $\text{Ca}^{2+}$  storage protein, calreticulin, I propose that LENA could serve as a  $\text{Ca}^{2+}$  storage protein in chloroplasts. SAMTL, on the other hand, is a  $\text{Ca}^{2+}$  signaling protein as it contains a single EF-hand. SAMTL is part of the mitochondrial carrier protein family and in-depth bioinformatic analysis suggests that it functions as plastid SAM transporter in addition to the known SAM transporter, SAMT1.

The discovery of SAMTL prompted us to investigate the other EF-hand containing mitochondrial carrier family proteins. This inevitably expanded our scope of finding  $\text{Ca}^{2+}$  binding proteins of the chloroplast to include  $\text{Ca}^{2+}$  binding proteins of the mitochondria. APC1, 2 and 3 are Arabidopsis isoforms of the calcium-dependent ATP-importer of

mitochondria that is best known from yeast and humans. I could provide good evidence that APC1,2 and 3 may play a similar role in plants, based on overall homology and the functional complementation of an ATP-importer deficient yeast strain. That is, during periods of anoxia, APC1, 2 and 3 may provide the mitochondria with external ATP to maintain the mitochondrial membrane potential by a reversal of the  $F_0F_1$   $H^+$ -ATP synthase, which is crucial to the viability of mitochondria and the cell.

The discovery that OEF18 is dually localized, led to the conclusion that eventually the peroxisome has to be included into the organellar  $Ca^{2+}$  signalling network. OEF18 is a novel single EF-hand protein that is dually targeted to the plastid outer envelope and peroxisomal membrane. Unlike LENA, SAMTL and APC1, 2 and 3, there is no precedent to OEF18, making it difficult to find a function. However, based on its localization and a chloroplast clustering phenotype we observed in transgenic plant lines, I hypothesize that OEF18 is involved in the process of organellar division.

In addition to my approaches to identify novel organellar  $Ca^{2+}$  binding proteins, I have investigated a potential crosstalk between calcium signaling and protein phosphorylation in chloroplasts. Calcium dependent protein phosphorylation is a common regulatory principle in plants and all prerequisites for calcium signaling can be found in chloroplasts as well. However, chloroplast protein phosphorylation is much better understood than organellar calcium signaling, so it provides a good experimental background to assess the impact of chloroplast calcium signaling on the plant by protein phosphorylation. I have identified three chloroplast proteins with good confidence to be calcium dependently phosphorylated: PsaN, CAS and VAR1. Most likely, more chloroplast proteins are calcium dependently phosphorylated as well, but they need further confirmation or are still waiting to be discovered.

The presented work lays only a base for further research and I am aware that more experimental work is necessary to proof some of the hypotheses in order to better understand the impact of organellar calcium signaling on the plant. Arabidopsis lines deficient in predicted organellar  $Ca^{2+}$  handling proteins could be crossed with  $Ca^{2+}$  reporter lines. For example, LENA (and LENB or double mutants) deficient plants could be crossed with stromal targeted aequorin transgenic Arabidopsis lines, in order to check if the reported  $Ca^{2+}$  flux on the transition from light to dark is affected. For similar reasons, knock-out plants of the plant homologs of the newly discovered human mitochondrial calcium channels (MICU and MCU, see review) could be crossed with

mitochondrial targeted aequorin transgenic Arabidopsis lines. For LENA and LENB it would be further required to investigate the properties and specificity of  $\text{Ca}^{2+}$  binding with biophysical techniques such as isothermal titration calorimetry (ITC) or circular dichroism (CD). The same should be done for OEF18 and its EF-hand mutant, OEF18-D2A. Furthermore for OEF18, the plastid clustering phenotype should be better documented both in *oef18-1*, *oef18-2*, OEF18-1, OEF18-2 and higher overexpressing OEF18 transgenic plants. Also, the impact of the EF-hand D2A mutation of OEF18 on plastid morphology should be checked in transgenic Arabidopsis plants. A search for interaction partners of OEF18 could include targeted Y2H assays with proteins of the organellar division machineries, a naïve Y2H screen or immunoprecipitation assays. For SAMTL, the predicted substrate transport of SAM should be assayed with purified recombinant protein reconstituted in liposomes, as it has been done for many other mitochondrial carrier family proteins. After that, it would be really interesting to investigate the effect of deleting SAMTL in Arabidopsis plants with a SAMT1 deficient background and to observe the *in vivo* levels of SAM in the chloroplast. In the case of APC1, 2 and 3, the genetic analysis of their function could be checked under specific conditions, such as anoxia or added sugars. Complications arising from gene redundancy might require the fabrication of triple knock-out Arabidopsis plants to assess the full implications of the loss of mitochondrial ATP import. The influence of  $\text{Ca}^{2+}$  on the function of SAMTL and APC1,2 and 3, could be checked by mutating the EF-hand regions in a similar way to the D2A mutation in the EF-hand of OEF18. To investigate the impact of calcium dependent protein phosphorylation on chloroplast function and plant physiology, known phosphorylated amino acids of PsaN, CAS and VAR1 could be point mutated. The clear phenotypes of CAS and VAR1 would be instrumental to the read-out of introducing point-mutated protein versions in a knock-out background.

It became evident that plastids, mitochondria and potentially peroxisomes are both subjected to  $\text{Ca}^{2+}$  dependent regulations and can influence  $\text{Ca}^{2+}$  signaling to the rest of the cell. The finding of novel  $\text{Ca}^{2+}$  binding proteins has led to the understanding that these organelles potentially undergo  $\text{Ca}^{2+}$  dependent regulation during stress conditions, such as anoxia, or during developmental processes, such as organellar division. Complementary to the photosynthetic ‘dark reactions’, the protein of the ‘light reactions’ might also undergo calcium dependent regulation, since important photosynthetic thylakoid membrane proteins are reversibly phosphorylated in a calcium dependent manner.

Further work on these proteins warrants exciting future developments. The next important question to address will be the role of the proteins involved in  $\text{Ca}^{2+}$  handling, such as the  $\text{Ca}^{2+}$  sensing proteins,  $\text{Ca}^{2+}$  channels and  $\text{Ca}^{2+}$  storage proteins of the organelles in order to measure their contribution to cellular  $\text{Ca}^{2+}$  signaling. Finally, more organellar  $\text{Ca}^{2+}$  binding proteins and  $\text{Ca}^{2+}$  regulated processes are awaiting discovery.



## 4. Material and methods

### 4.1. Used vectors

All vectors were made compatible for cloning *ApaI/NotI* or *NcoI/NotI* and are here listed in alphabetical order.

pBAT	derived from pBluescript; contains T3-promotor and rabbit myoglobin leader sequence to enhance protein expression; used for <i>in vitro</i> translation of proteins (Annweiler et al., 1991)
pBTM117	derived from pBTM116 (Bartel and Fields, 1995) modified by Dr. Markus Teige; contains Lex-A DNA-binding domain; used for yeast two hybrid assays
pBIN-Basta	derived from pBIN19 (Bevan, 1984); plant kanamycin resistance gene exchanged for bar gene (BASTA resistance marker) and one <i>ApaI</i> restriction site deleted by Norbert Mehlmer; binary plant transformation vector for protein YFP-fusion localization analysis and transformation of <i>Arabidopsis thaliana</i>
pBIN-Cherry	derived from pBIN19; created in this work by replacing YFP with mCherry; binary plant transformation vector for protein mCherry-fusion localization analysis
pBIN-Kan	pBIN19; plant kanamycin resistance gene; binary plant transformation vector for protein YFP-fusion localization analysis and transformation of <i>Arabidopsis thaliana</i>
pBin-Ncherry	derived from pBIN-Basta; created by removing YFP and adding N-terminal mCherry tag; binary plant transformation vector for protein YFP-fusion localization analysis
pBIN-saGFP1-10	derived from pBIN-Basta; created in this work by replacing YFP with saGFP1-10 tag; used for topology experiments
pBIN-saGFP11C	derived from pBIN-Basta; created in this work by replacing YFP with saGFP11C tag; used for topology experiments

pBIN-saGFP11N	derived from pBIN-Ncherry; created in this work by replacing Ncherry with saGFP11N tag; used for topology experiments
pBIN-Strep	derived from pBIN-Basta; created in this work by replacing YFP with StrepII-tag; binary plant transformation vector for transformation of <i>Arabidopsis thaliana</i>
pCRBlunt	Invitrogen; used as entry-vector for cloning of blunt-end PCR products
pGad424	Clontech; contains Gal4 activation domain; used for yeast two hybrid assays
pGEX4T-3	GE Healthcare; contains glutathione S-transferase (GST) tag; used for inducible protein expression in <i>E. coli</i>
pGreen-Strep	derived from pGREEN II (Hellens, 2000); created in this work by replacing YFP with StrepII-tag; plant kanamycin resistance gene; binary plant transformation vector for protein transformation of <i>Arabidopsis thaliana</i>
pTLT	created by Dr. Norbert Mehlmer; used as a shuttle-vector for cloning into pBIN
pTWIN1-N	derived from pTWIN1 (New England Biolabs, NEB); one intein tag removed by Dr. Norbert Mehlmer; used for inducible protein expression in <i>E. coli</i> ; chitin-tag is still cleaved by remaining intein to release untagged protein
YEpm351-HA	kindly provided by Markus Aleschko; contains a methionine-repressible promoter and a c-terminal triple hemagglutinin (HA) tag; used for constitutive expression in yeast

## 4.2. Bacteria and yeast strains

### Bacteria

strain DH5 $\alpha$	F-, $\Phi$ 80lacZ $\Delta$ M15 $\Delta$ (lacZYA-argF) U169 recA1 endA1 hsdR17 (rK-, mK+) phoA supE44 $\lambda$ - thi-1 gyrA96 relA1
strain ER2566	from NEB; F-, $\lambda$ - fhuA2 [lon] ompT lacZ::T7 gene1 gal sulA11 $\Delta$ (mcrC-mrr)114::IS10 R(mcr-73::miniTn10-TetS)2 R(zgb-210::Tn10)(TetS) endA1 [dcm]

**Agrobacteria**

AGL1 *recA::bla* pTiBo542ΔT Mop<sup>+</sup> Cb<sup>R</sup> (Lazo et al., 1991)

GV3101 pMP90RK *rpoH<sup>+</sup> hrcA<sup>+</sup> C58C1 Rif<sup>r</sup> Gm<sup>r</sup>*(Koncz and Schell, 1986)

**Yeast**

L40 *MATα hisΔ200 trp1-900 leu2-3.112 ade2 LYS2 :: (LexA op)<sub>4</sub>HIS3 URA3 :: (LexA op)<sub>8</sub> lacZ Gal4 gal 80*

W303 *MATα leu2-3,112 trp1-1 can1-100 ura3-1 ade2-1 his3-11,15*  
(kindly provided by Juraj Laco)

Δsal1 as W303, but *AAC1-3 Δsal1::kanMX4* (kindly provided by Juraj Laco)

**4.3. Plant material*****Arabidopsis thaliana***

Col-0 ecotype Columbia

WiscDsLox461-464A5 knock-out T-DNA insertion line for OEF18 (At1g64850) in Col-0 background; BASTA resistance marker (University of Wisconsin)

SK40148 knock-out T-DNA insertion line for OEF18 (At1g64850) in Col-4 background; BASTA resistance marker (Robinson et al., 2009)

C1S1-17 independent overexpression lines of OEF18, containing full length OEF18 (Ca1) with a C-terminal StrepII-tag under control of a single 35S promoter in Col-0 background; BASTA resistance marker (except C1S1 has kanamycin resistance due to cloning via pGREEN-Strep)

***Nicotiana tabacum***

cv. Petite Havana SR1

***Pisum sativum***

cv. Arvika ZS (BSV-Bayrische Futtersaatbau GmbH, Ismaning, Germany)

#### 4.4. Antibodies

##### Primary antibodies

Anti-

APX3 peroxisomal tail-anchored ascorbate peroxidase 3 protein (kindly provided by Dr.Hong Zhang); from rabbit; use 1:500 in TBS-T with 1% milk

Ca1N prepared by inoculating recombinant protein of a N-terminal part of OEF18 (first 102 amino acids, by Davids Biotechnology): from rabbit; use 1:500 in TBS-T with 1% milk

P-Thr phospho-threonine specific antibody (Cell Signaling #9381); from rabbit; use 1:1000 in TBS-T with 1% bovine serum albumine (BSA)

Porin mitochondrial porin (kindly provided by Dr. Harvey Millar); from mouse; use 1:3000 in TBS-T with 1% milk

Toc75 chloroplast outer envelope membrane translocon complex OEP75 protein (Agrisera #AS06150); from rabbit; use 1:1000 in TBS-T with 1% milk

GFP green fluorescent protein (Roche #11814460001); from Mouse; use 1:1000 in TBS-T with 1% BSA

##### Secondary antibodies

Anti-

Mouse ECL Mouse IgG, HRP-Linked Whole Ab (from sheep, GE healthcare #NA931)

Rabbit ECL Rabbit IgG, HRP-Linked Whole Ab (from donkey, GE healthcare #NA934)

#### 4.5. Media

Media were prepared with distilled water (dH<sub>2</sub>O) and autoclaved at 120°C for 20 minutes.

##### Lysogeny broth (LB) medium

For 1 litre of liquid medium, add 10 g tryptone, 5 g yeast extract and 5 g NaCl, adjust pH to 7.2 with 1M NaOH. For plates, add 20 g bacto-agar. For selection media, add 1 ml of a 1000x stock (100mg/ml ampicillin in dH<sub>2</sub>O stored at 4°C for LB-AMP or 50mg/ml kanamycin in dH<sub>2</sub>O stored at 4°C for LB-KAN).

**½ Murashige Skoog (MS) medium**

For 1 litre of liquid medium, add 2.2 g MS powder (Duchefa) and adjust pH to 5.8 with 0.1M KOH. For plates, add 7 g plant-agar (Duchefa). Optionally, add 1% sucrose.

**Synthetic drop-out (SD) medium**

Prepare yeast nitrogen base medium (YNB, 4.6 g/L) to which adenine, uracil and tyrosine are added (40mg/ml) and autoclaved. Autoclave separately a 40% glucose solution. Prepare separately a 100x stock solution of ‘complete amino acids’ (printed bold in the table) and a separate 100x stock of each ‘selection amino acid’ (leucine, tryptophane and histidine) and sterile filtrate these amino acid solutions. Before use, add to the YNB medium the glucose (final concentration of 2%) and all amino acids, except for those which are selected for. For plates, add 30 g bacto-agar.

Amino acids and bases	g/L
<b>Arginin</b>	3
<b>Isoleucin</b>	2
<b>Lysin</b>	4
<b>Methionin</b>	2
<b>Phenylalanin</b>	6
<b>Threonin</b>	15
<b>Valin</b>	6.5
<b>Aspartat</b>	10
(Histidin)	2
(Leucin)	8
(Tryptophan)	4
<i>Tyrosin</i>	4
<i>Uracil</i>	4
<i>Adenin</i>	4

**YPD (Yeast, Peptone, Dextrose) medium**

For 1 litre of liquid medium, add 20 g pepton and 10 g yeast-extract. Autoclave and store separately from glucose-solution (this is the YP-medium). Before use, add 50 ml of 40% glucose (-D, from dextrose; autoclave separately) to get YPD with a glucose endconcentration of 2%. For plates, add 30 g bacto-agar.

**4.6. Buffers and solutions**

Buffers and solutions were prepared with distilled water (dH<sub>2</sub>O) and autoclaved at 120°C for 20 minutes. Common buffers are listed here. Specific buffers are noted after each protocol.

**Coomassie staining solution**

10% acetic acid, 30% isopropanol, 2.5g/L Coomassie Brilliant Blue R-250

**Coomassie destaining solution**

10% acetic acid, 10% isopropanol

### **3x DNA loading buffer**

50 mM Tris-HCl pH 7.6, 60% glycerol, 0.25% bromophenol blue, 0.25% xylene cyanol. Buffer was used with 1x concentration.

### **Laemmli buffer (2x)**

125 mM Tris-HCl pH 6.8, 4% SDS, 20% glycerol, 5%  $\beta$ -mercaptoethanol, 0.005% bromophenol blue

### **SDS running buffer**

25 mM Tris, 250 mM glycine, 0.1% SDS

### **50x TAE buffer**

2 M Tris, 50 mM Na<sub>2</sub>EDTA, 5.70% glacial acetic acid, adjusted to pH 8 with HCl

### **TBS-T (Tris buffered saline – Tween )**

50 mM Tris-HCl pH 7.4, 150 mM NaCl. Before use add 0.1% TWEEN 20 (Sigma-Aldrich #P7949).

### **TE buffer (1x)**

10 mM Tris, 1 mM Na<sub>2</sub>EDTA, adjust pH to 8 with HCl

## **4.7. RNA methods**

To prevent degradation of RNA due to Rnase activity, diethylpyrocarbonate treated water (DEPC.ddH<sub>2</sub>O) was used for all steps and buffers in the following methods.

### **Total RNA extraction from Arabidopsis**

Arabidopsis plant material (appr. 150 mg) was frozen on liquid nitrogen in a 1.5 ml Eppendorf tube to which 2 metal beads (QIAGEN #69989) were added. The material was then ground for 2x 1 min in a TissueLyser II (QIAGEN) with refreezing in liquid nitrogen in between the two grinding steps. 530  $\mu$ l of RNA extraction buffer and 530  $\mu$ l of phenol (pH4, AppliChem) were added. Tubes were vortexed and centrifuged for 10 min at 16100g on 4°C. After centrifugation, two phases separated. The top phase (aqueous and containing the RNA) was transferred to a new Eppendorf tube and an equal volume of PCI (phenol/chloroform/isoamyl alcohol, ROTH) was added. Again, tubes were vortexed and centrifuged for 10 min at 16100g on 4°C. Afterwards, the extraction was repeated

with chloroform. Finally, the supernatant was transferred to a new Eppendorf tube, mixed with 1/3 volume of 10 M LiCl (in DEPC.ddH<sub>2</sub>O) and incubated overnight on 4°C. The next day, the tubes were centrifuged for 20 min at 16100g on 4°C. The pellet, containing RNA, was washed with 70% ethanol (in DEPC.ddH<sub>2</sub>O) and centrifuged for 10 min at 16100g on 4°C. After repeating the washing step, the pellet was dried on room temperature, resuspended in 25 µl DEPC.ddH<sub>2</sub>O and dissolved by shaking on room temperature for ½ hour. RNA concentration was measured on a nanodrop (Pqlab). RNA was stored on -80°C.

- **RNA extraction buffer**

200 mM NaCH<sub>3</sub>COO pH 5.2, 10 mM Na<sub>2</sub>EDTA, 1% SDS. In DEPC-treated water.

### **First strand cDNA synthesis**

First strand cDNA was synthesized from total RNA using the M-MLV reverse transcriptase according to the manufacturer's protocol (Promega #M1701). 2 µg of total RNA was used for each reaction. To obtain cDNA from total RNA, an oligo(dT) primer was used and dNTP's were provided in a mix (NEB #N0447 ). cDNA was stored at -20°C.

## **4.8. DNA methods**

### **Polymerase chain reaction (PCR)**

PCR was used for the cloning of genes (or other DNA-products) and for analytical purposes such as RT-PCR or colony-PCR. For the cloning of DNA-products, Phusion DNA polymerase (a proofreading polymerase, Finnzymes, #F-530) was used. For analytical purposes, where proofreading was not required, GoTaq DNA polymerase (Promega, #M300) was used. PCR's were run according to manufacturer's protocol. A primerlist of all cloned products is attached in the supplementary materials.

### **Mini-prep from *Escherichia coli* (*E. coli*) cultures**

For the isolation of plasmids from *E. coli*, single colonies were inoculated in 3 ml of LB containing an appropriate selection marker (5 ml for low-copy plasmids, such as pBIN) and grown overnight on 37°C. The next day, 2 ml of each culture (2x2 for low-copy plasmids) was transferred to an Eppendorf tube and centrifuged for 1 min at 20.000g on room temperature. After discarding the supernatant, the tubes were inverted on a paper

towel in order to remove as much of the supernatant as possible. The pellets were resuspended in 200 µl of Mini-prep buffer 1. Next, 200 µl of Mini-prep buffer 2 was added to lyse the cells (alkaline lysis). Finally, 200 µl of Mini-prep buffer 3 was added to neutralize the lysis-solution. In between each addition, the tubes were gently inverted so the nuclear *E. coli* DNA would not fragment. Afterwards, the tubes were kept on ice for 20 min and subsequently centrifuged for 5 min at 20.000g on room temperature. To precipitate the plasmid, 500 µl isopropanol was added to each tube and the tubes were vortexed and placed on ice for 20 min. The tubes were centrifuged for 10 min at 20.000g on room temperature, the supernatant was discarded, 500 µl of 70% ethanol was added and, after vortexing, each tube was rested on room temperature for 5 min. The tubes were centrifuged for 5 min and the supernatant removed as carefully as possible with a pipette, as not to lose the pellet. After removal of remaining liquids (quick-spin), pellets were dried for appr. 15 min on 40°C. Pellets were resuspended in 40 µl ddH<sub>2</sub>O (or 20 µl for low-copy plasmids) by shaking for 15 min on 40°C. On average, 20-30 µg of plasmid DNA could be isolated with this method.

- **Mini-prep buffer 1**

25 mM Tris, 10 mM Na<sub>2</sub>EDTA, adjust pH to 8 with HCl. Before use, add 250µg/ml RNase A and store afterwards at 4°C.

- **Mini-prep buffer 2**

0.2 M NaOH and 1% SDS

- **Mini-prep buffer 3**

5 M KCH<sub>3</sub>COO, 11.5% CH<sub>3</sub>COOH. pH was approximately 5.5.

### **Midi-prep from *E. coli* cultures**

To obtain greater quantities of plasmid DNA (on average 200-700 µg) the midi-prep protocol ‘Jetstar’ from the company Genomed was used. The protocol is based on the alkaline lysis of the cells, followed by binding and washing of the DNA on a novel anion exchange column. In general, a 200 ml *E. coli* culture was grown overnight to high optical density (OD600), thereby exceeding the theoretical maximum of the protocol. However, we have experienced this not to be a problem. For the further steps, the company protocol was followed until the elution of the plasmid. The plasmid DNA was eluted into a 12 ml tube (Kabe labortechnik #050301) to which 5 ml of isopropanol was added. Upon inverting the tubes the DNA visibly precipitated as a white strand. After



resting the tubes at -20°C for 30 min, they were centrifuged for 30 min at 12.000 g on 4°C (SS34 rotor, Beckman-Coulter). The supernatant was removed as complete as possible and the pellet was resuspended in 300 µl ½ TE-buffer to which 30 µl of 3 M NaCH<sub>3</sub>COO was added. The solution was transferred to an Eppendorf tube and the DNA was re-precipitated with 1 ml of 100% ethanol. The DNA again visibly precipitated as a white strand and was centrifuged for 2 min at 20000g on room temperature. The supernatant was removed, 700 µl of 70% ethanol was added and the tubes were rested on room temperature for 10 min. The tubes were centrifuged for 2 min and the supernatant removed as carefully as possible with a pipette. After removal of remaining liquids (quick-spin), pellets were dried for appr. 15 min on 40°C. Pellets were resuspended in 50 µl ddH<sub>2</sub>O by shaking for 15 min on 40°C. DNA concentration was measured on a nanodrop (Pepqlab) and the concentration was adjusted to 1 µg/µl. Plasmid DNA was stored on -20°C.

### **Cloning strategy**

In order to streamline the process of cloning, all DNA-products were cloned with primers (see supplementary table) containing ApaI/NotI(‘5’/3) or NcoI/NotI(‘5’/3) restriction enzymes (New England Biolabs). Accordingly, all vectors used in this work had these restriction sites in frame with their functional features. Because most Arabidopsis genes and cloning vectors are devoid of the ApaI, NcoI and NotI restriction sites, this cloning strategy proved usefull in most cases.

For the entry of new DNA-products in our vectors, PCR was performed on either Arabidopsis cDNA, Lacroute library DNA (Minet et al., 1992) or plasmid DNA with a proofreading DNA polymerase. These blunt-end products were ligated into the commercialy available vector pCRBlunt, using the Zero Blunt PCR Cloning kit (Invitrogen) according to manufacturer’s protocol. Alternatively, when ligation to pCRBlunt did not work out, the PCR-products were restricted immediately and cloned directly into the appropriate vectors (albeit with lower efficiency). All new gene-products were sequenced an inspected for their correct nucleotide composition (neutral substitutions were tolerated).

In the downstream cloning steps, correct DNA-products were restricted and subsequently ligated using the T4 DNA ligase from New England Biolabs (#M0202). Ligation mixes were transformed to DH5α. Positive transformants were screened by isolation of plasmid DNA (see Mini-prep from Escherichia coli (E. coli) cultures) followed by a restriction

digest of the plasmid with a restriction enzyme that cuts both the DNA-product and the vector backbone. From most new plasmids a Midi-prep was made for storage in a plasmid collection.

### **Agarose gel electrophoresis and DNA extraction**

DNA-products from restriction or PCR were mixed with appr. 1/5 of 1x DNA-loading buffer. The DNA-products were separated on agarose gels with varying percentage (0.8-2%) according to their expected size. Gels were run at a current of 100-150 mA in 1X TAE buffer and stained with Ethidium bromide (5 µl of 5mg/ml stock in 100 ml 1xTAE buffer). The size of DNA products was estimated by comparison with the size marker Generuler 1kb DNA ladder plus (Fermentas).

For extraction of DNA from gel slices the Wizard SV gel and PCR Clean-Up system (Promega) was used according to the manufacturer's protocol.

### **Genomic DNA extraction from Arabidopsis leaves (quick 'n dirty)**

Arabidopsis leaves (appr. 150 mg) were frozen on liquid nitrogen in 1.5 ml Eppendorf tubes to which 2 metal beads (QIAGEN #69989) were added. The material was then ground for 2x 1 min in a TissueLyser II (QIAGEN) with refreezing in liquid nitrogen in between the two grinding steps. To the Eppendorf tubes, 200 µl DNA extraction buffer was added and vortexed. At this point, the metal beads were removed with the help of a magnet and the tubes were centrifuged for 5 min at 20.000g on room temperature. The supernatants were transferred to new Eppendorf tubes and 200 µl isopropanol was added. The tubes were inverted and rested on room temperature for 5 min to precipitate the genomic DNA. After centrifugation for 5 min at 20.000g on room temperature, pellets are washed with 500 µl of 70% ethanol. The pellets are then dried on 40°C for 15 min and resuspended in 70 µl ddH<sub>2</sub>O. To improve solubilization and DNA purity, tubes are heated twice at 65°C for 5 min with stirring (pipet tip) in between heating. Finally, the tubes are centrifuged for 2 min at 20.000g on room temperature and the supernatants are transferred to fresh tubes.

- **Genomic DNA extraction buffer**

200 mM Tris-HCl pH7.5, 25 mM Na<sub>2</sub>EDTA, 0.5% SDS, 250 mM NaCl

**Plasmid DNA extraction from yeast**

2 ml of overnight yeast cultures were centrifuged in screw cap tubes (Sarstedt, #72.694) for 1 min at 20.000g on room temperature. To the pellets were added a 200  $\mu$ l lysis buffer, a 200  $\mu$ l PCI (ROTH) and an eppi-tip of glass beads (Sartorius, #BBI-8541701). The tubes were manually vortexed and the cells were disrupted in a FastPrep FP120 Homogenizer (Thermo Savant, 2x 10 sec at speed 6.0). The tubes were centrifuged for 5 min at 20.000g on 4°C to pellet cell debris and to separate the two phases (lysis buffer - PCI). The top phase (lysis buffer) was once more extracted with an equal volume of PCI and once more with chloroform to remove any remaining phenol. The top phase was transferred to a fresh Eppendorf tube, and the tubes were incubated with 5  $\mu$ l of Rnase (10mg/ml in ddH<sub>2</sub>O) for 1 hour on room temperature. Finally, the plasmid DNA was purified using the Wizard SV gel and PCR Clean-Up system (Promega) according to manufacturer's protocol.

**4.9. Protein methods****Recombinant protein expression and purification (pTWIN system)**

Most proteins were expressed using a modified version of the IMPACT System (NEB). Proteins of interest were cloned to the vector pTWIN1-N and transformed into the *E. coli* strain ER2566, which is a BL21 derivative that improves the expression of otherwise toxic proteins. A main culture of 200 ml LB-AMP was inoculated with an overnight *E. coli* culture to an OD600 of 0.2 and was then grown on 37°C to an OD600 of 0.6. Protein expression was achieved by the addition of 1mM Isopropyl  $\beta$ -D-1-thiogalactopyranoside (IPTG) and the incubation overnight on 16°C of the main culture. The next day, the culture was centrifuged for 10 min at 2900g on 4°C, resuspended in 10 ml of cold buffer B1 and transferred to a 50 ml tube (Greiner Bio One). From this point, all steps were carried out on ice or 4°C. The *E. coli* cells were disrupted by sonification; 3 times 1 min continuous on 80% of the maximum power level with 30s rest in between (Bandelin Sonopuls HD70). Immediately after, 1 ml of 10% Triton X-100 was added and the suspension was centrifuged for 20 min at 16000g on 4°C in a 12 ml tube (Kabe labortechnik #050301) with a SS34 rotor (Beckman-Coulter). During this step the affinity column with chitin beads (NEB) was prepared. The gravity-flow column (Thermo scientific #29920) was packed with a bed volume of 2 ml and equilibrated with buffer B1. After applying the protein (gravity flow), the column was washed with 20 ml of buffer B1

and flushed with 4 ml of buffer B2. To induce cleavage of the chitin binding tag by the intein protease, the column is left over night on room temperature. The next day, protein is eluted with 4 ml of buffer B2 and can optionally be concentrated with an Amicon Ultra Centrifugal Filter unit (Millipore). Protein is stored on  $-20^{\circ}\text{C}$ .

- **B1 buffer (pTWIN protein expression)**

20 mM Hepes pH 8.5, 1 mM  $\text{Na}_2\text{EDTA}$ , 1 M NaCl

- **B2 buffer (pTWIN protein expression)**

20 mM Hepes pH 7, 1 mM  $\text{Na}_2\text{EDTA}$ , 0.5 M NaCl

### **Recombinant GST-fusion protein expression and purification (pGEX system)**

In case of protein solubility problems with the pTWIN protein expression system, proteins were expressed with an N-terminal glutathione S-transferase (GST) tag to improve solubility of the recombinant fusion protein. Proteins of interest were cloned to the vector pGEX4T-3 and transformed into the *E. coli* strain ER2566. A main culture of 200 ml LB-AMP was inoculated with an overnight *E. coli* culture to an OD600 of 0.2 and was then grown on  $37^{\circ}\text{C}$  to an OD600 of 0.8. Protein expression was achieved by the addition of 1mM IPTG and the incubation of the culture for 4 hours on  $30^{\circ}\text{C}$ . The culture was centrifuged for 10 min at 2900g on  $4^{\circ}\text{C}$ , resuspended in 10 ml of cold GST wash buffer and transferred to a 50 ml tube (Greiner Bio One). From this point, all steps were carried out on ice or  $4^{\circ}\text{C}$ . The *E. coli* cells were disrupted by sonification; 3 times 1 min continuous on 80% of the maximum power level with 30s rest in between (Bandelin Sonopuls HD70). Immediately after, 1 ml of 10% Triton X-100 was added and the suspension was centrifuged for 20 min at 16000g on  $4^{\circ}\text{C}$  in a 12 ml tube (Kabe labortechnik #050301) with the SS34 rotor (Beckman-Coulter). During this step, the Glutathione Sepharose 4B beads (GE Healthcare) were prepared; 100  $\mu\text{l}$  of beads were centrifuged in an Eppendorf tube and washed twice with 1 ml of GST wash buffer by centrifugation for 5 min at 500g on room temperature (the beads should not be centrifuged at speeds higher than 500g). The beads were resuspended in 75  $\mu\text{l}$  of GST wash buffer. The protein was applied to the beads in a 15 ml tube (Greiner Bio One) and incubated on a spinning wheel for 1 hour at  $4^{\circ}\text{C}$ . Afterwards, the beads were washed twice with 5 ml of GST wash buffer. For elution of the GST-fusion protein, the beads were incubated with 300  $\mu\text{l}$  of GEB for 1 hour at  $4^{\circ}\text{C}$ . After centrifugation the supernatant is stored on  $-20^{\circ}\text{C}$ . The elution can be repeated up to 3 times for full recovery of protein.

- **Glutathione elution buffer (GEB)**

50 mM Tris-HCl pH 8, 10mM glutathione (reduced). Store at -20°C.

- **GST wash buffer**

50 mM Tris-HCl pH 8, 5mM Na<sub>2</sub>EDTA , 20mM MgSO<sub>4</sub>. Before use, add 2 mM dithiotreitol (DTT).

### **SDS-aceton protein extraction**

Plant material was frozen on liquid nitrogen in 1.5 ml Eppendorf tubes to which 2 metal beads (QIAGEN #69989) were added. The material was then ground for 2x 1 min in a TissueLyser II (QIAGEN) with refreezing in liquid nitrogen in between the two grinding steps. To an eppi-tip of grinded material, 250 µl of SDS extraction buffer was added and the tubes were vortexed well. The tubes were centrifuged for 10 min at 20.000g on room temperature and the supernatant was transferred to a fresh Eppendorf tube. To precipitate the protein, 4 volumes of cold acetone (-20°C) were added, the tubes were vortexed well and left to rest for 1 hour on -20°C. The tubes were centrifuged for 10 min at 10.000g on 4°C and the protein pellets were resuspended in cold acetone (by mixing with a pipette tip). The tubes were centrifuged for 2 min and the pellets were dried on 40°C. Pellets were resuspended in an appropriate volume of Laemmli buffer.

- **SDS extraction buffer**

0.175 mM Tris-HCl pH 8.8, 5% SDS, 15% glycerol, 300mM DTT

- **Laemmli buffer (2x)**

125 mM Tris-HCl pH 6.8, 4% SDS, 20% glycerol, 5% β-mercaptoethanol, 0.005% bromophenol blue

### **Phosphorylation assay for calcium dependent thylakoid phosphorylation experiment**

*Arabidopsis thaliana* or *Pisum sativa* chloroplasts (140 µg Chlorophyll of percoll purified chloroplasts for 2 reactions) were lysed by adding 5 volumes of lysis buffer for 5 min on ice. The thylakoids were spun down for 2 min at 20.000g on 4°C and washed with 5 volumes of lysis buffer. After centrifugation, the thylakoid pellet was resuspended in 80 µl lysis buffer and divided to 2 Eppendorf tubes (so each reaction uses 70 µg *Chl*). To one tube, 1 µl of CaCl<sub>2</sub> (of varying concentrations; 40, 10 or 1 mM) was added. To the other tube, 1 µl of ethylene glycol tetraacetic acid (EGTA, of varying concentrations; 40, 10 or 1 mM) was added. The tubes were gently mixed by tapping and they were incubated for 5 min on room temperature in the dark. The kinase reaction was started by adding 1 µl of

an 8 mM ATP solution (so, the final concentration is 0.2 mM ATP). The tubes were gently mixed by tapping and they were incubated for 20 min on room temperature in the dark. The kinase reaction was stopped by adding 400  $\mu$ l methanol and vortexing.

- **Lysis buffer**

25 mM Tris-HCl pH 7.8, 75 mM NaCl, 10 mM MgCl<sub>2</sub>, 1 mM NaF, 0.5 mM NaVO<sub>3</sub>, 15 mM  $\beta$ -Glycerophosphate. Before use, add 1 mM DTT and cOmplete, EDTA-free Protease Inhibitor Cocktail (Roche #04693132001, 1 tablet was soluted in 2 ml ddH<sub>2</sub>O for a 25x stock)

### **Chloroform/methanol protein precipitation for calcium dependent thylakoid phosphorylation experiment**

In order to use protein for isoelectric focusing (IEF) it was necessary to get rid of salts and detergents (when present) and other interfering plant compounds (lipids, sugars, phenolic compounds...). To this end, the thylakoid proteins were precipitated according to the protocol of Wessel and Fluge (1984, ratio Sample/chloroform/methanol/H<sub>2</sub>O: 1/1/4/3). To the samples, 400  $\mu$ l methanol was already added (see previous paragraph). Next, 100  $\mu$ l chloroform was added and the tubes were vortexed. After the addition of 360  $\mu$ l ddH<sub>2</sub>O, the tubes were vortexed and centrifuged for 2 min at 20.000g on room temperature in order for an organic and aqueous phase to separate. After centrifugation, the top phase is removed (protein precipitated as a white band in between the phases) and 400  $\mu$ l methanol was added. After vortexing, the tubes were centrifuged for 2 min at 20.000g on room temperature and the protein pellet was washed with 400  $\mu$ l methanol. Finally, the remaining methanol was removed and the pellets were left to dry on room temperature for 5 min.

### **Isoelectric focusing for calcium dependent thylakoid phosphorylation experiment**

The protein samples for isoelectric focusing were precipitated by chloroform/methanol method. The protein samples were resolubilised in 125  $\mu$ l rehydration buffer (125  $\mu$ l is an appropriate volume for the 7 cm strips, use 200  $\mu$ l for 11 cm strips). The rehydration buffer contained urea and CHAPS (a non-ionic detergent), to help solute more hydrophobic proteins. In addition, the use of thiourea was found to improve the solubilization of membrane proteins. The pellets were mechanically broken (by mixing with a pipette tip) and were shaken for ½ hour on room temperature. Next, the protein solutions were centrifuged for 1 min at 20.000g on room temperature and were applied to

Immobilized pH Gradient strips of various length and pH range (IPG strips Immobiline™ DryStrip gels, GE Healthcare). After covering of the strips with mineral oil (Immobiline™ DryStrip Cover Fluid, GE Healthcare), they were left to rehydrate overnight.

The day after, the strips were placed in a Multiphor II focusing unit (GE Healthcare) which was connected to an EPS 3501 XL power supply (GE Healthcare) and were run according protocol.

- **Rehydration buffer**

7 M urea (or 8 M in case thiourea was not used), 2M thiourea, 2% CHAPS, 2% IPG buffer (GE Healthcare, pH4-7 #17-6000-86 or pH3-11 NL #17-6004-40), 50 mM DTT (70mg DTT/25ml). Aliquots were stored on -80°C. Before use, 2 µl of a bromophenol blue stock solution (in rehydration buffer) was added.

### **Second dimension SDS-PAGE for calcium dependent thylakoid phosphorylation experiment**

To prepare the IEF strips for the second dimension they were equilibrated in SDS equilibration buffer. Furthermore, in order to guarantee optimal protein separation in the second dimension, the strips were incubated with DTT for reduction of disulfide bonds between cysteine residues. The reduced S-H groups were then alkylated with iodacetamid to prevent disulfide bonds from forming anew. The solutions were made fresh for each experiment. The IEF strips were equilibrated for 20 min on room temperature in a 15 ml tube (Greiner Bio One) on a platform shaker with SDS equilibration buffer containing DTT (100 mg/ 10 ml buffer). Next, the strips were transferred and incubated in a fresh tube of SDS equilibration buffer containing iodacetamid (250 mg/ 10 ml buffer). After 20 min of equilibration, the strips were placed on top of an SDS-PAGE gel (with varying concentration of acrylamid). In this step, the strips were pushed through a layer of hot agarose (1% in SDS running buffer). It was very important not to trap any bubbles in the contactzone between the strips and the SDS-PAGE gels. Furthermore, care had to be taken to work fast, so the agarose would not solidify while pushing the strips on top of the gels. A spacer was also inserted, to make a well for a protein size marker (PageRuler™ Plus Prestained Protein Ladder, Fermentas). The gels were run in a Mini-PROTEAN II system (Bio-Rad) at a current of 10 mA/gel until the protein from the strip had entered the SDS-PAGE, after which the current was increased to 30 mA/gel. After completion of the run, the gels were stained using silver stain or coomassie stain. Alternatively, the gels

were used further for Pro-Q Diamond Phosphoprotein gel stain (Invitrogen, according to protocol) or western blot.

- **SDS equilibration buffer**

75 mM Tris-HCl pH 8.8, 6 M urea, 29.3% glycerol, 2% SDS. A small spatula tip of bromophenol blue was added for coloration.

- **SDS running buffer**

25 mM Tris, 250 mM glycine, 0.1% SDS. pH was approximately 8.8.

### **Sample preparation for mass spectrometry (MS) analysis**

To minimize keratin contamination, all the following steps were carried out in a sterile bench, gloves and labcoat were worn at all time and prepacked pipette tips were used (Sarstedt #70.760.502). The sterile bench, glas slide, tweezers and razor were washed with 70% ethanol ('pro analysi') and acetone. Gel slices or spots were chopped in 1 mm<sup>2</sup> sized gel pieces with the help of the tweezers and razor on the glas slide. The gel pieces were transferred to a 600 µl tube (GenXpress) and were washed 3 times with 200 µl ddH<sub>2</sub>O (for 10 min on room temperature on a thermomixer at 800rpm). In the case of coomassie staining, the gel pieces were destained by adding 200 µl freshly prepared 50mM NH<sub>4</sub>HCO<sub>3</sub> and 160 µl acetonitrile (Chromasolv<sup>®</sup>; Sigma-Aldrich) and incubating for 15 min on room temperature while shaking. If the the color did not completely disappear, this step was repeated. Destaining was impossible for a silver stained gel. Next, to dry out the gel pieces, 160 µl acetonitrile was added and the tubes were incubated for 5 min on room temperature while shaking. Following removal of the acetonitrile, the gel pieces were left to dry in the sterile bench (approximately 10 min). In the next two steps, reactive thiol groups of the proteins inside the gel pieces were being reduced and blocked by soaking of the gel pieces in a DTT containing solution and a iodacetamid containing solution. For the gel spots that were retrieved from the calcium dependent thylakoid phosphorylation experiment, these steps were already performed before running the SDS-PAGE (see previous paragraph) and hence, were not necessary to repeat here. For the reduction step, the gel pieces were covered with 200 µl of a 10 mM DTT solution (in 50mM NH<sub>4</sub>HCO<sub>3</sub>) and were incubated for ½ hour on 56°C while shaking. Afterwards, the solution was pipetted of and 160 µl acetonitrile was added to dry the gel pieces again as before. For the alkylation step, the dried gel pieces were incubated for 20 min in the dark on room temperature with a 100 µl of freshly prepared iodacetamid solution



(10mg/ml in 50mM  $\text{NH}_4\text{HCO}_3$ ). The gel pieces were shortly spun down, the iodacetamid solution was carefully removed and the gel pieces were washed 3 times for 10 min with 200  $\mu\text{l}$  of 50mM  $\text{NH}_4\text{HCO}_3$  while shaking. Before the addition of the protease solution the gel pieces were dried again with the help of acetonitrile. To prepare the protease solution, a 196  $\mu\text{l}$  of 50mM  $\text{NH}_4\text{HCO}_3$  were added to a 4  $\mu\text{l}$  aliquot of trypsin (proteomics grade, Roche #03708969001; 1  $\mu\text{g}$  in 4  $\mu\text{l}$  of 1 mM HCl, stored at  $-80^\circ\text{C}$ ). The dried gel pieces were soaked with 40  $\mu\text{l}$  of protease solution for 10 min on  $4^\circ\text{C}$ . If the pieces absorbed all of the solution, a little more was added and they were again incubated for 10 min on  $4^\circ\text{C}$ . The protease solution was removed, the gel pieces were covered with a minimal volume of 50mM  $\text{NH}_4\text{HCO}_3$  and the protein digestion was carried out over night on  $37^\circ\text{C}$ . The next day, the protein digestion was ended by the addition of 10% HCOOH to a final concentration of 1% of the sample volume. To extract the peptides from the gel pieces, the tubes were placed in an ultrasonic bath (cooled with ice pack) for 10min. After a short spin, the supernatant was transferred to a 200  $\mu\text{l}$  tube with GELoader® tips (Eppendorf #0030 001.222, narrow tips prevented the transfer of gel pieces). The extraction was repeated twice with a minimal volume (that covers the gel pieces) of 5% HCOOH. In order to remove particles that may clog the liquid chromatography columns, the tubes were centrifuged for 2 min at 20.000g and the solution was transferred to a new 200  $\mu\text{l}$  tube. Subsequently, peptides were subjected to LC-MS/MS analysis.

### **Western blot (WB)**

A semi dry transfer protocol was used for western blotting. SDS-PAGE gels were incubated for 5 min in cathode buffer. In the meanwhile, a polyvinylidene fluoride membrane (PVDF, Immobilon-P, Millipore #IPVH00010) was wetted in 100% methanol and transferred to anode buffer 2. Blotting stacks were prepared inside the blotting apparatus (Trans-Blot SD semi-dry electrophoretic transfer cell, Bio-Rad #3030917), which consisted from bottom to top of: 2 Whatman® Papers (3MM Chr, GE Healthcare) soaked in anode buffer 1, 2 Whatman® Papers soaked in anode buffer 2, the PVDF membrane, the SDS-PAGE gel and 3 Whatman® Papers soaked in cathode buffer. Air bubbles inside the stacks were removed by rolling over it with a tube. The blotting apparatus was closed and was run at a current of  $1.3 \text{ mA/cm}^2$  for 1 hour per gel. Afterwards, the membranes were blocked for 1-2 hours on a platform shaker in TBS-T buffer containing 5% skimmed milk powder or 1% BSA, according to the primary antibody recommendations. Next, the membranes were incubated overnight with 5 ml of

the primary antibody solution in a 50 ml tube (Greiner Bio One) on a rolling platform on 4°C (for standard sized membranes of 6x9 cm). The next day, the membranes were washed 5x 5 min with TBS-T and incubated with 20 ml of secondary antibody solution for 2 hours on room temperature on a platform shaker. The membranes were again washed 5x 5 min with TBS-T. For the detection of antibody binding, a horseradish peroxidase substrate was used in all cases. The Pierce ECL Western Blotting Substrate was used for less sensitive western blots according to manufacturer's protocol. When higher sensitivity was needed (e.g. Ca1N antibody), the ECL Plus Western Blotting Detection System (GE Healthcare #RPN2132) was used. Blots were exposed to X-ray film (Fujifilm) in an EC-DW X-ray cassette (Fujifilm) and developed in a CURIX60 table-top processor (AGFA).

### **Fractionation of Arabidopsis membranes by sucrose density gradient centrifugation**

Approximately 10-12 g of Arabidopsis leaves was collected from 8-weeks-old plants, per gradient. The leaves were thoroughly homogenised in 100 ml of homogenisation buffer in a Waring blender (5 x 3 s, maximum speed). The homogenate was filtered through two layers of Miracloth (Merck) and centrifuged for 20 min at 10.000g in a SW28 rotor (Beckman Coulter) at 4°C, to remove most large debris including nuclei and thylakoids. The supernatant was centrifuged for 1 h at 100.000g in the same rotor, to precipitate the microsomal fraction. The microsomal pellet was rinsed with 1 ml of microsome resuspension buffer and was transferred with the help of a spatula to an Eppendorf tube filled with 200 µl of microsome resuspension buffer. To solubilize the microsome pellet, sea sand was added to the Eppendorf tube and the pellet was mechanically disrupted with a glass drill bit attached to a drill force (RW16 basic, IKA Labortechnik; 3 x 1 min at full speed with 1 min rests). Finally, microsome resuspension buffer was added to a total volume of 0.5 ml and the suspension was transferred, avoiding sea sand, to the bottom of a 14 ml thinwall polyallomer tube (Beckman Coulter). A linear sucrose gradient was layered over the suspension with the help of a gradient mixer (VWR) using 6 ml of the two centrifugation buffers, each with 20% or 50% sucrose (w/w). Afterwards, the gradient was centrifuged over night for 18 h at 100.000g in a SW40Ti rotor (Beckman Coulter). The next day, 12 fractions of 1 ml were carefully transferred starting from the top of the gradient and the sucrose concentration in each fraction was measured with a refractometer (Pal-1, Atago). Fractions were stored at -20°C. The fractionation can be performed in the presence or absence of Mg<sup>2+</sup> to change the fractionation pattern of the

ER, due to the association or dissociation of ribosomes, respectively, and the buffers are called accordingly (Lu and Hrabak, 2002). All steps were performed at 4°C.

- **Homogenisation buffer without Mg<sup>2+</sup>**  
50 mM Tris-HCl (pH 7.8), 400 mM sorbitol, 10 mM EDTA, 1 mM DTT and cComplete, EDTA-free Protease Inhibitor Cocktail (Roche #04693132001)
- **Homogenisation buffer with Mg<sup>2+</sup>**  
50 mM Tris-HCl (pH 7.8), 400 mM sorbitol, 2 mM EDTA, 15 mM MgCl<sub>2</sub>, 1 mM DTT and cComplete, EDTA-free Protease Inhibitor Cocktail (Roche #04693132001)
- **Microsome resuspension buffer without Mg<sup>2+</sup>**  
10 mM Tris-HCl (pH 7.5), 5 mM EDTA, 55% (w/w) sucrose
- **Microsome resuspension buffer with Mg<sup>2+</sup>**  
10 mM Tris-HCl (pH 7.5), 2 mM EDTA, 15 mM MgCl<sub>2</sub>, 55% (w/w) sucrose

#### 4.10. Bacteria methods

##### Preparation of competent *E. coli* strains DH5α and ER2566

*E. coli* cells from a -80 °C stock were streaked on an LB plate (withouth antibiotics) or alternitavely, were inoculated in 5 ml LB medium, and were incubated overnight at 37°C. The next day, a colony or a few microliter of culture were inoculated in 20 ml LB medium (supplied with 20 mM MgSO<sub>4</sub>) and incubated overnight on 23°C. From this preculture, 2 ml were inoculated the next day in 300 ml LB medium (supplied with 20 mM MgSO<sub>4</sub>) and were grown overnight at 23°C to an OD600 of approximately 0.4 to 0.6. To harvest the cells, they were transferred to 50 ml sterile tubes (Greiner Bio One), were incubated on ice for 10 min and were centrifuged for 10 min at 755g on 4°C. All further steps were carried out on ice. The supernatant was discarded and the pellets were resuspended in 10 ml TB buffer each. The cells were pooled to 2 tubes, were incubated on ice for 30min and were centrifuged for 10 min at 425g on 4°C. The supernatant was removed and each tube was resuspended in 5 ml TB buffer + 7% DMSO (sterile filtrated). After incubation on ice for 1 hour, the cells were aliquoted in Eppendorf tubes and immediately frozen on dry ice. Aliquots were stored at -80°C.

- **TB buffer**  
10 mM CaCl<sub>2</sub>, 15 mM KCl, 10 mM Pipes-NaOH, adjust pH to 6.7 with HCl. After adjusting the pH, 55 mM MnCl<sub>2</sub> was added and the buffer was sterile filtrated.

**Preparation of electrocompetent agrobacteria strains AGL1 and GV3101**

Agrobacteria cells from a -80 °C stock were inoculated in 2 ml LB medium and were incubated overnight on 30°C. The next day, the entire culture was inoculated in 200 ml LB medium (supplied with 25 µg/ml rifampicin) and again grown overnight on 30°C to an OD<sub>600</sub> of approximately 1 to 1.5. The culture was cooled on ice, transferred to a sterile 500 ml centrifuge tube and centrifuged for 6 min at 4066g on 4°C (GS3 rotor, Sorvall). To wash the pellet, it was resuspended in 50 ml of 1 mM Hepes pH7, transferred to a 50 ml tube (Greiner Bio One) and centrifuged for 12 min at 3166g on 4°C. The washing step was repeated twice with 50ml 1mM Hepes pH7 and once with sterile 10% glycerol. Finally, the pellet was resuspended in 4 ml of 10% glycerol, aliquoted in Eppendorf tubes and immediately frozen on dry ice. Aliquots were stored at -80°C.

**Transformation of *E. coli* by heat shock**

Aliquots of competent *E.coli* were thawed on ice. Plasmid DNA (from a ligation mix or plasmid stock) was mixed with 50 µl of cells and incubated on ice for 20 min. The cells were heat-shocked for 1 min at 42°C and were left to recover, after the addition of 800 µl LB medium (no antibiotics), while shaking for 1h at 37°C. The cells were centrifuged for 1 min at 10.000g on room temperature and were resuspended in a small rest volume of the supernatant, after it was discarded. The cell suspension was plated with the help of sterile glass beads on LB plates containing the appropriate antibiotic. The plates were incubated overnight on 37°C.

**Transformation of agrobacteria**

Aliquots of electrocompetent agrobacteria (AGL1 or GV3101) were thawed on ice. To 50 µl of cells, 1 µg of plasmid DNA was added and mixed in an electroporation cuvette (cellprojects #EP-102, 2 mm slit). The binary plant transformation vectors pBIN or pGreen were used. Electroporation was performed with a Gene Pulser (Bio-Rad) with a voltage of 1.6 kV, a resistance of 200 ohms and a capacitance of 25 µF. Immediately after, 1 ml of LB medium (no antibiotics) was added to the cells. The cell suspension was transferred to an Eppendorf tube and the cells were left to recover for 1 hour at 30°C. The cells were centrifuged for 1 min at 10.000g on room temperature and were resuspended in a small rest volume of the supernatant, after it was discarded. The cell suspension was

plated with the help of sterile glass beads on LB plates containing the appropriate antibiotics. The plates were incubated for 2 to 3 days at 30°C. To check for the presence of the correct DNA product, colony PCR was performed with an appropriate primer pair. To make a stock, a correct agrobacterium colony was grown overnight in 30 ml of LB-KAN (for AGL1 strain) or LB-KAN/Gentamycin (for GV3101 strain). The next day, the culture was centrifuged, resuspended in sterile 25% glycerol and frozen at -80°C.

#### **4.11. Yeast methods**

##### **Quick trafo**

A master trafo-mix was prepared containing 800 µl of 50% PEG 3.300, 100 µl of 2M lithium acetate, 100 µl of DTT and 20 µl of bacterial RNA (10µg/µl). Yeast from a fresh streaked plate was added to the master trafo-mix and resuspended well by light vortexing. Approximately 2 µg of plasmid DNA was added to a 150 µl of trafo-mix and resuspended by tapping the Eppendorf tube. Then, the Eppendorf tube was incubated for 20 min at 30 °C followed by 20 min at 44°C. Immediately after, 1 ml of sterile water was added and the Eppendorf tube was inverted end over end. After a short spin, the cell pellet was resuspended in 100 µl of sterile water, plated and incubated for 2-3 days on 30 °C.

#### **4.12. Plant methods**

##### **Agrobacterium-mediated transfection of tobacco leaf**

Tobacco plants (*Nicotiana tabacum* cv. Petite Havana SR1) were grown for 5-7 weeks under stable short day conditions in a plant growth chamber. Single agrobacterium colonies or stocks (AGL1) harbouring the desired DNA product were grown overnight in 5 ml of LB-KAN on 30°C. The next day, the cultures were filled up to 50 ml of LB-KAN and grown for 4 more hours on 30°C. Afterwards, the cultures were centrifuged for 10 min at 3000 g on room temperature in 50 ml tubes (Greiner Bio One) and the pellets were resuspended in 40 ml of LB (no antibiotics). To induce the virality of the agrobacteria, 150 µM acetosyringone was added and the cultures were grown for 2 more hours on 30°C in the 50 ml tubes. Next, the cultures were centrifuged and resuspended in approximately 30ml of a 5% sucrose solution (according to the size of the pellet). At this point, in case of co-infiltrations, the cultures were mixed 1:1. The leaves were infiltrated with the use of a 1 ml syringe (without a needle; Terumo), by pushing the solution through a punctured

hole. Afterwards, the plants were placed overnight in a plastic bag and the next day, they were transferred to a greenhouse for 2-3 days.

### **Agrobacterium-mediated transfection of Arabidopsis (floral dip method)**

*Arabidopsis thaliana* plants were grown relatively dense in stable long day conditions in a plant growth chamber. The first stalks of the bolting plants were cut off and the plants were left to grow another week, to promote the growth of numerous adventitious stalks. Single agrobacterium colonies or stocks (GV3101) harbouring the desired DNA product were grown overnight in 5 ml of LB-KAN/Gentamycin on 30°C. The next day, the cultures were filled up to 100 ml of LB-KAN/Gentamycin and grown for 4 more hours on 30°C. Afterwards, the cultures were centrifuged for 10 min at 3000 g on room temperature in 50 ml tubes (Greiner Bio One) and the pellets were resuspended in 50 ml of a 5% sucrose solution. Immediately before use, 0.02% of the detergent Silwet L-77 (VAC-IN-STUFF, Lehle Seeds) was added to the cells. On the day of transfection, siliques on the Arabidopsis plants that already had formed were removed, so only the flowers were left on the stalks. The agrobacterium suspensions were poured in square Petri dishes and the stalks of the Arabidopsis plants were pushed in the suspensions until all flowers were covered. Excess suspension was drained from the stalks, the plants were wrapped in common kitchen foil and were left to incubate overnight on room temperature. The next day, the plants were transferred to the greenhouse. To improve transformation rate, the plants were dipped a second time the next week (this time the siliques were not removed before dipping!).

### **Protoplast isolation from agrobacterium-mediated transformed tobacco leaf for microscopy**

Protoplasts were isolated from agrobacterium-mediated transformed tobacco leaves. Pieces of one leaf were cut out in between of the veins and infiltrated with 20 ml of enzyme solution in a 50 ml syringe. The suspension was transferred to a Petri dish and the pieces of leaf were cut in solution into stripes of 1 mm. They were left to incubate for 3 hours on room temperature in the dark without shaking. Afterwards, the Petri dishes were gently agitated in order to release the protoplasts. The suspension was filtered through a nylon mesh (125 µm pore size) and centrifuged for 2 min at 100g on room temperature. The protoplasts were washed with 5 ml of MMG buffer and rested on room temperature before proceeding with microscopy.

- **Enzyme solution**

20 mM MES (pH 5.7), 1.5% (weight/Vol) cellulase (Fluka), 0.4% macerozyme (Fluka #17389) , 0.4 M mannitol and 20 mM KCl. The buffer was warmed to 55°C for 10 min to inhibit possible DNase and protease activity. After cooling to room temperature, 10 mM CaCl<sub>2</sub> and 0.1% BSA was added. Finally, the solution is filtrated through a 0.45µm syringe filter device.

- **MMG buffer**

4 mM MES (pH 5.7), 0.4 M mannitol and 15 mM MgCl<sub>2</sub>

**Confocal microscopy**

Immediately before use, transformed pieces of tobacco leaves were infiltrated with dH<sub>2</sub>O and mounted on glass slides under a cover glass fixed with double-sided tape. Alternatively, protoplasts suspensions were dropped onto glass plates and fixed under a cover glass in between 2 pieces of parafilm. In all cases, viable leaf tissue was used expressing fluorescent proteins or stained with the chemical MitoTracker Red CMXRos (Molecular Probes; final concentration of 100 nM). Images were taken on a confocal laser scanning microscope Zeiss 510 model, with a Plan-Neofluar 40x/1.3 oil DIC objective. Excitation wavelength for GFP and chloroplasts was 488 nm (appr. 30% of argon laser strength); for YFP it was 514 nm (appr. 30% of argon laser strength); for mCherry and MitoTracker Red CMXRos (Molecular Probes) it was 561 nm. For GFP, emission was measured between 505-565 nm; YFP signal emission was measured between 530-600 nm; chloroplasts-autofluorescence was measured between 615-668 nm; mCherry and Mito-tracker red emission was measured between 575-615 nm. Afterwards, images were processed with the LSM image browser (Zeiss) and ImageJ.

**Chloroplast isolation from *Arabidopsis thaliana***

Chloroplast isolation from *Arabidopsis thaliana* was performed according protocol (Seigneurin-Berny et al., 2008). The chloroplast extracts were frozen on liquid nitrogen and stored on -80°C.

**Chloroplast isolation from *Pisum sativum***

Chloroplast isolation from *Pisum sativum* (Pea) was performed according protocol with minor modifications (Schleiff et al., 2003). One tray of Pea seedlings were grown for 8-9 days under standard long day conditions in a greenhouse. From here, all steps were

performed in the cold room or on ice. The leaves were collected in approximately 200 ml of P-ISO buffer and were homogenized using a Waring blender (3 x 3s pulses: low – high – low). The homogenate was filtered through four layers of Miracloth (Merck) and centrifugated for 2 min at 2800g in four round-bottom 50 ml tubes. Each pellet was resuspended in 1 ml P-WASH buffer, and the resulting 4 ml of resuspended pellets was loaded on top of two preformed and cooled Percoll gradients (12 ml 40% Percoll and 7 ml 80% Percoll). Gradients were centrifuged for 5 min at 8000g (brake “off”) in a HB-4 swing-out rotor (Sorvall) and intact chloroplasts were recovered from the 40% - 80% interphase. They were transferred into two round-bottom 50 ml tubes and washed with P-WASH buffer (centrifugation for 2min at 2800g). The supernatant was decanted and the pellets were resuspended in ~500µl P-WASH buffer. After the chlorophyll concentration was measured, the chloroplast suspension was frozen in liquid nitrogen and stored at -80°C.

- **Pea chloroplast isolation buffer (P-ISO)**

20 mM MOPS, 13 mM Tris, 330 mM sorbitol, 0.1% BSA, 3 mM MgCl<sub>2</sub>. Buffer should not be stored at 4°C longer than one week.

- **P-WASH I**

50 mM HEPES-KOH (pH 7.6), 330 mM sorbitol, 3 mM MgCl<sub>2</sub>. Buffer can be stored at -20°C.

- **40% Percoll for Pea chloroplast isolation**

50 mM HEPES-KOH (pH 7.6), 330 mM sorbitol, 40% Percoll (GE Healthcare # 17089101). Buffer can be stored at -20°C.

- **80% Percoll for Pea chloroplast isolation**

50 mM HEPES-KOH (pH 7.6), 330 mM sorbitol, 80% Percoll (GE Healthcare # 17089101). Buffer can be stored at -20°C.

### **Chlorophyll concentration measurement**

The chlorophyll content of chloroplast preparations was measured according to (Arnon, 1949). To 1 ml of 80% acetone was added 5 µl of chloroplast suspension. The solution was vortexed and centrifuged for 1 min at 20.000g on room temperature. The supernatant was transferred to a quartz cuvette and absorption was measured at wavelengths 645 nm and 663 nm. The chlorophyll concentration was calculated from the following formula:

$$(OD_{645} * 20.2 + OD_{663} * 8.02) * 200 (\text{dilution factor}) = \mu\text{g/ml chlorophyll}$$



## 5. References

- Abell BM, Mullen RT** (2011) Tail-anchored membrane proteins: exploring the complex diversity of tail-anchored-protein targeting in plant cells. *Plant Cell Rep* **30**: 137-151
- Abu-Abied M, Avisar D, Belausov E, Holdengreber V, Kam Z, Sadot E** (2009) Identification of an Arabidopsis unknown small membrane protein targeted to mitochondria, chloroplasts, and peroxisomes. *Protoplasma* **236**: 3-12
- Albrecht V, Ritz O, Linder S, Harter K, Kudla J** (2001) The NAF domain defines a novel protein-protein interaction module conserved in Ca<sup>2+</sup>-regulated kinases. *EMBO J* **20**: 1051-1063
- Aldridge C, Moller SG** (2005) The plastid division protein AtMinD1 is a Ca<sup>2+</sup>-ATPase stimulated by AtMinE1. *J Biol Chem* **280**: 31673-31678
- Ali R, Ma W, Lemtiri-Chlieh F, Tsaltas D, Leng Q, von Bodman S, Berkowitz GA** (2007) Death don't have no mercy and neither does calcium: Arabidopsis CYCLIC NUCLEOTIDE GATED CHANNEL2 and innate immunity. *Plant Cell* **19**: 1081-1095
- Ali R, Zielinski RE, Berkowitz GA** (2006) Expression of plant cyclic nucleotide-gated cation channels in yeast. *J Exp Bot* **57**: 125-138
- Allen GJ, Muir SR, Sanders D** (1995) Release of Ca<sup>2+</sup> from individual plant vacuoles by both InsP<sub>3</sub> and cyclic ADP-ribose. *Science* **268**: 735-737
- Anielska-Mazur A, Bernas T, Gabrys H** (2009) In vivo reorganization of the actin cytoskeleton in leaves of *Nicotiana tabacum* L. transformed with plastin-GFP. Correlation with light-activated chloroplast responses. *BMC Plant Biol* **9**: 64
- Annweiler A, Hippskind RA, Wirth T** (1991) A strategy for efficient in vitro translation of cDNAs using the rabbit beta-globin leader sequence. *Nucleic Acids Res* **19**: 3750
- Arnon DI** (1949) Copper Enzymes in Isolated Chloroplasts. Polyphenoloxidase in *Beta Vulgaris*. *Plant Physiol* **24**: 1-15
- Aro EM, McCaffery S, Anderson JM** (1993) Photoinhibition and D1 Protein Degradation in Peas Acclimated to Different Growth Irradiances. *Plant Physiol* **103**: 835-843
- Aro EM, Suorsa M, Rokka A, Allahverdiyeva Y, Paakkarinen V, Saleem A, Battchikova N, Rintamaki E** (2005) Dynamics of photosystem II: a proteomic approach to thylakoid protein complexes. *J Exp Bot* **56**: 347-356
- Arpagaus S, Rawyler A, Braendle R** (2002) Occurrence and characteristics of the mitochondrial permeability transition in plants. *J Biol Chem* **277**: 1780-1787
- Aung K, Zhang X, Hu J** (2010) Peroxisome division and proliferation in plants. *Biochem Soc Trans* **38**: 817-822
- Bae W, Lee YJ, Kim DH, Lee J, Kim S, Sohn EJ, Hwang I** (2008) AKR2A-mediated import of chloroplast outer membrane proteins is essential for chloroplast biogenesis. *Nat Cell Biol* **10**: 220-227
- Baekgaard L, Fuglsang AT, Palmgren MG** (2005) Regulation of plant plasma membrane H<sup>+</sup>- and Ca<sup>2+</sup>-ATPases by terminal domains. *J Bioenerg Biomembr* **37**: 369-374
- Baginsky S, Tiller K, Pfannschmidt T, Link G** (1999) PTK, the chloroplast RNA polymerase-associated protein kinase from mustard (*Sinapis alba*), mediates redox control of plastid in vitro transcription. *Plant Mol Biol* **39**: 1013-1023
- Balsera M, Goetze TA, Kovacs-Bogdan E, Schurmann P, Wagner R, Buchanan BB, Soll J, Bolter B** (2009) Characterization of Tic110, a channel-forming protein at the inner envelope membrane of chloroplasts, unveils a response to Ca<sup>2+</sup> and a stromal regulatory disulfide bridge. *J Biol Chem* **284**: 2603-2616
- Barran-Berdon AL, Rodea-Palomares I, Leganes F, Fernandez-Pinas F** (2011) Free Ca<sup>2+</sup> as an early intracellular biomarker of exposure of cyanobacteria to environmental pollution. *Anal Bioanal Chem* **400**: 1015-1029
- Batistic O, Kudla J** (2009) Plant calcineurin B-like proteins and their interacting protein kinases. *Biochim Biophys Acta* **1793**: 985-992
- Batistic O, Sorek N, Schultke S, Yalovsky S, Kudla J** (2008) Dual fatty acyl modification determines the localization and plasma membrane targeting of CBL/CIPK Ca<sup>2+</sup> signaling complexes in Arabidopsis. *Plant Cell* **20**: 1346-1362
- Batistic O, Waadt R, Steinhorst L, Held K, Kudla J** (2010) CBL-mediated targeting of CIPKs facilitates the decoding of calcium signals emanating from distinct cellular stores. *Plant J* **61**: 211-222
- Baughman JM, Perocchi F, Girgis HS, Plovianich M, Belcher-Timme CA, Sancak Y, Bao XR, Strittmatter L, Goldberger O, Bogorad RL, Kotliansky V, Mootha VK** (2011) Integrative

- genomics identifies MCU as an essential component of the mitochondrial calcium uniporter. *Nature*
- Bayer RG, Stael S, Csaszar E, Teige M** (2011) Mining the soluble chloroplast proteome by affinity chromatography. *Proteomics* **11**: 1287-1299
- Benetka W, Mehler N, Maurer-Stroh S, Sammer M, Koranda M, Neumuller R, Betschinger J, Knoblich JA, Teige M, Eisenhaber F** (2008) Experimental testing of predicted myristoylation targets involved in asymmetric cell division and calcium-dependent signalling. *Cell Cycle* **7**: 3709-3719
- Bennett J** (1977) Phosphorylation of chloroplast membrane polypeptides *Nature* **269**: 344 - 346
- Berkelman T, Garret-Engel P, Hoffman NE** (1994) The *pacL* gene of *Synechococcus* sp. strain PCC 7942 encodes a Ca(2+)-transporting ATPase. *J Bacteriol* **176**: 4430-4436
- Bianchini GM, Pastini AC, Muschietti JP, Tellez-Inon MT, Martinetto HE, Torres HN, Flavia MM** (1990) Adenylate cyclase activity in cyanobacteria: activation by Ca(2+)-calmodulin and a calmodulin-like activity. *Biochim Biophys Acta* **1055**: 75-81
- Biro RL, Daye S, Serlin BS, Terry ME, Datta N, Sopory SK, Roux SJ** (1984) Characterization of oat calmodulin and radioimmunoassay of its subcellular distribution. *Plant Physiol* **75**: 382-386
- Bonza MC, Morandini P, Luoni L, Geisler M, Palmgren MG, De Michelis MI** (2000) At-ACA8 encodes a plasma membrane-localized calcium-ATPase of Arabidopsis with a calmodulin-binding domain at the N terminus. *Plant Physiol* **123**: 1495-1506
- Bouche N, Scharlat A, Snedden W, Bouchez D, Fromm H** (2002) A novel family of calmodulin-binding transcription activators in multicellular organisms. *J Biol Chem* **277**: 21851-21861
- Bouche N, Yellin A, Snedden WA, Fromm H** (2005) Plant-specific calmodulin-binding proteins. *Annu Rev Plant Biol* **56**: 435-466
- Boudsocq M, Willmann MR, McCormack M, Lee H, Shan L, He P, Bush J, Cheng SH, Sheen J** (2010) Differential innate immune signalling via Ca(2+) sensor protein kinases. *Nature* **464**: 418-422
- Boursiac Y, Harper JF** (2007) The origin and function of calmodulin regulated Ca<sup>2+</sup> pumps in plants. *J Bioenerg Biomembr* **39**: 409-414
- Bouvier F, Linka N, Isner JC, Mutterer J, Weber AP, Camara B** (2006) Arabidopsis SAMT1 defines a plastid transporter regulating plastid biogenesis and plant development. *Plant Cell* **18**: 3088-3105
- Brautigam A, Kajala K, Wullenweber J, Sommer M, Gagneul D, Weber KL, Carr KM, Gowik U, Mass J, Lercher MJ, Westhoff P, Hibberd JM, Weber AP** (2011) An mRNA blueprint for C4 photosynthesis derived from comparative transcriptomics of closely related C3 and C4 species. *Plant Physiol* **155**: 142-156
- Brautigam A, Shrestha RP, Whitten D, Wilkerson CG, Carr KM, Froehlich JE, Weber AP** (2008) Low-coverage massively parallel pyrosequencing of cDNAs enables proteomics in non-model species: comparison of a species-specific database generated by pyrosequencing with databases from related species for proteome analysis of pea chloroplast envelopes. *J Biotechnol* **136**: 44-53
- Brautigam A, Weber AP** (2009) Proteomic analysis of the proplastid envelope membrane provides novel insights into small molecule and protein transport across proplastid membranes. *Mol Plant* **2**: 1247-1261
- Brookes PS, Parker N, Buckingham JA, Vidal-Puig A, Halestrap AP, Gunter TE, Nicholls DG, Bernardi P, Lemasters JJ, Brand MD** (2008) UCPs--unlikely calcium porters. *Nat Cell Biol* **10**: 1235-1237; author reply 1237-1240
- Buchanan BB, Gruissem W, Jones RL** (2000) Biochemistry and molecular biology of plants.
- Bullmann L, Haarmann R, Mirus O, Bredemeier R, Hempel F, Maier UG, Schleiff E** (2010) Filling the gap, evolutionarily conserved Omp85 in plastids of chromalveolates. *J Biol Chem* **285**: 6848-6856
- Bussemer J, Chigri F, Vothknecht UC** (2009) Arabidopsis ATPase family gene 1-like protein 1 is a calmodulin-binding AAA+-ATPase with a dual localization in chloroplasts and mitochondria. *FEBS J* **276**: 3870-3880
- Bussemer J, Vothknecht UC, Chigri F** (2009) Calcium regulation in endosymbiotic organelles of plants. *Plant Signal Behav* **4**: 805-808
- Campbell AK, Naseem R, Wann K, Holland IB, Matthews SB** (2007) Fermentation product butane 2,3-diol induces Ca<sup>2+</sup> transients in *E. coli* through activation of lanthanum-sensitive Ca<sup>2+</sup> channels. *Cell Calcium* **41**: 97-106
- Cardenas L, Lovy-Wheeler A, Kunkel JG, Hepler PK** (2008) Pollen tube growth oscillations and intracellular calcium levels are reversibly modulated by actin polymerization. *Plant Physiol* **146**: 1611-1621

- Carrie C, Giraud E, Whelan J** (2009) Protein transport in organelles: Dual targeting of proteins to mitochondria and chloroplasts. *FEBS J* **276**: 1187-1195
- Cavero S, Traba J, Del Arco A, Satrustegui J** (2005) The calcium-dependent ATP-Mg/Pi mitochondrial carrier is a target of glucose-induced calcium signalling in *Saccharomyces cerevisiae*. *Biochem J* **392**: 537-544
- Chai MF, Chen QJ, An R, Chen YM, Chen J, Wang XC** (2005) NADK2, an Arabidopsis chloroplastic NAD kinase, plays a vital role in both chlorophyll synthesis and chloroplast protection. *Plant Mol Biol* **59**: 553-564
- Chalmers S, Nicholls DG** (2003) The relationship between free and total calcium concentrations in the matrix of liver and brain mitochondria. *J Biol Chem* **278**: 19062-19070
- Charles SA, Halliwell B** (1980) Action of calcium ions on spinach (*Spinacia oleracea*) chloroplast fructose biphosphatase and other enzymes of the Calvin cycle. *Biochem J* **188**: 775-779
- Charpentier M, Bredemeier R, Wanner G, Takeda N, Schleiff E, Parniske M** (2008) Lotus japonicus CASTOR and POLLUX are ion channels essential for perinuclear calcium spiking in legume root endosymbiosis. *Plant Cell* **20**: 3467-3479
- Chen C, Fan C, Gao M, Zhu H** (2009) Antiquity and function of CASTOR and POLLUX, the twin ion channel-encoding genes key to the evolution of root symbioses in plants. *Plant Physiol* **149**: 306-317
- Chen XJ** (2004) Sallp, a calcium-dependent carrier protein that suppresses an essential cellular function associated With the Aac2 isoform of ADP/ATP translocase in *Saccharomyces cerevisiae*. *Genetics* **167**: 607-617
- Cheng NH, Liu JZ, Nelson RS, Hirschi KD** (2004) Characterization of CXIP4, a novel Arabidopsis protein that activates the H<sup>+</sup>/Ca<sup>2+</sup> antiporter, CAX1. *FEBS Lett* **559**: 99-106
- Cheng NH, Pittman JK, Shigaki T, Lachmansingh J, LeClere S, Lahner B, Salt DE, Hirschi KD** (2005) Functional association of Arabidopsis CAX1 and CAX3 is required for normal growth and ion homeostasis. *Plant Physiol* **138**: 2048-2060
- Chigri F, Hormann F, Stamp A, Stammers DK, Bolter B, Soll J, Vothknecht UC** (2006) Calcium regulation of chloroplast protein translocation is mediated by calmodulin binding to Tic32. *Proc Natl Acad Sci U S A* **103**: 16051-16056
- Chigri F, Soll J, Vothknecht UC** (2005) Calcium regulation of chloroplast protein import. *Plant J* **42**: 821-831
- Choi HI, Park HJ, Park JH, Kim S, Im MY, Seo HH, Kim YW, Hwang I, Kim SY** (2005) Arabidopsis calcium-dependent protein kinase AtCPK32 interacts with ABF4, a transcriptional regulator of abscisic acid-responsive gene expression, and modulates its activity. *Plant Physiol* **139**: 1750-1761
- Christensen A, Svensson K, Thelin L, Zhang W, Tintor N, Prins D, Funke N, Michalak M, Schulze-Lefert P, Saijo Y, Sommarin M, Widell S, Persson S** (2010) Higher plant calreticulins have acquired specialized functions in Arabidopsis. *PLoS One* **5**: e11342
- Cinco RM, Robblee JH, Messinger J, Fernandez C, McFarlane Holman KL, Sauer K, Yachandra VK** (2004) Orientation of calcium in the Mn<sub>4</sub>Ca cluster of the oxygen-evolving complex determined using polarized strontium EXAFS of photosystem II membranes. *Biochemistry* **43**: 13271-13282
- Clapham DE** (2007) Calcium signaling. *Cell* **131**: 1047-1058
- Coca M, San Segundo B** (2010) AtCPK1 calcium-dependent protein kinase mediates pathogen resistance in Arabidopsis. *Plant J*
- Coe H, Michalak M** (2009) Calcium binding chaperones of the endoplasmic reticulum. *Gen Physiol Biophys* **28 Spec No Focus**: F96-F103
- Collins S, Meyer T** (2010) Cell biology: A sensor for calcium uptake. *Nature* **467**: 283
- Conn S, Gilliham M** (2010) Comparative physiology of elemental distributions in plants. *Ann Bot* **105**: 1081-1102
- Conn SJ, Gilliham M, Athman A, Schreiber AW, Baumann U, Moller I, Cheng NH, Stancombe MA, Hirschi KD, Webb AA, Burton R, Kaiser BN, Tyerman SD, Leigh RA** (2011) Cell-specific vacuolar calcium storage mediated by CAX1 regulates apoplastic calcium concentration, gas exchange, and plant productivity in Arabidopsis. *Plant Cell* **23**: 240-257
- Contreras L, Gomez-Puertas P, Iijima M, Kobayashi K, Saheki T, Satrustegui J** (2007) Ca<sup>2+</sup> Activation kinetics of the two aspartate-glutamate mitochondrial carriers, aralar and citrin: role in the heart malate-aspartate NADH shuttle. *J Biol Chem* **282**: 7098-7106
- Costa A, Drago I, Behera S, Zottini M, Pizzo P, Schroeder JI, Pozzan T, Lo Schiavo F** (2010) H<sub>2</sub>O<sub>2</sub> in plant peroxisomes: an in vivo analysis uncovers a Ca(2+)-dependent scavenging system. *Plant J* **62**: 760-772
- Cunningham KW, Fink GR** (1994) Calcineurin-dependent growth control in *Saccharomyces cerevisiae* mutants lacking PMC1, a homolog of plasma membrane Ca<sub>2+</sub> ATPases. *J Cell Biol* **124**: 351-363

- Dammann C, Ichida A, Hong B, Romanowsky SM, Hrabak EM, Harmon AC, Pickard BG, Harper JF** (2003) Subcellular targeting of nine calcium-dependent protein kinase isoforms from *Arabidopsis*. *Plant Physiol* **132**: 1840-1848
- Davis DJ, Gross EL** (1975) Protein-protein interactions of light-harvesting pigment protein from spinach chloroplasts. I.  $\text{Ca}^{2+}$  binding and its relation to protein association. *Biochim Biophys Acta* **387**: 557-567
- Day IS, Reddy VS, Shad Ali G, Reddy AS** (2002) Analysis of EF-hand-containing proteins in *Arabidopsis*. *Genome Biol* **3**: RESEARCH0056
- de Brito OM, Scorrano L** (2010) An intimate liaison: spatial organization of the endoplasmic reticulum-mitochondria relationship. *EMBO J* **29**: 2715-2723
- de Castro E, Sigrist CJ, Gattiker A, Bulliard V, Langendijk-Genevaux PS, Gasteiger E, Bairoch A, Hulo N** (2006) ScanProsite: detection of PROSITE signature matches and ProRule-associated functional and structural residues in proteins. *Nucleic Acids Res* **34**: W362-365
- De Stefani D, Raffaello A, Teardo E, Szabo I, Rizzuto R** (2011) A forty-kilodalton protein of the inner membrane is the mitochondrial calcium uniporter. *Nature*
- DeFalco TA, Bender KW, Snedden WA** (2010) Breaking the code:  $\text{Ca}^{2+}$  sensors in plant signalling. *Biochem J* **425**: 27-40
- del Arco A, Satrustegui J** (2004) Identification of a novel human subfamily of mitochondrial carriers with calcium-binding domains. *J Biol Chem* **279**: 24701-24713
- Dhanao PK, Richardson LG, Smith MD, Gidda SK, Henderson MP, Andrews DW, Mullen RT** (2010) Distinct pathways mediate the sorting of tail-anchored proteins to the plastid outer envelope. *PLoS One* **5**: e10098
- Dodd AN, Kudla J, Sanders D** (2010) The language of calcium signaling. *Annu Rev Plant Biol* **61**: 593-620
- Dominguez DC** (2004) Calcium signalling in bacteria. *Mol Microbiol* **54**: 291-297
- Drago I, Giacomello M, Pizzo P, Pozzan T** (2008) Calcium dynamics in the peroxisomal lumen of living cells. *J Biol Chem* **283**: 14384-14390
- Duchene AM, Giritch A, Hoffmann B, Cognat V, Lancelin D, Peeters NM, Zaepfel M, Marechal-Drouard L, Small ID** (2005) Dual targeting is the rule for organellar aminoacyl-tRNA synthetases in *Arabidopsis thaliana*. *Proc Natl Acad Sci U S A* **102**: 16484-16489
- Dunkley TP, Hester S, Shadforth IP, Runions J, Weimar T, Hanton SL, Griffin JL, Bessant C, Brandizzi F, Hawes C, Watson RB, Dupree P, Lilley KS** (2006) Mapping the *Arabidopsis* organelle proteome. *Proc Natl Acad Sci U S A* **103**: 6518-6523
- Durek P, Schmidt R, Heazlewood JL, Jones A, MacLean D, Nagel A, Kersten B, Schulze WX** (2010) PhosPhAt: the *Arabidopsis thaliana* phosphorylation site database. An update. *Nucleic Acids Res* **38**: D828-834
- Dutta R, Robinson KR** (2004) Identification and characterization of stretch-activated ion channels in pollen protoplasts. *Plant Physiol* **135**: 1398-1406
- Duy D, Soll J, Philippar K** (2007) Solute channels of the outer membrane: from bacteria to chloroplasts. *Biol Chem* **388**: 879-889
- Dyall SD, Agius SC, De Marcos Lousa C, Trezeguet V, Tokatlidis K** (2003) The dynamic dimerization of the yeast ADP/ATP carrier in the inner mitochondrial membrane is affected by conserved cysteine residues. *J Biol Chem* **278**: 26757-26764
- Eilam Y, Othman M, Halachmi D** (1990) Transient increase in  $\text{Ca}^{2+}$  influx in *Saccharomyces cerevisiae* in response to glucose: effects of intracellular acidification and cAMP levels. *J Gen Microbiol* **136**: 2537-2543
- Ettlinger WF, Clear AM, Fanning KJ, Peck ML** (1999) Identification of a  $\text{Ca}^{2+}/\text{H}^{+}$  antiport in the plant chloroplast thylakoid membrane. *Plant Physiol* **119**: 1379-1386
- Faxen K, Andersen JL, Gourdon P, Fedosova N, Morth JP, Nissen P, Moller JV** (2011) Characterization of a *Listeria monocytogenes*  $\text{Ca}(2+)$  pump: a SERCA-type ATPase with only one  $\text{Ca}(2+)$ -binding site. *J Biol Chem* **286**: 1609-1617
- Ferro M, Brugiere S, Salvi D, Seigneurin-Berny D, Court M, Moyet L, Ramus C, Miras S, Mellal M, Le Gall S, Kieffer-Jaquinod S, Bruley C, Garin J, Joyard J, Masselon C, Rolland N** (2010) AT\_CHLORO, a comprehensive chloroplast proteome database with subplastidial localization and curated information on envelope proteins. *Mol Cell Proteomics* **9**: 1063-1084
- Ferro M, Salvi D, Brugiere S, Miras S, Kowalski S, Louwagie M, Garin J, Joyard J, Rolland N** (2003) Proteomics of the chloroplast envelope membranes from *Arabidopsis thaliana*. *Mol Cell Proteomics* **2**: 325-345

- Fiermonte G, Palmieri L, Todisco S, Agrimi G, Palmieri F, Walker JE** (2002) Identification of the mitochondrial glutamate transporter. Bacterial expression, reconstitution, functional characterization, and tissue distribution of two human isoforms. *J Biol Chem* **277**: 19289-19294
- Finkler A, Kaplan B, Fromm H** (2007) Ca-Responsive cis-Elements in Plants. *Plant Signal Behav* **2**: 17-19
- Fiore C, Trezeguet V, Le Saux A, Roux P, Schwimmer C, Dianoux AC, Noel F, Lauquin GJ, Brandolin G, Vignais PV** (1998) The mitochondrial ADP/ATP carrier: structural, physiological and pathological aspects. *Biochimie* **80**: 137-150
- Friso G, Giacomelli L, Ytterberg AJ, Peltier JB, Rudella A, Sun Q, Wijk KJ** (2004) In-depth analysis of the thylakoid membrane proteome of *Arabidopsis thaliana* chloroplasts: new proteins, new functions, and a plastid proteome database. *Plant Cell* **16**: 478-499
- Fristedt R, Carlberg I, Zygadlo A, Piippo M, Nurmi M, Aro EM, Scheller HV, Vener AV** (2009) Intrinsically unstructured phosphoprotein TSP9 regulates light harvesting in *Arabidopsis thaliana*. *Biochemistry* **48**: 499-509
- Fristedt R, Granath P, Vener AV** (2010) A protein phosphorylation threshold for functional stacking of plant photosynthetic membranes. *PLoS One* **5**: e10963
- Fristedt R, Willig A, Granath P, Crevecoeur M, Rochaix JD, Vener AV** (2009) Phosphorylation of photosystem II controls functional macroscopic folding of photosynthetic membranes in *Arabidopsis*. *Plant Cell* **21**: 3950-3964
- Fujisawa M, Wada Y, Tsuchiya T, Ito M** (2009) Characterization of *Bacillus subtilis* YfkE (ChaA): a calcium-specific Ca<sup>2+</sup>/H<sup>+</sup> antiporter of the CaCA family. *Arch Microbiol* **191**: 649-657
- Furuichi T, Mori IC, Takahashi K, Muto S** (2001) Sugar-induced increase in cytosolic Ca<sup>2+</sup> in *Arabidopsis thaliana* whole plants. *Plant Cell Physiol* **42**: 1149-1155
- Furuichi T, Muto S** (2005) H<sup>+</sup>-Coupled sugar transporter, an initiator of sugar-induced Ca<sup>2+</sup>-signaling in plant cells. *Z Naturforsch C* **60**: 764-768
- Galon Y, Finkler A, Fromm H** (2010) Calcium-regulated transcription in plants. *Mol Plant* **3**: 653-669
- Gao H, Kadirjan-Kalbach D, Froehlich JE, Osteryoung KW** (2003) ARC5, a cytosolic dynamin-like protein from plants, is part of the chloroplast division machinery. *Proc Natl Acad Sci U S A* **100**: 4328-4333
- Geisler DA, Broselid C, Hederstedt L, Rasmusson AG** (2007) Ca<sup>2+</sup>-binding and Ca<sup>2+</sup>-independent respiratory NADH and NADPH dehydrogenases of *Arabidopsis thaliana*. *J Biol Chem* **282**: 28455-28464
- Geisler M, Axelsen KB, Harper JF, Palmgren MG** (2000) Molecular aspects of higher plant P-type Ca<sup>2+</sup>-ATPases. *Biochim Biophys Acta* **1465**: 52-78
- George L, Romanowsky SM, Harper JF, Sharrock RA** (2008) The ACA10 Ca<sup>2+</sup>-ATPase regulates adult vegetative development and inflorescence architecture in *Arabidopsis*. *Plant Physiol* **146**: 716-728
- Ger MF, Rendon G, Tilson JL, Jakobsson E** (2010) Domain-based identification and analysis of glutamate receptor ion channels and their relatives in prokaryotes. *PLoS One* **5**: e12827
- Giacomello M, Drago I, Pizzo P, Pozzan T** (2007) Mitochondrial Ca<sup>2+</sup> as a key regulator of cell life and death. *Cell Death Differ* **14**: 1267-1274
- Gifford JL, Walsh MP, Vogel HJ** (2007) Structures and metal-ion-binding properties of the Ca<sup>2+</sup>-binding helix-loop-helix EF-hand motifs. *Biochem J* **405**: 199-221
- Givens RM, Lin MH, Taylor DJ, Mechold U, Berry JO, Hernandez VJ** (2004) Inducible expression, enzymatic activity, and origin of higher plant homologues of bacterial RelA/SpoT stress proteins in *Nicotiana tabacum*. *J Biol Chem* **279**: 7495-7504
- Gong D, Guo Y, Jagendorf AT, Zhu JK** (2002) Biochemical characterization of the *Arabidopsis* protein kinase SOS2 that functions in salt tolerance. *Plant Physiol* **130**: 256-264
- Gowik U, Brautigam A, Weber KL, Weber AP, Westhoff P** (2011) Evolution of c4 photosynthesis in the genus flaveria: how many and which genes does it take to make c4? *Plant Cell* **23**: 2087-2105
- Grabarek Z** (2006) Structural basis for diversity of the EF-hand calcium-binding proteins. *J Mol Biol* **359**: 509-525
- Groppi S, Belotti F, Brandao RL, Martegani E, Tisi R** (2011) Glucose-induced calcium influx in budding yeast involves a novel calcium transport system and can activate calcineurin. *Cell Calcium* **49**: 376-386
- Gross EL, Hess SC** (1974) Correlation between calcium ion binding to chloroplast membranes and divalent cation-induced structural changes and changes in chlorophyll a fluorescence. *Biochim Biophys Acta* **339**: 334-346
- Gupta D, Tuteja N** (2011) Chaperones and foldases in endoplasmic reticulum stress signaling in plants. *Plant Signal Behav* **6**: 232-236

- Gutierrez-Ford C, Levay K, Gomes AV, Perera EM, Som T, Kim YM, Benovic JL, Berkovitz GD, Slepak VZ** (2003) Characterization of tescalcin, a novel EF-hand protein with a single Ca<sup>2+</sup>-binding site: metal-binding properties, localization in tissues and cells, and effect on calcineurin. *Biochemistry* **42**: 14553-14565
- Hajnoczky G, Csordas G** (2010) Calcium signalling: fishing out molecules of mitochondrial calcium transport. *Curr Biol* **20**: R888-891
- Han S, Tang R, Anderson LK, Woerner TE, Pei ZM** (2003) A cell surface receptor mediates extracellular Ca<sup>2+</sup> sensing in guard cells. *Nature* **425**: 196-200
- Han S, Tang R, Anderson LK, Woerner TE, Pei ZM** (2003) A cell surface receptor mediates extracellular Ca(2+) sensing in guard cells. *Nature* **425**: 196-200
- Hansson M, Dupuis T, Stromquist R, Andersson B, Vener AV, Carlberg I** (2007) The mobile thylakoid phosphoprotein TSP9 interacts with the light-harvesting complex II and the peripheries of both photosystems. *J Biol Chem* **282**: 16214-16222
- Harper JF, Breton G, Harmon A** (2004) Decoding Ca(2+) signals through plant protein kinases. *Annu Rev Plant Biol* **55**: 263-288
- Harper JF, Harmon A** (2005) Plants, symbiosis and parasites: a calcium signalling connection. *Nat Rev Mol Cell Biol* **6**: 555-566
- Harper JF, Hong B, Hwang I, Guo HQ, Stoddard R, Huang JF, Palmgren MG, Sze H** (1998) A novel calmodulin-regulated Ca<sup>2+</sup>-ATPase (ACA2) from Arabidopsis with an N-terminal autoinhibitory domain. *J Biol Chem* **273**: 1099-1106
- Haswell ES, Meyerowitz EM** (2006) MscS-like proteins control plastid size and shape in Arabidopsis thaliana. *Curr Biol* **16**: 1-11
- He X, Wu C, Yarbrough D, Sim L, Niu G, Merritt J, Shi W, Qi F** (2008) The cia operon of *Streptococcus mutans* encodes a unique component required for calcium-mediated autoregulation. *Mol Microbiol* **70**: 112-126
- Heazlewood JL, Durek P, Hummel J, Selbig J, Weckwerth W, Walther D, Schulze WX** (2008) PhosPhAt: a database of phosphorylation sites in Arabidopsis thaliana and a plant-specific phosphorylation site predictor. *Nucleic Acids Res* **36**: D1015-1021
- Hepler PK** (2005) Calcium: a central regulator of plant growth and development. *Plant Cell* **17**: 2142-2155
- Hepler PK, Winship LJ** (2010) Calcium at the cell wall-cytoplasm interface. *J Integr Plant Biol* **52**: 147-160
- Herbaud ML, Guiseppi A, Denizot F, Haiech J, Kilhoffer MC** (1998) Calcium signalling in *Bacillus subtilis*. *Biochim Biophys Acta* **1448**: 212-226
- Hetherington AM, Brownlee C** (2004) The generation of Ca(2+) signals in plants. *Annu Rev Plant Biol* **55**: 401-427
- Hoppe UC** (2010) Mitochondrial calcium channels. *FEBS Lett* **584**: 1975-1981
- Hrabak EM, Chan CW, Gribskov M, Harper JF, Choi JH, Halford N, Kudla J, Luan S, Nimmo HG, Sussman MR, Thomas M, Walker-Simmons K, Zhu JK, Harmon AC** (2003) The Arabidopsis CDPK-SnRK superfamily of protein kinases. *Plant Physiol* **132**: 666-680
- Hu Y, Zhang X, Shi Y, Zhou Y, Zhang W, Su XD, Xia B, Zhao J, Jin C** (2011) Structures of Anabaena calcium-binding protein CcbP: insights into Ca<sup>2+</sup> signaling during heterocyst differentiation. *J Biol Chem* **286**: 12381-12388
- Hua BG, Mercier RW, Leng Q, Berkowitz GA** (2003) Plants do it differently. A new basis for potassium/sodium selectivity in the pore of an ion channel. *Plant Physiol* **132**: 1353-1361
- Huang L, Berkelman T, Franklin AE, Hoffman NE** (1993) Characterization of a gene encoding a Ca(2+)-ATPase-like protein in the plastid envelope. *Proc Natl Acad Sci U S A* **90**: 10066-10070
- Ifuku K, Ishihara S, Sato F** (2010) Molecular functions of oxygen-evolving complex family proteins in photosynthetic electron flow. *J Integr Plant Biol* **52**: 723-734
- Ikura M, Osawa M, Ames JB** (2002) The role of calcium-binding proteins in the control of transcription: structure to function. *Bioessays* **24**: 625-636
- Imaizumi-Anraku H, Takeda N, Charpentier M, Perry J, Miwa H, Umehara Y, Kouchi H, Murakami Y, Mulder L, Vickers K, Pike J, Downie JA, Wang T, Sato S, Asamizu E, Tabata S, Yoshikawa M, Murooka Y, Wu GJ, Kawaguchi M, Kawasaki S, Parniske M, Hayashi M** (2005) Plastid proteins crucial for symbiotic fungal and bacterial entry into plant roots. *Nature* **433**: 527-531
- Ishijima J, Nagasaki N, Maeshima M, Miyano M** (2007) RVCaB, a calcium-binding protein in radish vacuoles, is predominantly an unstructured protein with a polyproline type II helix. *J Biochem* **142**: 201-211
- Ishitani M, Liu J, Halfter U, Kim CS, Shi W, Zhu JK** (2000) SOS3 function in plant salt tolerance requires N-myristoylation and calcium binding. *Plant Cell* **12**: 1667-1678

- Jarrett HW, Brown CJ, Black CC, Cormier MJ** (1982) Evidence that calmodulin is in the chloroplast of peas and serves a regulatory role in photosynthesis. *J Biol Chem* **257**: 13795-13804
- Jiang D, Zhao L, Clapham DE** (2009) Genome-wide RNAi screen identifies Letm1 as a mitochondrial  $\text{Ca}^{2+}/\text{H}^{+}$  antiporter. *Science* **326**: 144-147
- Johnson CH, Knight MR, Kondo T, Masson P, Sedbrook J, Haley A, Trewavas A** (1995) Circadian oscillations of cytosolic and chloroplastic free calcium in plants. *Science* **269**: 1863-1865
- Jones HE, Holland IB, Baker HL, Campbell AK** (1999) Slow changes in cytosolic free  $\text{Ca}^{2+}$  in *Escherichia coli* highlight two putative influx mechanisms in response to changes in extracellular calcium. *Cell Calcium* **25**: 265-274
- Kanamaru K, Kashiwagi S, Mizuno T** (1993) The cyanobacterium, *Synechococcus* sp. PCC7942, possesses two distinct genes encoding cation-transporting P-type ATPases. *FEBS Lett* **330**: 99-104
- Kaplan B, Davydov O, Knight H, Galon Y, Knight MR, Fluhr R, Fromm H** (2006) Rapid transcriptome changes induced by cytosolic  $\text{Ca}^{2+}$  transients reveal ABRE-related sequences as  $\text{Ca}^{2+}$ -responsive cis elements in *Arabidopsis*. *Plant Cell* **18**: 2733-2748
- Kaplan B, Sherman T, Fromm H** (2007) Cyclic nucleotide-gated channels in plants. *FEBS Lett* **581**: 2237-2246
- Kaplan RS, Mayor JA, Gremse DA, Wood DO** (1995) High level expression and characterization of the mitochondrial citrate transport protein from the yeast *Saccharomyces cerevisiae*. *J Biol Chem* **270**: 4108-4114
- Karnik SK, Trelease RN** (2007) *Arabidopsis* peroxin 16 trafficks through the ER and an intermediate compartment to pre-existing peroxisomes via overlapping molecular targeting signals. *J Exp Bot* **58**: 1677-1693
- Kasai M, Muto S** (1990)  $\text{Ca}^{2+}$  pump and  $\text{Ca}^{2+}/\text{H}^{+}$  antiporter in plasma membrane vesicles isolated by aqueous two-phase partitioning from corn leaves. *J Membr Biol* **114**: 133-142
- Kato M, Nagasaki-Takeuchi N, Ide Y, Maeshima M** (2010) An *Arabidopsis* hydrophilic  $\text{Ca}^{2+}$ -binding protein with a PEVK-rich domain, PCaP2, is associated with the plasma membrane and interacts with calmodulin and phosphatidylinositol phosphates. *Plant Cell Physiol* **51**: 366-379
- Kato Y, Miura E, Ido K, Ifuku K, Sakamoto W** (2009) The variegated mutants lacking chloroplastic FtsHs are defective in D1 degradation and accumulate reactive oxygen species. *Plant Physiol* **151**: 1790-1801
- Keller A, Nesvizhskii AI, Kolker E, Aebersold R** (2002) Empirical statistical model to estimate the accuracy of peptide identifications made by MS/MS and database search. *Anal Chem* **74**: 5383-5392
- Kim MC, Chung WS, Yun DJ, Cho MJ** (2009) Calcium and calmodulin-mediated regulation of gene expression in plants. *Mol Plant* **2**: 13-21
- Kim TH, Bohmer M, Hu H, Nishimura N, Schroeder JI** (2010) Guard cell signal transduction network: advances in understanding abscisic acid,  $\text{CO}_2$ , and  $\text{Ca}^{2+}$  signaling. *Annu Rev Plant Biol* **61**: 561-591
- Kim YY, Choi H, Segami S, Cho HT, Martinoia E, Maeshima M, Lee Y** (2009) AtHMA1 contributes to the detoxification of excess Zn(II) in *Arabidopsis*. *Plant J* **58**: 737-753
- Knight MR, Campbell AK, Smith SM, Trewavas AJ** (1991) Recombinant aequorin as a probe for cytosolic free  $\text{Ca}^{2+}$  in *Escherichia coli*. *FEBS Lett* **282**: 405-408
- Kobayashi M, Ohura I, Kawakita K, Yokota N, Fujiwara M, Shimamoto K, Doke N, Yoshioka H** (2007) Calcium-dependent protein kinases regulate the production of reactive oxygen species by potato NADPH oxidase. *Plant Cell* **19**: 1065-1080
- Kong SG, Wada M** (2011) New Insights into Dynamic Actin-Based Chloroplast Photorelocation Movement. *Mol Plant*
- Kornmann B, Currie E, Collins SR, Schuldiner M, Nunnari J, Weissman JS, Walter P** (2009) An ER-mitochondria tethering complex revealed by a synthetic biology screen. *Science* **325**: 477-481
- Kreimer** (1985) Characterization of calcium fluxes across the envelope of intact spinach chloroplasts. *Planta*: 515-523
- Kreimer** (1987) Calcium binding by spinach stromal proteins. *Planta* **171**: 259-265
- Kretsinger RH, Nockolds CE** (1973) Carp muscle calcium-binding protein. II. Structure determination and general description. *J Biol Chem* **248**: 3313-3326
- Kriechbaumer V, Shaw R, Mukherjee J, Bowsher CG, Harrison AM, Abell BM** (2009) Subcellular distribution of tail-anchored proteins in *Arabidopsis*. *Traffic* **10**: 1753-1764
- Kudla J, Batistic O, Hashimoto K** (2010) Calcium signals: the lead currency of plant information processing. *Plant Cell* **22**: 541-563
- Kuhn S, Bussemer J, Chigri F, Voithknecht UC** (2009) Calcium depletion and calmodulin inhibition affect the import of nuclear-encoded proteins into plant mitochondria. *Plant J* **58**: 694-705

- Kunji ER, Robinson AJ** (2010) Coupling of proton and substrate translocation in the transport cycle of mitochondrial carriers. *Curr Opin Struct Biol* **20**: 440-447
- Kurokawa M, Kornbluth S** (2009) Caspases and kinases in a death grip. *Cell* **138**: 838-854
- Laco J, Zeman I, Pevala V, Polcic P, Kolarov J** (2010) Adenine nucleotide transport via Sall carrier compensates for the essential function of the mitochondrial ADP/ATP carrier. *FEMS Yeast Res* **10**: 290-296
- Lasorsa FM, Pinton P, Palmieri L, Scarcia P, Rottensteiner H, Rizzuto R, Palmieri F** (2008) Peroxisomes as novel players in cell calcium homeostasis. *J Biol Chem* **283**: 15300-15308
- Laude AJ, Simpson AW** (2009) Compartmentalized signalling: Ca<sup>2+</sup> compartments, microdomains and the many facets of Ca<sup>2+</sup> signalling. *FEBS J* **276**: 1800-1816
- Lazo GR, Stein PA, Ludwig RA** (1991) A DNA transformation-competent Arabidopsis genomic library in Agrobacterium. *Biotechnology (N Y)* **9**: 963-967
- Lecourieux D, Lamotte O, Bourque S, Wendehenne D, Mazars C, Ranjeva R, Pugin A** (2005) Proteinaceous and oligosaccharidic elicitors induce different calcium signatures in the nucleus of tobacco cells. *Cell Calcium* **38**: 527-538
- Lee J, Lee H, Kim J, Lee S, Kim DH, Kim S, Hwang I** (2011) Both the hydrophobicity and a positively charged region flanking the C-terminal region of the transmembrane domain of signal-anchored proteins play critical roles in determining their targeting specificity to the endoplasmic reticulum or endosymbiotic organelles in Arabidopsis cells. *Plant Cell* **23**: 1588-1607
- Lee SM, Kim HS, Han HJ, Moon BC, Kim CY, Harper JF, Chung WS** (2007) Identification of a calmodulin-regulated autoinhibited Ca<sup>2+</sup>-ATPase (ACA11) that is localized to vacuole membranes in Arabidopsis. *FEBS Lett* **581**: 3943-3949
- Lee YJ, Kim DH, Kim YW, Hwang I** (2001) Identification of a signal that distinguishes between the chloroplast outer envelope membrane and the endomembrane system in vivo. *Plant Cell* **13**: 2175-2190
- Lee YJ, Sohn EJ, Lee KH, Lee DW, Hwang I** (2004) The transmembrane domain of AtToc64 and its C-terminal lysine-rich flanking region are targeting signals to the chloroplast outer envelope membrane [correction]. *Mol Cells* **17**: 281-291
- Leganes F, Forchhammer K, Fernandez-Pinas F** (2009) Role of calcium in acclimation of the cyanobacterium *Synechococcus elongatus* PCC 7942 to nitrogen starvation. *Microbiology* **155**: 25-34
- Leng Q, Mercier RW, Yao W, Berkowitz GA** (1999) Cloning and first functional characterization of a plant cyclic nucleotide-gated cation channel. *Plant Physiol* **121**: 753-761
- Lerch-Bader M, Lundin C, Kim H, Nilsson I, von Heijne G** (2008) Contribution of positively charged flanking residues to the insertion of transmembrane helices into the endoplasmic reticulum. *Proc Natl Acad Sci U S A* **105**: 4127-4132
- Lewis NE, Marty NJ, Kathir KM, Rajalingam D, Kight AD, Daily A, Kumar TK, Henry RL, Goforth RL** (2010) A dynamic cpSRP43-Albino3 interaction mediates translocase regulation of chloroplast signal recognition particle (cpSRP)-targeting components. *J Biol Chem* **285**: 34220-34230
- Lewit-Bentley A, Rety S** (2000) EF-hand calcium-binding proteins. *Curr Opin Struct Biol* **10**: 637-643
- Li J, Wang DY, Li Q, Xu YJ, Cui KM, Zhu YX** (2004) PPF1 inhibits programmed cell death in apical meristems of both G2 pea and transgenic Arabidopsis plants possibly by delaying cytosolic Ca<sup>2+</sup> elevation. *Cell Calcium* **35**: 71-77
- Li X, Chanroj S, Wu Z, Romanowsky SM, Harper JF, Sze H** (2008) A distinct endosomal Ca<sup>2+</sup>/Mn<sup>2+</sup> pump affects root growth through the secretory process. *Plant Physiol* **147**: 1675-1689
- Liang F, Cunningham KW, Harper JF, Sze H** (1997) ECA1 complements yeast mutants defective in Ca<sup>2+</sup> pumps and encodes an endoplasmic reticulum-type Ca<sup>2+</sup>-ATPase in *Arabidopsis thaliana*. *Proc Natl Acad Sci U S A* **94**: 8579-8584
- Liao B, Gawienowski MC, Zielinski RE** (1996) Differential stimulation of NAD kinase and binding of peptide substrates by wild-type and mutant plant calmodulin isoforms. *Arch Biochem Biophys* **327**: 53-60
- Lindahl M, Spetea C, Hundal T, Oppenheim AB, Adam Z, Andersson B** (2000) The thylakoid FtsH protease plays a role in the light-induced turnover of the photosystem II D1 protein. *Plant Cell* **12**: 419-431
- Linka N, Theodoulou FL, Haslam RP, Linka M, Napier JA, Neuhaus HE, Weber AP** (2008) Peroxisomal ATP import is essential for seedling development in *Arabidopsis thaliana*. *Plant Cell* **20**: 3241-3257
- Liu J, Zhu JK** (1998) A calcium sensor homolog required for plant salt tolerance. *Science* **280**: 1943-1945
- Logan DC, Knight MR** (2003) Mitochondrial and cytosolic calcium dynamics are differentially regulated in plants. *Plant Physiol* **133**: 21-24



- Lu SX, Hrabak EM** (2002) An Arabidopsis calcium-dependent protein kinase is associated with the endoplasmic reticulum. *Plant Physiol* **128**: 1008-1021
- Malmstrom S, Askerlund P, Palmgren MG** (1997) A calmodulin-stimulated  $\text{Ca}^{2+}$ -ATPase from plant vacuolar membranes with a putative regulatory domain at its N-terminus. *FEBS Lett* **400**: 324-328
- Marmol P, Pardo B, Wiederkehr A, del Arco A, Wollheim CB, Satrustegui J** (2009) Requirement for aralar and its  $\text{Ca}^{2+}$ -binding sites in  $\text{Ca}^{2+}$  signal transduction in mitochondria from INS-1 clonal beta-cells. *J Biol Chem* **284**: 515-524
- Maruyama K, Mikawa T, Ebashi S** (1984) Detection of calcium binding proteins by  $^{45}\text{Ca}$  autoradiography on nitrocellulose membrane after sodium dodecyl sulfate gel electrophoresis. *J Biochem* **95**: 511-519
- Masuda S, Mizusawa K, Narisawa T, Tozawa Y, Ohta H, Takamiya K** (2008) The bacterial stringent response, conserved in chloroplasts, controls plant fertilization. *Plant Cell Physiol* **49**: 135-141
- Matzke AJ, Weiger TM, Matzke M** (2010) Ion channels at the nucleus: electrophysiology meets the genome. *Mol Plant* **3**: 642-652
- Mazars C, Bourque S, Mithofer A, Pugin A, Ranjeva R** (2009) Calcium homeostasis in plant cell nuclei. *New Phytol* **181**: 261-274
- Mazars C, Briere C, Bourque S, Thuleau P** (2011) Nuclear calcium signaling: An emerging topic in plants. *Biochimie*
- McAinsh MR, Pittman JK** (2009) Shaping the calcium signature. *New Phytol* **181**: 275-294
- McCormack E, Tsai YC, Braam J** (2005) Handling calcium signaling: Arabidopsis CaMs and CMLs. *Trends Plant Sci* **10**: 383-389
- McCormack EaB, J.** (2003) Calmodulins and related potential calcium sensors of Arabidopsis. *New Phytol* **159**: 585-598
- McCormack JG, Halestrap AP, Denton RM** (1990) Role of calcium ions in regulation of mammalian intramitochondrial metabolism. *Physiol Rev* **70**: 391-425
- Mehlmer N, Wurzinger B, Stael S, Hofmann-Rodrigues D, Cszasz E, Pfister B, Bayer R, Teige M** (2010) The  $\text{Ca}^{2+}$ -dependent protein kinase CPK3 is required for MAPK-independent salt-stress acclimation in Arabidopsis. *Plant J* **63**: 484-498
- Mehlmer N, Wurzinger B, Stael S, Hofmann-Rodrigues D, Cszasz E, Pfister B, Bayer R, Teige M** (2010) The  $\text{Ca}^{2+}$ -dependent protein kinase CPK3 is required for MAPK-independent salt-stress acclimation in Arabidopsis. *Plant J*
- Mei H, Zhao J, Pittman JK, Lachmansingh J, Park S, Hirschi KD** (2007) In planta regulation of the Arabidopsis  $\text{Ca}^{2+}/\text{H}^{+}$  antiporter CAX1. *J Exp Bot* **58**: 3419-3427
- Meskauskiene R, Nater M, Goslings D, Kessler F, op den Camp R, Apel K** (2001) FLU: a negative regulator of chlorophyll biosynthesis in Arabidopsis thaliana. *Proc Natl Acad Sci U S A* **98**: 12826-12831
- Meyer RC, Steinfath M, Lisek J, Becher M, Witucka-Wall H, Torjek O, Fiehn O, Eckardt A, Willmitzer L, Selbig J, Altmann T** (2007) The metabolic signature related to high plant growth rate in *Arabidopsis thaliana*. *Proc Natl Acad Sci U S A* **104**: 4759-4764
- Michalak M, Groenendyk J, Szabo E, Gold LI, Opas M** (2009) Calreticulin, a multi-process calcium-buffering chaperone of the endoplasmic reticulum. *Biochem J* **417**: 651-666
- Michard E, Lima PT, Borges F, Silva AC, Portes MT, Carvalho JE, Gilliam M, Liu LH, Obermeyer G, Feijo JA** (2011) Glutamate receptor-like genes form  $\text{Ca}^{2+}$  channels in pollen tubes and are regulated by pistil D-serine. *Science* **332**: 434-437
- Michiels J, Xi C, Verhaert J, Vanderleyden J** (2002) The functions of  $\text{Ca}^{2+}$  in bacteria: a role for EF-hand proteins? *Trends Microbiol* **10**: 87-93
- Miernyk JA, Fang TK, Randall DD** (1987) Calmodulin antagonists inhibit the mitochondrial pyruvate dehydrogenase complex. *J Biol Chem* **262**: 15338-15340
- Mills RF, Doherty ML, Lopez-Marques RL, Weimar T, Dupree P, Palmgren MG, Pittman JK, Williams LE** (2008) ECA3, a Golgi-localized P2A-type ATPase, plays a crucial role in manganese nutrition in Arabidopsis. *Plant Physiol* **146**: 116-128
- Minet M, Dufour ME, Lacroute F** (1992) Complementation of *Saccharomyces cerevisiae* auxotrophic mutants by *Arabidopsis thaliana* cDNAs. *Plant J* **2**: 417-422
- Mithofer A, Mazars C** (2002) Aequorin-based measurements of intracellular  $\text{Ca}^{2+}$ -signatures in plant cells. *Biol Proced Online* **4**: 105-118
- Mochizuki N, Brusslan JA, Larkin R, Nagatani A, Chory J** (2001) Arabidopsis genomes uncoupled 5 (GUN5) mutant reveals the involvement of Mg-chelatase H subunit in plastid-to-nucleus signal transduction. *Proc Natl Acad Sci U S A* **98**: 2053-2058

- Monshausen GB, Messerli MA, Gilroy S** (2008) Imaging of the Yellow Cameleon 3.6 indicator reveals that elevations in cytosolic  $\text{Ca}^{2+}$  follow oscillating increases in growth in root hairs of Arabidopsis. *Plant Physiol* **147**: 1690-1698
- Moreno I, Norambuena L, Maturana D, Toro M, Vergara C, Orellana A, Zurita-Silva A, Ordenes VR** (2008) AtHMA1 is a thapsigargin-sensitive  $\text{Ca}^{2+}$ /heavy metal pump. *J Biol Chem* **283**: 9633-9641
- Morgan RO, Martin-Almedina S, Garcia M, Jhoncon-Kooyip J, Fernandez MP** (2006) Deciphering function and mechanism of calcium-binding proteins from their evolutionary imprints. *Biochim Biophys Acta* **1763**: 1238-1249
- Mori IC, Murata Y, Yang Y, Munemasa S, Wang YF, Andreoli S, Tiriach H, Alonso JM, Harper JF, Ecker JR, Kwak JM, Schroeder JI** (2006) CDPKs CPK6 and CPK3 function in ABA regulation of guard cell S-type anion- and  $\text{Ca}^{2+}$ -permeable channels and stomatal closure. *PLoS Biol* **4**: e327
- Morre DJ, Sellden G, Sundqvist C, Sandelius AS** (1991) Stromal low temperature compartment derived from the inner membrane of the chloroplast envelope. *Plant Physiol* **97**: 1558-1564
- Munnik T, Testerink C** (2009) Plant phospholipid signaling: "in a nutshell". *J Lipid Res* **50 Suppl**: S260-265
- Murray JD** (2011) Invasion by invitation: rhizobial infection in legumes. *Mol Plant Microbe Interact* **24**: 631-639
- Nagata T, Iizumi S, Satoh K, Ooka H, Kawai J, Carninci P, Hayashizaki Y, Otomo Y, Murakami K, Matsubara K, Kikuchi S** (2004) Comparative analysis of plant and animal calcium signal transduction element using plant full-length cDNA data. *Mol Biol Evol* **21**: 1855-1870
- Nakajima-Shimada J, Iida H, Tsuji FI, Anraku Y** (1991) Monitoring of intracellular calcium in *Saccharomyces cerevisiae* with an apoaequorin cDNA expression system. *Proc Natl Acad Sci U S A* **88**: 6878-6882
- Narendra S, Venkataramani S, Shen G, Wang J, Pasapula V, Lin Y, Kornyejev D, Holaday AS, Zhang H** (2006) The Arabidopsis ascorbate peroxidase 3 is a peroxisomal membrane-bound antioxidant enzyme and is dispensable for Arabidopsis growth and development. *J Exp Bot* **57**: 3033-3042
- Navazio L, Bewell MA, Siddiqua A, Dickinson GD, Galione A, Sanders D** (2000) Calcium release from the endoplasmic reticulum of higher plants elicited by the NADP metabolite nicotinic acid adenine dinucleotide phosphate. *Proc Natl Acad Sci U S A* **97**: 8693-8698
- Nazarenko LV, Andreev IM, Lyukevich AA, Pisareva TV, Los DA** (2003) Calcium release from *Synechocystis* cells induced by depolarization of the plasma membrane: MscL as an outward  $\text{Ca}^{2+}$  channel. *Microbiology* **149**: 1147-1153
- Nesvizhskii AI, Keller A, Kolker E, Aebersold R** (2003) A statistical model for identifying proteins by tandem mass spectrometry. *Anal Chem* **75**: 4646-4658
- Niefind K, Putter M, Guerra B, Issinger OG, Schomburg D** (1999) GTP plus water mimic ATP in the active site of protein kinase CK2. *Nat Struct Biol* **6**: 1100-1103
- Nobel PS** (1969) Light-induced changes in the ionic content of chloroplasts in *Pisum sativum*. *Biochim Biophys Acta* **172**: 134-143
- Nomura H, Komori T, Kobori M, Nakahira Y, Shiina T** (2008) Evidence for chloroplast control of external  $\text{Ca}^{2+}$ -induced cytosolic  $\text{Ca}^{2+}$  transients and stomatal closure. *Plant J* **53**: 988-998
- Ogrzewalla K, Piotrowski M, Reinbothe S, Link G** (2002) The plastid transcription kinase from mustard (*Sinapis alba* L.). A nuclear-encoded CK2-type chloroplast enzyme with redox-sensitive function. *Eur J Biochem* **269**: 3329-3337
- Oldroyd GE, Downie JA** (2006) Nuclear calcium changes at the core of symbiosis signalling. *Curr Opin Plant Biol* **9**: 351-357
- Palmieri F** (1994) Mitochondrial carrier proteins. *FEBS Lett* **346**: 48-54
- Palmieri F, Pierri CL, De Grassi A, Nunes-Nesi A, Fernie AR** (2011) Evolution, structure and function of mitochondrial carriers: a review with new insights. *Plant J* **66**: 161-181
- Palmieri L, Arrigoni R, Blanco E, Carrari F, Zanor MI, Studart-Guimaraes C, Fernie AR, Palmieri F** (2006) Molecular identification of an Arabidopsis S-adenosylmethionine transporter. Analysis of organ distribution, bacterial expression, reconstitution into liposomes, and functional characterization. *Plant Physiol* **142**: 855-865
- Palty R, Silverman WF, Hershinkel M, Caporale T, Sensi SL, Parnis J, Nolte C, Fishman D, Shoshan-Barmatz V, Herrmann S, Khananshvilid D, Sekler I** (2010) NCLX is an essential component of mitochondrial  $\text{Na}^+/\text{Ca}^{2+}$  exchange. *Proc Natl Acad Sci U S A* **107**: 436-441
- Paulsen IT, Nguyen L, Sliwinski MK, Rabus R, Saier MH, Jr.** (2000) Microbial genome analyses: comparative transport capabilities in eighteen prokaryotes. *J Mol Biol* **301**: 75-100

- Pauly N, Knight MR, Thuleau P, van der Luit AH, Moreau M, Trewavas AJ, Ranjeva R, Mazars C** (2000) Control of free calcium in plant cell nuclei. *Nature* **405**: 754-755
- Peiter E** (2011) The plant vacuole: Emitter and receiver of calcium signals. *Cell Calcium*
- Peiter E, Maathuis FJ, Mills LN, Knight H, Pelloux J, Hetherington AM, Sanders D** (2005) The vacuolar Ca<sup>2+</sup>-activated channel TPC1 regulates germination and stomatal movement. *Nature* **434**: 404-408
- Perocchi F, Gohil VM, Girgis HS, Bao XR, McCombs JE, Palmer AE, Mootha VK** (2010) MICU1 encodes a mitochondrial EF hand protein required for Ca(2+) uptake. *Nature* **467**: 291-296
- Persson S, Wyatt SE, Love J, Thompson WF, Robertson D, Boss WF** (2001) The Ca(2+) status of the endoplasmic reticulum is altered by induction of calreticulin expression in transgenic plants. *Plant Physiol* **126**: 1092-1104
- Picault N, Hodges M, Palmieri L, Palmieri F** (2004) The growing family of mitochondrial carriers in Arabidopsis. *Trends Plant Sci* **9**: 138-146
- Pohlmeier K, Soll J, Grimm R, Hill K, Wagner R** (1998) A high-conductance solute channel in the chloroplastic outer envelope from Pea. *Plant Cell* **10**: 1207-1216
- Portis AR, Jr., Heldt HW** (1976) Light-dependent changes of the Mg<sup>2+</sup> concentration in the stroma in relation to the Mg<sup>2+</sup> dependency of CO<sub>2</sub> fixation in intact chloroplasts. *Biochim Biophys Acta* **449**: 434-436
- Postis V, De Marcos Lousa C, Arnou B, Lauquin GJ, Trezeguet V** (2005) Subunits of the yeast mitochondrial ADP/ATP carrier: cooperation within the dimer. *Biochemistry* **44**: 14732-14740
- Pottosin I, Wherrett T, Shabala S** (2009) SV channels dominate the vacuolar Ca<sup>2+</sup> release during intracellular signaling. *FEBS Lett* **583**: 921-926
- Qi Z, Stephens NR, Spalding EP** (2006) Calcium entry mediated by GLR3.3, an Arabidopsis glutamate receptor with a broad agonist profile. *Plant Physiol* **142**: 963-971
- Qiu QS, Guo Y, Dietrich MA, Schumaker KS, Zhu JK** (2002) Regulation of SOS1, a plasma membrane Na<sup>+</sup>/H<sup>+</sup> exchanger in *Arabidopsis thaliana*, by SOS2 and SOS3. *Proc Natl Acad Sci U S A* **99**: 8436-8441
- Qudeimat E, Faltusz AM, Wheeler G, Lang D, Brownlee C, Reski R, Frank W** (2008) A PIIB-type Ca<sup>2+</sup>-ATPase is essential for stress adaptation in *Physcomitrella patens*. *Proc Natl Acad Sci U S A* **105**: 19555-19560
- Racker E, Schroeder EA** (1958) The reductive pentose phosphate cycle. II. Specific C-1 phosphatases for fructose 1,6-diphosphate and sedoheptulose 1,7-diphosphate. *Arch Biochem Biophys* **74**: 326-344
- Raeymaekers L, Wuytack E, Willems I, Michiels CW, Wuytack F** (2002) Expression of a P-type Ca(2+)-transport ATPase in *Bacillus subtilis* during sporulation. *Cell Calcium* **32**: 93
- Randall SK** (1992) Characterization of vacuolar calcium-binding proteins. *Plant Physiol* **100**: 859-867
- Raychaudhury B, Gupta S, Banerjee S, Datta SC** (2006) Peroxisome is a reservoir of intracellular calcium. *Biochim Biophys Acta* **1760**: 989-992
- Reddy AS, Ali GS, Celesnik H, Day IS** (2011) Coping with stresses: roles of calcium- and calcium/calmodulin-regulated gene expression. *Plant Cell* **23**: 2010-2032
- Reddy AS, Ben-Hur A, Day IS** (2011) Experimental and computational approaches for the study of calmodulin interactions. *Phytochemistry* **72**: 1007-1019
- Reddy VS, Ali GS, Reddy AS** (2002) Genes encoding calmodulin-binding proteins in the Arabidopsis genome. *J Biol Chem* **277**: 9840-9852
- Reddy VS, Day IS, Thomas T, Reddy AS** (2004) KIC, a novel Ca<sup>2+</sup> binding protein with one EF-hand motif, interacts with a microtubule motor protein and regulates trichome morphogenesis. *Plant Cell* **16**: 185-200
- Reddy VS, Safadi F, Zielinski RE, Reddy AS** (1999) Interaction of a kinesin-like protein with calmodulin isoforms from Arabidopsis. *J Biol Chem* **274**: 31727-31733
- Reiland S, Finazzi G, Endler A, Willig A, Baerenfaller K, Grossmann J, Gerrits B, Rutishauser D, Gruissem W, Rochaix JD, Baginsky S** (2011) Comparative phosphoproteome profiling reveals a function of the STN8 kinase in fine-tuning of cyclic electron flow (CEF). *Proc Natl Acad Sci U S A* **108**: 12955-12960
- Reiland S, Messerli G, Baerenfaller K, Gerrits B, Endler A, Grossmann J, Gruissem W, Baginsky S** (2009) Large-scale Arabidopsis phosphoproteome profiling reveals novel chloroplast kinase substrates and phosphorylation networks. *Plant Physiol* **150**: 889-903
- Reumann S, Quan S, Aung K, Yang P, Manandhar-Shrestha K, Holbrook D, Linka N, Switzenberg R, Wilkerson CG, Weber AP, Olsen LJ, Hu J** (2009) In-depth proteome analysis of Arabidopsis leaf peroxisomes combined with in vivo subcellular targeting verification indicates novel metabolic and regulatory functions of peroxisomes. *Plant Physiol* **150**: 125-143

- Reusch RN** (1989) Poly-beta-hydroxybutyrate/calcium polyphosphate complexes in eukaryotic membranes. *Proc Soc Exp Biol Med* **191**: 377-381
- Reusch RN, Huang R, Bramble LL** (1995) Poly-3-hydroxybutyrate/polyphosphate complexes form voltage-activated Ca<sup>2+</sup> channels in the plasma membranes of *Escherichia coli*. *Biophys J* **69**: 754-766
- Rigden DJ, Woodhead DD, Wong PW, Galperin MY** (2011) New Structural and Functional Contexts of the Dx[DN]xDG Linear Motif: Insights into Evolution of Calcium-Binding Proteins. *PLoS One* **6**: e21507
- Robinson AJ, Kunji ER** (2006) Mitochondrial carriers in the cytoplasmic state have a common substrate binding site. *Proc Natl Acad Sci U S A* **103**: 2617-2622
- Robinson SJ, Tang LH, Mooney BA, McKay SJ, Clarke WE, Links MG, Karcz S, Regan S, Wu YY, Gruber MY, Cui D, Yu M, Parkin IA** (2009) An archived activation tagged population of *Arabidopsis thaliana* to facilitate forward genetics approaches. *BMC Plant Biol* **9**: 101
- Rochaix JD** (2007) Role of thylakoid protein kinases in photosynthetic acclimation. *FEBS Lett* **581**: 2768-2775
- Roh MH, Shingles R, Cleveland MJ, McCarty RE** (1998) Direct measurement of calcium transport across chloroplast inner-envelope vesicles. *Plant Physiol* **118**: 1447-1454
- Romeis T, Ludwig AA, Martin R, Jones JD** (2001) Calcium-dependent protein kinases play an essential role in a plant defence response. *EMBO J* **20**: 5556-5567
- Rosch JW, Sublett J, Gao G, Wang YD, Tuomanen EI** (2008) Calcium efflux is essential for bacterial survival in the eukaryotic host. *Mol Microbiol* **70**: 435-444
- Rossi AE, Dirksen RT** (2006) Sarcoplasmic reticulum: the dynamic calcium governor of muscle. *Muscle Nerve* **33**: 715-731
- Sachs F** (2010) Stretch-activated ion channels: what are they? *Physiology (Bethesda)* **25**: 50-56
- Sai J, Johnson CH** (2002) Dark-stimulated calcium ion fluxes in the chloroplast stroma and cytosol. *Plant Cell* **14**: 1279-1291
- Sakamoto W, Zaltsman A, Adam Z, Takahashi Y** (2003) Coordinated regulation and complex formation of yellow variegated1 and yellow variegated2, chloroplastic FtsH metalloproteases involved in the repair cycle of photosystem II in *Arabidopsis* thylakoid membranes. *Plant Cell* **15**: 2843-2855
- Sanders D, Pelloux J, Brownlee C, Harper JF** (2002) Calcium at the crossroads of signaling. *Plant Cell* **14 Suppl**: S401-417
- Sato M, Takahashi K, Ochiai Y, Hosaka T, Ochi K, Nabeta K** (2009) Bacterial alarmone, guanosine 5'-diphosphate 3'-diphosphate (ppGpp), predominantly binds the beta' subunit of plastid-encoded plastid RNA polymerase in chloroplasts. *Chembiochem* **10**: 1227-1233
- Schattat M, Barton K, Baudisch B, Klosgen RB, Mathur J** (2011) Plastid stromule branching coincides with contiguous endoplasmic reticulum dynamics. *Plant Physiol* **155**: 1667-1677
- Schattat M, Barton K, Mathur J** (2011) Correlated behavior implicates stromules in increasing the interactive surface between plastids and ER tubules. *Plant Signal Behav* **6**: 715-718
- Schiott M, Romanowsky SM, Baekgaard L, Jakobsen MK, Palmgren MG, Harper JF** (2004) A plant plasma membrane Ca<sup>2+</sup> pump is required for normal pollen tube growth and fertilization. *Proc Natl Acad Sci U S A* **101**: 9502-9507
- Schleiff E, Soll J, Kuchler M, Kuhlbrandt W, Harrer R** (2003) Characterization of the translocon of the outer envelope of chloroplasts. *J Cell Biol* **160**: 541-551
- Schliebner I, Pribil M, Zuhlke J, Dietzmann A, Leister D** (2008) A Survey of Chloroplast Protein Kinases and Phosphatases in *Arabidopsis thaliana*. *Curr Genomics* **9**: 184-190
- Schroers A, Burkovski A, Wohlrab H, Kramer R** (1998) The phosphate carrier from yeast mitochondria. Dimerization is a prerequisite for function. *J Biol Chem* **273**: 14269-14276
- Schwacke R, Schneider A, van der Graaff E, Fischer K, Catoni E, Desimone M, Frommer WB, Flugge UI, Kunze R** (2003) ARAMEMNON, a novel database for *Arabidopsis* integral membrane proteins. *Plant Physiol* **131**: 16-26
- Schweer J, Turkeri H, Link B, Link G** (2010) AtSIG6, a plastid sigma factor from *Arabidopsis*, reveals functional impact of cpCK2 phosphorylation. *Plant J* **62**: 192-202
- Sedbrook JC, Kronebusch PJ, Borisy GG, Trewavas AJ, Masson PH** (1996) Transgenic AEQUORIN reveals organ-specific cytosolic Ca<sup>2+</sup> responses to anoxia and *Arabidopsis thaliana* seedlings. *Plant Physiol* **111**: 243-257
- Seigneurin-Berny D, Gravot A, Auroy P, Mazard C, Kraut A, Finazzi G, Grunwald D, Rappaport F, Vavasseur A, Joyard J, Richaud P, Rolland N** (2006) HMA1, a new Cu-ATPase of the chloroplast envelope, is essential for growth under adverse light conditions. *J Biol Chem* **281**: 2882-2892

- Seigneurin-Berny D, Salvi D, Joyard J, Rolland N** (2008) Purification of intact chloroplasts from Arabidopsis and spinach leaves by isopycnic centrifugation. *Curr Protoc Cell Biol* **Chapter 3**: Unit 3 30
- Shen G, Koppu S, Venkataramani S, Wang J, Yan J, Qiu X, Zhang H** (2010) ANKYRIN REPEAT-CONTAINING PROTEIN 2A is an essential molecular chaperone for peroxisomal membrane-bound ASCORBATE PEROXIDASE3 in Arabidopsis. *Plant Cell* **22**: 811-831
- Shi J, Kim KN, Ritz O, Albrecht V, Gupta R, Harter K, Luan S, Kudla J** (1999) Novel protein kinases associated with calcineurin B-like calcium sensors in Arabidopsis. *Plant Cell* **11**: 2393-2405
- Shi Y, Zhao W, Zhang W, Ye Z, Zhao J** (2006) Regulation of intracellular free calcium concentration during heterocyst differentiation by HetR and NtcA in *Anabaena* sp. PCC 7120. *Proc Natl Acad Sci U S A* **103**: 11334-11339
- Shigaki T, Rees I, Nakhleh L, Hirschi KD** (2006) Identification of three distinct phylogenetic groups of CAX cation/proton antiporters. *J Mol Evol* **63**: 815-825
- Sieberer BJ, Chabaud M, Timmers AC, Monin A, Fournier J, Barker DG** (2009) A nuclear-targetedameleon demonstrates intranuclear Ca<sup>2+</sup> spiking in *Medicago truncatula* root hairs in response to rhizobial nodulation factors. *Plant Physiol* **151**: 1197-1206
- Silva MA, Carnieri EG, Vercesi AE** (1992) Calcium transport by corn mitochondria : evaluation of the role of phosphate. *Plant Physiol* **98**: 452-457
- Snyders S, Kohorn BD** (1999) TAKs, thylakoid membrane protein kinases associated with energy transduction. *J Biol Chem* **274**: 9137-9140
- Sommer MS, Daum B, Gross LE, Weis BL, Mirus O, Abram L, Maier UG, Kuhlbrandt W, Schleiff E** (2011) Chloroplast Omp85 proteins change orientation during evolution. *Proc Natl Acad Sci U S A* **108**: 13841-13846
- Stael S, Bayer RG, Mehler N, Teige M** (2011) Protein N-acylation overrides differing targeting signals. *FEBS Lett* **585**: 517-522
- Starkov AA** (2010) The molecular identity of the mitochondrial Ca<sup>2+</sup> sequestration system. *FEBS J* **277**: 3652-3663
- Stephens NR, Qi Z, Spalding EP** (2008) Glutamate receptor subtypes evidenced by differences in desensitization and dependence on the GLR3.3 and GLR3.4 genes. *Plant Physiol* **146**: 529-538
- Storey R, Leigh RA** (2004) Processes modulating calcium distribution in citrus leaves. An investigation using x-ray microanalysis with strontium as a tracer. *Plant Physiol* **136**: 3838-3848
- Subbaiah CC, Bush DS, Sachs MM** (1994) Elevation of cytosolic calcium precedes anoxic gene expression in maize suspension-cultured cells. *Plant Cell* **6**: 1747-1762
- Subbaiah CC, Bush DS, Sachs MM** (1998) Mitochondrial contribution to the anoxic Ca<sup>2+</sup> signal in maize suspension-cultured cells. *Plant Physiol* **118**: 759-771
- Sulpice R, Trenkamp S, Steinfath M, Usadel B, Gibon Y, Witucka-Wall H, Pyl ET, Tschoep H, Steinhäuser MC, Guenther M, Hoehne M, Rohwer JM, Altmann T, Fernie AR, Stitt M** (2010) Network analysis of enzyme activities and metabolite levels and their relationship to biomass in a large panel of Arabidopsis accessions. *Plant Cell* **22**: 2872-2893
- Sundberg E, Slaughter JG, Fridborg I, Cleary SP, Robinson C, Coupland G** (1997) ALBINO3, an Arabidopsis nuclear gene essential for chloroplast differentiation, encodes a chloroplast protein that shows homology to proteins present in bacterial membranes and yeast mitochondria. *Plant Cell* **9**: 717-730
- Szabadkai G, Duchen MR** (2008) Mitochondria: the hub of cellular Ca<sup>2+</sup> signaling. *Physiology (Bethesda)* **23**: 84-94
- Takahashi H, Watanabe A, Tanaka A, Hashida SN, Kawai-Yamada M, Sonoike K, Uchimiya H** (2006) Chloroplast NAD kinase is essential for energy transduction through the xanthophyll cycle in photosynthesis. *Plant Cell Physiol* **47**: 1678-1682
- Takahashi K, Kasai K, Ochi K** (2004) Identification of the bacterial alarmone guanosine 5'-diphosphate 3'-diphosphate (ppGpp) in plants. *Proc Natl Acad Sci U S A* **101**: 4320-4324
- Tikkanen M, Aro EM** (2011) Thylakoid protein phosphorylation in dynamic regulation of photosystem II in higher plants. *Biochim Biophys Acta*
- Tikkanen M, Grieco M, Kangasjarvi S, Aro EM** (2010) Thylakoid protein phosphorylation in higher plant chloroplasts optimizes electron transfer under fluctuating light. *Plant Physiol* **152**: 723-735
- Tikkanen M, Nurmi M, Kangasjarvi S, Aro EM** (2008) Core protein phosphorylation facilitates the repair of photodamaged photosystem II at high light. *Biochim Biophys Acta* **1777**: 1432-1437
- Tiwari BS, Belenghi B, Levine A** (2002) Oxidative stress increased respiration and generation of reactive oxygen species, resulting in ATP depletion, opening of mitochondrial permeability transition, and programmed cell death. *Plant Physiol* **128**: 1271-1281

- Tlalka M, Fricker M** (1999) The role of calcium in blue-light-dependent chloroplast movement in *lemna trisulca* L. *Plant J* **20**: 461-473
- Torrecilla I, Leganes F, Bonilla I, Fernandez-Pinas F** (2000) Use of recombinant aequorin to study calcium homeostasis and monitor calcium transients in response to heat and cold shock in cyanobacteria. *Plant Physiol* **123**: 161-176
- Torrecilla I, Leganes F, Bonilla I, Fernandez-Pinas F** (2004) A calcium signal is involved in heterocyst differentiation in the cyanobacterium *Anabaena* sp. PCC7120. *Microbiology* **150**: 3731-3739
- Torrecilla I, Leganes F, Bonilla I, Fernández-Piñas F** (2001) Calcium transients in response to salinity and osmotic stress in the nitrogen-fixing cyanobacterium *Anabaena* sp. PCC7120 expressing cytosolic apoaequorin. *Plant Cell and Environment* **24**: 641-648
- Tozawa Y, Nozawa A, Kanno T, Narisawa T, Masuda S, Kasai K, Nanamiya H** (2007) Calcium-activated (p)ppGpp synthetase in chloroplasts of land plants. *J Biol Chem* **282**: 35536-35545
- Traba J, Froschauer EM, Wiesenberger G, Satrustegui J, Del Arco A** (2008) Yeast mitochondria import ATP through the calcium-dependent ATP-Mg/Pi carrier Sal1p, and are ATP consumers during aerobic growth in glucose. *Mol Microbiol* **69**: 570-585
- Traba J, Satrustegui J, del Arco A** (2009) Transport of adenine nucleotides in the mitochondria of *Saccharomyces cerevisiae*: interactions between the ADP/ATP carriers and the ATP-Mg/Pi carrier. *Mitochondrion* **9**: 79-85
- Trenker M, Malli R, Fertschai I, Levak-Frank S, Graier WF** (2007) Uncoupling proteins 2 and 3 are fundamental for mitochondrial Ca<sup>2+</sup> uniport. *Nat Cell Biol* **9**: 445-452
- Turano FJ, Thakkar SS, Fang T, Weisemann JM** (1997) Characterization and expression of NAD(H)-dependent glutamate dehydrogenase genes in *Arabidopsis*. *Plant Physiol* **113**: 1329-1341
- Turner WL, Waller JC, Vanderbeld B, Snedden WA** (2004) Cloning and characterization of two NAD kinases from *Arabidopsis*. identification of a calmodulin binding isoform. *Plant Physiol* **135**: 1243-1255
- Urquhart W, Gunawardena AH, Moeder W, Ali R, Berkowitz GA, Yoshioka K** (2007) The chimeric cyclic nucleotide-gated ion channel ATCNGC11/12 constitutively induces programmed cell death in a Ca<sup>2+</sup> dependent manner. *Plant Mol Biol* **65**: 747-761
- Vainonen JP, Sakuragi Y, Stael S, Tikkanen M, Allahverdiyeva Y, Paakkarinen V, Aro E, Suorsa M, Scheller HV, Vener AV, Aro EM** (2008) Light regulation of CaS, a novel phosphoprotein in the thylakoid membrane of *Arabidopsis thaliana*. *FEBS J* **275**: 1767-1777
- Van Aken O, Zhang B, Carrie C, Uggalla V, Paynter E, Giraud E, Whelan J** (2009) Defining the mitochondrial stress response in *Arabidopsis thaliana*. *Mol Plant* **2**: 1310-1324
- van Der Luit AH, Olivari C, Haley A, Knight MR, Trewavas AJ** (1999) Distinct calcium signaling pathways regulate calmodulin gene expression in tobacco. *Plant Physiol* **121**: 705-714
- van der Zand A, Braakman I, Tabak HF** (2010) Peroxisomal membrane proteins insert into the endoplasmic reticulum. *Mol Biol Cell* **21**: 2057-2065
- Virolainen E, Blokhina O, Fagerstedt K** (2002) Ca(2+)-induced high amplitude swelling and cytochrome c release from wheat (*Triticum aestivum* L.) mitochondria under anoxic stress. *Ann Bot* **90**: 509-516
- von Zychlinski A, Kleffmann T, Krishnamurthy N, Sjolander K, Baginsky S, Gruissem W** (2005) Proteome analysis of the rice etioplast: metabolic and regulatory networks and novel protein functions. *Mol Cell Proteomics* **4**: 1072-1084
- Vothknecht U.C. WRDaKCG** (1995) Sinefungin inhibits chlorophyll synthesis by blocking the S-adenosylmethionine : Mg-Protoporphyrin IX O-methyltransferase in greening barley leaves. *Plant Physiology and Biochemistry* **33**: 759-763
- Waditee R, Hossain GS, Tanaka Y, Nakamura T, Shikata M, Takano J, Takabe T, Takabe T** (2004) Isolation and functional characterization of Ca<sup>2+</sup>/H<sup>+</sup> antiporters from cyanobacteria. *J Biol Chem* **279**: 4330-4338
- Waller JC, Dhanoa PK, Schumann U, Mullen RT, Snedden WA** (2010) Subcellular and tissue localization of NAD kinases from *Arabidopsis*: compartmentalization of de novo NADP biosynthesis. *Planta* **231**: 305-317
- Walter A, Mazars C, Maitrejean M, Hopke J, Ranjeva R, Boland W, Mithofer A** (2007) Structural requirements of jasmonates and synthetic analogues as inducers of Ca<sup>2+</sup> signals in the nucleus and the cytosol of plant cells. *Angew Chem Int Ed Engl* **46**: 4783-4785
- Wang D, Xu Y, Li Q, Hao X, Cui K, Sun F, Zhu Y** (2003) Transgenic expression of a putative calcium transporter affects the time of *Arabidopsis* flowering. *Plant J* **33**: 285-292
- Wang SL, Fan KQ, Yang X, Lin ZX, Xu XP, Yang KQ** (2008) CabC, an EF-hand calcium-binding protein, is involved in Ca<sup>2+</sup>-mediated regulation of spore germination and aerial hypha formation in *Streptomyces coelicolor*. *J Bacteriol* **190**: 4061-4068

- Wang Y, Zhu Y, Ling Y, Zhang H, Liu P, Baluska F, Samaj J, Lin J, Wang Q** (2010) Disruption of actin filaments induces mitochondrial  $\text{Ca}^{2+}$  release to the cytoplasm and  $[\text{Ca}^{2+}]_c$  changes in Arabidopsis root hairs. *BMC Plant Biol* **10**: 53
- Weber AP, Fischer K** (2007) Making the connections--the crucial role of metabolite transporters at the interface between chloroplast and cytosol. *FEBS Lett* **581**: 2215-2222
- Weinl S, Held K, Schlucking K, Steinhorst L, Kuhlert S, Hippler M, Kudla J** (2008) A plastid protein crucial for  $\text{Ca}^{2+}$ -regulated stomatal responses. *New Phytol* **179**: 675-686
- Weinl S, Kudla J** (2009) The CBL-CIPK  $\text{Ca}^{2+}$ -decoding signaling network: function and perspectives. *New Phytol* **184**: 517-528
- Weinl S, Kudla J** (2009) The CBL-CIPK  $\text{Ca}^{2+}$ -decoding signaling network: function and perspectives. *New Phytol* **184**: 517-528
- Wessel D, Flugge UI** (1984) A method for the quantitative recovery of protein in dilute solution in the presence of detergents and lipids. *Anal Biochem* **138**: 141-143
- Westphal S, Soll J, Voithknecht UC** (2001) A vesicle transport system inside chloroplasts. *FEBS Lett* **506**: 257-261
- Westphal S, Soll J, Voithknecht UC** (2003) Evolution of chloroplast vesicle transport. *Plant Cell Physiol* **44**: 217-222
- Wheeler GL, Brownlee C** (2008)  $\text{Ca}^{2+}$  signalling in plants and green algae--changing channels. *Trends Plant Sci* **13**: 506-514
- Williams LE, Lemoine R, Sauer N** (2000) Sugar transporters in higher plants--a diversity of roles and complex regulation. *Trends Plant Sci* **5**: 283-290
- Wilson ME, Jensen GS, Haswell ES** (2011) Two Mechanosensitive Channel Homologs Influence Division Ring Placement in Arabidopsis Chloroplasts. *Plant Cell*
- Wohlrab H** (2010) Homodimeric intrinsic membrane proteins. Identification and modulation of interactions between mitochondrial transporter (carrier) subunits. *Biochem Biophys Res Commun* **393**: 746-750
- Woody ST, Austin-Phillips S, Amasino RM, Krysan PJ** (2007) The WiscDsLox T-DNA collection: an arabidopsis community resource generated by using an improved high-throughput T-DNA sequencing pipeline. *J Plant Res* **120**: 157-165
- Wu SJ, Ding L, Zhu JK** (1996) SOS1, a Genetic Locus Essential for Salt Tolerance and Potassium Acquisition. *Plant Cell* **8**: 617-627
- Wurzinger B, Mair A, Pfister B, Teige M** (2011) Cross-talk of calcium-dependent protein kinase and MAP kinase signaling. *Plant Signal Behav* **6**: 8-12
- Xi C, Schoeters E, Vanderleyden J, Michiels J** (2000) Symbiosis-specific expression of Rhizobium etli casA encoding a secreted calmodulin-related protein. *Proc Natl Acad Sci U S A* **97**: 11114-11119
- Xiong TC, Coursol S, Grat S, Ranjeva R, Mazars C** (2008) Sphingolipid metabolites selectively elicit increases in nuclear calcium concentration in cell suspension cultures and in isolated nuclei of tobacco. *Cell Calcium* **43**: 29-37
- Xiong TC, Jauneau A, Ranjeva R, Mazars C** (2004) Isolated plant nuclei as mechanical and thermal sensors involved in calcium signalling. *Plant J* **40**: 12-21
- Yamaguchi T, Aharon GS, Sottosanto JB, Blumwald E** (2005) Vacuolar  $\text{Na}^+/\text{H}^+$  antiporter cation selectivity is regulated by calmodulin from within the vacuole in a  $\text{Ca}^{2+}$ - and pH-dependent manner. *Proc Natl Acad Sci U S A* **102**: 16107-16112
- Yang T, Poovaiah BW** (2000) Arabidopsis chloroplast chaperonin 10 is a calmodulin-binding protein. *Biochem Biophys Res Commun* **275**: 601-607
- Yang T, Poovaiah BW** (2002) Hydrogen peroxide homeostasis: activation of plant catalase by calcium/calmodulin. *Proc Natl Acad Sci U S A* **99**: 4097-4102
- Yoo SD, Cho YH, Sheen J** (2007) Arabidopsis mesophyll protoplasts: a versatile cell system for transient gene expression analysis. *Nat Protoc* **2**: 1565-1572
- Ytterberg AJ, Peltier JB, van Wijk KJ** (2006) Protein profiling of plastoglobules in chloroplasts and chromoplasts. A surprising site for differential accumulation of metabolic enzymes. *Plant Physiol* **140**: 984-997
- Yuasa K, Maeshima M** (2001) Organ specificity of a vacuolar  $\text{Ca}^{2+}$ -binding protein RVCaB in radish and its expression under  $\text{Ca}^{2+}$ -deficient conditions. *Plant Mol Biol* **47**: 633-640
- Zakharov SD, Ewy RG, Dilley RA** (1993) Subunit III of the chloroplast ATP-synthase can form a  $\text{Ca}^{2+}$ -binding site on the lumenal side of the thylakoid membrane. *FEBS Lett* **336**: 95-99
- Zhang D, Kato Y, Zhang L, Fujimoto M, Tsutsumi N, Sodmergen, Sakamoto W** (2010) The FtsH protease heterocomplex in Arabidopsis: dispensability of type-B protease activity for proper chloroplast development. *Plant Cell* **22**: 3710-3725

- Zhang H, Li X, Zhang Y, Kuppu S, Shen G** (2010) Is AKR2A an essential molecular chaperone for a class of membrane-bound proteins in plants? *Plant Signal Behav* **5**: 1520-1522
- Zhang X, Hu J** (2010) The Arabidopsis chloroplast division protein DYNAMIN-RELATED PROTEIN5B also mediates peroxisome division. *Plant Cell* **22**: 431-442
- Zhao Y, Shi Y, Zhao W, Huang X, Wang D, Brown N, Brand J, Zhao J** (2005) CcbP, a calcium-binding protein from *Anabaena* sp. PCC 7120, provides evidence that calcium ions regulate heterocyst differentiation. *Proc Natl Acad Sci U S A* **102**: 5744-5748
- Zheng M, Beck M, Muller J, Chen T, Wang X, Wang F, Wang Q, Wang Y, Baluska F, Logan DC, Samaj J, Lin J** (2009) Actin turnover is required for myosin-dependent mitochondrial movements in Arabidopsis root hairs. *PLoS One* **4**: e5961
- Zhou Y, Yang W, Kirberger M, Lee HW, Ayalasomayajula G, Yang JJ** (2006) Prediction of EF-hand calcium-binding proteins and analysis of bacterial EF-hand proteins. *Proteins* **65**: 643-655
- Zhu SY, Yu XC, Wang XJ, Zhao R, Li Y, Fan RC, Shang Y, Du SY, Wang XF, Wu FQ, Xu YH, Zhang XY, Zhang DP** (2007) Two calcium-dependent protein kinases, CPK4 and CPK11, regulate abscisic acid signal transduction in Arabidopsis. *Plant Cell* **19**: 3019-3036
- Zimmermann P, Hirsch-Hoffmann M, Hennig L, Gruissem W** (2004) GENEVESTIGATOR. Arabidopsis microarray database and analysis toolbox. *Plant Physiol* **136**: 2621-2632



**6. Supplementary material**

# PROTEOMICS

Supporting Information  
for Proteomics

DOI 10.1002/pmic.201000495

Roman G. Bayer, Simon Stael, Edina Csaszar and Markus Teige  
Mining the soluble chloroplast proteome by affinity chromatography

**FIGURE LEGENDS**

**Supporting Information Figure S1. Saturation curves of ATP/PurB and Eu<sup>3+</sup> runs.** X-axis shows the number of biological replicates. Y-axis shows identified proteins in percentage of all proteins identified with the respective affinity strategy. The number of uniquely identified proteins with consecutive biological samples was added up.

**Supporting Information Figure S2. Comparison of ATP, PurB, and Eu<sup>3+</sup> affinity runs.**

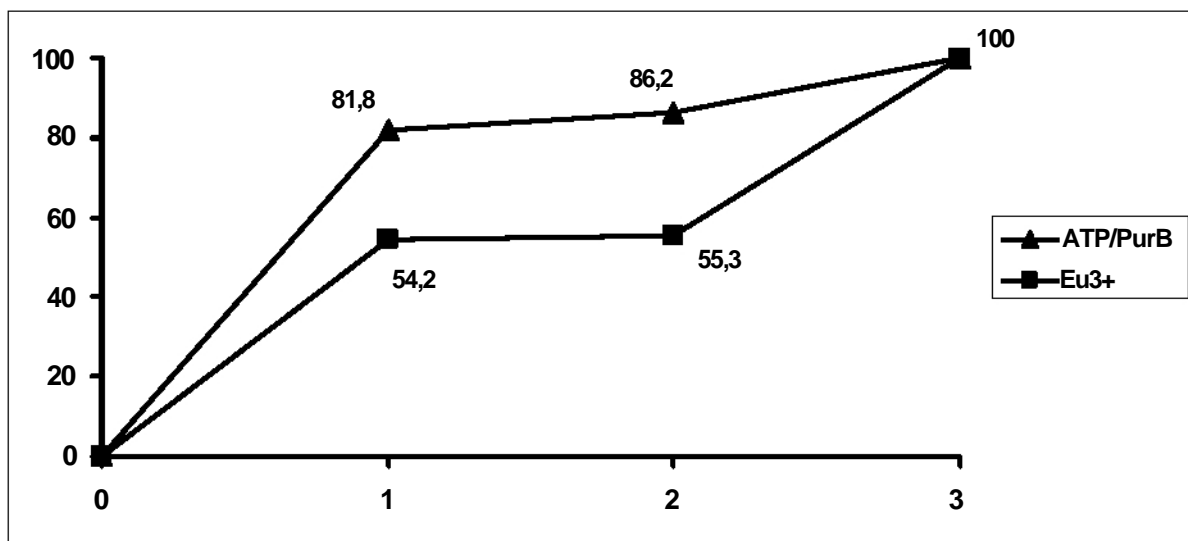
Numbers and overlaps of proteins identified by ATP-, PurB-, and Eu<sup>3+</sup>-affinity chromatography are shown in this Venn diagram.

**Supporting Information Fig. S3. YFP localization of known chloroplast proteins.**

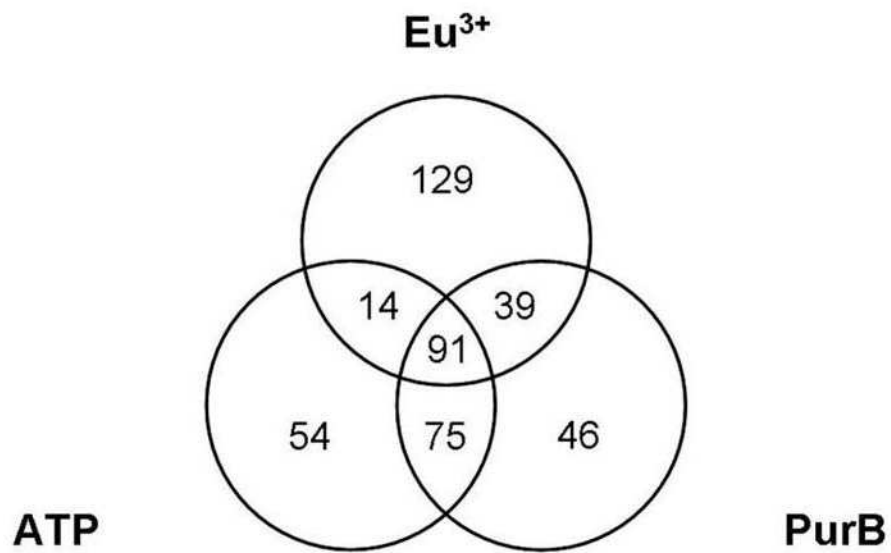
Tobacco leaves expressing ferredoxin-NADP<sup>+</sup> reductase (A) and Rubisco activase (B) fused in front of YFP were analyzed by confocal laser scanning microscopy. Chlorophyll autofluorescence is shown in the first channel and the YFP signal in the second channel. The third channel is a merged image of the previous two plus transmitted light. Bar = 20 μm.

**Tables S1-S3** are too large to be included and can be found at:

<http://onlinelibrary.wiley.com/doi/10.1002/pmic.201000495/supinfo>

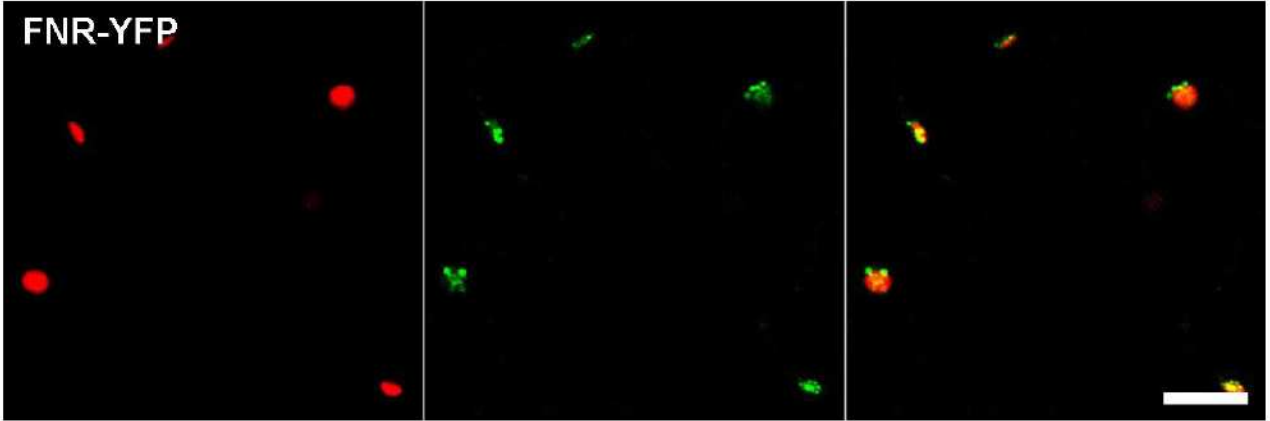
*Bayer et al. suppl. Fig. S1*

*Bayer et al. suppl. Fig. S2*

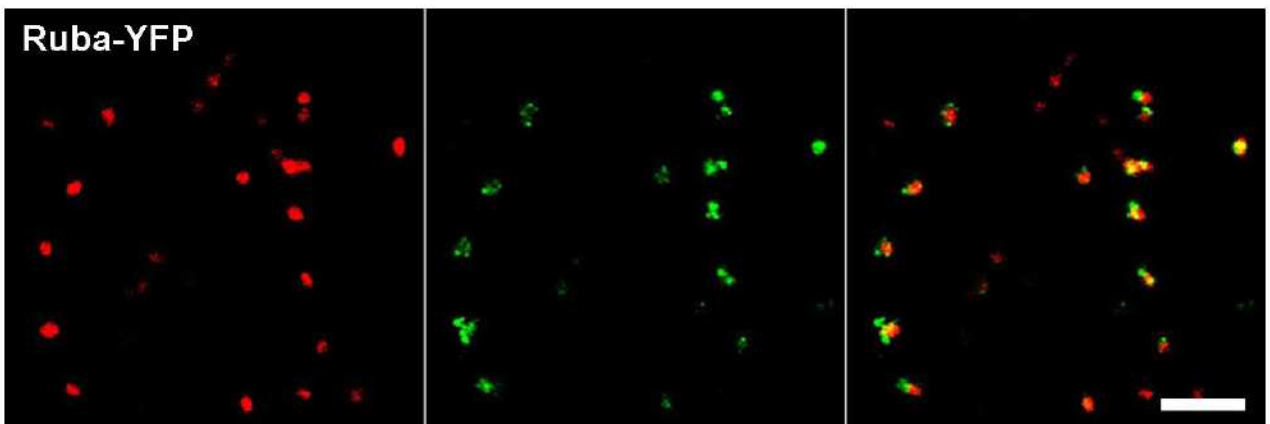


*Bayer et al. suppl. Fig. S3*

**A**



**B**



**FEBS**  
*Letters*journal homepage: [www.FEBSLetters.org](http://www.FEBSLetters.org)

## Protein N-acylation overrides differing targeting signals

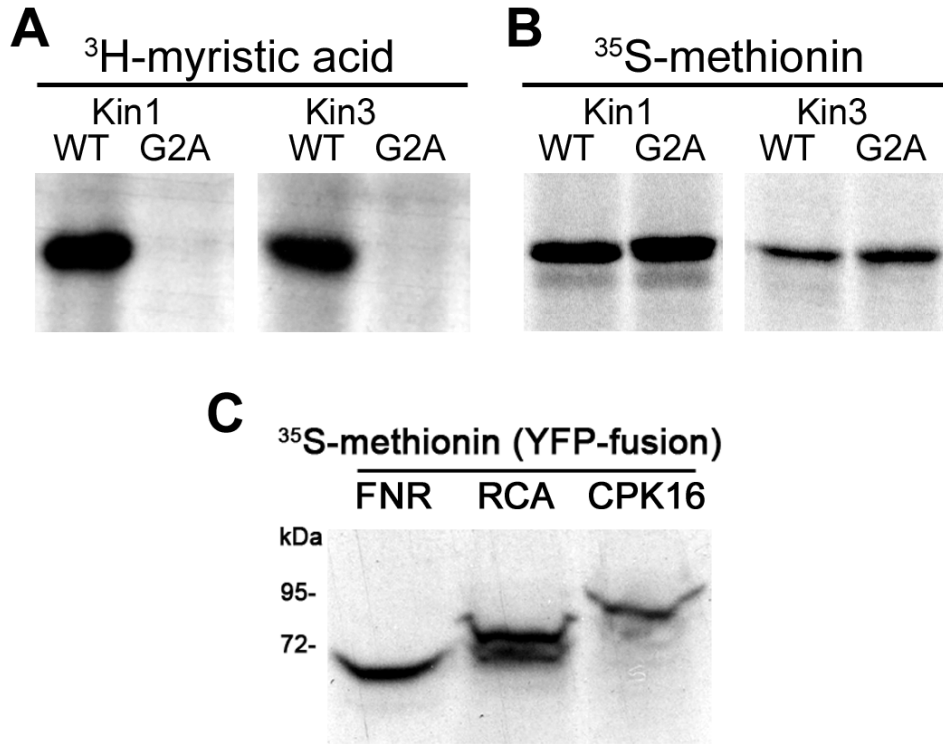
Simon Stael<sup>1</sup>, Roman G. Bayer<sup>1</sup>, Norbert Mehlmer<sup>2</sup>, Markus Teige<sup>\*</sup>*Department of Biochemistry and Cell Biology, MFPL, University of Vienna, Dr. Bohrgasse 9, A-1030 Vienna, Austria*

### Supplemental Figure Legends

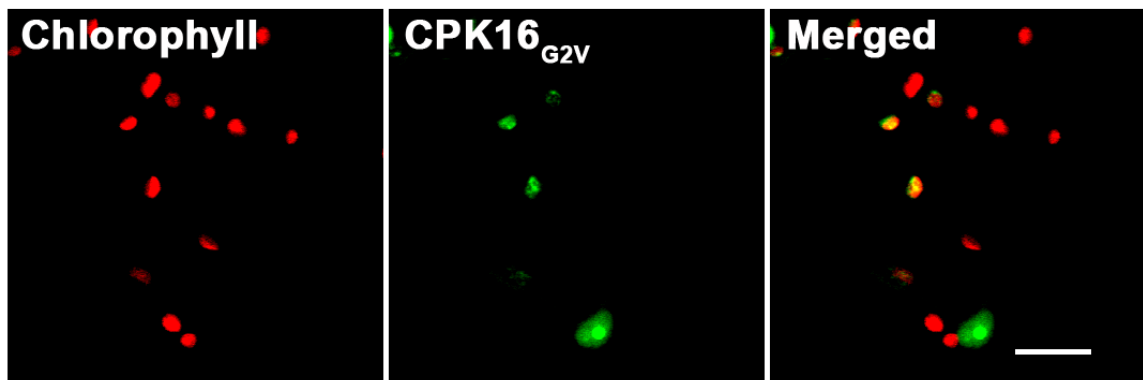
**Suppl. Fig. 1.** *In vitro* translation of predicted chloroplast-localized protein Kinases Kin1 and Kin3, and of the YFP-fusion proteins of FNR, RCA, and CPK16. A) Autoradiograph of *in vitro* myristoylation assays of Kin1 and Kin3 showing incorporation of <sup>3</sup>H-labelled myristic acid in the wild-type (WT), but not in the G2A mutant protein. B) Autoradiograph of the corresponding translation controls using <sup>35</sup>S-methionin. C) Autoradiograph of an *in vitro* translation of YFP-fusion proteins of FNR, RCA, and CPK16 with <sup>35</sup>S-methionin.

**Suppl. Fig. 2.** Localization of the CPK16 G2V mutant in tobacco epidermal leaf cells. Tobacco epidermal leaf cells were infiltrated with agrobacteria and the leaves were analysed two days after infiltration using confocal microscopy. CPK16, green channel; chlorophyll, red channel; scale bar = 20 μm).

*Stael et al. Supplemental figure 1*



*Stael et al. Supplemental figure 2*



**Arabidopsis calcium-binding mitochondrial carrier proteins as potential facilitators of mitochondrial ATP-import and plastid SAM-import**

Simon Stael<sup>1</sup>, Agostinho G. Rocha<sup>2</sup>, Alan J. Robinson<sup>3</sup>, Przemyslaw Kmiecik<sup>1</sup>, Ute C. Vothknecht<sup>2,4</sup>, and Markus Teige<sup>1\*</sup>

**Suppl. Fig. 1.** Multiple sequence alignment of green plant SAMTL proteins. Shown above the alignment are the motifs of the predicted proton-binding site ([ST]), contact points of the binding site ([SHxxR]) and ([RE]) and the salt bridge networks ([Px(D/E)xxK] and [(F/Y)ExxK]).

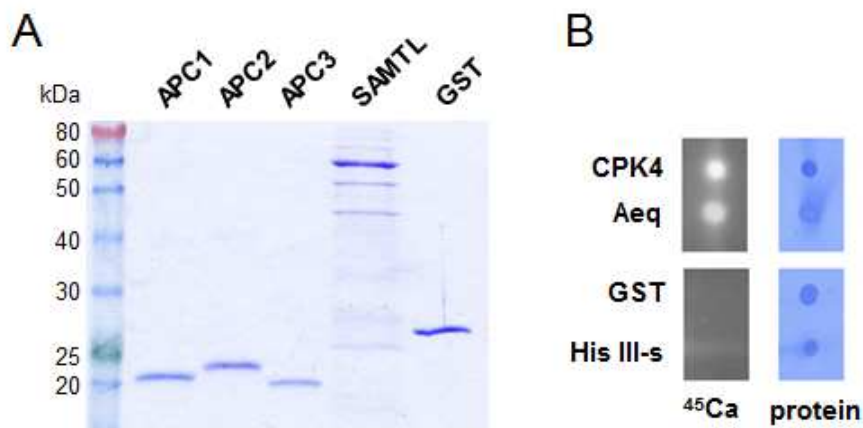
**Suppl. Fig. 2.** Additional controls to the radiolabeled calcium (<sup>45</sup>Ca) overlay assay. **(A)** Coomassie Brilliant Blue stain of an SDS-PAGE gel demonstrates the purity of the purified SAMTL and APC1, 2 and 3 proteins. **(B)** <sup>45</sup>Ca overlay assay displaying calcium-dependent protein kinase 4 (CPK4) and aequorin (Aeq) as positive controls and glutathione *S*-transferase (GST) and histone type III-S (His III-S) as negative controls. GST, like CPK4 and Aeq were purified with the IMPACT™ System (NEB) from *E. coli*. The contamination of any calcium-binding activity from *E. coli* seems unlikely, considering the purity of the protein samples and the lack of <sup>45</sup>Ca signal in the GST sample.



Stael et al. Supplementary figure 1

	555	561	605	613	650	692	704	741	786	798
	[ST]	[PxDxxK]	[SHxxR]	[FExxK]	[PxExxK]	[RE]	[YExxK]	[PxDxxK]	[W]	[YExxK]
A_thaliana	:	-SSSLMRFVDTIP	--SSEGLRTGIFBAS	---	PCEVIF	RE	YASSF	ESIVMS	W	YELAK
V_vinifera	:	-SSLLRFVDTIP	--SSEGLRTGIFBAS	---	PCEVIF	RE	YASSF	ESIVMS	W	YELAK
C_papaya	:	-SSLLRFVDTIP	--SSEGLRTGIFBAS	---	PCEVIF	RE	YASSF	ESIVMS	W	YELAK
R_occumunis	:	-SSSLMRFVDTIP	--SSEGLRTGIFBAS	---	PCEVIF	RE	YASSF	ESIVMS	W	YELAK
M_esculenta	:	-SSAMRFVDTIP	--SSEGLRTGIFBAS	---	PCEVIF	RE	YASSF	ESIVMS	W	YELAK
P_trichocarpa	:	-SSSLMRFVDTIP	--TSEGLRTGIFBATE	---	PCEVIF	RE	YASSF	ESIVMS	W	YELAK
G_max	:	-SSALLRFVDTIP	--SSEGLRTGIFBAS	---	PCEVIF	RE	YASSF	ESIVMS	W	YELAK
M_truncatula	:	-SSALLRFVDSIF	--SSEGLRTGIFBAS	---	PCEVIF	RE	YASSF	ESIVMS	W	YELAK
A_lyrata	:	-SSSLMRFVDTIP	--SSEGLRTGIFBAS	---	PCEVIF	RE	YASSF	ESIVMS	W	YELAK
M_guttatus	:	-SSLLRFVDTIP	--SSEGLRTGIFBAS	---	PCEVIF	RE	YASSF	ESIVMS	W	YELAK
S_bicolor	:	-SSLLRFVDSMF	--SSEGLRTGIFBATE	---	PCEVIF	RE	YASSF	ESIVMS	W	YELAK
Z_mays	:	-SSLLRFVDSMF	--SSEGLRTGIFBAS	---	PCEVIF	RE	YASSF	ESIVMS	W	YELAK
B_distachyon	:	-SSSMLRFVDTMF	--SSEGLRTGIFBAS	---	PCEVIF	RE	YASSF	ESIVMS	W	YELAK
O_nativa	:	-SSSVMRFVDSMF	--SSEGLRTGIFBAS	---	PCEVIF	RE	YASSF	ESIVMS	W	YELAK
S_moellendorffii	:	-SSLLRFVDTLF	--SSEGLRTGIFBAS	---	PCEVIF	RE	YASSF	ESIVMS	W	YELAK
P_patens	:	-TSSMLRFVDTVF	--TSEGLRTGIFBAS	---	PCEVIF	RE	YASSF	ESIVMS	W	YELAK
M_pusilla	:	-SSACMRFVDTLF	--SSEGLRTATVAVV	---	PCEVIF	RE	YASSF	ESIVMS	W	YELAK
O_tauri	:	-TSSMRFVDTLF	--ASEGLRTATVAVV	---	PCEVIF	RE	YASSF	ESIVMS	W	YELAK

Stael et al. Supplementary figure 2



**Stael et al. suppl. Table S1****Suppl. Table 1** NCBI protein accession codes for the MCF proteins used for phylogeny

<b>NCBI accession</b>	<b>protein</b>	<b>annotation</b>	<b>species</b>
NP_568060	AtSAMT1	S-adenosylmethionine carrier 1 AT4G39460	<i>Arabidopsis thaliana</i>
NP_850252	AtSUC	mitochondrial substrate carrier At2g35800	<i>Arabidopsis thaliana</i>
XP_002529704	RcSUC	mitochondrial carrier protein	<i>Ricinus communis</i>
XP_002277407	VvSUC	hypothetical protein	<i>Vitis vinifera</i>
NP_001065524	OsSUC1	Os11g0103700	<i>Oryza sativa Japonica</i>
NP_001065240	OsSUC2	Os12g0103000	<i>Oryza sativa Japonica</i>
XP_002442640	SbSUC	hypothetical protein 08g000350	<i>Sorghum bicolor</i>
XP_001751862	PpSUC1	predicted protein	<i>Physcomitrella patens</i>
XP_001763497	PpSUC2	predicted protein	<i>Physcomitrella patens</i>
XP_002965835	SmSUC	EF-hand protein 20804	<i>Selaginella moellendorffii</i>
XP_003061528	MpSUC	predicted protein	<i>Micromonas pusilla</i>
XP_003082063	OtSUC	putative mitochondrial carrier	<i>Ostreococcus tauri</i>
NP_568940	AtAPC1	Mitochondrial substrate carrier AT5G61810	<i>Arabidopsis thaliana</i>
NP_199918	AtAPC2	Mitochondrial substrate carrier AT5G51050	<i>Arabidopsis thaliana</i>
NP_196349	AtAPC3	Mitochondrial substrate carrier AT5G07320	<i>Arabidopsis thaliana</i>
CBI15774	VvAPC2.1	unnamed protein	<i>Vitis vinifera</i>
XP_002277297	VvAPC2.2	hypothetical protein	<i>Vitis vinifera</i>
EAZ22133	OsAPC2.1	hypothetical protein OsJ_05795	<i>Oryza sativa Japonica</i>
NP_001058018	OsAPC2.2	hypothetical protein Os06g0604500	<i>Oryza sativa Japonica</i>
XP_002437252	SbAPC2	hypothetical protein 10g023640	<i>Sorghum bicolor</i>
XP_001769325	PpAPC2.1	predicted protein	<i>Physcomitrella patens</i>
XP_001777279	PpAPC2.2	predicted protein	<i>Physcomitrella patens</i>
XP_002966208	SmAPC2.1	hypothetical protein	<i>Selaginella moellendorffii</i>
XP_002983817	SmAPC2.2	hypothetical protein	<i>Selaginella moellendorffii</i>
NP_014316	ScSal1p	calcium-binding mitochondrial carrier Sal1	<i>Saccharomyces cerevisiae</i>
NP_037518	HsSCaMC-1	calcium-binding mitochondrial carrier SCaMC-1	<i>Homo sapiens</i>
NP_001006642	HsSCaMC-2	calcium-binding mitochondrial carrier SCaMC-2	<i>Homo sapiens</i>
NP_077008	HsSCaMC-3	calcium-binding mitochondrial carrier SCaMC-3	<i>Homo sapiens</i>

## CROSSTALK BETWEEN CALCIUM SIGNALING AND PROTEIN PHOSPHORYLATION AT THE THYLAKOID

Simon Stael<sup>1</sup>, Agostinho G. Rocha<sup>2</sup>, Terje Wimberger<sup>1</sup>, Dorothea Anrather<sup>3</sup>, Ute C. Vothknecht<sup>2,4</sup> and Markus Teige<sup>1\*</sup>

**Supplementary Table 1.** Overview of all identified calcium dependent phosphorylated proteins and EGTA dependent phosphorylated proteins.

### Calcium

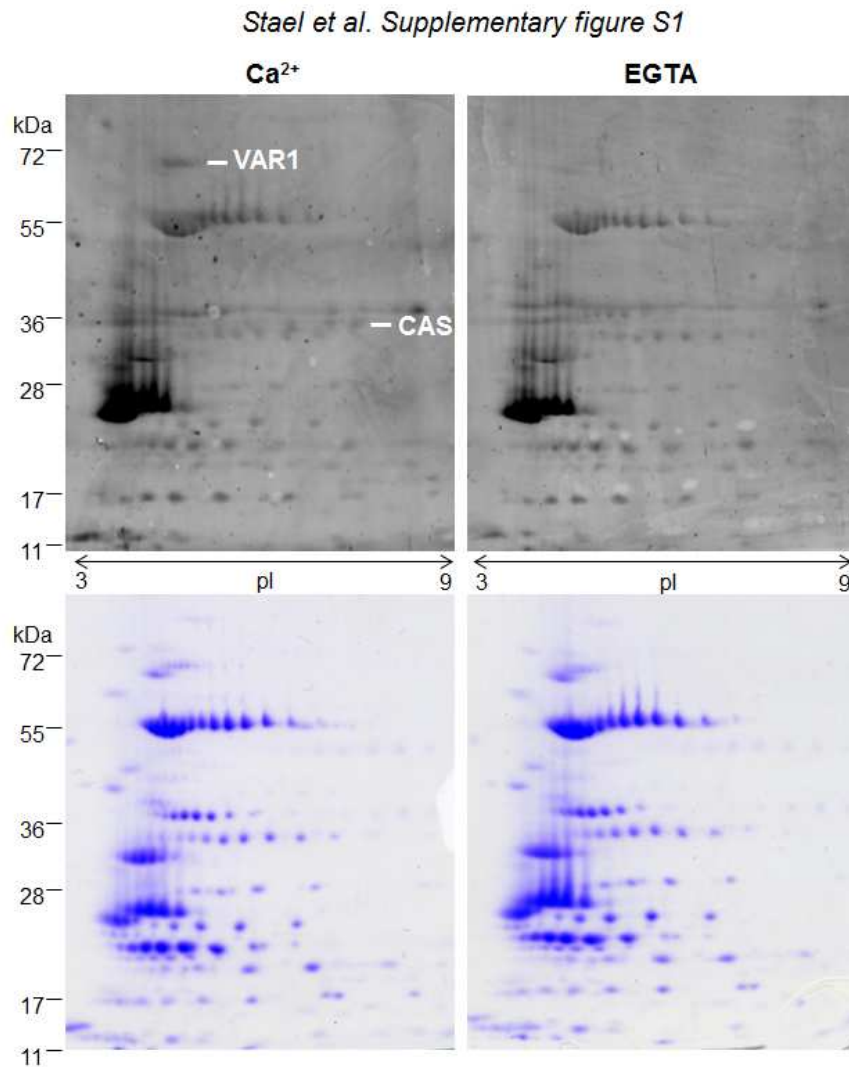
#	ID	AGI code	Description	Species	pro-Q	p-Thr	Phos Phat	Experiment
1	PsaN	At5g64040	Subunit N of photosystem I	At	4	4	y	(3)(4)(5) (6)(7)
2	CAS	At5g23060	'Calcium sensing' protein	Ps/At	2	1	y	(1)(2)(4)
3	VAR1/ VAR2	At5g42270/ At2G30950	Variegated 1 and 2, proteases	FtsH Ps/At	2	0	y/n	(1)(4)
4	PsbP-1	At1g06680	Subunit P-1 of photosystem II	At	1	1	y	(2)(7)
5	PsaH-2	At1g52230	Subunit H-2 of photosystem I	At	1	1	n	(3)(4)
6	PsbO-1	At5g66570	Subunit O-1 of photosystem II	At	0	1	n	7
7	PsbQ-2	At4g05180	Subunit Q-2 of photosystem II	At	0	1	y	3
8	PsbQ-1	At4g21280	Subunit Q-1 of photosystem II	At	0	1	y	3
9	PsaC	AtCg01060	Subunit C of photosystem I	At	0	1	n	7
10	PsaP	At2g46820	Subunit P of photosystem I	At	1	0	y	4
11	ATPF	AtCg00130	ATPase subunit F	At	0	1	n	3
12	PTAC16	At3g46780	Plastid transcriptionally active 16	At	0	1	y	6
13	Unknown1	At4g27700	Cell cycle control phosphatase superfamily	At	0	1	n	7
14	Unknown2	At3g63170	Chalcone-flavanone isomerase family protein	At	0	1	n	7

### EGTA

#	ID	AGI code	Description	Species	pro-Q	p-Thr	Phos Phat	Experiment
1	ATPC1	At4g04640	ATPase subunit gamma	At	1	0	y	4
2	FNR2	At1g20020	ferredoxin:NADP(H) oxidoreductase 2	At	0	1	n	6
3	Unknown3	At2g37660	3-beta hydroxysteroid dehydrogenase /isomerase family protein	At	0	1	y	7
4	PsaG	At1g55670	Subunit G of photosystem I	At	0	1	n	2
5	MFP1	At3g16000	MAR binding filament-like protein 1	At	0	1	y	3

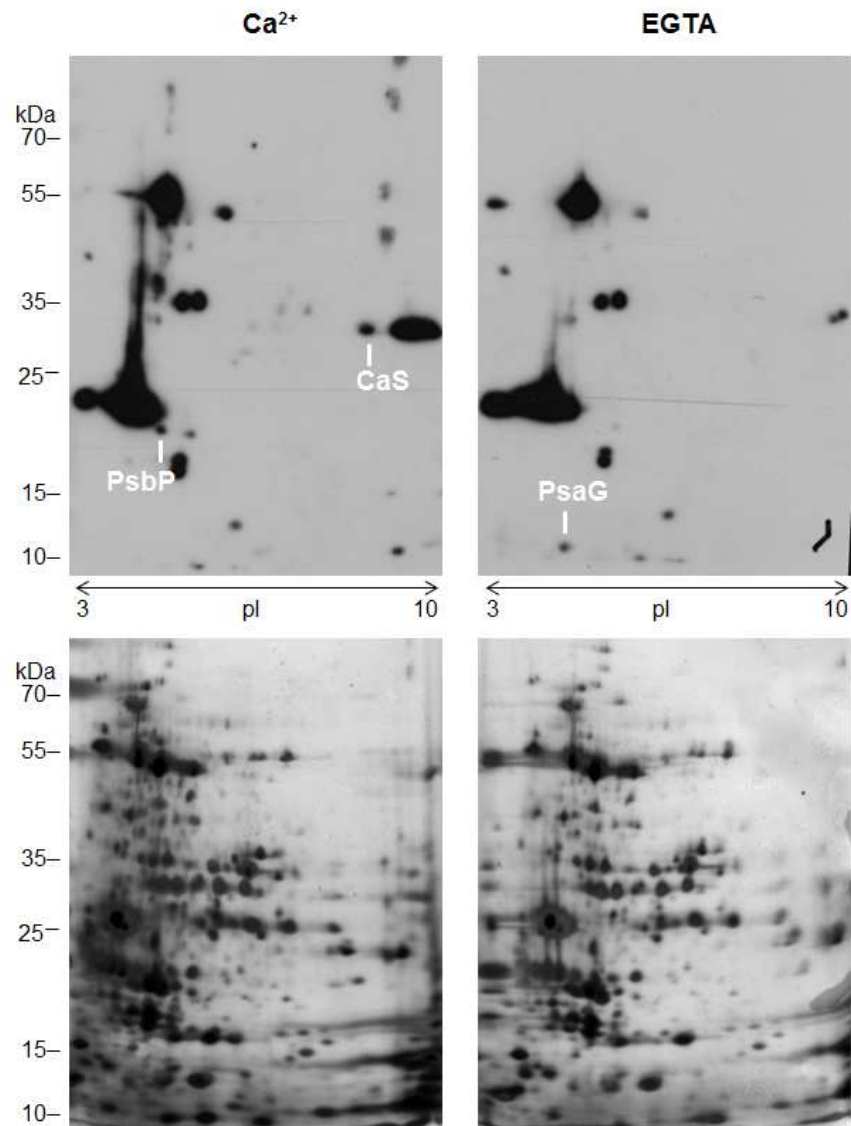
Indicated is in which species the proteins were identified (At = *Arabidopsis thaliana*; Ps = *Pisum sativum*), which stain was used to reveal the phosphorylated proteins (Pro-Q = Pro-Q Diamond phosphoprotein gel stain; pThr = phosphor-Threonine specific antibody), if the protein is included in the phospho-peptide database PhosPhat 3.0 (Heazlewood et al., 2008;

Durek et al., 2010), and in which experiment the protein was identified. Images to the seven experiments are included in the supplementary figures.



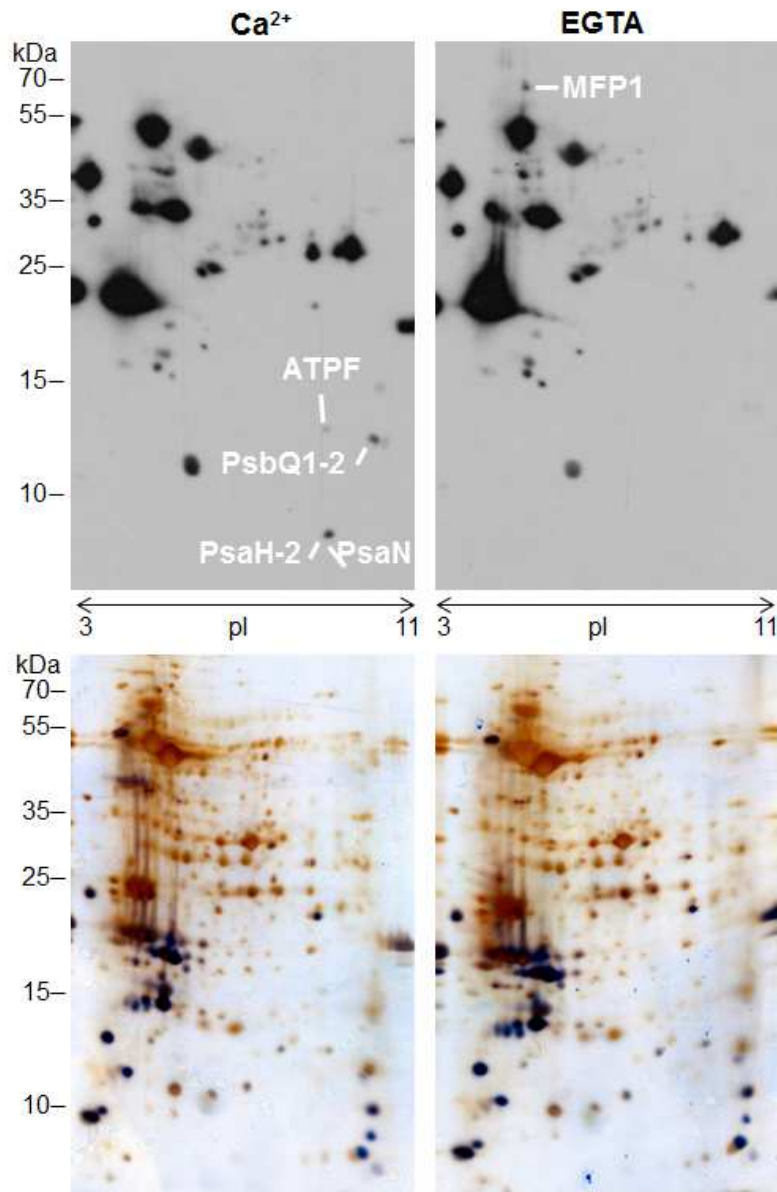
**Suppl. Figure S1 Experiment 1.** Pea thylakoid proteins phosphorylated in the presence of 1 mM Ca<sup>2+</sup> or 1 mM EGTA. Phosphorylated proteins were revealed with Pro-Q Diamond phosphoprotein gel stain and subsequently the gel was stained with CBB. Identified proteins are the FtsH protease, Variegated 1 (VAR1) and ‘Calcium sensing’ protein (CAS).

## Stael et al. Supplementary figure S2



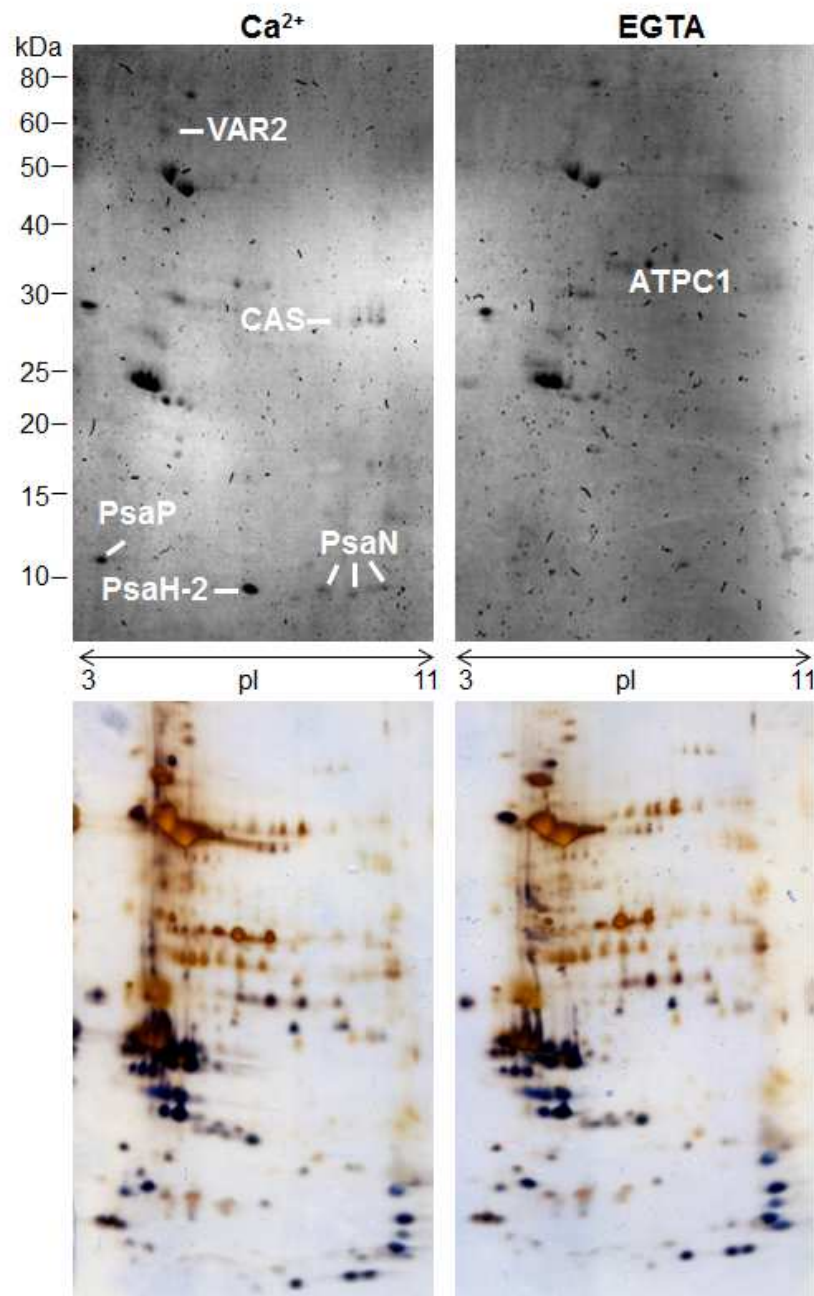
**Suppl. Figure S2 Experiment 2.** Arabidopsis thylakoid proteins phosphorylated in the presence of 250  $\mu\text{M}$   $\text{Ca}^{2+}$  or 250  $\mu\text{M}$  EGTA. Phosphorylated proteins were revealed with a phospho-threonine specific antibody and subsequently the gel was silver-stained. Identified proteins are ‘Calcium sensing’ protein (CAS), subunit P-1 of photosystem II (PsbP-1) and subunit G of photosystem I (PsaG).

## Stael et al. Supplementary figure S3

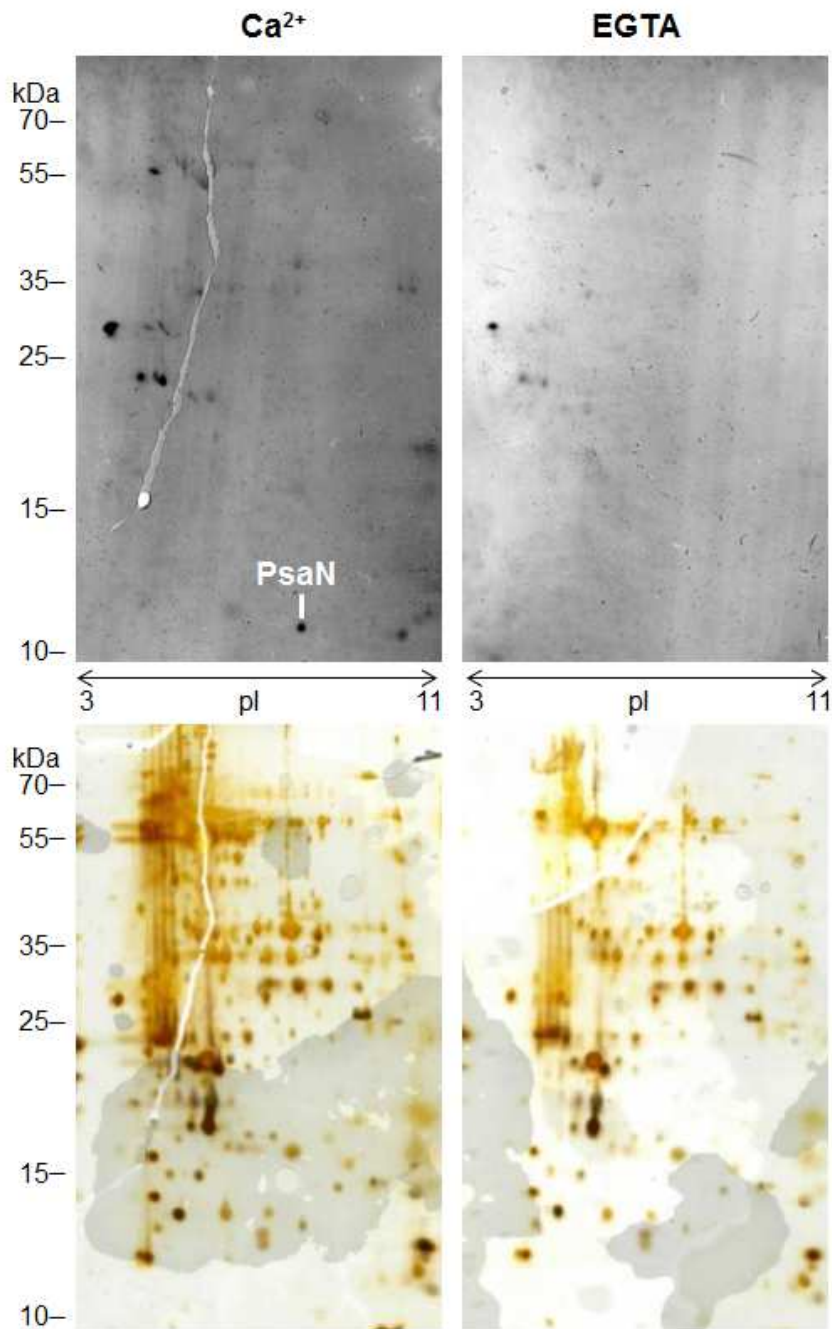


**Suppl. Figure S2 Experiment 3.** Arabidopsis thylakoid proteins phosphorylated in the presence of 250  $\mu\text{M}$   $\text{Ca}^{2+}$  or 250  $\mu\text{M}$  EGTA. Phosphorylated proteins were revealed with a phospho-threonine specific antibody and subsequently the gel was silver-stained. Identified proteins are the ATPase subunit F (ATPF), subunit Q-1 and Q-2 of photosystem II (PsbQ1-2), subunit H-2 of photosystem I (PsaH-2), subunit N of photosystem I (PsaN) and MAR binding filament-like protein 1 (MFP1).

## Stael et al. Supplementary figure S4



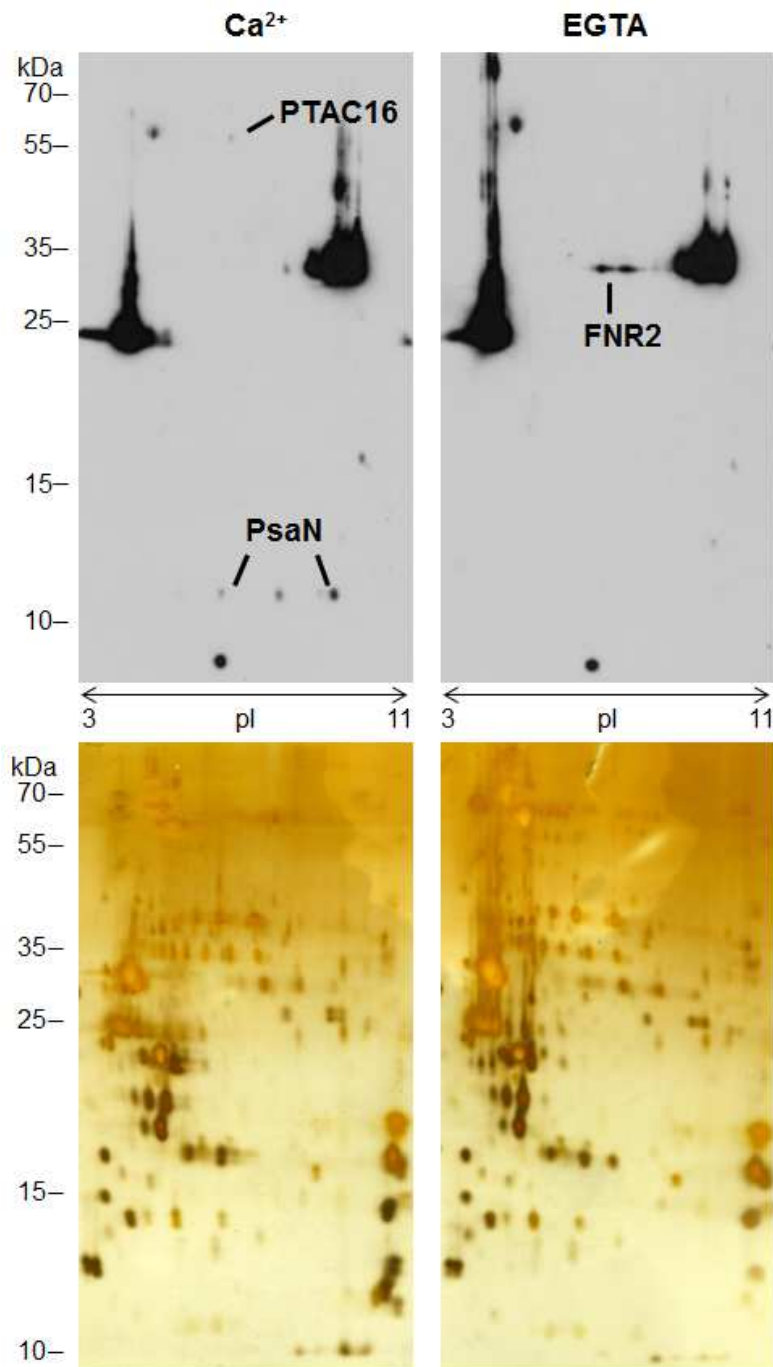
**Suppl. Figure S4 Experiment 4.** Arabidopsis thylakoid proteins phosphorylated in the presence of 250  $\mu\text{M}$   $\text{Ca}^{2+}$  or 250  $\mu\text{M}$  EGTA. Phosphorylated proteins were revealed with a Pro-Q Diamond phosphoprotein gel stain and subsequently the gel was silver-stained. Identified proteins are the FtsH protease, Variegated 2 (VAR2), ‘Calcium sensing’ protein (CAS), subunit H-2 of photosystem I (PsaH-2), subunit N of photosystem I (PsaN; three times identified), subunit P of photosystem I (PsaP) and the ATPase subunit gamma (ATPC1).

*Stael et al. Supplementary figure S5*

**Suppl. Figure S5 Experiment 5.** Arabidopsis thylakoid proteins phosphorylated in the presence of 25  $\mu\text{M}$   $\text{Ca}^{2+}$  or 25  $\mu\text{M}$  EGTA. Phosphorylated proteins were revealed with a Pro-Q Diamond phosphoprotein gel stain and subsequently the gel was silver-stained. The identified protein is subunit N of photosystem I (PsaN).

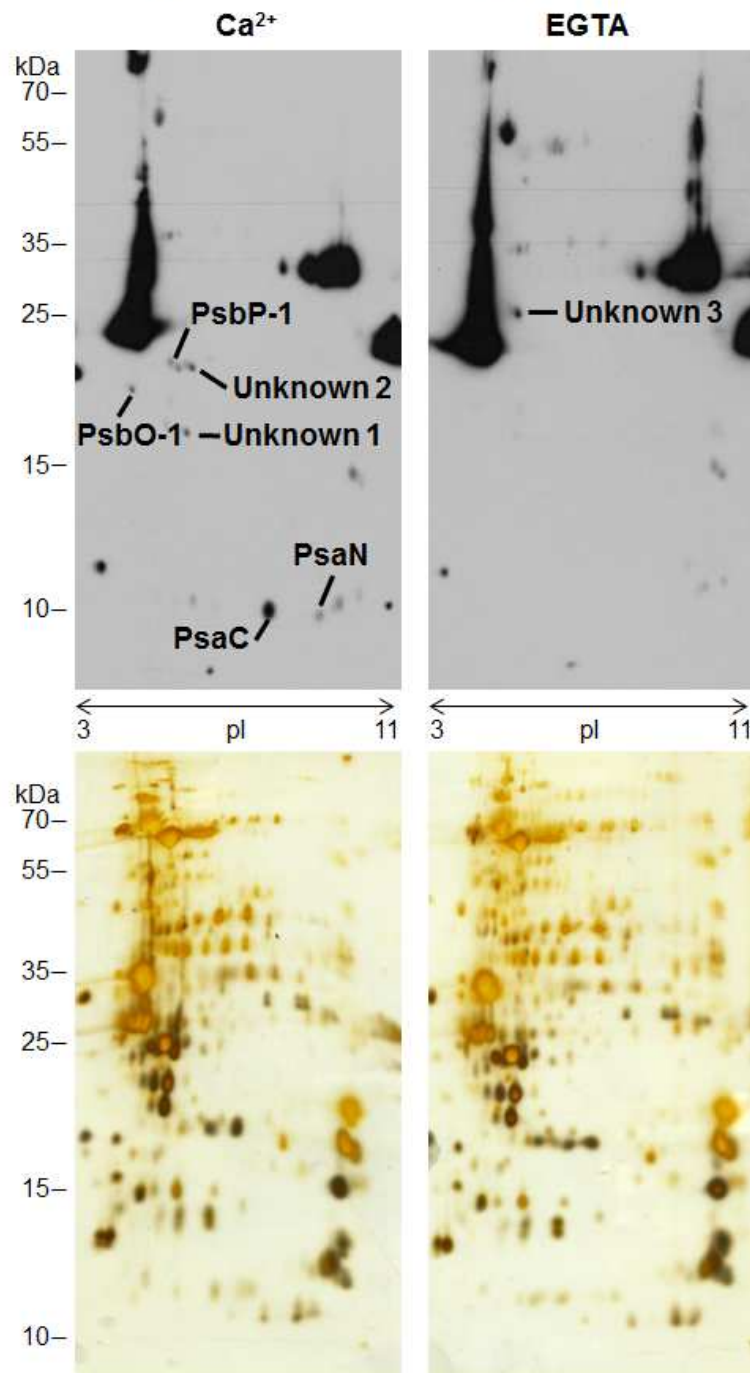


Stael et al. Supplementary figure S6



**Suppl. Figure S6 Experiment 6.** Arabidopsis thylakoid proteins phosphorylated in the presence of 25  $\mu\text{M}$   $\text{Ca}^{2+}$  or 25  $\mu\text{M}$  EGTA. Phosphorylated proteins were revealed with a phospho-threonine specific antibody and subsequently the gel was silver-stained. Identified proteins are Plastid transcriptionally active 16 (PTAC16), subunit N of photosystem I (PsaN; twice identified) and ferredoxin:NADP(H) oxidoreductase 2 (FNR2).

Stael et al. Supplementary figure S7



**Suppl. Figure S7 Experiment 7.** Arabidopsis thylakoid proteins phosphorylated in the presence of 25  $\mu\text{M}$   $\text{Ca}^{2+}$  or 25  $\mu\text{M}$  EGTA. Phosphorylated proteins were revealed with a phospho-threonine specific antibody and subsequently the gel was silver-stained. Identified proteins are subunit P-1 of photosystem II (PsbP-1), subunit O-1 of photosystem II (PsbO-1), subunit C of photosystem I (PsaC), subunit N of photosystem I (PsaN), the cell cycle control phosphatase superfamily protein (Unknown 1), the chalcone-flavanone isomerase family protein (Unknown 2) and the 3-beta hydroxysteroid dehydrogenase /isomerase family protein (Unknown 3).

## ORGANELLAR EF-HAND PROTEIN OF 18 KDA (OEF18) is a novel calcium signalling protein

### Supplementary table 1 – OEF18 toolkit

- **OEF18 T-DNA insertion lines:**

SAIL_123_B11	no KO
SALK_058430C	no KO
WiscDsLox461-464A5	<i>oef18-1</i> (Col-0)
SK40148	<i>oef18-2</i> (Col-4)

- **OEF18 overexpressor lines:**

C1S1-17 (Ca1-Strep)	35S::Ca1-Strep from pBinBasta vector in Col-0
C1GS1-17 (Ca1G2A-Strep)	35S::Ca1G2A-Strep from pBinBasta vector in Col-0
8C1S1-17	inducible Ca1-Strep from pER8 vector in Col-0
C1YFP	35S::Ca1-YFP from pBinBasta vector in Col-0
C1YFP-PR	1000bpPROM::Ca1-YFP from pBinBasta vector in Col-0

- **OEF18 Antibody (also called Ca1N)**

prepared by inoculating recombinant protein of a N-terminal part of OEF18 (first 102 amino acids, by Davids Biotechnology); from rabbit; use 1:500 in TBS-T with 1% milk

## 7. Curriculum vitae

**Simon Lander Stael**

E-mail address [simon.stael@univie.ac.at](mailto:simon.stael@univie.ac.at)

Date of birth 15/11/1985 Place of birth Bruges, Belgium

### EDUCATION

- University of Vienna, Vienna, Austria*  
**Ph.D. in Molecular biology** **2007**  
 Under supervision of Dr. Markus Teige, in Marie-Curie initial training network 'COSI'  
 (Chloroplast signals)
- University of Ghent and University of Turku, Turku, Finland*  
**Master ('Licentiaat') in Biotechnology** **2005**  
 Thesis: "Phosphoprotein CaS is required for efficient protein translocation to thylakoid  
 lumen of plant chloroplasts" under supervision of Prof. Dr. Dominique Van Der Straeten  
 and Prof. Dr. Eva-Mari Aro
- University of Ghent, Ghent, Belgium*  
**Bachelor ('Kandidatuur') in Biology** **2003**

### TEACHING EXPERIENCE

- University of Vienna, Vienna, Austria*  
**Tutor** – "Hefe als Modellorganismus für die Signaltransduktion in  
 eukaryotischen Zellen" – A student practical course **2008-2010**
- University of Vienna, Vienna, Austria*  
**Tutor** – "COSI Workshop II – Mass spectrometry and  
 phosphoproteomics" **2010**  
 Developed syllabus and overall course structure.

### RELATED EXPERIENCE

- Gregor Mendel Institute, Vienna, Austria*  
 "COSI soft skill workshop I – Scientific writing and presentations, project  
 management and grant writing" **2010**
- University of Florida, Gainesville, Florida*  
 "Proteomics Workshop and symposium – Proteomic, Redox and  
 Metabolomic Networks" **2009**
- Ludwig-Maximilians-Universität Munich, Munich, Germany*  
 "COSI workshop I – Functional genomics and bio-imaging" **2009**

### LANGUAGES

- Dutch – native language  
 English – speak fluently and read/write with high proficiency  
 German and French – speak, read, and write with basic competence

## 8. List of publications

- 1) **Stael S**, Rocha AG, Wimberger T, Anrather D, Vothknecht UC, Teige M. Crosstalk between calcium signaling and protein phosphorylation at the thylakoid. **Journal of Experimental Botany** (first submission, 07/10/2011).
- 2) **Stael S**, Rocha AG, Robinson AJ, Kmiecik P, Vothknecht UC, Teige M. Arabidopsis calcium-binding mitochondrial carrier proteins as potential facilitators of mitochondrial ATP-import and plastid SAM-import. **FEBS Lett** (first revision submitted, 07/10/2011)
- 3) **Stael S**, Wurzinger B, Mehlmer N, Vothknecht UC, Teige M. The magical life of calcium as a secondary messenger: A journey to the organelles. **Journal of Experimental Botany** (first revision, 26/09/2011).
- 4) Bayer RG, **Stael S**, Rocha AG, Mair A, Vothknecht UC, Teige M. The mystery of chloroplast-localised protein kinases. **Journal of Experimental Botany** (first revision, 18/09/2011)
- 5) Bayer RG, **Stael S**, Csaszar E, Teige M. Mining the soluble chloroplast proteome by affinity chromatography. **Proteomics**. 2011 Apr. PMID: 21365755.
- 6) **Stael S**, Bayer RG, Mehlmer N, Teige M. Protein N-acylation overrides differing targeting signals. **FEBS Lett**. 2011 Feb 4. PMID: 21219905.
- 7) Mehlmer N, Wurzinger B, **Stael S**, Hofmann-Rodrigues D, Csaszar E, Pfister B, Bayer R, Teige M. The Ca(2+)-dependent protein kinase CPK3 is required for MAPK-independent salt-stress acclimation in Arabidopsis. **Plant J**. 2010 May 20. PMID: 20497378.
- 8) Vainonen JP, Sakuragi Y, **Stael S**, Tikkanen M, Allahverdiyeva Y, Paakkanen V, Aro E, Suorsa M, Scheller HV, Vener AV, Aro EM. Light regulation of CaS, a novel phosphoprotein in the thylakoid membrane of Arabidopsis thaliana. **FEBS J**. 2008 Apr. PMID: 18331354.